Estudio de la aplicación de ultrasonidos de alta intensidad en sistemas sólido-líquido y sólido-gas. Influencia en la cinética de transporte de materia y en la estructura de los productos

CÉSAR OZUNA LÓPEZ

EDITORIAL
UNIVERSITAT POLITÈCNICA DE VALÈNCIA

DEPARTAMENTO DE TECNOLOGÍA DE ALIMENTOS

UNIVERSITAT POLITÈCNICA DE VALÈNCIA

Estudio de la Aplicación de Ultrasonidos de Alta Intensidad en Sistemas Sólido-Líquido y Sólido-Gas. Influencia en la Cinética de Transporte de Materia y en la Estructura de los Productos

TESIS DOCTORAL

Presentada por:
César Ozuna López
Dirigida por:
Dr.Juan Andrés Cárcel Carrión
Dr.José Vicente García Pérez

Valencia, 2013

Colección Tesis Doctorales

Telf.: 963 877 012 / www.lalibreria.upv.es

ISBN: 978-84-9048-182-0 (versión CD)

UNIVERSITAT POLITÈCNICA DE VALÈNCIA

DEPARTAMENTO DE TECNOLOGÍA DE ALIMENTOS

D. JUAN ANDRÉS CÁRCEL CARRIÓN Y D. JOSÉ VICENTE GARCÍA PÉREZ, AMBOS PROFESORES TITULARES DE UNIVERSIDAD DEL DEPARTAMENTO DE TECNOLOGÍA DE ALIMENTOS DE LA UNIVERSITAT POLITÈCNICA DE VALÈNCIA

CERTIFICAN: Que la memoria titulada "ESTUDIO DE LA APLICACIÓN DE ULTRASONIDOS DE ALTA INTENSIDAD EN SISTEMAS SÓLIDO-LÍQUIDO Y SÓLIDO-GAS. INFLUENCIA EN LA CINÉTICA DE TRANSPORTE DE MATERIA Y EN LA ESTRUCTURA DE LOS PRODUCTOS", que para aspirar al grado de **Doctor en Ciencia, Tecnología y Gestión Alimentaria**, presenta **D. César Ozuna López**, realizada bajo nuestra dirección en el Departamento de Tecnología de Alimentos de la Universitat Politècnica de València, cumple las condiciones adecuadas para su aceptación como **Tesis Doctoral**, por lo que

AUTORIZAN: Al interesado a su presentación en el Departamento de Tecnología de Alimentos de la Universitat Politècnica de València.

Y para que conste a los efectos oportunos, presentamos la referida memoria, firmando el presente certificado en Valencia 13 de Noviembre de 2013.

Fdo. Dr. D. Juan Andrés Cárcel Carrión

Fdo. Dr. D. José Vicente García Pérez

"He llegado… ahora entiendo que no podré parar…"

A mis padres, por el apoyo para iniciar esta gran aventura,

A las dos mujercitas que más amo en este mundo, Edith y Mariana,

¡Gracias por existir!

Agradecimientos

A la Universitat Politècnica de València (UPV) por la concesión de las becas "Formación de Personal de Investigación (2009-02)" y "Estancias de Personal Docente e Investigador de la UPV en Centros de Investigación de Prestigio (PAID-00-12)".

A todas las personas que integran el Grupo de Análisis y Simulación de Procesos Agroalimentarios del Departamento de Tecnología de Alimentos de la UPV. A su director, el Dr. Antonio Mulet Pons.

A mis directores de tesis, Dr. Juan Andrés Cárcel Carrión y Dr. José Vicente García Pérez, por la dedicación e interés en la realización de esta Tesis Doctoral.

A la Dra. Consuelo Ana Puig Gómez del Grupo de Microestructura y Química de Alimentos (MIQUALI) del Departamento de Tecnología de Alimentos de la UPV, por su ayuda y consejos en el análisis microestructural de este trabajo.

Al Dr. Per Magne Walde por su cálido recibimiento, su apoyo e interés en mi proyecto de investigación realizado durante mi estancia en Høgskolen i Ålesund, Noruega.

A Tanja Hespos y a Marta Silva, por su colaboración en la etapa experimental de esta Tesis Doctoral.

A mis compañeros de laboratorio, Edith, Elvira, Ingrid, Jader, Juan Vicente, Julián, Marta, Neus, Nieves, Rosa Isela y Sergio, por darle vida, calor y diversión al laboratorio. Siempre los llevaré en mi corazón.

A María, Julia, Annamaria, José Luis y Luis Miguel, del grupo de investigación MIQUALI, gracias por la amistad y por los buenos momentos compartidos.

A Carmina y a Marga, a estas dos personitas únicas y tan "fantásticas", por la amistad, el cariño, las sonrisas y el apoyo en todo momento. Las quiero con todo mi corazón.

A Jaime, por la amistad, su ayuda en los momentos más difíciles y por esas divertidas cenas en el "chino".

A Ana Brocal, por su amistad y por el diseño de la portada de esta Tesis Doctoral.

A mis padres y a mis hermanas, que a pesar de los miles de kilómetros de distancia que separan México de España, siempre he sentido tan cerca su amor.

A Dios, por regalarme la vida y darme fuerzas para seguir adelante.

A Stan. Gracias por tu inmenso amor.

César Ozuna

Noviembre 2013

Contenido

Abstract

Resumen

Resum

Study of High Intensity Ultrasound Application in Solid-Liquid and Solid-Gas Systems. Influence on Mass Transport Kinetics and Product Structure

Author
César Ozuna López

Supervisors
Dr. Juan Andrés Cárcel Carrión
Dr. José Vicente García Pérez

Abstract

Nowadays, food technology is becoming considerably interested in the application of High Intensity Ultrasound (**US**) due to its ability to induce mass-transfer intensification. When traveling through a medium, US causes a series of effects that can affect both the external and internal resistance to mass transfer, but it can also influence the structure and the quality of the final product. In order to achieve a better understanding of the effects of US on both the mass transfer and the food quality, it is important to be aware of the interactions between ultrasonic energy and the food structure. Therefore, the main aim of this thesis was to evaluate the influence of US on mass transport and its interaction with the structure of treated materials in some relevant applications in solid-liquid and solid-gas systems.

Regarding the US application in solid-liquid systems, the study of meat brining and cod desalting have been addressed. In both of them, the main objective was to evaluate the influence of US application on moisture and NaCl transport kinetics, as well as how microstructure and other physical properties are affected by US. Moreover, in meat brining (5±1 ºC), the effect of NaCl concentration in the brine (50, 100, 150, 200, 240 and 280 kg NaCl/m^3) was evaluated. In this sense, the brine concentration affected the moisture transport direction. Thus, at brine concentrations lower than 200 kg NaCl/m^3, samples were hydrated, and at higher concentrations they suffered dehydration. In the case of cod desalting (4±1 ºC), two acoustic powers were tested. Mass transport was analyzed, considering a separate diffusion of both moisture and NaCl. Microstructure was characterized by SEM, Cryo-SEM and Light

Microscopy, and, among other physical parameters, sample hardness and swelling have been determined.

The diffusion models were accurate for describing moisture and NaCl transport kinetics in both brining and desalting processes, providing a similar trend between the calculated and experimental data. In all the cases studied, US application significantly ($p<0.05$) intensified mass transport, increasing both moisture and NaCl effective diffusivities and not affecting the mass transport direction. In cod desalting, it was also observed that the higher the applied ultrasonic power, the larger the enhancement of mass transport induced by US.

The NaCl gain during meat brining promoted changes in the meat texture, and thus, higher NaCl contents led to harder samples. Then, the higher values of hardness of US-treated samples, compared with the conventionally brined ones, could be linked to the higher NaCl content. On the other hand, the desalting process produced swelling and hardness reduction, which were more evident in the US-treated samples. Microstructural analysis showed that US brought about noticeable effects on the product structure. For example, a more homogeneous NaCl distribution was observed in the US-brined meat and thicker cod fibers were observed in US-desalted samples.

In solid-gas systems, the air-borne US application was addressed in both hot-air and low-temperature drying. First of all, the feasibility of US application in low-temperature drying of salted cod was addressed by quantifying its influence on the drying kinetics and on some physical properties of the final dried product. For that purpose, drying experiments at -10, 0, 10, 20 °C were carried out with salted-cod slabs at constant air velocity (2±0.1 m/s) and relative humidity (9±4 %) with (20.5 kW/m^3) and without US application. The dried-salted cod rehydration capacity (4 ºC) as well as microstructural, textural and color changes were determined. Diffusion and empirical models were used in order to quantify the influence of US application and the drying temperature on drying and rehydration kinetics, respectively.

At every temperature tested, US application sped up the drying rate, the drying time being shortened by up to 50%. The diffusion model described the drying kinetics adequately, with percentages of explained variance up to 99%. The US application significantly ($p<0.05$) increased the effective moisture diffusivity up to 110%. Regarding the physical properties, US-dried samples were softer and presented a

higher rehydration capacity than those conventionally dried. This fact was linked to induced structural changes, such as the formation of large spaces between myofibrils and a more intense salt redistribution on the sample surface, such as the microstructural analysis highlighted. In addition, significant ($p<0.05$) color changes were brought about by US application.

In the air-borne US application on the hot-air drying, the response of different types of fruit and vegetables to the acoustic energy was addressed. For that purpose, experimental drying kinetics (40 ºC and 1 m/s) of eggplant, potato, cassava and apple were carried out by applying different ultrasonic powers (0, 6, 12, 19, 25 and 31 kW/m^3). US application shortened the drying times in all cases, with the magnitude of the reduction ranging from 27% (cassava) to 68% (eggplant), depending on the product considered.

In order to study the influence of US in both internal and external resistance to mass transfer, diffusion models with differing degrees of complexity were used. For the experimental conditions tested, the external resistance was found significant. Thus, its inclusion in the diffusion model increased the explained variance from 84% (the obtained value neglecting external resistance in the model) to above 98%. However, overestimated effective diffusivity was noticed an when the shrinkage was significant, such as in the case of eggplant. Thereby, a more complex model, which considered both external resistance and shrinkage to be significant phenomena, was used to accurately describe the drying kinetics of eggplant (explained variances higher than 99% and mean relative errors of under 1.2%).

The ultrasonic power had a significant ($p<0.05$) influence on the kinetic parameters, thus significant ($p<0.05$) linear relationships were found between both the effective moisture diffusivity and the mass transfer coefficient with the ultrasonic power applied. Although, the magnitude of the improvement for the kinetic parameters was greatly product-dependent.

In order to contribute to the understanding of how the properties of the material being dried affect the effectiveness of air-borne ultrasonic application, the experimental results obtained in this work for eggplant, potato, cassava and apple were completed with others already published in previous works for orange and lemon peel, and carrot. Drying kinetics were analyzed considering a pure diffusion

model in which the effective diffusivity was considered a global mass transport parameter. Moreover, structural, textural and acoustic properties were assessed for every product. The **S**lope of the relationship between the effective **D**iffusivity and the **U**ltrasonic **P**ower (**SDUP**) was used as an index of the effectiveness of the ultrasonic application, thus the higher the slope, the more effective the US application. SDUP was well correlated ($r \geq 0.95$) with the porosity and the hardness of the samples. Then, the larger the porosity and the lower the hardness, the higher the SDUP figure. In addition, SDUP was greatly affected by the acoustic impedance of the material being dried. In such a way, the relationship between SDUP vs. impedance and SDUP vs. transmission coefficient of the acoustic energy in the interface showed a similar pattern. This fact illustrates that the ultrasonic application is at least partially controlled by the way US is transmitted through the air-solid interface. On the one hand, products with softer and more open-porous structure showed a better transmission of the acoustic energy and were more prone to the mechanical effects produced by US. On the other hand, materials with a harder and more closed-compact structure were less affected by the acoustic energy due to the high impedance mismatch between the product and the air causing high energy losses on the interface.

Summarizing, common facts have been highlighted between the US applications in liquid-solid and solid-gas systems. First of all, the ability of US to intensify mass transport kinetics in both systems has been illustrated. In both cases, the mechanical effects induced by US produced changes in the product structure as well as in the physical properties of the treated product, which have to be considered aiming to a better preservation of quality traits. Moreover, in solid-gas systems, the influence of product structure on the effectiveness of US during drying was observed. This fact was linked to the large impedance mismatch between the air and the product.

Estudio de la Aplicación de Ultrasonidos de Alta Intensidad en Sistemas Sólido-Líquido y Sólido-Gas. Influencia en la Cinética de Transporte de Materia y en la Estructura de los Productos

Autor
César Ozuna López

Directores
Dr. Juan Andrés Cárcel Carrión
Dr. José Vicente García Pérez

Resumen

En los últimos años, la aplicación de Ultrasonidos de Alta Intensidad (**US**) en procesos alimentarios ha despertado un gran interés debido a su capacidad para intensificar los fenómenos de transporte de materia. Esta capacidad es atribuida a una serie de mecanismos inducidos por los US que pueden afectar tanto la resistencia interna como la resistencia externa al transporte de materia. Además, la aplicación de US puede influir en la estructura del producto tratado y en consecuencia en su calidad final. Para poder tener un mejor conocimiento de los efectos de los US, tanto en el transporte de materia como en la calidad del producto final, es importante profundizar en la interacción entre la energía acústica y la estructura del alimento. Por lo tanto, el principal objetivo de esta Tesis Doctoral fue evaluar la influencia de los US en el transporte de materia y en la interacción ultrasonidos-estructura del producto en varios sistemas sólido-líquido y sólido-gas.

Respecto a las aplicaciones en sistemas sólido-líquido, se estudió el efecto de los US en el salado de carne y en el desalado de bacalao. En ambos estudios, el principal objetivo fue evaluar la influencia de la aplicación de US en las cinéticas de transporte de agua y NaCl, así como en la microestructura y en las propiedades físicas del producto final. Además, en el salado de carne (5±1 ºC), se estudió el efecto de la concentración de NaCl en la salmuera (50, 100, 150, 200, 240 y 280 kg NaCl/m^3). En este sentido, se observó que la concentración de la salmuera afectó a la dirección del transporte de agua. Así, a concentraciones inferiores a 200 kg NaCl/m^3, las muestras se rehidrataron, mientras que a concentraciones mayores, la muestras sufrieron una

deshidratación. En el caso del desalado de bacalao (4±1 ºC), se evaluó la aplicación de dos potencias acústicas diferentes. En ambos procesos, se analizó el transporte de materia mediante modelos difusivos. El análisis microestructural se realizó a través de diferentes técnicas: SEM, Cryo-SEM y microscopia óptica. Además, se evaluaron ciertos parámetros físicos del producto final, tales como la dureza y el hinchamiento de las muestras.

Los modelos difusivos describieron de manera adecuada las cinéticas de transporte de agua y NaCl, tanto en salado como desalado, proporcionando una tendencia similar entre los datos experimentales y los calculados. En todos los casos estudiados, la aplicación de US intensificó significativamente ($p<0.05$) el transporte de materia, incrementando ambas difusividades efectivas (agua y NaCl). Además, en el caso del desalado de bacalao, se observó que al aumentar la potencia acústica aplicada al medio, la intensificación del transporte de materia fue más acusada.

La ganancia de sal en el salado de carne provocó cambios en la textura, así, altos contenidos de NaCl conllevaron muestras más duras. La mayor dureza de la carne salada con US, comparada con la salada de manera convencional, pudo deberse a su contenido más alto de sal. Por otro lado, en el bacalao, el desalado produjo el hinchamiento y el ablandamiento de las muestras. Dichos efectos fueron más evidentes al aplicar US. Mediante el análisis microestructural se observó que, la carne salada con la aplicación de US presentó una distribución más homogénea de NaCl, mientras que en el bacalao desalado, los US produjeron un incremento de la anchura de las fibras musculares.

En sistemas sólido-gas, se estudió la aplicación de US sin contacto directo tanto en el secado por aire caliente como en el secado a baja temperatura. En primer lugar, se estudió la aplicación de US en el secado a baja temperatura de bacalao salado. En este estudio se cuantificó la influencia de los US en las cinéticas de secado y en algunas propiedades físicas del producto final. Así, se realizaron experiencias de secado (2 ± 0.1 m/s) de bacalao salado a diferentes temperaturas (-10, 0, 10 y 20 °C) con (20.5 kW/m^3) y sin la aplicación de US. En las muestras deshidratadas se analizó la capacidad de rehidratación (4 °C), el color, la textura y la microestructura. Con el fin de cuantificar la influencia de la aplicación de US y la temperatura durante el secado, las cinéticas de secado y de rehidratación se modelizaron mediante modelos difusivos y empíricos.

En todas las temperaturas estudiadas, la aplicación de US durante el secado de bacalao incrementó la velocidad del proceso, alcanzando reducciones de tiempo de hasta un 50%. Por otro lado, el modelo difusivo describió adecuadamente las cinéticas de secado proporcionando porcentajes de varianza superiores al 99%. La aplicación de US incrementó significativamente ($p<0.05$) la difusividad efectiva hasta un 110%. Respecto a las propiedades físicas, las muestras secadas con US fueron más blandas y presentaron una mayor capacidad de rehidratación que las muestras secadas de manera convencional. Este hecho se relacionó con los cambios microestructurales observados, tales como, mayores espacios entre las miofibrillas y una mayor migración de la sal a la superficie de las muestras. Finalmente, la aplicación de US produjo cambios significativos ($p<0.05$) de color en el producto deshidratado.

En el caso de la aplicación de US en el secado por aire caliente, se evaluó la respuesta de diferentes vegetales ante la energía acústica. Así, se estudió la aplicación de US en el secado por aire caliente (40 ºC y 1 m/s) de berenjena, patata, manzana y yuca aplicando diferentes niveles de potencia acústica (0, 6, 12, 19, 25 y 31 kW/m^3). La aplicación de US redujo el tiempo de secado en todos los productos analizados. Sin embargo, las reducciones dependieron del producto tratado, oscilando entre un 27%, en el caso de la yuca, y un 68%, para la berenjena.

Con la finalidad de estudiar la influencia de los US tanto en la resistencia interna como en la resistencia externa al transporte de materia, las cinéticas de secado fueron modelizadas mediante modelos difusivos con diferente nivel de complejidad. Para las condiciones experimentales estudiadas, la resistencia externa resultó ser significativa. Así, su consideración en el modelo difusivo incrementó el porcentaje de varianza explicada de un 84%, valor obtenido por el modelo que no considera la resistencia externa, a un 98%. Sin embargo, cuando el encogimiento de la muestra resultó un fenómeno significativo, como en el caso de la berenjena, la difusividad efectiva identificada fue sobreestimada. Es por ello que, el modelo difusivo que considera ambos fenómenos (resistencia externa y encogimiento) se utilizó para describir con mayor precisión las cinéticas de secado de berenjena, alcanzándose porcentajes de varianza explicada superiores al 99% y errores relativos medios inferiores al 1.2%.

La potencia ultrasónica influyó significativamente ($p<0.05$) en los parámetros cinéticos. Así, se observaron relaciones lineales significativas entre la difusividad efectiva y el coeficiente de transferencia de materia con la potencia ultrasónica

aplicada. Por otro lado, la magnitud del incremento de los parámetros cinéticos con el aumento de la potencia acústica aplicada se vio muy influenciado por el producto secado.

Con el objetivo de mejorar la comprensión de cómo la estructura interna del material influye en la efectividad de los US durante el secado, los resultados experimentales de este trabajo para berenjena, patata, yuca y manzana fueron completados con otros ya publicados en trabajos previos sobre zanahoria, piel de naranja y piel de limón. Las cinéticas de secado fueron analizadas mediante un modelo difusivo en el cual se consideró la difusividad efectiva como un parámetro global del transporte de materia. Además, en todos los productos se determinó experimentalmente la porosidad y diversos parámetros texturales, como por ejemplo la dureza, la microestructura y las propiedades acústicas.

La **P**endiente de la relación lineal entre la **D**ifusividad efectiva y la **P**otencia **U**ltrasónica aplicada (**PDPU**) calculada para cada producto se utilizó como una estimación de la efectividad de los US, de manera que mientras mayor fue dicha pendiente, la efectividad de los US se incrementó. Se observó la existencia de una correlación lineal ($r \geq 0.95$) entre PDPU y la porosidad y dureza del producto. Así, en productos que presentaron una mayor porosidad y una menor dureza, la PDPU fue mayor. Además, se observó que las relaciones PDPU vs. impedancia y PDPU vs. coeficiente de transmisión de la energía acústica mostraron un patrón muy similar. Este hecho pone de manifiesto que la aplicación de US en el proceso de secado depende en gran medida de la fracción de energía ultrasónica que penetra en el sólido. Por un lado, los productos más blandos y con una estructura más porosa mostraron una mejor transmisión de la energía acústica y fueron más sensibles a los efectos mecánicos producidos por los US. Por otro lado, los materiales más duros y con una estructura más compacta fueron menos afectados por la energía acústica, debido a la gran diferencia de impedancias entre el producto y el aire, lo cual puede inducir grandes pérdidas de energía en la interfase.

En resumen, a partir de los resultados obtenidos en este trabajo, se han encontrado diversos factores que son comunes en las aplicaciones de los US en sistemas sólido-líquido y en sólido-gas. En primer lugar, se ha demostrado el potencial de los US para intensificar las cinéticas de transporte de materia en ambos sistemas. Además, en ambos casos, los efectos mecánicos atribuidos a la aplicación de US provocaron

cambios en la estructura del producto, así como también en las propiedades físicas del material tratado que deben de tenerse en cuenta en vistas a preservar la calidad de los productos. Además, en los sistemas sólido-gas, se ha observado la influencia de la estructura del producto en la efectividad de los US durante el secado. Esto se ha atribuido a la diferencia de impedancias entre el aire y el producto.

Estudi de l'aplicació d'ultrasons d'alta intensitat en sistemes sòlid-líquid i sòlid-gas. Influència en la cinètica de transport de matèria i en l'estructura dels productes

Autor
César Ozuna López

Directors
Dr. Juan Andrés Cárcel Carrión
Dr. José Vicente García Pérez

Resum

En els últims anys, l'aplicació d'ultrasons d'alta intensitat (**US**) en processos alimentaris ha despertat un gran interès a causa de la capacitat que tenen per a intensificar els fenòmens de transport de matèria. Aquesta capacitat és atribuïda a una sèrie de mecanismes induïts pels US que poden afectar tant la resistència interna com la resistència externa al transport de matèria. A més, l'aplicació d'US pot influir en l'estructura del producte tractat i, en conseqüència, en la qualitat final d'aquest. Per a poder tenir un millor coneixement dels efectes dels US, tant en el transport de matèria com en la qualitat del producte final, és important tenir en compte la interacció entre l'energia acústica i l'estructura de l'aliment. Per tant, el principal objectiu d'aquesta tesi doctoral ha sigut avaluar la influència dels US en el transport de matèria i en la interacció ultrasons-estructura del producte en diversos sistemes sòlid-líquid i sòlid-gas.

Respecte a les aplicacions en sistemes sòlid-líquid, hem estudiat l'efecte dels US en el salatge de carn i en el dessalatge de bacallà. En tots dos estudis, el principal objectiu ha sigut avaluar la influència de l'aplicació d'US en les cinètiques de transport d'aigua i NaCl, com també en la microestructura i en les propietats físiques del producte final. A més, en el salatge de carn (5±1 ºC), hem estudiat l'efecte de la concentració de NaCl en la salmorra (50, 100, 150, 200, 240 i 280 kg NaCl/m^3). En aquest sentit, s'ha observat que la concentració de la salmorra afecta la direcció del transport d'aigua. Així, a concentracions inferiors a 200 kg NaCl/m^3, les mostres es van rehidratar, mentre que a concentracions majors, les mostres van sofrir una deshidratació. En el cas del dessalatge de bacallà (4±1 ºC), hem avaluat l'aplicació de dues potències

acústiques diferents. En tots dos processos, hem analitzat el transport de matèria mitjançant models difusius. L'anàlisi microestructural s'ha realitzat a través de diferents tècniques: SEM, Cryo-SEM i microscòpia òptica. A més, hem avaluat certs paràmetres físics del producte final, tals com la duresa i l'inflament de les mostres.

Els models difusius van descriure de manera adequada les cinètiques de transport d'aigua i NaCl, tant en salatge com en dessalatge, i proporcionaren una tendència semblant entre les dades experimentals i les calculades. En tots els casos estudiats, l'aplicació d'US va intensificar significativament ($p<0.05$) el transport de matèria, amb la qual cosa ambdues difusivitats efectives (aigua i NaCl) van augmentar. En el cas del dessalatge de bacallà, es va observar que l'augment de la potència acústica aplicada al medi va produir una major intensificació del procés.

El guany de sal en el salatge de carn va provocar canvis en la textura, de manera que alts continguts de NaCl van comportar mostres més dures. La major duresa de la carn salada amb US, comparada amb la salada de manera convencional, pot ser causada pel contingut més alt de sal. D'altra banda, el dessalatge va produir l'inflament i l'ablaniment de les mostres. Aquests efectes van ser més evidents en aplicar-hi US.

Mitjançant l'anàlisi microestructural es va observar que, en aplicar-hi US, la carn salada va presentar una distribució més homogènia de NaCl, mentres que en el bacallà dessalat es va observar un increment de l'amplària de les fibres musculars.

En sistemes sòlid-gas hem estudiat l'aplicació d'US sense contacte directe, tant en l'assecatge per aire calent com en l'assecatge a baixa temperatura. En primer lloc, es va estudiar l'aplicació d'US en l'assecatge a baixa temperatura de bacallà salat. En aquest estudi s'ha quantificat la influència dels US en les cinètiques d'assecatge i en algunes propietats físiques del producte final. Així, es van realitzar experiències d'assecatge ($2 \pm 0{,}1$ m/s) de bacallà salat a diferents temperatures (-10, 0, 10 i 20 °C) amb ($20{,}5$ kW/m^3) i sense l'aplicació d'US. En les mostres tractades es va analitzar la capacitat de rehidratació (4 °C), el color, la textura i la microestructura. A fi de quantificar la influència de l'aplicació d'US i la temperatura durant l'assecatge, les cinètiques d'assecatge i de rehidratació es modelitzaren mitjançant models difusius i empírics.

Per a totes les temperatures estudiades, l'aplicació d'US durant l'assecatge de bacallà salat va incrementar la velocitat del procés, i s'aconseguiren reduccions de temps de

fins a un 50%. D'altra banda, el model difusiu va descriure adequadament les cinètiques d'assecatge, i va proporcionar percentatges de variància superiors al 99%. L'aplicació d'US va incrementar significativament ($p<0,05$) la difusivitat efectiva fins a un 110%. Respecte a les propietats físiques, les mostres assecades amb US van ser més blanes i van presentar una major capacitat de rehidratació que les mostres assecades de manera convencional. Aquest fet es va relacionar amb els canvis microestructurals observats, tals com majors espais entre les miofibril·les i una major migració de la sal a la superfície de les mostres. Finalment, l'aplicació d'US va produir canvis significatius ($p<0,05$) de color en el producte deshidratat.

En el cas de l'aplicació d'US en l'assecatge per aire calent, hem avaluat la resposta de diverses fruites i vegetals davant de l'energia acústica. Així, es va estudiar l'aplicació d'US en l'assecatge per aire calent (40 ºC i 1 m/s) d'albergínia, creïlla, poma i iuca aplicant diferents nivells de potència acústica (0, 6, 12, 19, 25 i 31 kW/m^3). L'aplicació d'US va reduir el temps d'assecatge en tots els productes analitzats, però, no obstant això, les reduccions van dependre del producte tractat i van oscil·lar a l'entorn d'un 27%, en el cas de la iuca, i un 68%, per a l'albergínia.

Amb la finalitat d'estudiar la influència dels US tant en la resistència interna com en la resistència externa al transport de matèria, les cinètiques d'assecatge van ser modelitzades mitjançant models difusius amb diferent nivell de complexitat. Per a les condicions experimentals estudiades, la resistència externa va ser significativa. Així, en considerar-la dins del model difusiu, va incrementar el percentatge de variància explicada d'un 84%, valor obtingut pel model que no considera la resistència externa, a un 98%. No obstant això, es va observar que quan l'encongiment de la mostra és un fenomen significatiu, com en el cas de l'albergínia, la difusivitat efectiva identificada està sobreestimada. Per tant, el model difusiu que considera aquests dos fenòmens (resistència externa i encongiment) es va utilitzar per a descriure amb major precisió les cinètiques d'assecatge d'albergínia. S'aconseguiren percentatges de variància explicada superiors al 99% i errors relatius mitjans inferiors a l'1,2%

La potència ultrasònica va influir significativament ($p<0,05$) en els paràmetres cinètics. Així, s'hi van observar relacions lineals significatives entre la difusivitat efectiva i el coeficient de transferència de matèria amb la potència ultrasònica aplicada. Encara que la magnitud de l'increment dels paràmetres cinètics es va veure molt influïda pel producte assecat.

Amb l'objectiu de millorar la comprensió de com l'estructura interna del material influeix en l'efectivitat dels US durant l'assecatge, els resultats experimentals d'aquest treball van ser completats amb altres ja publicats en treballs previs sobre carlota, pell de taronja i pell de llima. Les cinètiques d'assecatge van ser analitzades mitjançant un model difusiu en el qual es va considerar la difusivitat efectiva com un paràmetre global del transport de matèria. A més, en tots els productes es va determinar experimentalment la porositat, diversos paràmetres texturals, com per exemple la duresa, la microestructura i les propietats acústiques.

El pendent de la relació lineal entre la difusivitat efectiva i la potència ultrasònica aplicada (**PDPU**) calculada per a cada producte es va utilitzar com una estimació de l'efectivitat dels US. Per a valors majors del pendent, l'efectivitat dels US es va incrementar. Es va observar l'existència d'una correlació lineal (r=0,95) entre PDPU i la porositat i la duresa del producte. Així, en productes que van presentar una major porositat i una menor duresa, la PDPU va ser major. A més, es va observar que la relació PDPU i la impedància i PDPU i el coeficient de transmissió de l'energia acústica van mostrar una tendència molt semblant. Per tant, aquest fet posa de manifest que l'aplicació d'US en el procés d'assecatge depèn en gran manera de la fracció d'energia ultrasònica que penetra en el sòlid. D'una banda, els productes més blans i amb una estructura més porosa van mostrar una millor transmissió de l'energia acústica i van ser més sensibles als efectes mecànics produïts pels US. D'una altra banda, els materials més durs i amb una estructura més compacta van ser menys afectats per l'energia acústica, a causa de la gran diferència d'impedàncies entre el producte i l'aire, la qual cosa pot induir grans pèrdues d'energia en la interfase.

En resum, amb els resultats obtinguts en aquest treball, s'han trobat diversos fets que són comuns en les aplicacions dels US tant en sistemes sòlid-líquid com en sòlid-gas. En primer lloc, s'ha demostrat el potencial dels US per a intensificar les cinètiques de transport de matèria en aquests dos sistemes. A més, en tots dos casos, els efectes mecànics atribuïts a l'aplicació d'US van provocar canvis en l'estructura del producte, com també en les propietats físiques del material tractat que han de ser considerades per a preservar la qualitat dels productes. No obstant això, també s'han trobat alguns fets particulars dels sistemes estudiats. Per exemple, en sistemes sòlid-gas, l'estructura del producte va influir en gran manera en l'efectivitat dels US durant l'assecatge a causa de la gran diferència d'impedàncies entre l'aire i el producte.

1. Introducción

1.1. Aplicación de nuevas tecnologías en la industria de alimentos

La industria de alimentos se encuentra en constante evolución en respuesta a un mercado que demanda cada día productos más seguros, de elevada calidad y asequibles (Cardello et al., 2007). Por tal motivo, este sector ha mostrado un interés creciente en la aplicación de "**nuevas tecnologías**" o "**tecnologías emergentes**" a los procesos convencionales de elaboración, transformación y conservación de alimentos (Knorr et al., 2011).

La definición de "nuevas tecnologías" o "tecnologías emergentes" ha evolucionado. En un principio, estas tecnologías fueron definidas como procesos no térmicos, diseñados para desarrollar alimentos nutritivos, seguros y de elevada calidad. Actualmente, esta definición considera la capacidad de estas tecnologías para modificar las propiedades funcionales del alimento y además contribuir a intensificar los procesos ya existentes (Roupas, 2008).

La **intensificación de procesos** tiene como objetivo mejorar los procesos tradicionales y desarrollar nuevas tecnologías que permitan alcanzar mayores rendimientos de producción, disminuir el consumo de energía, aumentar la calidad del producto y la seguridad del proceso (Benali & Kundra, 2010; Gerven & Stankiewicz, 2009). En los últimos años, un gran número de investigaciones han centrado sus objetivos en la aplicación de nuevas tecnologías que contribuyan a la intensificación de procesos en la industria de alimentos tales como las microondas (Venkatesh & Raghavan, 2004), las altas presiones hidrostáticas (Oey et al., 2008), los pulsos eléctricos (Toepfl et al., 2006), los fluidos supercríticos (Ortuño et al., 2012) y los ultrasonidos de alta intensidad (Cárcel et al., 2012; Chemat et al., 2011), entre otras.

La aplicación de **microondas** en la intensificación de procesos ha sido estudiada en diversas aplicaciones como el secado, la pasteurización, la descongelación y el horneado (Chandrasekaran et al., 2013). En el secado, una de sus principales limitaciones es el sobrecalentamiento que puede sufrir el producto en algunas zonas del mismo si el control del proceso no es óptimo (Zhang et al., 2006). Las **altas presiones** y los **pulsos eléctricos** resultan de gran interés en procesos de conservación de alimentos y han demostrado ser efectivos en la eliminación o reducción del contenido de microorganismos, tanto patógenos como causantes del

deterioro del alimento (Jaeger et al., 2009; Patterson, 2005). Sin embargo, los productos sometidos a estos tratamientos a menudo sufren alteraciones que repercuten en sus propiedades sensoriales, tales como el color, sabor y textura (Fuentes et al., 2010). En cuanto a los **fluidos supercríticos,** se han utilizado para mejorar procesos de extracción, pasteurización e inactivación de microorganismos y enzimas (Ortuño et al., 2013; Perrut, 2012; Spilimbergo et al., 2007).

Finalmente, la aplicación de **ultrasonidos de alta intensidad** en procesos alimentarios supone una opción innovadora, capaz de reducir el consumo energético y respetuosa con el medio ambiente (Gallego-Juárez et al., 2010). Esta tecnología, que se ha utilizado en numerosas aplicaciones como operaciones de lavado, desespumado, extracción, etc., ha despertado un gran interés debido a su capacidad para acelerar procesos de transferencia de materia tanto en sistemas sólido-líquido como en sistemas sólido-gas (Tao & Sun, 2013; Chemat et al., 2011).

1.2. Ultrasonidos

1.2.1. Definición

Los **ultrasonidos** son ondas elásticas de frecuencia superior al límite de audición humano (20 kHz), las cuales necesitan un medio para propagarse (Mason & Lorimer, 2002). La fuente de producción de ultrasonidos suele ser un cuerpo vibrante. Así, el movimiento de vibración de dicho cuerpo se comunica a las partículas del medio que le rodean, que a su vez comienzan a oscilar, comunicando la energía de forma también oscilante a las partículas vecinas. Las ondas acústicas, como cualquier otro tipo de onda, se caracterizan por una serie de parámetros que a continuación se exponen.

Frecuencia

La frecuencia (f, kHz) de una onda se define como el número de vibraciones o ciclos completados por la onda en una unidad de tiempo. Al inverso de la frecuencia se le denomina periodo y se define como el tiempo necesario para que cada onda realice un ciclo (Fig. 1).

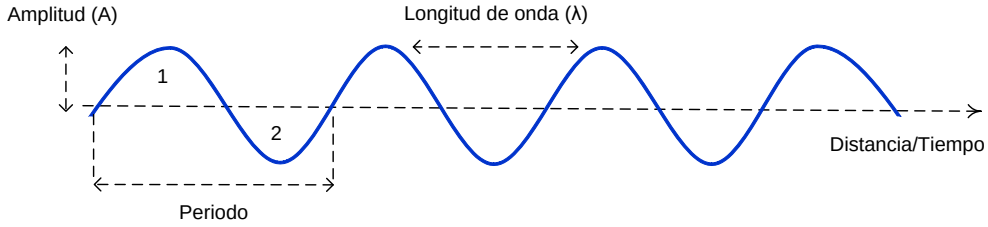

Fig. 1 Propagación de una onda ultrasónica. Parámetros característicos (García-Pérez, 2007). 1) Zona de compresión, 2) Zona de descompresión.

Velocidad acústica

La velocidad acústica (v, m/s) se define como la velocidad de propagación de la onda. La velocidad de propagación de las ondas longitudinales y transversales es característica del medio de propagación y, en general, puede considerarse constante para un determinado medio. Sin embargo, la velocidad puede verse afectada por variables ambientales como la temperatura o la presión.

Longitud de onda

La longitud de onda (λ, m) se define como la distancia entre dos planos en los que las partículas se encuentran en el mismo estado de vibración (Fig. 1). Se determina a partir de la velocidad acústica (v) y la frecuencia (f) (Ec. 1).

$$\lambda = \frac{v}{f} \tag{1}$$

Amplitud

La amplitud de la onda (A, m) es el máximo desplazamiento de la partícula desde la posición de equilibrio (Fig. 1).

Presión acústica

La presión acústica (P_A, N/m^2) es la presión existente en las diversas zonas del medio. Esta presión será mayor en las zonas de contracción de partículas que la zona normal, y menor en las zonas dilatadas. Por lo tanto, la presión acústica es alterna (Fig. 1). La desviación máxima en relación a la normal se denomina amplitud de la presión acústica y está relacionada con la amplitud de oscilación de la onda.

Intensidad acústica

La intensidad de una onda acústica (I, W/m^2) se define como la energía media transmitida a través de la unidad de área, perpendicular a la dirección de propagación de la onda, por unidad de tiempo. La intensidad acústica es proporcional al cuadrado de la presión acústica máxima (Ec. 2).

$$I = \frac{P_A^2}{2\rho v} \tag{2}$$

donde ρ es la densidad del medio (kg/m^3).

Densidad de energía

Al propagarse una onda, se transmite energía que puede ser disipada en forma de calor debido al trabajo realizado al desplazar las partículas en un medio sujeto a fuerzas contrarias al desplazamiento de las mismas. La densidad de energía (E) puede expresarse como el cociente entre la intensidad acústica (I) y la velocidad de propagación de la onda (v) (Ec. 3):

$$E = \frac{I}{v} \tag{3}$$

La densidad de energía se mide en unidades de J/m^3. Si la energía se expresa en Newton por metro (N.m), las unidades de la densidad de energía se transforman en N/m^2, es decir en unidades de presión. Por lo tanto, la densidad de energía es equivalente al nivel de presión acústica.

Potencia acústica

La potencia acústica (P, W) es la energía total irradiada por la fuente ultrasónica por unidad de tiempo. Se puede calcular a partir de la intensidad acústica y del área de la superficie radiante (S) (Ec. 4).

$$P = IS \tag{4}$$

La potencia puede expresarse en notación decibélica (P_{dB}) a partir de la relación logarítmica entre la intensidad (o potencia) acústica existente en un medio (I) y la intensidad (o potencia) acústica de referencia (I_0) (Ec. 5).

$$P_{dB} = 10 \log \frac{I}{I_0} \tag{5}$$

De igual manera que en el caso de la potencia, la presión acústica puede referirse en notación decibélica (P_{AdB}) (Ec. 6), lo que se denomina como nivel de presión sonora.

$$P_{AdB} = 10 \log \frac{P_A^2}{P_{A0}^2} \tag{6}$$

Generalmente se toman como valores de referencia de I_0, 1 x 10^{-12} W/m^2, y de P_{A0}, 2 x 10^{-5} Pa.

Finalmente, cabe destacar que la amplitud de la onda, la densidad de energía, la presión, intensidad y potencia acústica son medidas que indican la **cantidad de energía acústica** en el medio. Sin embargo, a efectos prácticos y en aplicaciones concretas, realizar estas medidas puede resultar complejo, por lo que frecuentemente sólo se indica la potencia eléctrica consumida por los dispositivos ultrasónicos, lo cual puede llevar a cierta confusión cuando se comparan diferentes trabajos.

Impedancia acústica

La impedancia acústica (Z, MRayl) se define como la relación entre la presión acústica y la velocidad de vibración de la partícula. Se puede calcular a partir de la velocidad acústica (v) y la densidad del medio (ρ) (Ec. 7).

$$Z = \rho \cdot v \tag{7}$$

Al igual que le ocurre a la luz, cuando la onda ultrasónica llega a una interfase, una parte es reflejada y otra transmitida. La proporción de energía reflejada depende en gran medida de la diferencia de impedancia entre los dos medios. Mientras mayor sea la diferencia, mayor será la energía reflejada y menor la transmitida. Por lo tanto, esta característica presenta una gran importancia en las aplicaciones de los ultrasonidos. Si la proporción de energía reflejada es mayor que la transmitida, los efectos de los ultrasonidos podrían ser más intensos en la interfase. Si por el contrario, la energía transmitida es mayor, se incrementan los efectos de los ultrasonidos en el interior del segundo medio (García-Pérez, 2007).

Atenuación

Durante la propagación de la onda ultrasónica por un medio, la intensidad de la onda disminuye al aumentar la distancia a la fuente que la produce. Este fenómeno es conocido como atenuación. La Ec. 8 muestra la expresión para el cálculo de la intensidad acústica de la onda en un punto situado a una cierta distancia (d) de la fuente productora.

$$I = I_0 e^{(-\alpha_a d)} \tag{8}$$

donde α_a es el coeficiente de atenuación.

La atenuación puede ser consecuencia de la reflexión, la dispersión o la difracción de la onda durante su propagación, o como consecuencia de la conversión de parte de la energía cinética de la onda en calor.

1.2.2. Clasificación

Las aplicaciones de los ultrasonidos se pueden clasificar en dos grandes grupos. Por un lado se encuentran las aplicaciones de **ultrasonidos de alta frecuencia** (>100 kHz) y **baja potencia** (<1 W/cm^2), también denominados como "ultrasonidos de señal". Estas aplicaciones se centran en el control de calidad de productos y/o procesos (Chandrapala 2012a; Coupland, 2004). Su utilización se basa principalmente en la medida de la velocidad ultrasónica, la atenuación de la señal o el análisis del espectro de frecuencia, y a partir de ahí se obtiene información del medio en el que se propagan los ultrasonidos. Con estas técnicas, se han caracterizado una amplia gama de productos (Awad et al., 2012). En este sentido, los ultrasonidos han sido empleados para la evaluación de la calidad de las frutas y vegetales (Mizrach, 2008), procesos de fermentación durante la fabricación de pan (Ross et al., 2004), en la estimación del contenido de grasa sólida, los cambios en la cristalización y el estado físico de grasas (Awad, 2004; McClements & Povey, 1992) o la caracterización de productos cárnicos (Corona et al., 2013).

Por otro lado, se encuentran los **ultrasonidos de baja frecuencia** (20-100 kHz) y **alta potencia** (>1 W/cm^2) también conocidos como "ultrasonidos de alta intensidad" o "ultrasonidos de potencia" (**US**). En este caso, los US se utilizan para provocar cambios en el producto o en los procesos en los que son aplicados (Tao & Sun, 2013;

Picó, 2013; Chemat et al., 2011). En la siguiente sección se abordará con más detalle los efectos producidos por los US en función del medio donde se propagan y sus principales aplicaciones en procesos alimentarios tanto en sistemas sólido-líquido como sólido-gas.

1.3. Ultrasonidos de alta intensidad

1.3.1. Efectos en el medio de propagación

Los US generan una serie de efectos cuando atraviesan un medio, algunos de los cuales pueden afectar a los fenómenos de transporte, tanto de materia como de calor. Estos efectos pueden explicarse mediante varios mecanismos asociados, que varían en función del medio donde se propaga la onda acústica.

Medio líquido

La mayoría de los efectos atribuidos a los US en medio líquido están producidos por la cavitación (Esclapez et al., 2011; Chandrapala et al., 2012b). La propagación de los US en un líquido induce una serie de compresiones y descompresiones provocando desplazamientos moleculares (Fig. 1). Cuando la potencia acústica alcanza cierto umbral, las presiones negativas que se producen durante el ciclo de descompresión pueden vencer las fuerzas atractivas de las moléculas del líquido, principalmente la tensión superficial, formándose una burbuja de gas en el líquido (Picó, 2013; Soria & Villamiel, 2010). Una vez formada, la burbuja puede seguir creciendo por el mecanismo de difusión rectificada, caracterizado por un flujo neto de gas desde el líquido a la burbuja (Fig. 2A). En el ciclo de presión negativa, el flujo de gas se produce desde el líquido hacia la burbuja, que se expande aumentando de tamaño. Cuando la presión es negativa, el flujo es contrario y la burbuja disminuye de tamaño. La cantidad de vapor perdido siempre es inferior al ganado, por lo que el tamaño de la burbuja crece cada ciclo (Luque de Castro & Priego Capote, 2007).

Las burbujas de cavitación pueden alcanzar un tamaño estable con una variación constante debido a las sucesivas compresiones y descompresiones, generando microagitaciones en el líquido. Este fenómeno se denomina "**cavitación estable**". Sin embargo, el tamaño de las burbujas puede ser inestable, el ciclo de crecimiento de la burbuja es mayor que el ciclo de disminución, lo que provoca un crecimiento rápido que acaba en el colapso de la burbuja generando altas temperaturas (5000 K) y

presiones (100 MPa) (Luque de Castro & Priego Capote, 2007) (Fig. 2B). Este tipo de cavitación conocida como "**cavitación transitoria**" puede producir fuerzas cortantes y turbulencia en la zona de cavitación (Pingret et al., 2013; Cárcel et al., 2012).

En sistemas sólido-líquido, los efectos mecánicos provocados por la cavitación dependen en gran medida de las características del medio (viscosidad, tensión superficial, presión de vapor del líquido) y de los parámetros ultrasónicos (frecuencia, intensidad) (Chemat et al., 2011; Chandrapala et al., 2012b).

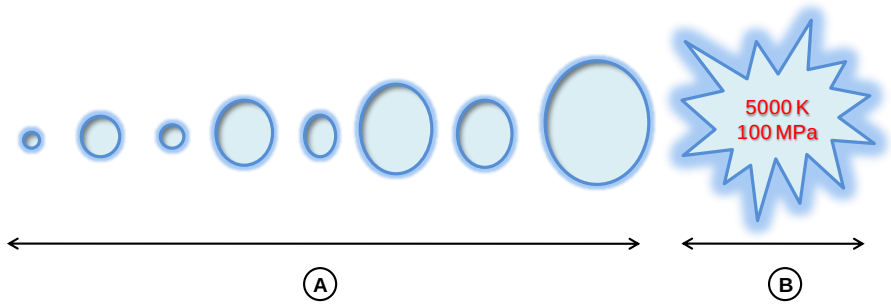

Fig. 2 A) Formación y crecimiento de la burbuja de cavitación por difusión rectificada. B) Implosión de la burbuja de cavitación (Luque de Castro & Priego Capote, 2007).

Por otro lado, el colapso de las burbujas de cavitación es asimétrico cuando se produce en posiciones cercanas a la superficie del sólido. Como consecuencia, se genera una corriente de líquido hacia el interior de la burbuja, es decir, un "microjet" que la atraviesa y golpea la superficie del sólido (Fig. 3). Este fenómeno también puede incrementar la transferencia de materia y energía entre el líquido y el sólido disminuyendo el espesor de la capa límite.

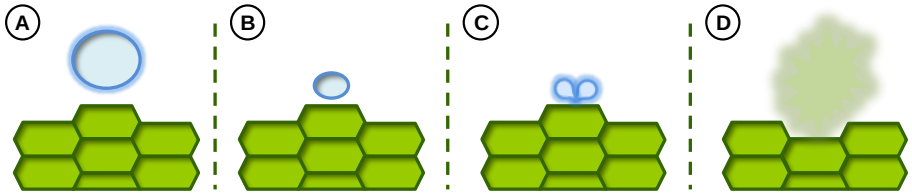

Fig. 3 Ciclo de descompresión (A) y compresión (B) de una burbuja de cavitación, (C) Colapso de la burbuja y formación de un microjet en la superficie del sólido, (D) Liberación del material interno del sólido (Esclapez et al., 2011).

Finalmente, la resistencia viscosa a la vibración que ejercen los líquidos produce la conversión de parte de energía en calor. Esta absorción de energía acústica es particularmente importante en las intefases (Mason & Lorimer, 2002). Este fenómeno, junto con la cavitación, puede provocar un calentamiento significativo del medio líquido, el cual debe tenerse en cuenta a la hora de diseñar tratamientos que se tengan que realizar a una determinada temperatura. Este hecho es importante cuando el proceso se realiza a baja temperatura, ya que un aumento de la misma puede influir en los fenómenos de transporte de materia (Esclapez et al., 2011; Cárcel, 2003).

Medio gas

En medio gas, los US pueden provocar efectos intensos en las interfases, tales como variaciones de presión, velocidades oscilantes y microcorrientes. Estos efectos pueden contribuir a la disminución del espesor de la capa límite de difusión, y por tanto, a la reducción de la resistencia externa a la transferencia de calor y de materia (Mulet et al., 2010). Estos efectos también aparecen en medio líquido pero son enmascarados por los efectos de la cavitación. Por último, los US también pueden producir un ligero calentamiento en medio gas, aunque este incremento de temperatura no es tan importante como el que se genera en medio líquido al no darse cavitación y considerando la baja viscosidad de los gases.

Material sólido

Cuando la energía ultrasónica atraviesa un medio sólido causa una serie de contracciones y expansiones alternantes. El proceso, a nivel microscópico, podría asimilarse a lo que ocurre cuando una esponja se aprieta y se relaja, por eso a este fenómeno se le conoce como "efecto esponja". Este estrés facilita el intercambio con el medio que rodea al sólido. Así, en el caso de ser un gas, se favorece la salida de líquido durante la fase de compresión (Tao & Sun, 2013; Cárcel et al., 2012). En el caso de estar el sólido sumergido en un líquido, éste puede penetrar en la matriz sólida durante la fase expansión. Además, el estrés mecánico puede inducir la creación de microcanales que facilitan estos intercambios (Muralidhara et al., 1985). Por último, hay que tener en cuenta que el fenómeno de cavitación podría aparecer en la fase líquida incluida en la matriz sólida, contribuyendo de este modo a eliminar el líquido más fuertemente retenido en la estructura del producto.

1.3.2. Aplicaciones en procesos alimentarios

La efectividad de las aplicaciones de US en procesos alimentarios depende en gran medida de la eficiencia del sistema de aplicación. A continuación se muestran las aplicaciones más relevantes tanto en medio líquido como en gases.

Dentro de los sistemas de aplicación de US en medios líquidos destacan los **baños de ultrasonidos** y los **sistemas tipo sonda**. Los baños de ultrasonidos están constituidos por una serie de transductores acoplados a la base de una carcasa metálica (Luque de Castro & Priego Capote, 2007). Al vibrar todos ellos en fase, hacen que toda la carcasa vibre y transmita la energía ultrasónica al líquido contenido en ella. Por otro lado, en los sistemas tipo sonda, el transductor se encuentra acoplado a una sonda que es la encargada de transmitir la vibración al medio. La geometría de la sonda varía en función de la aplicación específica de que se trate (Cárcel, 2003). Utilizando ambos sistemas de generación de US, se han desarrollado diversas aplicaciones en procesos tales como la deshidratación osmótica de vegetales (Cárcel et al., 2007a; Gabaldón-Leyva et al., 2007), el salado de carne (Siró et al., 2009; Cárcel et al., 2007b) y queso (Sánchez et al. 2001a, b), procesos de extracción de productos naturales (Ahmad-Qasem et al., 2013; Esclapez et al., 2011) o también en pretratamientos, tanto osmóticos (Oliveira et al., 2011; Stojanovic & Silva, 2007) como de escaldado (Gamboa-Santos et al., 2013; Rawson et al., 2011) previos al secado por aire caliente. Finalmente, cabe mencionar que en los últimos años se han desarrollado aplicaciones de US combinados con fluidos supercríticos, tanto en procesos de extracción (Riera et al., 2010) como en procesos de inactivación de microorganismos (Ortuño et al., 2013).

La aplicación de US en medios gaseosos es mucho más compleja que en medios líquidos debido principalmente a que la transmisión de energía acústica se ve dificultada por la gran diferencia de impedancias entre los sistemas emisores de US y los gases. A esto se une que los gases producen una elevada atenuación de las ondas acústicas (Riera et al., 2011; García-Pérez, 2007). Sin embargo, y a pesar de las dificultades existentes, recientemente se han desarrollado sistemas ultrasónicos eficientes, con mejor acople de impedancias con el aire y alta capacidad de potencia, que han permitido desarrollar aplicaciones en procesos tan diferentes como la aglomeración de polvos, la destrucción de espumas (Rodríguez et al., 2010; Riera et al., 2006) o el secado de alimentos (Cárcel et al., 2012; De la Fuente et al., 2006).

En procesos de secado, se han utilizado **transductores de placa escalonada** para irradiar la energía acústica al aire (Gallego-Juárez et al., 1999). Estos dispositivos se han aplicado tanto **con contacto directo** entre el emisor y el alimento, como **sin ningún tipo de contacto** (Sabarez et al., 2012; De la Fuente et al., 2006). Otra alternativa que ha sido explorada consiste en que la propia **cámara de secado sea el elemento vibrante** y transmita la energía a las partículas presentes en su interior. Basado en esta premisa, García-Pérez et al. (2006a) desarrollaron un sistema de aplicación ultrasónico consistente en un cilindro vibrando a flexión, excitado por un vibrador compuesto por un transductor tipo sándwich (frecuencia 21.7 kHz, impedancia 369 Ω, capacidad de potencia 90 W) y un amplificador mecánico (Fig. 4). Este dispositivo se ha utilizado en el secado por aire caliente de diversos productos vegetales (Rodriguez et al., 2013; Cárcel et al., 2011; García-Pérez et al., 2009). Recientemente, García-Pérez et al. (2012a) han modificado este sistema de generación de US para la aplicación en el secado a baja temperatura de productos vegetales.

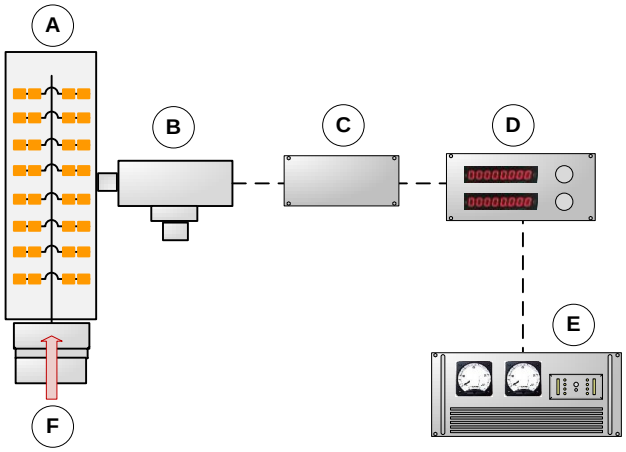

Fig. 4 Principales elementos de la cámara de secado vibrante. A) Cilindro vibrante/cámara de secado, B) Transductor ultrasónico, C) Adaptador de impedancias, D) Medidor de potencia, E) Generador ultrasónico de potencia, F) Flujo de aire (García-Pérez et al., 2006a).

Por otra parte, otros autores han utilizado **transductores comerciales**, diseñados para otros usos, en procesos de secado. Así, Bantle & Eikevik (2011) incorporaron un transductor comercial (20 kHz; DN 20/2000, Sonotronic) a un secadero convectivo a baja temperatura. Por otro lado, Schössler et al. (2012a y 2012b) aplicaron US por contacto directo durante en el secado de vegetales por aire caliente mediante un

sonotrodo tipo anillo (RIS 200, Hielscher Ultrasonics), excitado por un transductor ultrasónico (24 kHz; UIS250L, Hielscher Ultrasonics), para transmitir la energía acústica a un tamiz donde las muestras fueron depositadas. En procesos de liofilización, Schössler et al. (2012c), adaptaron un dispositivo similar a un liofilizador comercial. Sin embargo, a pesar de los esfuerzos realizados por estos autores, la eficiencia de los US en estas aplicaciones es relativamente baja en comparación con los otros sistemas descritos anteriormente y desarrollados específicamente para aplicaciones en medios gaseosos.

1.4. Intensificación de procesos de transferencia de materia mediante aplicación de ultrasonidos

1.4.1. Sólido-líquido

Los US se han aplicado en diversos sistemas sólido-líquido con el objetivo común de acelerar la transferencia de materia y así reducir los tiempos de tratamiento. La influencia de los US en las cinéticas de transporte depende de ciertas variables de proceso tales como la potencia acústica y la temperatura del medio, aspectos que se trataran a continuación.

Potencia acústica

El nivel de potencia acústica suministrada al medio tiene un papel muy importante sobre la efectividad de los US en la intensificación de procesos de transferencia de materia. De acuerdo con la bibliografía, es necesario alcanzar cierto umbral de energía acústica para observar efectos significativos en los fenómenos de transporte de materia. Así, estudiando la deshidratación osmótica de manzana (30 °Brix, 30 °C), Cárcel et al. (2007a) observaron que tanto para el transporte de agua como para el de solutos existe un umbral de potencia acústica en torno a 10 W/cm^2 que limita la efectividad de la aplicación de US. Cuando la intensidad ultrasónica superó dicho umbral, las difusividades efectivas del agua y de los solutos se incrementaron en un 117% y un 137%, respectivamente, en comparación con el tratamiento convencional. La existencia de este umbral de energía acústica también se observó en el salado de carne (salmuera saturada, 2 °C). En este caso, los valores de intensidad umbral se situaron por encima de 51 W/cm^2 y 39 W/cm^2, para el transporte de NaCl y agua, respectivamente (Cárcel et al., 2007b). Por lo tanto, a partir de los resultados obtenidos por dichos autores, puede observarse que el umbral mínimo de energía

acústica podría tener cierta relación con la estructura de la materia prima utilizada, siendo menores para productos porosos, como es el caso de la manzana, que para productos proteicos y de alta densidad, como lo es la carne.

En procesos de extracción asistidos por US, se ha observado que la cantidad de energía suministrada al medio influye de manera significativa en el rendimiento del proceso (Tao & Sun, 2013; Picó, 2013). Así, en algunos estudios se ha observado que al incrementar la potencia ultrasónica aplicada, los rendimientos en la extracción son mayores (Ahmad-Qasem et al., 2013; Zou et al., 2010; Ji et al., 2006). Sin embargo, otras investigaciones han demostrado que una vez superado un valor de potencia ultrasónica, el rendimiento de la extracción se mantiene constante y en algunos casos incluso disminuye (Lou et al., 2010; Zhao et al., 2007; Wei et al., 2008). Además, se ha observado que una elevada potencia acústica transmitida al solvente puede generar la extracción de compuestos no deseados y en algunos casos la descomposición química de los compuestos extraídos (Esclapez et al., 2011; Ying et al., 2011). Por lo tanto, habría una potencia acústica óptima en la que se alcanzarían un máximo en los efectos beneficiosos y un mínimo en los desfavorables.

Por otro lado, el nivel de potencia acústica también puede afectar la dirección del transporte de materia. Los niveles de intensidad acústica aplicados por Cárcel et al. (2007a) durante la deshidratación osmótica de manzana incrementaron los dos principales transportes de materia, ganancia de solutos y la pérdida de agua. Por el contrario, Cárcel et al. (2007b) durante el salado de carne con salmuera, observaron que las muestras tratadas con aplicación de intensidades acústicas más bajas (< 30 W/cm^2) experimentaron una deshidratación similar a los tratamientos realizados sin la aplicación de US, mientras que las muestras tratadas con intensidades más elevadas (> 64 W/cm^2) no sólo no se deshidrataron, si no que presentaron contenidos de agua superiores al de la carne fresca. Por lo tanto, a esas intensidades, se invirtió el sentido del transporte de agua.

Finalmente, la potencia acústica puede verse afectada por la presencia de turbulencias en el medio. Así, Cárcel (2003), al comparar la variación de presión acústica generada en un baño de US con y sin agitación en el medio, observó que la agitación produjo una importante disminución de la presión acústica en el sistema. Este autor concluyó que la presencia de turbulencias en el medio puede dificultar la transmisión de la onda

acústica, lo cual puede aumentar la atenuación en el medio y en consecuencia la disminución de la presión acústica.

Temperatura

El aumento de la temperatura es un factor que puede acelerar el transporte de materia en procesos alimentarios. Sin embargo, esta variable debe ser optimizada y controlada para una aplicación eficiente (Esclapez et al., 2011). En sistemas sólido-líquido, la temperatura puede tener una influencia sobre la efectividad de los US debido a que altas temperaturas puede disminuir la tensión superficial, lo que incrementa la presión de vapor, y en consecuencia disminuye la energía que se libera en el colapso de las burbujas de cavitación (Tao & Sun, 2013; Mason & Lorimer, 2002). En este sentido, Simal et al. (1998) en tratamientos osmóticos de manzana, observaron que tanto la ganancia de solutos como la pérdida de agua fueron mayores en las experiencias donde se aplicaron US, aunque las diferencias entre tratamientos disminuyeron a medida que aumentó la temperatura.

En procesos de extracción de compuestos naturales asistida por US, el efecto de la temperatura en los rendimientos de extracción parece estar ligada a la materia prima utilizada (Picó, 2013; Esclapez et al., 2011). En este sentido, en la extracción de compuestos fenólicos en hojas de olivo, Ahmad-Qasem et al. (2013) no encontraron una clara influencia de la temperatura en el rendimiento del proceso en el rango de temperaturas estudiado (25-50ºC). No obstante, estos autores observaron un ligero incremento de la actividad antioxidante a una temperatura de 45 °C. Zhang et al. (2009) mostraron que los rendimientos en la extracción de Epimedium C fueron mayores al incrementar la temperatura de 15 a 45 °C. Sin embargo, al superar los 45 °C, el rendimiento de la extracción disminuyó. Por el contrario, Zhang et al. (2011) afirmaron que las altas temperaturas (79 ºC) son las que favorecen la extracción de flavonoides totales en *Prunella vulgaris* L.

1.4.2. Sólido-gas

Una de las principales aplicaciones de los US en la intensificación de procesos en sistemas sólido-gas, es el secado. De acuerdo a la bibliografía previa, la eficacia de los US para acelerar los procesos de transferencia de materia en el secado depende en gran medida a las variables del proceso aplicadas tales como la **potencia acústica**, la

velocidad o la **temperatura** del aire de secado. A continuación se describe como dichas variables influyen en la efectividad de los US.

Potencia acústica

En el secado asistido por US, la potencia acústica presente en el medio influye en gran medida en la intensificación de los fenómenos de transporte. En diversos trabajos se ha observado que al incrementar los niveles de potencia acústica, las reducciones de tiempo de secado son mayores (Puig et al., 2012; Sabarez et al., 2012). Además, de igual forma que en sistemas sólido-líquido, se ha identificado que en algunas aplicaciones es necesario superar cierto umbral de energía para producir efectos en el transporte de materia. Así, García-Pérez et al. (2009) observaron que en un intervalo comprendido entre 0 y 37 kW/m^3 (energía eléctrica suministrada al transductor ultrasónico dividida por el volumen de la cámara de secado), los efectos asociados a la aplicación de US en el secado de zanahoria aparecieron a partir de un umbral de potencia aplicada situado en torno a 12 kW/m^3. Una vez superado este umbral, la difusividad efectiva del agua aumentó de forma proporcional con la potencia aplicada (Fig. 5A). Por el contrario, en el secado de piel de limón en las mismas condiciones, no se observó ningún umbral de potencia acústica y la proporcionalidad entre potencia y difusividad efectiva fue válida en todo el rango de potencia evaluado (Fig. 5B).

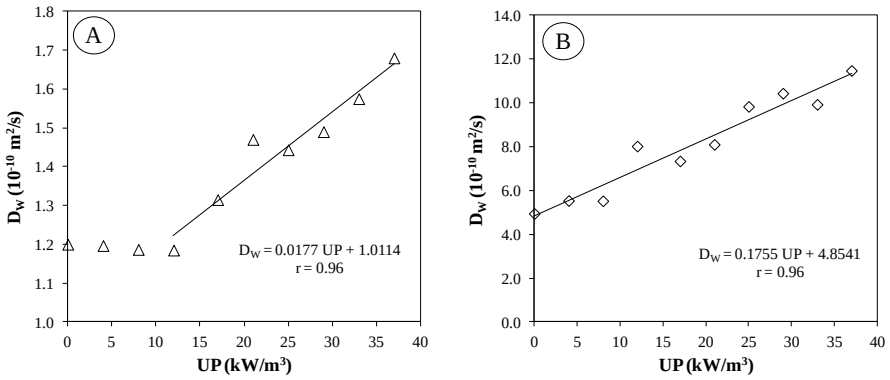

Fig. 5 Difusividades efectivas del agua (D_W) obtenidas para el secado (40 ºC, 1 m/s) de zanahoria (A) y piel de limón (B) con y sin aplicación de US a diferentes potencias acústicas (UP) (García-Pérez et al., 2009).

Por otro lado, es necesario recalcar que la energía acústica disponible en el medio puede verse afectada por la densidad de carga másica en la cámara de secado. Así, Cárcel et al. (2011) en el secado de zanahoria asistido por US, observaron que en densidades inferiores a los 90 kg/m^3, la difusividad efectiva y el coeficiente de transferencia de materia se incrementaron con la aplicación de US. Sin embargo, al superar esta densidad, las diferencias dejaron de ser estadísticamente significativas. Los autores, atribuyeron este hecho a la disminución de la cantidad de energía acústica que le llega a cada partícula debido al aumento de la masa presente en la cámara de secado.

Velocidad de aire

La influencia de la velocidad del aire en los efectos de los US en el secado ha sido otro de los parámetros estudiados debido a su importancia. Así, utilizando un sistema de aplicación de US de cilindro vibrante (Fig. 4), Cárcel et al. (2007c) evaluaron la influencia de la velocidad del aire (de 0.5 hasta 12 m/s) en la efectividad de los US durante el secado (40 ºC) de caqui. Estos autores observaron una reducción de la efectividad de los US en velocidades de aire superiores a 4 m/s. Por otro lado, Riera et al. (2011) midieron el efecto del incremento de la velocidad del aire sobre la presión acústica generada dentro del cilindro vibrante. Así, estos autores observaron una clara disminución de la presión acústica al aumentar la velocidad de secado, llegando a ser constante a partir de una velocidad de 8 m/s. Los autores concluyeron que el aumento de flujo de aire durante el proceso puede crear turbulencias en el medio que pueden disminuir la intensidad del campo acústico y, en consecuencia, la energía acústica disponible para intensificar los fenómenos de transporte de materia.

Por otro lado, utilizando los transductores de placa escalonada, también se han obtenido conclusiones similares. Así, Gallego-Juárez et al. (1999), observaron que la influencia de los US (20 kHz, 155 dB) durante el secado de zanahoria fue menos importante a 3 m/s que a 1.3 y 1.6 m/s. En el secado de surimi (40 ºC), Nakagawa et al. (1996) encontraron una clara influencia de los US (19.5 kHz, 155 dB) en todo el rango de velocidades de aire evaluado (1.6-2.8 m/s).

Temperatura

La temperatura es otra variable del proceso que puede afectar a la efectividad de los US durante el secado, tal y como observaron García-Pérez et al. (2006b) en el secado convectivo de zanahoria. Estos autores encontraron que la aplicación de US

incrementó de forma significativa ($p<0.05$) los valores de la difusividad efectiva y del coeficiente de transferencia de materia cuando se aplicaron temperaturas de secado comprendidas entre 30 y 50 ºC. Sin embargo, dicha influencia dejó de ser significativa para la temperatura de 60 ºC y resultó totalmente despreciable a 70 ºC. Rodríguez et al. (2013) obtuvieron que las temperaturas adecuadas para intensificar el secado de hojas de tomillo con US deben ser inferiores a 60 ºC. En este mismo sentido, Sabarez et al. (2012) utilizando transductores de placa escalonada sin contacto directo entre el emisor y el producto, observaron una reducción de la efectividad de los US al aumentar la temperatura de secado de 40 a 60 °C. Utilizando este mismo sistema, Gallego-Juárez et al. (1999) observaron que la influencia de los US en la pérdida de peso del producto durante el secado disminuyó a medida que la temperatura fue más elevada, desapareciendo al utilizar temperaturas superiores a 100 °C. Probablemente, cuando se aplican temperaturas elevadas, el nivel de energía térmica en el sistema sea suficiente para enmascarar los efectos de los US, que sí son significativos a temperaturas inferiores.

Considerando, entre otros factores, que la efectividad de los US se reduce a una temperatura elevada, su aplicación puede tener un gran potencial para intensificar los procesos de secado a baja temperatura. Uno de los primeros intentos para intensificar el proceso de secado a baja temperatura utilizando energía acústica fue realizado por Moy & DiMarco (1970). En este estudio, los autores utilizaron un sistema tipo silbato (10.8-12.2 kHz) para aplicar energía acústica durante el secado (-15 y -26 °C) de productos líquidos (agua, extractos de café y té). Los resultados obtenidos por estos autores mostraron un incremento en la velocidad de secado desde un 10% hasta un 100%. Sin embargo, el intenso ruido producido por el equipo, al trabajar a frecuencias audibles, podría ser el principal impedimento para implementar esta tecnología a nivel industrial. En los últimos años se han realizado más estudios para aplicar la energía acústica en el secado a baja temperatura mediante transductores comerciales. Bantle & Eikevik (2011) obtuvieron una máxima reducción de tiempo de hasta el 10% en el secado de guisantes (-3 ºC). De igual forma, Schössler et al. (2012c) aplicando US de manera intermitente durante un proceso de liofilización a vacio encontraron una reducción de hasta un 11.5% en el tiempo de secado de pimiento. Resultados más prometedores fueron obtenidos por García-Pérez et al. (2012a) en la aplicación de los US en el secado a baja temperatura. Así, utilizando un cilindro vibrante (Fig. 4), estos autores obtuvieron reducciones de tiempo de secado de hasta un 70% en el secado

convectivo (-14 ºC y 2 m/s) asistido por US (19.5 kW/m^3) de zanahoria, manzana y berenjena. La aplicación de US incrementó la difusividad efectiva del agua para estos productos entre un 407 y un 428% mientras que el coeficiente de transferencia de materia lo hizo entre 96 y 170%. Los estudios realizados hasta el momento actual en procesos de secado a baja temperatura pueden considerarse como preliminares, ya que simplemente se han centrado en mostrar el potencial de esta tecnología. Sin embargo, todavía existen muchos aspectos a esclarecer, como determinar la influencia de las variables del proceso y cómo los US influyen en la calidad del producto.

1.5. Interacción ultrasonidos-estructura del producto

La aplicación de US puede influir en la estructura del alimento y en consecuencia en su calidad final (Pingret et al., 2013). Para poder tener un mejor conocimiento de los efectos de los US, tanto en el transporte de materia como en la calidad del producto final, es importante conocer la interacción entre la energía acústica y la estructura del alimento (Jaeger et al., 2012; Lee & Feng, 2011). Así, en los siguientes apartados se abordará como el material tratado influye en la efectividad de los US y como estos afectan a la calidad final del alimento tanto en sistemas sólido-líquido como en sistemas sólido-gas.

1.5.1. Sólido-líquido

En base a los trabajos presentados por Simal et al. (1998), Sanchez et al. (1999) y Gisbert (2001) en deshidratación osmótica de manzana, salado de queso y carne, respectivamente, se puede establecer cierta influencia del material tratado en los efectos de los US (Mulet el al., 2003). Así, utilizado el mismo sistema de aplicación de US en todos estos casos, en la manzana, con una estructura porosa, la influencia de los US fue más evidente (Simal et al., 1998). En el caso del queso, cuyos poros se encuentran llenos de líquido, la influencia de los US disminuyó (Sanchez et al., 1999). Y por último, en el caso de la carne cuya estructura es fibrosa y no presenta poros, la influencia de los US, a los niveles de potencia acústica aplicados, resultó despreciable. De igual forma, Fernandes & Rodrigues (2008), estudiando la aplicación de US en un pretratamiento sólido-líquido (agua destilada y disoluciones osmóticas) previo al secado por aire caliente de diversas frutas, observaron que la efectividad de los US dependió en gran medida a la estructura inicial del producto. Por un lado, en tratamientos con agua destilada, el melón fue un producto muy sensible a los efectos de los US, observándose un aumento en la difusividad de los sólidos solubles de un

52.5%. Por el contrario, los efectos de los US disminuyeron en la papaya, donde los incrementos en el transporte de sólidos solubles fueron prácticamente despreciables (1.5%).

Por otro lado, la influencia de la aplicación de US en sistemas sólido-líquido en la estructura y en los parámetros de la calidad final del producto, tales como la **textura**, el **color** y el **contenido de nutrientes**, han sido ampliamente estudiados (Pingret et al., 2013; Lee & Feng, 2011). Así, Stojanovic & Silva (2007) observaron que la deshidratación osmótica asistida por US provocó cambios en el color de los arándanos deshidratados. Además, estas muestras presentaron una mayor pérdida de antocianinas y ácido ascórbico después de un tratamiento osmótico (180 min). De igual forma, se observó que el escaldado asistido por US provocó una mayor disminución del contenido de vitamina C (Gamboa-Santos et al., 2013), sólidos totales y azúcares solubles (Gamboa et al., 2012) en comparación con el tratamiento convencional. Esta pérdida de nutrientes durante la aplicación de US fue atribuida a la formación de microroturas en el tejido provocadas por la cavitación, lo cual facilitó la salida de estos compuestos (Rawson et al., 2011). De igual manera, Fernandes & Rodrigues (2008) observaron que el incremento en las difusividades efectivas (agua y solutos) producidas por la aplicación de US dependió en gran medida de los efectos mecánicos de las ondas acústicas sobre el material tratado, tales como las microroturas celulares y la formación de canales microscópicos en el tejido. De acuerdo a micrografías realizadas en melón, Fernandes & Rodrigues (2008) observaron la formación de una gran cantidad de canales microscópicos en el material, lo que contribuyó a un aumento en la difusividad de los sólidos solubles.

Por otro lado, la aplicación de US también puede producir cambios favorables en las propiedades organolépticas del producto. Es el caso de los estudios presentados por Sánchez et al. (2001a y 2001b), donde se observó que los quesos salados en presencia de US mostraron un sabor y un aroma más intenso que los salados de manera tradicional. Estos autores atribuyeron este cambio a un incremento del contenido de ácidos grasos y aminoácidos libres durante la maduración. Este incremento pudo ser consecuencia de la rotura de los glóbulos grasos y de la desnaturalización de las proteínas en presencia del campo acústico.

Respecto a los cambios texturales inducidos por la aplicación de US, en el salado de carne asistido por US, Siró et al. (2009) observaron un ablandamiento de la carne

tratada. Sin embargo, al incrementar la potencia acústica en el medio, la dureza del producto se incrementó, lo cual fue atribuido a una mayor desnaturalización de las proteínas. En el salado de pimiento, Gabaldón-Leyva et al., 2007 observaron que la aplicación de US produjo un ablandamiento del tejido durante los primeros 30 min del proceso, mientras que en el tratamiento convencional, el ablandamiento únicamente se observó a partir de los 120 min. Estos resultados fueron similares a los obtenidos por Deng & Zhao (2008), quienes también mostraron que la aplicación de US durante la deshidratación osmótica de manzana produjo productos más blandos. En ambos casos se asoció el ablandamiento con el aumento de la permeabilidad de las paredes celulares vegetales como consecuencia de los efectos asociados a la energía acústica (Lee & Feng, 2011).

1.5.2. Sólido-gas

Como se puede observar en el apartado anterior, existe un gran número de trabajos que han abordado el estudio de la interacción entre los US y la estructura del producto en sistemas sólido-líquido. Sin embargo, son pocas las referencias bibliográficas que han centrado sus estudios en aplicaciones sólido-gas.

En el secado por aire caliente se ha observado que la porosidad del material tiene una cierta influencia en la efectividad de los US durante el proceso. García-Pérez et al. (2007) analizaron la influencia de la velocidad del aire sobre las cinéticas de secado asistidas por US de zanahoria, caqui (productos con baja porosidad) y piel de limón (producto con alta porosidad). Los resultados mostraron que la aplicación de US aumentó la velocidad de secado de las muestras de zanahoria y caqui únicamente a bajas velocidades de aire (< 6 m/s). En el caso de la piel de limón, la influencia de los US fue apreciable en todo el rango de velocidades de aire (0.5-9 m/s). De igual forma, en el secado por contacto directo, Schössler et al. (2012a) observaron que la aplicación de US provocó una reducción en el tiempo de secado del 10.3% para el caso de la patata (producto con baja porosidad), mientras que en productos con mayor porosidad tales como la manzana y el pimiento, la reducción de tiempo llego a ser superior al 27% (Schössler et al., 2012b). En ambos trabajos, se puso en manifiesto que productos con alta porosidad pueden ser más sensibles a los ciclos de compresión-descompresión producidos por las ondas acústicas ("efecto esponja"). Además, los efectos de los US en las interfases gas-sólido de los productos porosos pueden ser más intensos al poseer una red interna de espacios intercelulares mayor.

Sin embargo, las conclusiones obtenidas en bibliografía son meramente cualitativas. Por lo tanto, es necesario profundizar en el estudio de la interacción ultrasonidos-estructura del producto y poder correlacionar otras propiedades del material con la efectividad de los US.

Respecto a los efectos de los US sobre la calidad del producto final, Soria et al. (2010) observaron que la aplicación de US en el secado de zanahoria previamente escaldada produjo ligeros cambios en las propiedades físico-químicas (contenido de azúcar, capacidad antioxidante y perfiles de proteína) y una mejora en las características del producto rehidratado. De igual forma, Frias et al. (2010) mostraron que el secado asistido por US de zanahoria produjo una mayor retención de vitamina C y beta caroteno respecto al secado convencional.

Por otro lado, se ha encontrado una clara influencia de los US en la estructura interna del producto final. Así, García-Pérez et al. (2012b) y Puig et al. (2012) observaron que el nivel de potencia acústica aplicada (45 y 90 W) en el secado de piel de naranja y berenjena, respectivamente, influyó en la intensidad de los efectos de los US sobre la estructura interna del producto. De acuerdo a las micrografías obtenidas por Cryo-SEM de piel de naranja secada con (90 W) y sin aplicación de US (Fig. 6), García-Pérez et al. (2012b) observaron que al incrementar la potencia ultrasónica, la degradación de la estructura interna del producto fue mayor. Así, en las muestras secadas con la máxima potencia ultrasónica (90 W), los poros que se encuentran en la piel de naranja se difuminaron totalmente (Fig. 6C), sin apreciarse el cerco céreo característico de los mismos (Fig. 6A, P). Este hecho fue atribuido a las microcorrientes que los US generan en la interfase. Además, estos autores también observaron que la aplicación de US incrementó la degradación de las células del albedo (Fig. 6F) en comparación con el secado convencional (Fig. 6E). El tejido presentó una estructura más destruida con restos celulares visibles y con grandes huecos. En este mismo sentido, Puig et al. (2012) observaron que el uso de una potencia ultrasónica moderada, 45 W, puede contribuir a una mejor preservación de la estructura interna de la berenjena, ya que se reduce el tiempo de secado y los efectos mecánicos de los US sobre el endocarpio son menores. Finalmente, Sabarez et al. (2012) observaron, tanto a 40 °C como a 60 °C, que una potencia ultrasónica de 75 W es la óptima para contribuir a preservar la estructura interna de la manzana.

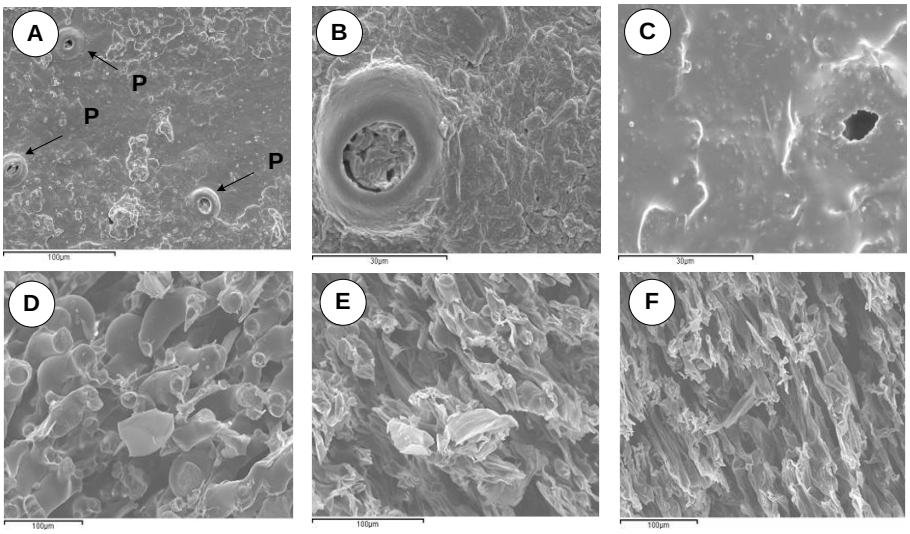

Fig. 6 Micrografías de piel de naranja obtenidas por Cryo-SEM. A) Superficie de la cutícula (x500; P: Poro), B) Detalle de poro secado con aire caliente (40 º C, 1 m/s, x2000), C) Detalle de poro secado con aire caliente y US (40 º C, 1 m/s, 90 W; x2000), D) Células de albedo (x 350), E) Células de albedo secadas por aire caliente (40 º C, 1 m/s, x350), F) Células de albedo secadas por aire caliente y con US (40 º C , 1 m/s, 90 W, x350) (García-Pérez et al., 2012b).

En el caso del secado a baja temperatura, la aplicación de US parece no tener un efecto significativo sobre la calidad del producto final. Schössler et al. (2012c) observaron que el proceso de liofilización asistida por US no afectó a los parámetros de calidad tales como la densidad aparente, el color, el contenido de ácido ascórbico y la capacidad de rehidratación del pimiento deshidratado. De igual forma, en el secado de guisantes, Bantle & Eikevik (2011) afirmaron que la aplicación de US no afectó al color del producto deshidratado. Sin embargo, en ambos trabajos se observó una escasa influencia de los US en el transporte de materia, con lo que cabe pensar que la potencia acústica real que recibieron las muestras no fue muy elevada.

Como puede observarse en este apartado, los trabajos que han analizado la influencia de los US sobre la calidad del producto final en el secado por aire caliente y a baja temperatura han centrado sus estudios en productos vegetales. Sin embargo, no se ha encontrado ninguna referencia bibliográfica que estudie el efecto de los US en matrices proteicas. Por tanto, resulta de gran interés profundizar en estudios que permitan conocer la interacción de los US en otro tipo de productos.

1.6. Conclusiones

Tal y como se desprende de la revisión bibliográfica, la aplicación de US tiene un gran potencial para intensificar procesos de transferencia de materia en sistemas sólido-líquido y en sistemas sólido-gas. Dicho potencial es atribuido a una serie de mecanismos inducidos por los US que pueden afectar, tanto a la resistencia interna como a la resistencia externa al transporte de materia. En sistemas sólido-líquido se puede encontrar un número importante de trabajos de investigación, probablemente debido a la existencia de sistemas de aplicación comerciales. Además, en los últimos años se han desarrollado sistemas ultrasónicos que permiten irradiar energía acústica de manera eficiente en medio gas, lo cual ha permitido grandes avances en el secado por aire caliente y, recientemente, en el secado a baja temperatura.

A pesar de las numerosas aplicaciones donde ha quedado probada la efectividad de los US para intensificar los procesos de transporte de materia, es necesario profundizar en estudios que permitan explicar la interacción que existe entre la efectividad de los US y las variables de procesos. En este sentido, resultaría de gran interés conocer como la estructura del producto tratado influye y es afectada por la aplicación de US.

2. Objetivos

El objetivo principal de la presente Tesis Doctoral consistió en evaluar la influencia de la aplicación de Ultrasonidos de Alta Intensidad (**US**) en sistemas sólido-líquido y sólido-gas en los fenómenos de transporte de materia y en la interacción ultrasonidos-estructura del producto. Para alcanzar este objetivo se establecieron los siguientes objetivos parciales:

1. Evaluar la influencia de la aplicación de US durante el salado de lomo de cerdo (*Longissimus dorsi*) en salmueras de diferente concentración en el transporte de materia, la microestructura y la textura de la carne tratada.
2. Determinar la influencia de la aplicación de US durante el desalado de bacalao (*Gadus morhua*) en el transporte de materia, la microestructura y textura del producto final.
3. Estudiar el secado de bacalao salado (*Gadus morhua*) a baja temperatura asistido por US. Determinar la influencia de la temperatura y la aplicación de US en el transporte de materia y propiedades físicas del producto deshidratado.
4. Evaluar la influencia de la aplicación de US en el secado por aire caliente de berenjena (*Solanum melongena* var. Black Enorma), patata (*Solanum tuberosum* var. Monalisa), yuca (*Manihot esculenta*) y manzana (*Malus domestica* var. Granny Smith) en función de la potencia acústica aplicada.
5. Analizar la influencia de la estructura, textura y propiedades acústicas de los productos en la eficiencia de aplicación de US durante el secado por aire caliente.

3.Metodología

3.1. Plan de trabajo

En base a los objetivos planteados en esta Tesis Doctoral, se elaboró el plan de trabajo que se muestra en la Fig. 1. La misma estructura que se muestra en dicha figura se ha utilizado para mostrar los resultados obtenidos y la discusión de los mismos organizando la información en **cuatro capítulos**.

El plan de trabajo se puede agrupar en dos apartados principales. El primero de ellos hace referencia a la aplicación de Ultrasonidos de Alta Intensidad (**US**) en sistemas **sólido-líquido**. Para ello, se estudió la influencia de US en el salado de carne (**Capítulo 1**) y en el proceso de desalado de bacalao (**Capítulo 2**). Así, se realizaron experiencias de salado (5±1 °C) de lomo de cerdo (*Longissimus dorsi*) en salmueras de diferente concentración (50, 100, 200, 240 y 280 kg NaCl/m^3) con (40 kHz; 37.5 kW/m^3) y sin la aplicación de US. Posteriormente, las cinéticas de transporte de agua y sal fueron modelizadas mediante la aplicación de modelos difusivos. También, se analizó la textura (análisis de punción) y la microestructura (Cryo-SEM y SEM) de la materia prima y de las muestras tratadas. Las experiencias de desalado (4±1 °C) de bacalao salado (*Gadus morhua*) se realizaron a diferentes potencias acústicas (0, 28 y 56 kW/m^3), determinando las cinéticas de transporte de agua y NaCl, así como la evolución de la dureza y el hinchamiento de las muestras durante el proceso de desalado. Se utilizaron dos tipos de técnicas para la caracterización del campo acústico del baño de US donde se realizaron los experimentos de desalado: la medida de la presión acústica mediante un hidrófono y un método calorimétrico basado en el registro del incremento de temperatura. Las cinéticas de transporte (agua y NaCl) fueron modelizadas con modelos difusivos, mientras que se utilizaron modelos empíricos para describir la evolución de la dureza y el hinchamiento de las muestras. Además, este estudio se complementó mediante un análisis microestructural (SEM y LM) de las muestras tratadas.

El segundo apartado del plan de trabajo hace referencia a la aplicación de US en sistemas **sólido-gas** (Fig. 1). Por un lado, se abordó el estudio de la aplicación de US en el secado a baja temperatura de bacalao salado (**Capítulo 3**). Por otro lado, se analizó la aplicación de US en el secado por aire caliente de diferentes vegetales (**Capítulo 4**).

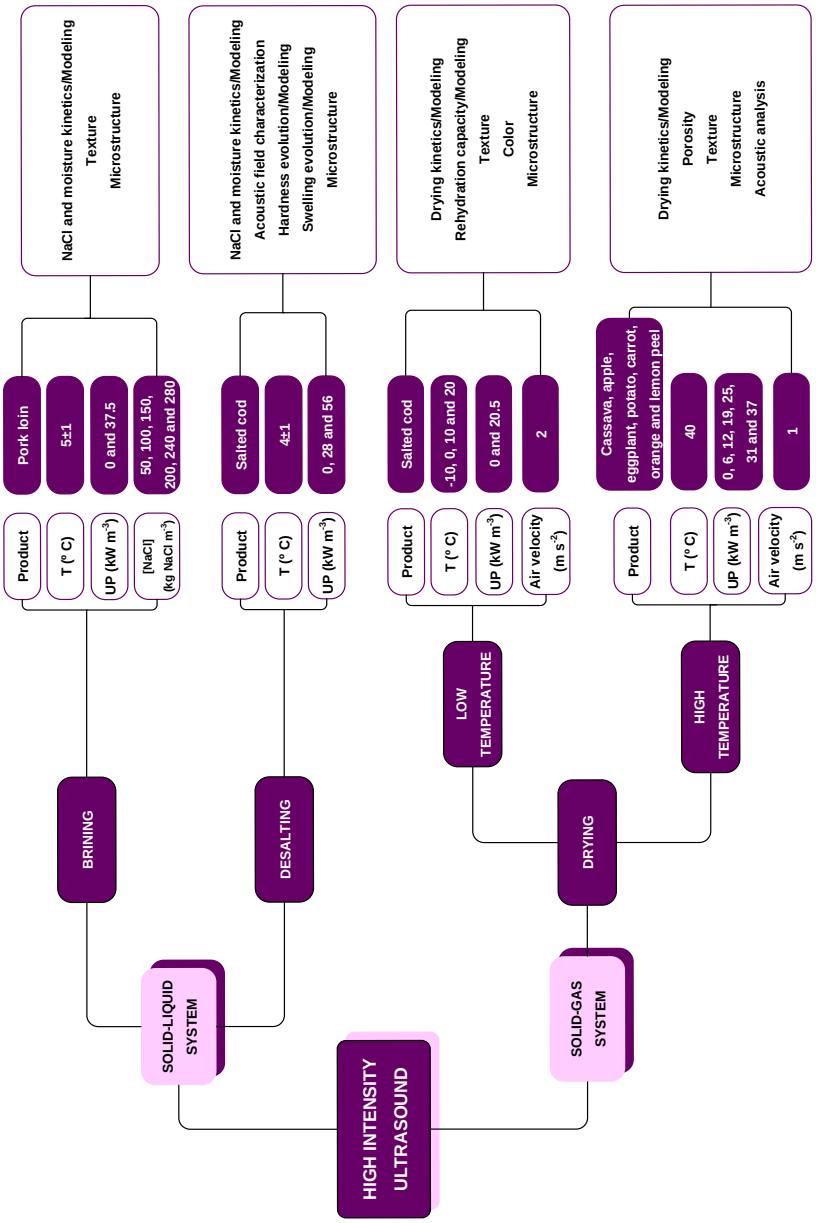

Fig. 1 Plan de trabajo (Working Plan).

Así, se realizaron experiencias de secado (2 ± 0.1 m/s) de bacalao salado (*Gadus morhua*) a diferentes temperaturas (-10, 0, 10 y 20 °C) con (20.5 kW/m^3) y sin la aplicación de US. Con la finalidad de evaluar las propiedades físicas del producto final, se realizaron determinaciones de la capacidad de rehidratación (4 °C, 27 h), color y análisis textural (punción) y microestructural (SEM) de las muestras tratadas. Las cinéticas de secado fueron modelizadas utilizando un modelo difusivo y las de rehidratación con un modelo empírico.

Respecto a la aplicación de US en el secado con aire caliente, se realizaron experiencias de secado (40 °C y 1 m/s) de berenjena (*Solanum melongena* var. Black Enorma), patata (*Solanum tuberosum* var. Monalisa), yuca (*Manihot esculenta*) y manzana (*Malus domestica* var. Granny Smith) a diferentes potencias acústicas (0, 6, 12, 19, 25 y 31 kW/m^3). Las cinéticas de secado fueron modelizadas utilizando modelos difusivos con diferente nivel de complejidad con el propósito de evaluar la influencia de la aplicación de US tanto en la resistencia interna a la transferencia de materia como en la externa. A partir de los resultados obtenidos (secado de berenjena, patata, manzana y yuca), y analizando también trabajos previamente publicados con productos tales como zanahoria (*Daucus carota* var. Nantesa), piel de naranja (*Citrus sinensis* var. Navelina) y piel limón (*Citrus limon* var. Fino), se estudió cómo la estructura del producto influye en la eficiencia de la aplicación de los US en el proceso de secado. Para ello, en todos los productos se determinó experimentalmente la porosidad, diversos parámetros texturales (análisis de TPA) como por ejemplo la dureza, la microestructura (Cryo-SEM) y las propiedades acústicas, tales como la velocidad ultrasónica, la impedancia acústica y el coeficiente de transmisión en la interfase.

En cada capítulo del apartado de **Resultados** de esta Tesis Doctoral se detalla la metodología específica de cada trabajo realizado, por tanto, en esta sección se procede únicamente a describir la materia prima, la preparación de las muestras y los montajes experimentales utilizados.

3.2. Materias primas

Para analizar la influencia de los US en las cinéticas de transporte de materia y en la estructura de los productos, tanto en sistemas sólido-líquido como en sólido-gas, se utilizaron diversas materias primas con estructura y composición muy diferente. Estos materiales pueden ser clasificados en dos grandes grupos: productos de **matrices proteicas** y productos de **matrices vegetales**. A continuación se hace una breve descripción de las materias primas utilizadas:

3.2.1. Matrices proteicas

Lomo de cerdo

La materia prima utilizada para la realización de las experiencias de salado de carne asistido con US fue el músculo *Longissimus dorsi* procedente de cerdos de raza (Large White x Landrace) x Pietrain (Fig. 2A). Este músculo forma parte del corte comercial conocido como lomo cinta. Su situación anatómica corresponde al espacio existente entre las apófisis espinosas y transversas de las vértebras dorsolumbares. Dispuesto longitudinalmente y adosado a la columna vertebral, se extiende desde la región cervical hasta la iniciación del sacro. Las fibras musculares que constituyen la cinta de lomo son de textura blanda, sobre todo el músculo ileoespinal, base anatómica de la pieza (Cárcel, 2003). La composición del *Longissimus dorsi*, se muestra en la Tabla 1.

Bacalao salado

El bacalao salado (*Gadus morhua*) es un producto altamente apreciado en del sur de Europa y América Latina. Durante su procesado, el pescado se eviscera, se descabeza y escinde longitudinalmente dejando la espina central adherida a uno de los laterales del pescado y posteriormente, es lavado y salado. La sal contenida en el bacalao oscila desde el 4% correspondiente a un producto ligeramente salado hasta el 20% que se encuentra en el producto intensamente salado durante unos 21 días (Oliveira et al., 2012). El proceso de salado conserva el bacalao y además, concentra sus nutrientes (Tabla 2).

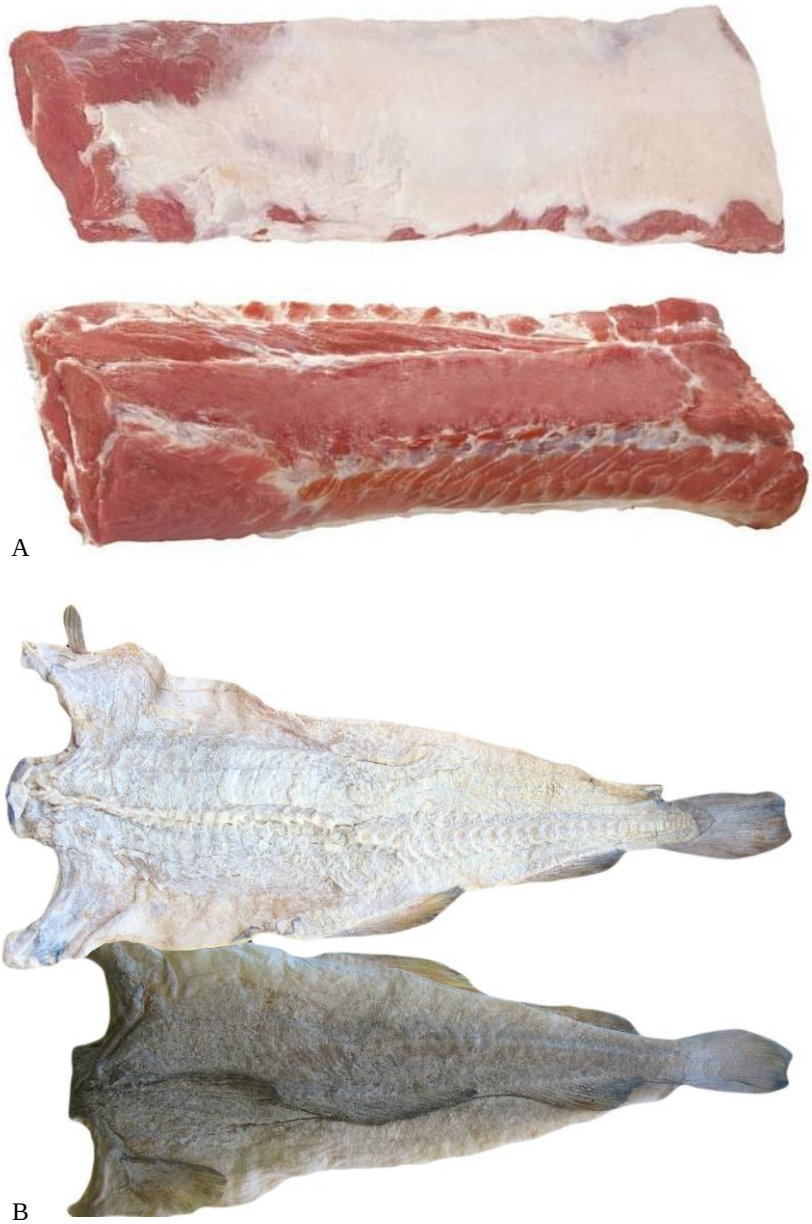

Fig. 2 Matrices proteicas. A) Lomo de cerdo, B) Bacalao salado.

Tabla 1 Composición (en 100 g) de lomo de cerdo (USDA, 2013).

Componente	Valor	Unidades
Agua	72.23	g
Proteína	21.43	g
Lípidos	5.66	g
Minerales		
Calcio	17	mg
Hierro	0.84	mg
Magnesio	23	mg
Fósforo	211	mg
Potasio	389	mg
Sodio	52	mg
Zinc	1.84	mg
Vitaminas		
A	7	IU
D	22	IU
C	0.6	mg
Tiamina	0.989	mg
Riboflavina	0.267	mg
Niacina	4.915	mg
B_6	0.527	mg
Lípidos		
Ác. grasos saturados	1.950	g
Ác. grasos insaturados	2.560	g
Ác. grasos poliinsaturados	0.610	g
Colesterol	59	mg

IU: Unidad internacional.

Para las experiencias de desalado y secado de bacalao asistido con US se empleó como materia prima bacalao salado (Fig. 2 B). Los bacalaos salados utilizados en este trabajo fueron suministrados por una empresa local (CARMEN CAMBRA S.L., España). De acuerdo a las especificaciones de la empresa, los bacalaos fueron capturados en altamar y procesados inmediatamente. Todos los bacalaos suministrados presentaron un peso aproximado de 1.5±0.25 kg.

Tabla 2 Composición (en 100 g) de bacalao fresco y salado (Rodríguez-Barona, 2003).

Componente	Bacalao fresco	Bacalao salado
Proteínas (g)	17	62
Grasa (mg)	0.3	1.4
Calcio (mg)	20	160
Fósforo (mg)	200	950
Hierro (mg)	0.6	2.5
Yodo (mg)	0.5	-
Vitaminas (μg)		
A	-	15
Tiamina	50	-
Riboflavina	110	240
Ác. Pantoténico	50	-
B_{12}	0.8	10

3.2.2. Matrices vegetales

Dentro de este apartado, dado que se pretendía evaluar la relación entre la estructura inicial del producto y la efectividad de los US durante el secado convectivo, se engloban diversas frutas y vegetales con estructuras muy diferentes (Fig. 3).

Yuca

Una de las materias primas empleadas para las experiencias de secado por aire caliente asistido por US fueron raíces de yuca (*Manihot esculenta*) (Fig. 3A). La yuca se caracteriza por su forma cilíndrica y su corteza dura, leñosa e incomestible. La pulpa es firme y muy compacta, surcada por fibras longitudinales más rígidas. Se compone principalmente de agua y carbohidratos y es un alimento altamente energético, cuyos carbohidratos son fácilmente asimilables. Posee ciertos polisacáridos no amiláceos como celulosa, pectinas y hemicelulosas así como otras proteínas y ligninas estructurales asociadas que se denominan fibra alimentaria (Cunha-Alves, 2002). La composición general de esta raíz se muestra en la Tabla 3.

Las raíces de yuca utilizadas para las experiencias de secado se adquirieron en un mercado local. Se verificó que las unidades estuvieran enteras, sanas (libres de podredumbres y otros defectos), fueran de consistencia dura y no presentaran ningún olor extraño. Las yucas se mantuvieron en refrigeración a 4±0.5 °C un máximo de 5 días hasta el momento de la realización de las experiencias.

Manzana

En las experiencias de secado se utilizó manzana de la variedad Granny Smith (Fig. 3B). Esta manzana se caracteriza por su color verde intenso y uniforme, con numerosas lenticelas de color blanquecino (Agustí, 2010). La pulpa destaca por su marcada acidez (8-8.5 g de ácido málico por litro de zumo) y su textura firme y compacta. La composición general de esta fruta se muestra en la Tabla 3.

Las manzanas fueron adquiridas en un mercado local y se seleccionaron de manera que todas presentasen una coloración y un tamaño similar. La concentración de sólidos solubles se situó en todos los casos dentro del rango 10.5-12 °Brix. Las manzanas se mantuvieron en refrigeración a 4±0.5 °C un máximo de cinco días hasta el momento de realización de las experiencias.

Berenjena

Para las experiencias de secado se utilizaron berenjenas (*Solanum melongena*) de la variedad Black Enorma (Fig. 3C). Esta variedad se caracteriza por su forma alargada y su piel lisa de color morado muy intenso y brillante. La pulpa blanca, de textura esponjosa, tiene cierto sabor amargo, presenta pequeñas semillas planas y blandas de color amarillo. El valor energético y nutritivo de la berenjena es pequeño comparado con otros frutos, verduras y hortalizas como puede apreciarse en la Tabla 3. Contiene escasas vitaminas, proteínas y minerales, siendo el componente mayoritario el agua.

Las berenjenas fueron adquiridas en un mercado local y se seleccionaron de manera que presentasen un tamaño y color similar. Posteriormente, fueron almacenadas en refrigeración (4±0.5 °C) un máximo de cinco días hasta el momento de la realización de las experiencias de secado.

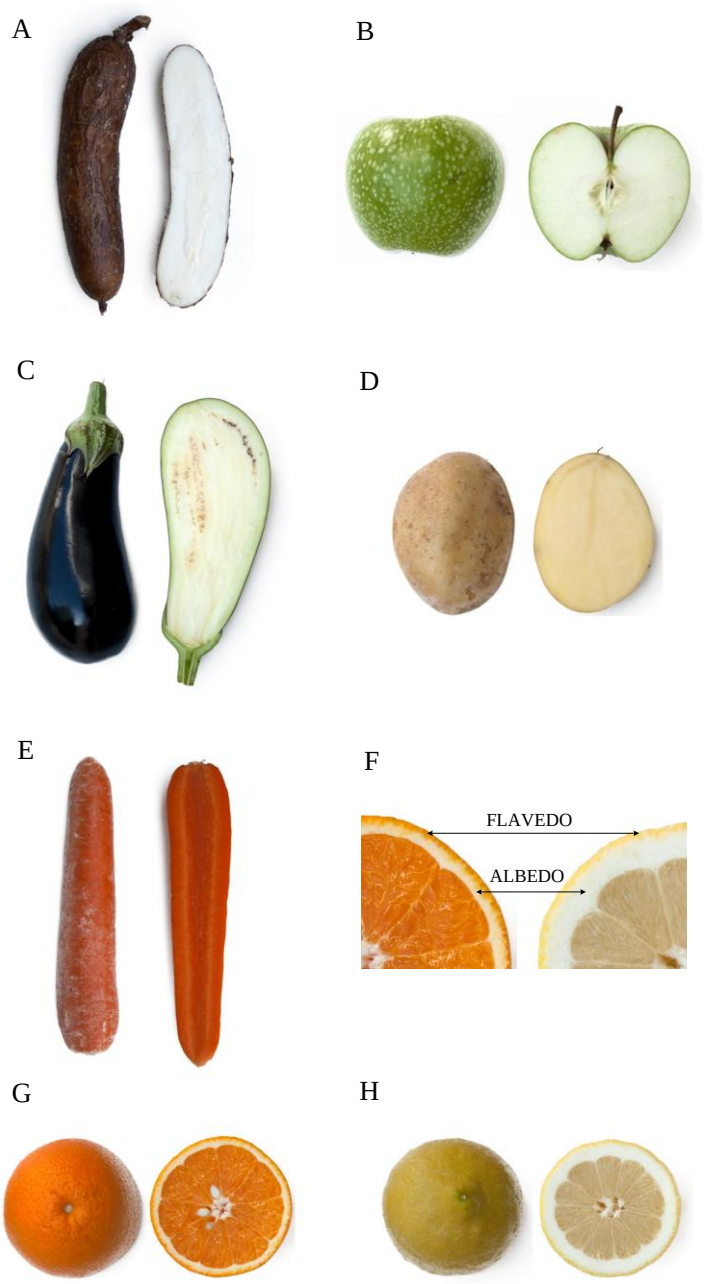

Fig. 3 Matrices vegetales. A) Yuca, B) Manzana, C) Berenjena, D) Patata, E) Zanahoria, F) Tejidos de la piel de cítricos, G) Naranja, H) Limón.

Tabla 3 Composición (en 100 g) de diferente frutas y vegetales (USDA, 2013).

Componente	Yuca	Manzana	Berenjena	Patata	Piel de naranja	Piel de limón	Zanahoria
Agua (g)	59.68	85.56	92.30	79.34	72.50	81.60	88.29
Proteína (g)	1.36	0.26	0.98	2.02	1.50	1.50	0.93
Grasa (g)	0.28	0.17	0.18	0.09	0.20	0.30	0.24
Carbohidratos (g)	38.06	13.81	5.88	17.47	25	16	9.58
Fibra (g)	1.8	2.4	3	2.2	10.6	10.6	2.8
Azúcares totales (g)	1.7	10.39	3.53	0.78		4.17	4.74
Minerales (mg)							
Calcio	16	6	9	12	161	134	33
Hierro	0.27	0.12	0.23	0.78	0.8	0.8	0.30
Magnesio	21	5	14	23	22	15	12
Fósforo	27	11	24	57	21	12	35
Potasio	271	107	229	421	212	160	320
Sodio	14	1	2	6	3	6	69
Zinc	0.34	0.04	0.16	0.29	0.25	0.25	0.24
Vitaminas *(mg)							
A (IU)	13	54	23	2	420	50	16706
C*	20.6	4.6	2.2	19.7	136	129	5.9
Tiamina*	0.087	0.017	0.039	0.080	0.120	0.06	0.066
Riboflavina*	0.048	0.026	0.037	0.032	0.090	0.08	0.058
Niacina*	0.854	0.091	0.649	1.054	0.9	0.4	0.983
B_6*	0.088	0.041	0.084	0.295	0.176	0.172	0.138
E*	0.19	0.18	0.30	0.01	0.25	0.25	0.66

Patata

En términos generales, la patata es un alimento rico en hidratos de carbono, contiene un alto porcentaje de agua, su materia seca está constituida por almidones, azúcares y proteínas y, además, contiene sustancias minerales tales como el potasio y el magnesio (Tabla 3). Las experiencias de secado se realizaron con patatas de la variedad Monalisa (Fig. 3D). Esta variedad es de una gran calidad caracterizada especialmente por su forma ovalada. Tanto su piel como su carne son de un color amarillento claro.

Las patatas utilizadas en este trabajo fueron adquiridas en un mercado local y se seleccionaron de manera que presentasen un tamaño y color uniforme. Las patatas se mantuvieron en refrigeración a 4±0.5 °C un máximo de 5 días hasta el momento de la realización de las experiencias.

Zanahoria

En este trabajo se utilizaron zanahorias de la variedad Nantesa (Fig. 3E). Esta variedad se caracteriza por presentar una raíz de 15 a 18 cm de longitud y de 2.5 a 5 cm de diámetro, de forma cilíndrica, con extremo redondeado y sin corazón. El tejido de la zanahoria, es fundamentalmente parénquima con poco o nulo tejido lignificado y las paredes celulares son ricas en polisacáridos pécticos (Ravigione, 2002). Desde el punto de vista nutritivo, la zanahoria es una excelente fuente de vitaminas y minerales (Tabla 3).

Las zanahorias utilizadas en este trabajo se adquirieron en un mercado local. Se verificó que las piezas estuvieran enteras, presentasen una coloración similar y fueran de consistencia dura. Las zanahorias se mantuvieron en refrigeración a 4±0.5 °C un máximo de 5 días hasta el momento de la realización de las experiencias

Piel de naranja y limón

En general, la naranja y el limón están formados por un ovario simple de 8-10 carpelos soldados (segmentos) rodeados por una corteza o piel resistente. Su forma variable desde esférica a esférico-aplanada u oval. La pulpa está formada por vesículas, que contienen el zumo, unidas por un filamento vascular a las paredes de los segmentos. La piel contiene numerosas glándulas de aceites esenciales y su color varía de amarillo-verdoso a naranja más o menos rojizo (Agustí, 2010). En la piel de la naranja y el limón se puede diferenciar tres tejidos diferentes (Fig. 3F):

- *Cutícula externa*: Constituye una capa cérea que actúa de protección para el fruto y está formada por ceras, cutina y otros lípidos.
- *Flavedo*: Compuesto por células poligonales e isodiamétricas sin espacios intercelulares. Sus componentes son pigmentos, glucósidos, vitaminas y aceites esenciales.
- *Albedo*: Tejido de color blanco constituido por células de forma irregular en tamaño y forma estructuradas en capas esponjosas con grandes espacios intercelulares. Está compuesto principalmente por hemicelulosa y pectinas.

Las naranjas utilizadas en este trabajo fueron de la variedad Navelina (Fig. 3G). En cuanto a los limones, se utilizó la variedad Fino (Fig. 3H). Ambos tipos de frutos se adquirieron en un mercado local seleccionando aquellas que presentaron un estado de madurez avanzada, y se mantuvieron en refrigeración (4±0.5 ºC) un máximo de 5 días hasta el momento de la realización de las experiencias. La materia prima utilizada en las experiencias fue la piel de ambos cítricos, ya que representa un subproducto de la industria de los zumos con alto contenido nutricional (Tabla 3).

3.3. Preparación de la materia prima

En la Fig. 4 se esquematiza la forma y las dimensiones de las muestras obtenidas a partir de la materia prima y que fueron utilizadas en las experiencias realizadas tanto en sistemas sólido-líquido como en sistemas sólido-gas. Como puede observarse, se obtuvieron muestras con geometrías simples para facilitar la posterior modelización de los fenómenos de transporte.

En la Fig. 4, se incluye también el tamaño de muestra utilizada para caracterizar las propiedades de interés de los productos como: textura, microestructura, color y propiedades acústicas. Cabe destacar que en cada uno de los cuatro apartados de la sección de **Resultados** se describe con mayor profundidad la manera en que se obtuvieron las muestras para las experiencias y el procedimiento que se llevó a cabo para los análisis de textura, microestructura, color y las medidas de las propiedades acústica realizados en cada caso específico.

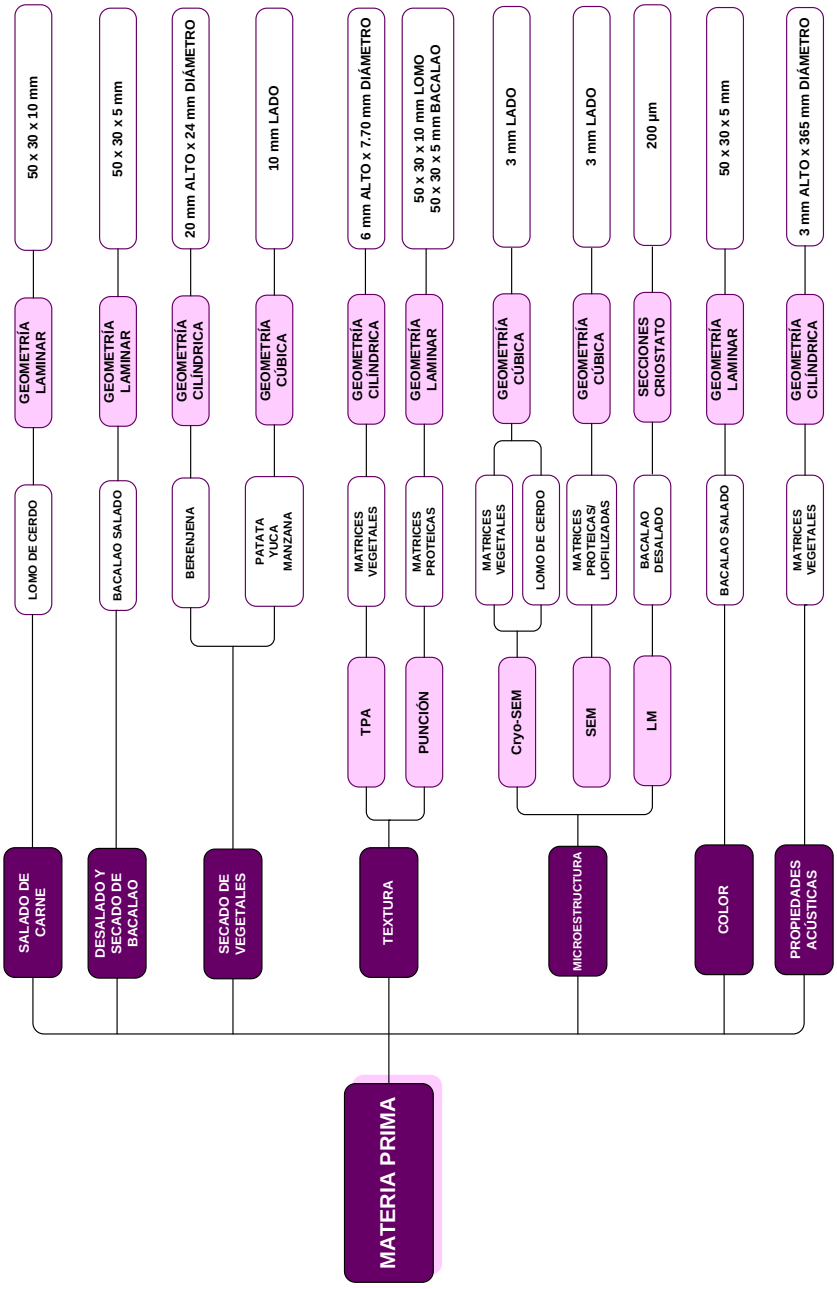

Fig. 4 Preparación de la material prima.

3.4. Montajes experimentales

Como se ha comentado, en la presente **Tesis Doctoral** se estudió la aplicación de US en sistemas **sólido-líquido** y **sólido-gas**. A continuación se describen los montajes experimentales utilizados en ambos casos.

3.4.1. Sistemas sólido-líquido

Para el estudio de la aplicación de US en sistemas sólido-líquido (salado y desalado) se utilizaron dos montajes diferentes. En ambos casos, se utilizaron baños ultrasónicos comerciales.

Salado de carne

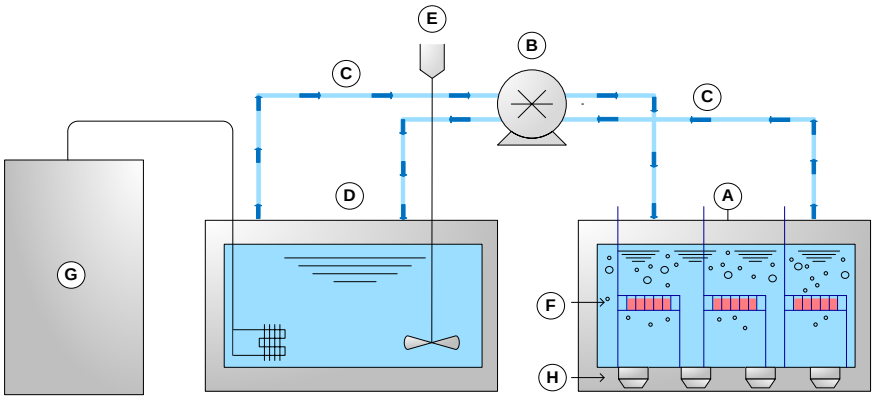

Fig. 5 Esquema del dispositivo US de salado. A) Baño de ultrasonidos, B) Bomba peristáltica, C) Conducción de salmuera, D) Depósito pulmón de salmuera, E) Sistema de agitación, F) Sistemas portamuestras, G) Unidad enfriadora, H) Transductores.

El montaje utilizado para realizar las experiencias de salado asistido con US se muestra en la Fig. 5. Los experiencias de salado de carne con y sin aplicación de US se realizaron a una temperatura de 5±1 °C con un baño de US (40 kHz; 37.5 kW/m^3, Selecta S. A., España) (Fig. 5A) con capacidad de 4 L. El control de temperatura se consiguió mediante la recirculación de salmuera desde un depósito pulmón (Fig. 5D) equipado con un equipo de refrigeración (3000778, J. P. Selecta S.A., España) (Fig. 5G) y un agitador portátil Heidolph (modelo RZR1, Heidolph Instruments GMBH & Co., Alemania) (Fig. 5E). Dicha recirculación se realizó con una bomba peristáltica Watson/Marlow (302S, Watson-Marlow Limited, Reino Unido) (Fig. 5B) que suministró un flujo de salmuera fría (Fig. 5C) suficiente para mantener la

temperatura del baño a 5±1 °C pero no tan grande como para perturbar el campo ultrasónico, lo cual se constató a partir de experiencias previas. Las muestras se colocaron en sistemas portamuestras (Fig. 5F) que permitieron mantenerlas en posiciones fijas durante el salado.

Desalado de bacalao

El montaje experimental utilizado para el proceso de desalado de bacalao asistido por US se esquematiza en la Fig. 6. El montaje consta de un baño de US de 72 L de capacidad máxima provisto de una camisa para refrigeración (40 kHz; 1500 W, ATU Ultrasonidos, España) (Fig. 6F). El control de la temperatura (4±1 °C) se realiza mediante la recirculación de agua glicolada que a su vez es enfriada en un intercambiador de placas (Fig. 6C) conectado a un equipo de refrigeración (KAE evo-121, MTA, Italia) (Fig. 6A). La disolución de agua glicolada se impulsa desde un sistema pulmón hacia la camisa de refrigeración del baño mediante una bomba (1-38023 CLES, EBARA, Italia) (Fig. 6D). El registro de temperatura se realizó mediante 7 sondas termopar tipo K (Fig. 6H) conectadas a un equipo de adquisición de datos (34970 A, Hewlett-Packard S.A., España) (Fig. 6K). A su vez, el equipo de adquisición de datos se conectó a un PC (Fig. 6M) provisto de un software, que permitió almacenar los datos de tiempo y temperatura durante las diferentes experiencias.

3.4.2. Sistemas sólido-gas

En los siguientes apartados se describen los equipos utilizados para la realización de las experiencias de secado asistido por US.

Secado a baja temperatura

Las experiencias de secado de bacalao salado se llevaron a cabo en un secadero convectivo asistido por US con capacidad para trabajar a bajas temperaturas (hasta -14 °C). Este secadero ha sido descrito originalmente por García-Pérez et al. (2012a). Se trata de un sistema con recirculación de aire a baja temperatura previamente enfriado por su paso por un intercambiador de tubos por donde circula agua glicolada (-22 °C). El sistema está totalmente automatizado y realiza pesadas de la muestra a tiempos prefijados por el usuario. En la Fig. 7 se muestra un diagrama del equipo, y sus principales componentes se detallan a continuación.

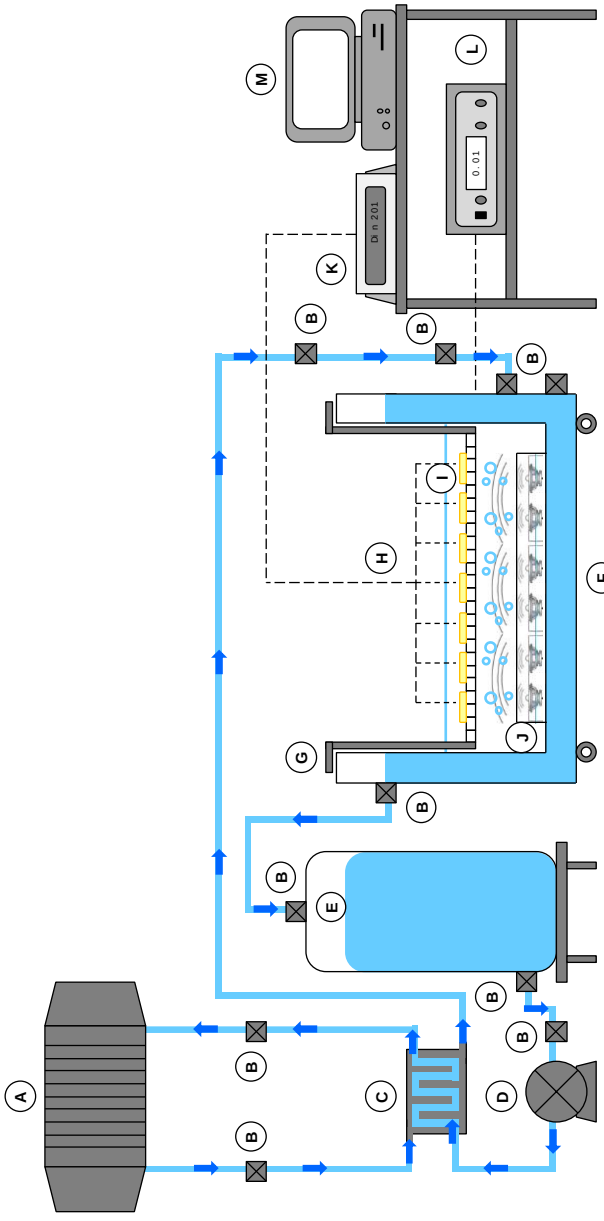

Fig. 6 Esquema del dispositivo de desalado. A) Equipo de refrigeración, B) Válvula, C) Intercambiador de placas, D) Bomba, E) Depósito pulmón, F) Baño de ultrasonidos, G) Sistema portamuestra, H) Sondas de temperatura, I) Muestras de bacalao, J) Transductores, K) Equipo de adquisición de datos de temperatura, L) Generador de ultrasonidos, M) PC.

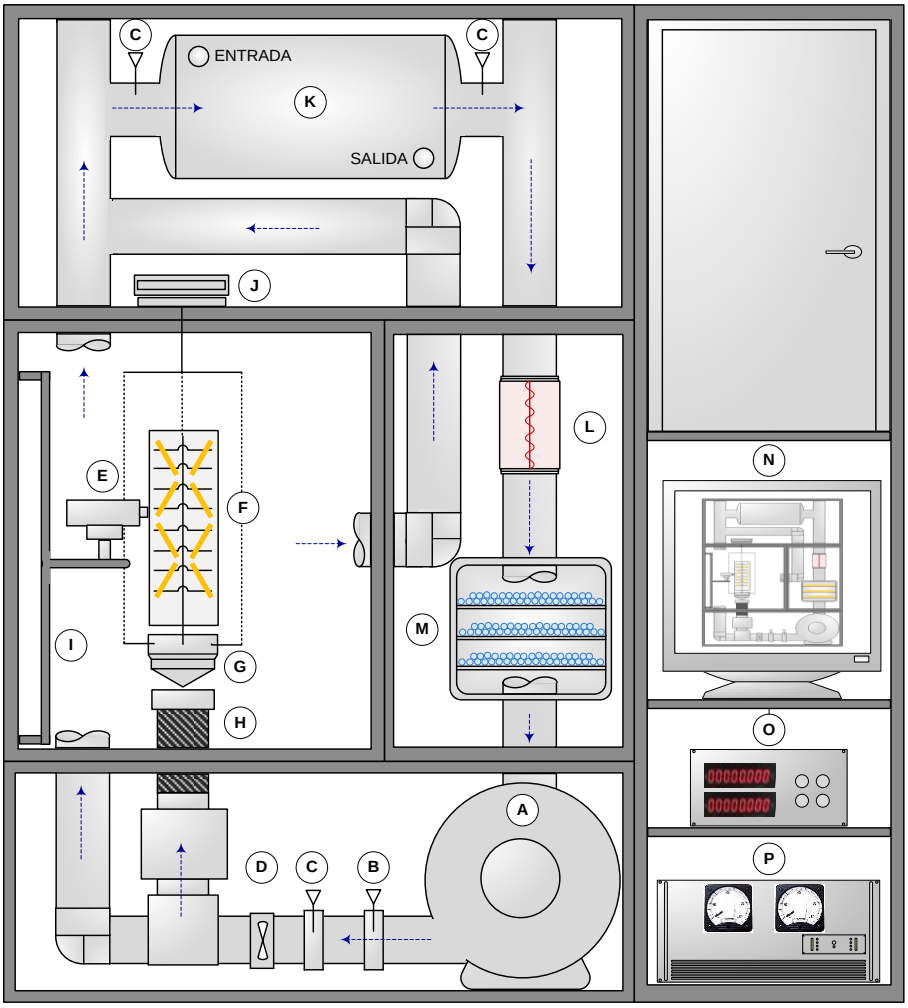

Fig. 7 Diagrama del secadero de baja temperatura asistido por ultrasonidos de alta intensidad. A) Soplante, B) Pt-100, C) Sensores de temperatura y humedad relativa, D) Anemómetro, E) Transductor ultrasónico, F) Cilindro vibrante, G) Dispositivo de carga de la muestra, H) Conducción retráctil, I) Brazo eléctrico de deslizamiento, J) Módulo de pesada, K) Intercambiador de calor, L) Resistencias eléctricas, M) Cámara de bandejas de material desecante, N) PC, O) Amplificador, P) Controlador dinámico de resonancia.

- **Sistema de ventilación**

El sistema de ventilación está compuesto por un soplante centrífugo de media presión (COT-100, Soler & Palau, España) (Fig. 7A). La velocidad del aire es medida mediante un anemómetro de rueda alada con una precisión de ±0.1 m/s (Wilh. Lambrecht GmbH, Alemania) (Fig. 7D). Para el control de la velocidad del aire, se utiliza un algoritmo PID que actúa sobre un variador de frecuencia (MX2, Omron, Japón) regulándose de esta manera la velocidad de giro del soplante.

- **Sistema de control de temperatura y humedad relativa**

El secadero cuenta con un intercambiador de calor de carcasa y tubos de cobre (área 13 m², espacio de aleta 9 mm; Frimetal, España) (Fig. 7K) por donde circula una solución de agua-glicol (45%, v/v, -22 °C, 150 L/min) proveniente de un equipo de refrigeración (KAE evo-121, MTA, Italia) localizado fuera del secadero.

La temperatura del aire de secado y su humedad relativa son medidas mediante sensores combinados de temperatura (±0.5 °C) y humedad relativa (±2.5%) (KDK, Galltec+Mela, Alemania) (Fig. 7C), tanto a la entrada de la cámara de secado como a la entrada y a la salida del intercambiador de calor. El control de la temperatura del aire de secado (de 60 a -15 °C) se realiza mediante un algoritmo PID que actúa sobre unas resistencias eléctricas (potencia máxima 2500 W, 230 V). El control de velocidad y temperatura del aire se realiza a través de un Compact FieldPoint (cFP-2220, National Instruments, EE.UU) donde están conectados todos los sensores y actuadores.

Para controlar la humedad relativa, el flujo de aire es forzado a atravesar tres bandejas que contienen gel de sílice (Fig. 7M). Estas bandejas son periódicamente retiradas del equipo para reponer el gel de sílice agotado, el cual se regenera en una estufa de aire caliente (250 °C). De esta manera, la humedad relativa del aire de secado se mantiene comprendida entre un 5 y un 20%.

- **Cámara de secado ultrasónica y sistema de pesada**

La cámara de secado (Fig. 7F) está constituida por un cilindro de aluminio de 100 mm de diámetro externo, 10 mm de espesor y una longitud de 310 mm. Este cilindro es excitado por un transductor de tipo sándwich (frecuencia 21.7 kHz, impedancia 369 Ω, capacidad de potencia 90 W). De esta manera, la propia

cámara de secado puede generar un campo acústico en su interior (Fig. 8) donde están colocadas las muestras.

Un controlador dinámico de resonancia (APG-AC01, Pusonics, España) (Fig. 7P) se encarga de generar y ajustar la señal eléctrica a la frecuencia de trabajo. La capacidad de potencia se fija mediante un amplificador de potencia (RMX 4050HD, QSC, EE.UU). Finalmente, un adaptador de impedancias (APG-AC01 Punsonics) permite la optimización eléctrica del sistema adaptando la impedancia de salida del generador a la del sistema de aplicación ultrasónico. Este adaptador consta de un transformador con una impedancia de 50 a 500 Ω, además de una inductancia con salida variable entre 5 y 9 mH. El sistema ultrasónico es capaz de generar un campo de alta intensidad ultrasónica en el medio (aire) alcanzando un nivel de presión acústica de 155 dB sin flujo de aire. El controlador dinámico de resonancia está conectado a un PC mediante una interfase RS-232 que monitoriza los principales parámetros eléctricos de la señal ultrasónica (potencia, intensidad, voltaje, fase, frecuencia e impedancia).

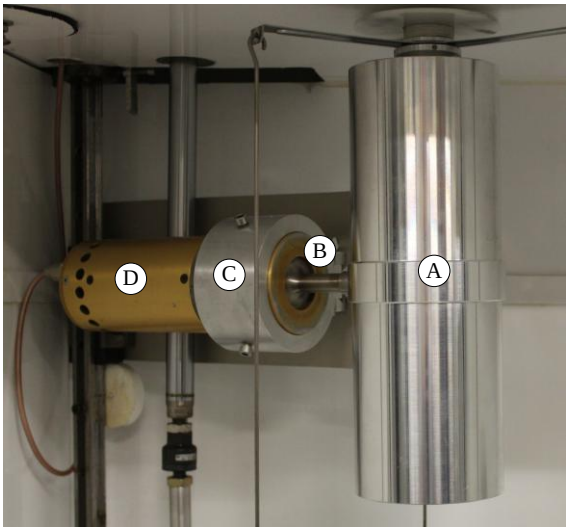

Fig. 8 Detalle del montaje del sistema ultrasónico de alta intensidad en el secadero convectivo a baja temperatura. A) Cilindro vibrante, B) Amplificador mecánico, C) Brida de anclaje, D) Transductor ultrasónico tipo sándwich.

Las muestras a secar se colocan en un sistema portamuestras que las mantiene en posiciones fijas durante la realización de las experiencias (Fig. 7G). Para determinar las

cinéticas de secado, el portamuestra se pesa de forma periódica mediante un módulo de pesada industrial (6000±0.01 g; VM6002-W22, Mettler Toledo, EE.UU) (Fig. 7J), el cual está conectado al sistema Compact FieldPoint mediante una interfase RS-422. En cada pesada, y para mantener la estabilidad de la balanza, se detiene el giro del soplante.

- **Sistema de control y adquisición de datos**

Una aplicación informática desarrollada en el lenguaje de programación de LABVIEW™ 2009 se utiliza como interfaz para el control de las experiencias de secado integrando la información sobre el flujo de aire, la temperatura, la evolución del peso de las muestras durante el secado, la humedad relativa del sistema y los parámetros ultrasónicos. La aplicación puede funcionar indistintamente ya sea en el PC (Fig. 7N) o el sistema Compact FieldPoint.

Secado por aire caliente

Para la realización de las experiencias de secado de berenjena, patata, manzana y yuca se utilizó un secadero de aire caliente asistido por US (García-Pérez, 2007). Se trata de un secadero convectivo de flujo vertical y horizontal totalmente automatizado que realiza pesadas de la muestra a tiempos prefijados por el usuario. Dispone de un control de velocidad y la temperatura del aire de secado. En la Fig. 9 se muestra un diagrama del equipo y a continuación se detallan sus principales componentes:

- **Sistema de ventilación**

El sistema de ventilación está compuesto por un soplante centrífugo de media presión (COT-100, Soler & Palau, España) (Fig. 9A) que impulsa el aire hacia el lecho de muestra. La velocidad del aire se controla por medio de un PC (Fig. 9M) que actúa sobre un variador de frecuencia (Inverter DV-551, Panasonic, EE.UU). La velocidad del aire es medida mediante un anemómetro de rueda alada con una precisión de ±0.1 m/s (Wilh. Lambrecht GmbH, Alemania) (Fig. 9C), el cual está conectado a un instrumento indicador/convertidor (TTM-104, EE.UU) que digitaliza el valor de la velocidad del aire.

- **Sistema de control de temperatura y humedad relativa**

El secadero dispone de resistencias para el calentamiento del aire de secado (Fig. 9B), colocadas después del soplante y antes de la cámara de secado. El sistema presenta

una potencia total de 3000 W a 220 V. La temperatura del aire se mide con un sensor Pt-100 que está conectado a un instrumento indicador/convertidor (TM-109, TOHO, Japón) para la digitalización del valor medido. El control de temperatura se realiza con un PC mediante un algoritmo PID que actúa sobre un variador de intensidad (80 A, Nixa, España).

La temperatura y humedad relativa ambiental son registradas utilizando un sensor de parámetros ambientales (TG 80, Galltec+mela, Alemania) conectado a sendos instrumentos indicadores/convertidores (TM-109, TOHO, Japón).

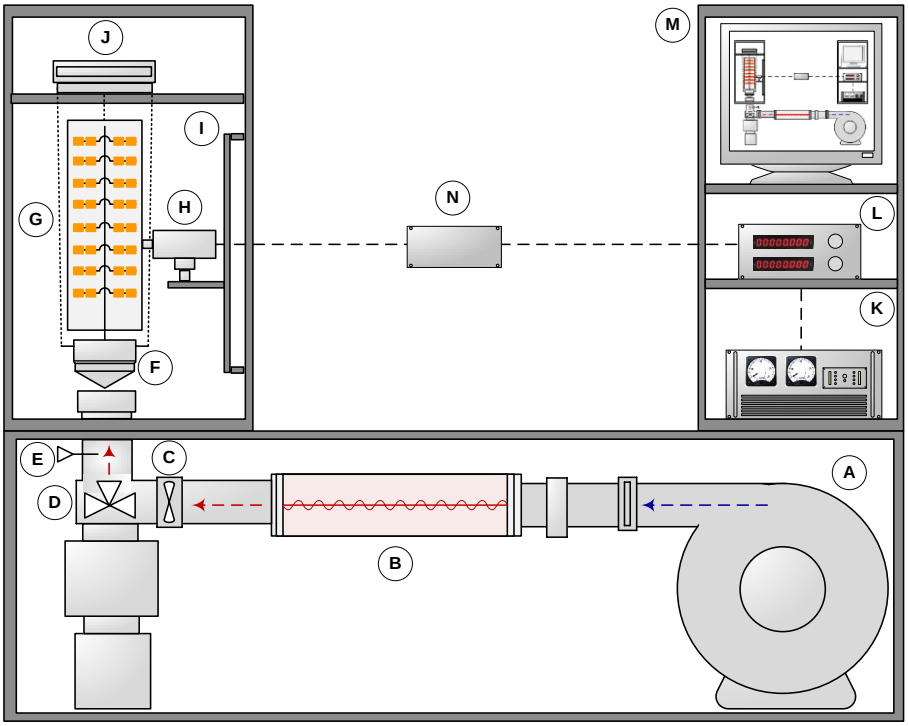

Fig. 9 Diagrama del secadero por aire caliente asistido por ultrasonidos. A) Soplante, B) Resistencias eléctricas, C) Anemómetro, D) Válvula de tres vías, E) Pt-100, F) Dispositivo de carga de la muestra, G) Cilindro vibrante, H) Transductor ultrasónico, I) Brazo neumático de deslizamiento, J) Balanza, K) Generador de ultrasonidos, L) Medidor de potencia, M) PC, N) Caja de impedancias.

- **Cámara de secado y sistema de pesada**

La cámara de secado está constituida por un cilindro de aluminio vibrando a flexión, excitado por un vibrador compuesto por un transductor tipo sándwich y un

amplificador mecánico con características similares al sistema descrito en el secadero a baja temperatura (Fig. 8). En este sistema, la generación de la señal ultrasónica y la amplificación de la misma se realizan ajustando manualmente la frecuencia y potencia en el generador ultrasónico (Fig. 9K) (LC-9601, Instituto de Acústica, CSIC, España). Con el objetivo de supervisar y controlar el comportamiento del dispositivo de US, los principales parámetros eléctricos de la señal (frecuencia, potencia, intensidad, voltaje y desfase) fueron medidos con un medidor de potencia digital (WT210, Japón) conectado a una aplicación desarrollada en LabVIEW™ (National Instruments, EE.UU) para la visualización y adquisición de los parámetros eléctricos.

Durante las experiencias de secado, el portamuestras es pesado de forma periódica mediante una balanza (PM4000, Mettler Toledo, EE.UU) (Fig. 9J) conectada a un PC mediante un puerto RS-232. En cada pesada, y para mantener la estabilidad de la balanza, una válvula neumática de 3 vías (Fig. 9D) desvía momentáneamente la salida del aire para evitar que éste incida sobre la misma.

- **Sistema de control y adquisición de datos**

Una aplicación informática desarrollada en Microsoft Visual Basic se utiliza como interfaz para el control de las experiencias de secado integrando la información sobre el flujo de aire, la temperatura, la evolución del peso de las muestras durante el secado y temperatura y la humedad relativa ambiental. El PC (Fig. 9M) está conectado al cuadro de control y a los distintos instrumentos indicadores/convertidores del secadero mediante una tarjeta de adquisición de datos (PCL-812, UCS, Reino Unido).

4.Resultados

CHAPTER 1

Meat Brining

Journal of Food Engineering, 2013, 119, 84-93

Influence of High Intensity Ultrasound Application on Mass Transport, Microstructure and Textural Properties of Pork Meat (*Longissimus dorsi*) Brined at Different NaCl Concentrations

César Ozuna[a], Ana Puig[b], Jose V. García-Pérez[a], Antonio Mulet[a] and Juan A. Cárcel[a,]*

[a] Grupo de Análisis y Simulación de Procesos Agroalimentarios. Departamento de Tecnología de Alimentos. Universitat Politècnica de València.

Camino de Vera. s/n. E46022. Valencia, Spain

[b] Grupo de Microestructura y Química de Alimentos. Departamento de Tecnología de Alimentos. Universitat Politècnica de València.

Camino de Vera. s/n. E46022. Valencia, Spain

Abstract

The aim of this work was to evaluate the effect of high intensity ultrasound and NaCl concentration on the brining kinetics (5±1 ºC) of pork loin as well as its influence on the textural and microstructural changes. In order to identify the effect of both factors on NaCl and moisture transport, kinetics were analyzed by taking the diffusion theory into account. The textural and microstructural analysis of raw and brined meat both with and without ultrasound application was carried out. The experimental results showed that the brine NaCl concentration not only determined the final NaCl content in meat samples but also the direction of water transport. The NaCl and moisture effective diffusivities were improved by ultrasound application. The final NaCl and moisture content and the ultrasound application promoted changes in instrumentally measured meat texture, which were confirmed via microstructural observations.

Keywords:
mass transfer, power ultrasound, modeling, diffusivity, texture, Cryo-SEM, SEM.

1. Introduction

Over 1.2 million tons of meat products produced per year makes Spain the fourth most important country in the European Union in this regard, being the dry-cured products the most valuable ones in the Spanish meat industry (AICE, 2011). One of the main stages during the processing of dry-cured products is salting. Actually, this operation is mainly carried out by salting the meat pieces with solid salts (NaCl), but it could also be performed by brining (Barat et al., 2006). Compared with other food processes, brining is a slow process and, for that reason, the food industry is searching for alternative technologies for improving the mass transfer kinetics (Rastogi et al., 2002), such as high intensity ultrasound application (Cárcel et al., 2007a).

In liquid medium, ultrasound induces cavitation (Leighton, 1998), temperature gradients within the material (Mason and Lorimer, 2002), mechanical phenomena, such as the "sponge effect", generation of microchannels and microstirring on interfaces (Muralidhara et al., 1985). These effects can not only increase the mass transport kinetics but also imply structural changes and, consequently, changes in textural properties. Thereby, textural changes induced by ultrasound have been observed in, among others, tomato juice (Vercet et al., 2002), yoghurt (Wu et al., 2000), bell peppers (Gabaldón-Leyva et al. 2007) or meat (Jayasooriya et al., 2007; Pohlman et al., 1997).

Meat has great biochemical and structural complexity. During meat brining, changes in NaCl and moisture content take place (Graiver et al., 2006), which extend meat's shelf life and modify organoleptic characteristics, such as juiciness, texture and flavor. Mass transfer driving forces between meat and brine are linked to chemical gradients and NaCl-induced changes in the water holding capacity (WHC) of meat proteins (Shi and Le Maguer, 2002; Vestergaard et al., 2005). The NaCl concentration in brine affects the direction of moisture transport as well as the equilibrium state (Cheng and Sun, 2008). A low NaCl content in the meat increases the water holding capacity (WHC) (Nguyen et al., 2010), a phenomenon known as "salting-in" which is linked to the meat protein net charge modification. However, a high NaCl content in meat could also bring about a decrease in WHC, probably due to the insolubilization of proteins ("salting-out") (Graiver et al., 2009). Therefore, the NaCl concentration in the brine solution can not only affect the chemical gradients, but also the WHC, thus affecting the magnitude of mass transport.

Modeling is a fundamental tool to quantify the mass transport (Cárcel et al., 2007a), as well as to evaluate the effectiveness on that of new technologies, such as ultrasound. But in addition, modeling also provides relevant information to understand the changes undergone by foodstuffs during processing, which usefulness complements the information given by other techniques, such as textural and microstructural ones (Pérez-Munuera et al., 2008). Thereby, different electron microscopy techniques, Larrea et al. (2007) have been used to characterize the microstructure of *Biceps femoris* and *Semimebranousus* muscles during the processing of Teruel dry-cured ham. Ruiz-Ramírez et al. (2005) described the effect of NaCl and pH on the relationship between water content and textural parameters in dry-cured muscles.

The main aim of this work was to evaluate the influence of high intensity ultrasound application on the meat brining kinetics using different NaCl concentrations in the brine solution. Moreover, the ultrasonic effects in transport phenomena have been quantified by modeling and linked to the induced changes in microstructural and textural meat properties.

2. Materials and methods

2.1. Raw material and sample preparation

Fresh pork loins (*Longissimus dorsi)* were purchased at a local slaughterhouse (Valencia, Spain). The pieces selected had a pH of 5.3 ± 0.30, which was measured in-situ by means of a pH-meter (pH STAR, Matthäus, Germany) at three different points along the muscle avoiding fatty areas. Parallelepiped shaped samples (length 50 x width 30 x thickness 10 mm) were obtained from the central part of loin pieces using a sharp knife. Before brining, samples were wrapped in plastic waterproof film and kept frozen at -18 ± 0.5 ºC (maximum storage time 120 hours).

2.2. Brining treatments

Brining experiments with (US, 40 kHz; 37.5 W/dm^3) and without ultrasound application (CONTROL) were carried out using brine solutions of different NaCl concentrations (50, 100, 150, 200, 240 and 280 kg NaCl/m^3). The highest NaCl concentration used (280 kg NaCl/m^3) involved brine saturation at 5±1 ºC, which was pointed to by the presence of NaCl crystals in the solution.

Brining treatments were carried out in an ultrasonic cleaning bath (4 L, Selecta, Spain) where the temperature was held at 5±1 ºC by brine recirculation from a cooling reservoir. A peristaltic pump (302S Limited, Watson/Marlow, United Kingdom) drove the brine from the cooling reservoir equipped with a chiller (3000778, J.P. Selecta, Spain) and a mechanical stirrer (RZR 1, Heidolph Instruments, Germany).

Before each brining experiment, 6 meat samples were thawed at constant temperature (2±1 ºC) for 24 h. Then, the samples were blotted, weighed (PB3002-S/PH, J.P., Mettler Toledo, Spain) and their size was measured by using a Vernier caliper. Afterwards, they were placed in a hollow sample holder and simultaneously introduced in the brine. For a homogenous brining, the position of the meat samples was changed every 5 min. In the US experiments, ultrasound was continuously applied. Samples were taken out of the brine at preset times (15, 30, 45, 60, 90 and 120 minutes) and immersed in distilled water for 20 s to remove any adhered surface brine. Finally, samples were blotted, wrapped in plastic waterproof film and frozen (-18 ± 0.5 ºC) until moisture and NaCl measurements were taken.

After brining, moisture and NaCl content were measured from ground meat (at 300 r.p.m., Blixer® 2, Robot coupe, France). The moisture content was determined following AOAC standards (Method No. 950.46 AOAC, 1997). While in the case of NaCl, the procedure reported by Cárcel et al. (2007b) was used. Both measurements were carried out in triplicate at least.

2.3. Mass transfer modeling

A mathematical model based on Fick's 2nd law was used to separately describe the evolution of moisture and NaCl content in the sample during brining (Cranck 1975). Samples were considered to become slab geometry bodies due to the fact that they were not nearly as thick (10 mm) as they were high (50 mm) and wide (30 mm), thus, mass transfer was simplified as a one-dimensional problem. Constant effective diffusivities (D_s and D_w), negligible changes in temperature and sample volume, solid symmetry, homogeneous NaCl and moisture initial content and negligible external resistance (Gou et al., 2003) were assumed during processing. Eqs. 1 and 2 show the solution of the diffusion model in terms of average moisture and NaCl content.

$$W = W_{eq} + (W_0 - W_{eq})\left[2\sum_{n=0}^{\infty}\frac{1}{\lambda_n^2 L^2}e^{-D_W\lambda_n^2 t}\right] \quad (1)$$

$$S = S_{eq} + (S_0 - S_{eq})\left[2\sum_{n=0}^{\infty}\frac{1}{\lambda_n^2 L^2}e^{-D_S\lambda_n^2 t}\right] \quad (2)$$

Where λ_n are the eigenvalues obtained from $\lambda_n L = (2n+1)\frac{\pi}{2}$. The equilibrium moisture and NaCl content values (S_e, W_e) were determined by immersing meat samples in the different brine solutions for at least 48 h. From previous experiments, this time was considered to be long enough to achieve the equilibrium.

Both effective diffusivity values, D_s and D_w, were identified by separately fitting Eqs. 1 and 2 to moisture and NaCl transport kinetics. The identification was performed by minimizing the squared differences between the experimental and calculated average sample moisture and NaCl content. For that purpose, the Generalized Reduced Gradient (GRG) optimization method, available in the Microsoft Excel spreadsheet from Microsoft Office XP Professional, was used.

2.4. Textural and microstructural analysis

Meat texture and microstructure were studied in raw material, US (40 kHz; 37.5 W/dm^3) and CONTROL brined samples for 120 minutes using low, intermediate and high NaCl concentrations (50, 200 and 280 kg NaCl/m^3, respectively). Samples were brined in triplicate at least.

2.4.1. Texture

Hardness, characterized as maximum penetration force, was evaluated in brined samples using a Texture Analyzer (TAX-T2®, Stable Micro System, United Kingdom). Penetration tests were conducted with a 2 mm flat cylinder probe (SMS P/2N), a crosshead speed of 1 mm/s and a strain of 60 % (penetration distance 6 mm). In each meat slice, penetration tests were carried out at 12 points at least.

2.4.2. Cryo-scanning electron microscopy (Cryo-SEM)

Cubic samples (side 3 mm) of raw and brined meat were immersed in slush Nitrogen (-210 ºC), and quickly transferred to a cryo-trans (CT 15000 C, Oxford Instruments, England) linked to a scanning electron microscope (JSM-5410, Jeol, Japan). Samples were cryo-fractured at -180 ºC, etched at -90 ºC and gold-coated, allowing cross-section visualization. The microscopic observations were carried out at 10 kV, a working distance of 15 mm and a temperature below -130 ºC.

2.4.3. Scanning electron microscopy (SEM) with combined dispersion X-ray analysis (SEM-EDX)

Cubic samples (side 3 mm) from raw and brined meat were immersed in liquid N_2 and then freeze-dried at 1 Pa for 3 days (LIOALFA-6, Telstar, Spain). Then, samples were vacuum sealed in vials in the same freeze-drier so that they would remain stable (Llorca et al., 2001). After that, they were individually placed on SEM slides with the aid of colloidal silver and then gold-coated with carbon (SCD005, Baltec, Germany) at 10-2 Pa and an ionization current of 40 mA. The samples were observed in a scanning electron microscope (JSM-5410, Jeol, Japan) equipped with an X-ray detector and LINK data-processing system (INCA 4.09, Oxford Instruments, England) at an acceleration voltage of 10-20 kV which provides internal information about the standards of energy dispersive X-ray spectra of the elements analyzed (Na^+ and Cl^-). This technique is an analytical tool that allows identifying the ions Cl^- and Na^+ inside the samples (Grote and George, 1984). For EDX (energy-dispersive X-ray) analysis, samples were carbon-coated (CEA035, Baltec, Germany). Mapping images of Cl^- and Na^+ distribution in meat samples were made using a voltage of 20 kV and at a working distance of 15 mm.

2.5. Fitting model evaluation and statistical analysis

In order to evaluate the ability of the models to fit the experimental data, the percentage of explained variance (%VAR) was computed (Eq. 3) (Cárcel et al., 2007a). Confidence intervals for the estimation of the effective diffusivities (D_s and D_w) were assessed in order to determine the reliability of the model prediction.

$$\%VAR = \left[1 - \frac{S^2_{tw}}{S^2_w}\right] x100 \quad (3)$$

Where S^2_w and S^2_{tw} are the variance of the sample and the estimation, respectively.

Multifactor ANOVA and LSD (Least Significant Difference) intervals were estimated to perform a statistical evaluation of the influence of ultrasound application and NaCl concentration on the textural properties. The statistical analysis was carried out using the Statgraphics Centurion XVI software package (Statistical Graphics Corp., Herdorn, USA).

3. Results and discussion

3.1. NaCl and water transport

3.1.1. NaCl and water content

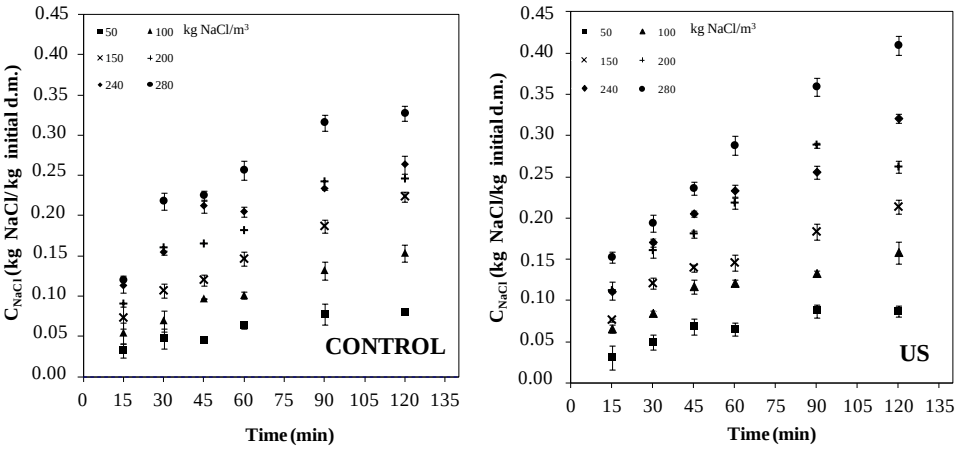

Fig. 1 Experimental NaCl transport kinetics in pork loin slices (thickness 10 mm) brined at different NaCl concentrations with (US, 40 kHz, 37.5 W/dm³) and without ultrasound application (CONTROL). In this figure, each point represents the average of 9 measurements: three independently brined samples analyzed in triplicate. Average ± standard deviation being plotted.

Fig. 1 shows the NaCl content of loin samples during brining, which is also considered the NaCl gain, due to the fact that the NaCl content in meat samples was negligible. NaCl concentration in the brine influenced significantly on NaCl content (Fig. 2A). Thus, when using a brine solution of 50 kg NaCl/m^3, the NaCl content in the meat after 120 min of brining was almost four times lower than when using 280 kg NaCl/m^3. The NaCl gain is mainly linked to osmotic mechanisms, thus the hydrodynamic flux increases as the pressure gradients between the meat and brine get higher (Schmidt et al., 2008). Other factors, such as temperature, pH and muscle microstructure, can also affect the NaCl gain (Barat et al., 2006).

Ultrasound also significantly ($p<0.05$) influenced the NaCl gain (Fig. 2 B); as an example, for a brining time of 90 min and using the highest NaCl concentration (280 kg NaCl/m^3) (Fig. 1), the NaCl content in the CONTROL samples was 0.315±0.020 kg NaCl/kg initial d.m. while the content in US samples reached 0.359±0.033 kg NaCl/kg initial d.m. Among other phenomena, the US application in liquid media induces cavitation, temperature gradients within the material, alternative compression and decompression of the material, the generation of microchannels and microstirring on interfaces, which are responsible for the increased gain in NaCl. Cárcel et al. (2007a) and Gabaldón-Leyva et al. (2007) also found significant differences ($p<0.05$) in the net increase of dry matter content during the ultrasound assisted osmotic treatment of apple and red bell pepper.

Regarding the moisture content, pork loin showed average initial moisture content of 3.10±0.12 kg water/kg initial d.m. As can be observed in Fig. 3, the concentration of NaCl in the brine solution was a key parameter in moisture transport, since it determined the direction of water flux. The ANOVA carried out with samples brined for 120 min reflected that samples could be classified in three significantly different groups according to the moisture content (Fig. 2 C). The first group included samples brined using 50 and 100 kg NaCl/m^3, which showed a significant ($p<0.05$) water gain. Samples brined using 150 and 200 kg NaCl/m^3 (the second group) neither lost nor gained water, having similar moisture content to raw meat. This result coincided with what was reported by Graiver et al. (2009) and Nguyen et al. (2010), who did not find a clear moisture transport when using brines close to 200 kg NaCl/m^3, either. The water activity of meat samples and the 200 kg NaCl/m^3 brine were 0.868±0.001 and 0.980±0.007 respectively (Aqua Lab Serie 3, Decagon Devices, Inc., USA).

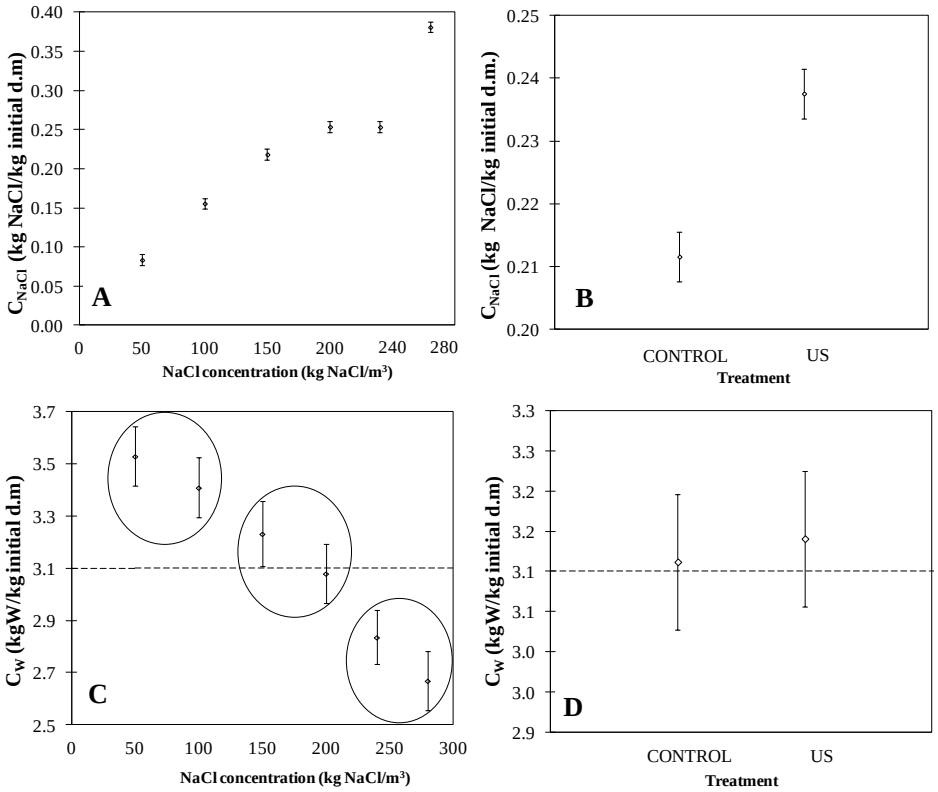

Fig. 2 Least Significant Difference intervals ($p<0.05$) for moisture and NaCl contents of pork loin slices (thickness 10 mm) brined at 5±1 ºC for 120 min with different brine concentrations with (US, 40 kHz, 37.5 W/dm³) and without ultrasound application (CONTROL). Dotted line (---) represents the average initial moisture content of pork loin.

Therefore, the no net moisture transport observed at this concentration can not to be explained from a water activity point of view. Finally, the third group included samples brined at 240 and 280 kg NaCl/m³, which underwent dehydration. During brining however, hydration or dehydration are not only affected by chemical potential gradient (Shi and Le Maguer, 2002) but also by structural changes brought about in the meat by salt gain (Schmidt et al., 2008). On the one side, the low NaCl content increases the muscle's WHC by protein solubilization, which is known, as aforementioned, the "salting-in" phenomenon (Offer and Trinick, 1983). On the other side, the high NaCl content reduces the WHC and meat muscle shrinks, which is the "salting-out" phenomenon (Graiver et al., 2006).

Regarding ultrasound effect on moisture content, US and CONTROL brined samples for 120 min did not show significant differences. (Fig. 2 D). This fact has been also been observed in ultrasound assisted brining of beef muscles (Pohlman et al., 1997; Jayasooriya et al. 2007) and pork meat (Siró et al. 2009). The negligible effect of ultrasound on water content could be linked to the great variability in moisture content of samples (Fig. 3). In addition, it should be considered that the ultrasound intensity may be not enough to provoke significant differences in water transport due to a minim amount of ultrasonic energy is necessary in the medium, and that threshold could be different for water and NaCl content. Cárcel et al., (2007b) reported that in high intensity ultrasound fields, brine could be microinjected into the meat leading to a direct increase of NaCl and water content.

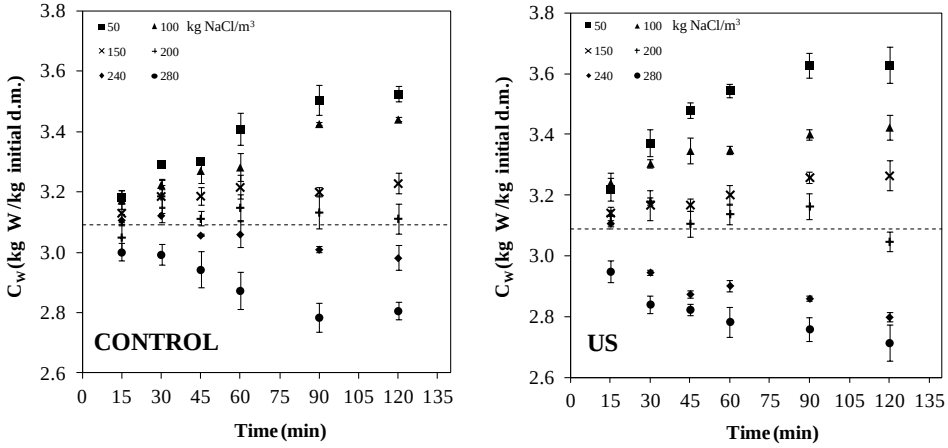

Fig. 3 Experimental moisture transport kinetics in pork loin slices (thickness 10 mm) brined at different NaCl concentrations with (US, 40 kHz, 37.5 W/dm3) and without ultrasound application (CONTROL). In this figure, each point represents the average of 9 measurements: three independently brined samples analyzed in triplicate. Average ± standard deviation being plotted.

3.2. Modeling transport kinetics

The analysis of the experimental results has been focused on the final salt and moisture content (samples brined for 120 min). Modeling the experimental transport kinetics (Figs. 1 and 3) will help to identify whether the brining conditions (US application and/or NaCl concentration) affect the process rate. The fit of the models to experimental kinetics achieved percentages of explained variance (Table 1) for NaCl transport ranging from 93 to 99%. These values were lower for moisture transport

(81.1 to 95.6%), which could indicate a poor fit in this case. However, as can be observed in Fig. 4, there exists a similar trend between calculated and experimental moisture contents, which highlights that the proposed diffusion model was adequate to describe the brining process.

Table 1 Modeling NaCl transport in pork meat brining (5±1 ºC) at different NaCl concentrations with (US, 40 kHz, 37.5 W/dm^3) and without (CONTROL) ultrasound application. Effective diffusivity and percentage of explained variance. Average ± confidence intervals (95%) are shown.

NaCl concentration (kg/m^3)	CONTROL		US		Increment (%)
	D_s (10^{-10} m^2/s)	% VAR	D_s (10^{-10} m^2/s)	% VAR	
50	1.24±0.11	98.1	1.73±0.51	97.5	40
100	2.04±0.16	99.2	2.93±0.54	96.6	44
150	2.11±0.19	99.0	2.60±0.24	98.9	23
200	1.99±0.32	96.4	2.68±0.51	95.1	35
240	1.73±0.18	96.1	2.51±0.52	93.8	45
280	1.96±0.32	96.1	2.62±0.16	99.5	34

The low explained variance provided by the diffusion model in the moisture transport should mostly linked to the great variability of the initial composition of raw meat. Therefore, diffusion could be considered the predominant mass transport mechanism during brining.

The D_s values were similar for all the different brine concentrations tested; a lower figure was only found for all NaCl concentration of 50 kg NaCl/m^3, probably due to the structural changes in meat samples brought about by low salt gain. The effective NaCl diffusivities identified for the CONTROL samples agree closely with the values reported in the literature (Graiver et al., 2006; Vestergaard et al., 2007), which actually range between 2–4×10^{-10} m^2/s. Regarding moisture transport, the D_w values identified in experiments where meat was hydrated (NaCl concentration lower than 200 kg NaCl/m^3) decreased as the NaCl content rose. Thus, in CONTROL experiments using a brining solution of 50 kg NaCl/m^3, the D_w was 0.76x10^{-10} m^2/s, while D_w decreased to 0.17x10^{-10} m^2/s for experiments at 150 kg NaCl/m^3, where hydration was almost negligible. The same fact was also observed in US experiments and has also been previously reported by Gou et al., (2003), who found that the D_w

decreased when the NaCl content of the salting solutions increased from 20 to 80 kg NaCl/m^3. On the other hand, the D_w values were higher when meat was dehydrated (NaCl concentration higher than 200 kg NaCl/m^3) than when meat was hydrated (NaCl concentration lower than 200 kg NaCl/m^3) (Table 2).

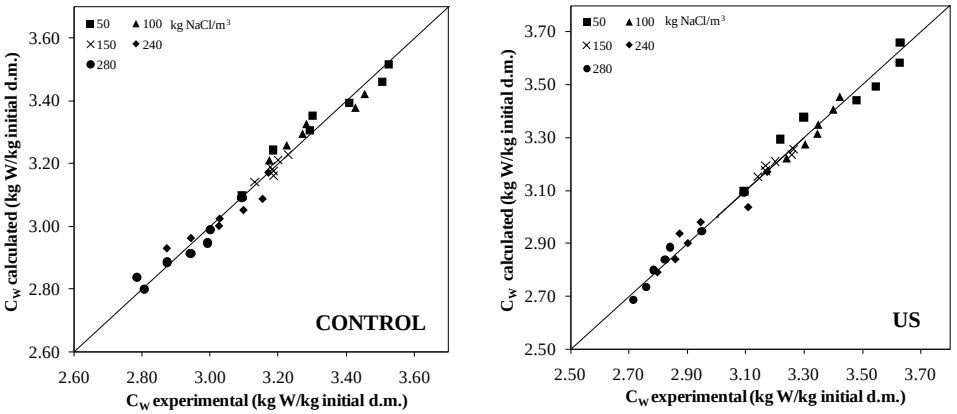

Fig. 4 Experimental vs calculated moisture content of pork loin slices (thickness 10 mm) brined with (US, 40 kHz, 37.5 W/dm^3) and without (CONTROL) ultrasound application.

It must to be clarified that the model did not fit to the experimental data of moisture content obtained for the 200 kg NaCl/m^3 brine due to no net moisture transport was observed. For this reason in Table 2 is not show diffusivity value for this case. These differences could be ascribed to the different product structure induced and controlled by NaCl transport (Schmidt et al., 2008; Gou et al., 2003; Offer and Trinick, 1983). Therefore, the NaCl concentration in the brining solution is not only affecting the direction of water flux (hydration or dehydration) but also the water transport rate as a consequence of the structural changes brought about by the NaCl content in the meat.

Ultrasound application led to a significant ($p<0.05$) improvement in both D_s and D_w, which points to an acceleration of both the global bring process. The increase in D_s ranged from 23 to 45% and is in a similar range to other improvements reported for solid transport in the literature. Thus, Siró et al. (2009) found increases of 96% in D_s meat brining and Gabaldón-Leyva et al. (2007) stated an improvement of 190% in the total solid diffusion coefficients. In the case of D_w, the improvement was higher than in D_s for the lowest and highest NaCl concentrations used (50 and 280 kg NaCl/m^3)

(Table 1), being in this case the improvement close to 100%. Gabaldón-Leyva et al., 2007 and Cárcel et al., 2007a reported increases in D_w of around 128 and 117% when ultrasound was applied in bell pepper brining and osmotic dehydration of apple. Smaller increases were observed in the D_w values for intermediate NaCl concentration brines tested, these being 76% and 41% for 100 and 150 kg NaCl/m^3, respectively. The different effectiveness of ultrasound application, depending on brine NaCl concentration, could be explained considering that the ultrasound effects on mass transport are largely dependent on product structure (Gabaldón-Leyva et al., 2007).

Table 2 Modeling moisture transport in pork meat brining (5±1 ºC) at different NaCl concentrations with (US, 40 kHz, 37.5 W/dm^3) and without (CONTROL) ultrasound application. Effective diffusivity and percentage of explained variance. Average ± confidence intervals (95%) are shown.

NaCl concentration (kg/m^3)	CONTROL		US		Increment (%)
	D_W (10^{-10}m^2/s)	VAR (%)	D_W (10^{-10} m^2/s)	VAR (%)	
50	0.76±0.21	90.7	1.92±0.27	91.6	153
100	0.62±0.19	90.2	1.09±0.14	94.7	76
150	0.17±0.04	89.1	0.24±0.07	92.2	41
200	-	-	-	-	-
240	1.04±0.52	81.1	2.60±0.83	88.8	150
280	1.83±0.57	90.0	3.67±0.68	95.6	101

Finally, it should be remarked that, as stated before, there was not a significant ($p<0.05$) difference on the moisture content at the end of the brining process (120 min) for CONTROL and US samples, however, the analysis of transport kinetics showed an improvement on the moisture transport rate by ultrasound. The effective moisture diffusivities identified from experimental results are kinetic parameters that not only include diffusion mechanisms but also other existing phenomena not considered in the model, such as external mass transport. Ultrasound may affect both internal mass transport resistance, by alternating cycles of expansions and contractions ("sponge effect") and the generation of microchannels, and external by microstirring at the interfaces (Muralidhara et al., 1985, Cárcel et al., 2007b). These effects that US induce into the medium are responsible for the kinetic improvement.

3.3. Texture

In order to study the influence of ultrasound application and NaCl concentration on meat texture, instrumental penetration tests were carried out in raw material, US (40 kHz; 37.5 W/dm^3) and CONTROL samples brined for 120 min using NaCl concentrations of 50, 200 and 280 kg NaCl/m^3. At least 12 points were measured in each meat slice.

Raw material showed a hardness value of 1.60 ± 0.49 N. With regard to brined samples, the hardness measured depended on the conditions of salting used. CONTROL samples brined at 200 and 280 kg NaCl/m^3 were significantly ($p<0.05$) harder than those brined at 50 kg NaCl/m^3 (Table 3). As aforementioned, the higher the NaCl concentration in the brine, the greater the NaCl gain. In such a way, the NaCl gain promoted changes in meat texture, leading to harder samples, a fact already showed by Ruiz-Ramírez et al. (2005). Non-significant differences ($p<0.05$) in hardness were found in samples brined at 200 and 280 kg NaCl/m^3 (Table 3). This indicates that the level of NaCl gained by both samples was enough to produce the same change in meat texture. The effect of the NaCl concentration in US samples was similar to that reported in CONTROL ones.

Table 3 Hardness (N) of pork meat brined for 120 min in different NaCl concentrations with (US, 40 kHz, 37.5 W/dm^3) and without (CONTROL) ultrasound application. Average ± standard deviations are shown. Subscripts (a,b,c,d) show homogeneous group established from LSD intervals ($p<0.05$).

Treatment	Hardness (N)		
	50 kg NaCl/m^3	200 kg NaCl/m^3	280 kg NaCl/m^3
CONTROL	$1.27\pm0.39_{a}$	$1.78\pm0.60_{b,c}$	$1.69\pm0.70_{b,c}$
US	$1.65\pm0.52_{b,c}$	$1.94\pm0.46_{b,c,d}$	$2.08\pm0.66_{d}$

On the other hand, the application of ultrasound during brining significantly increased ($p<0.05$) the meat hardness. As already explained, ultrasound application intensified NaCl transport during brining, increasing not only the NaCl diffusivity but also the final NaCl content (brining time 120 min, CONTROL 0.326±0.007 kg NaCl/kg initial

d.m. and US 0.409.29±0.11 kg NaCl/kg initial d.m.). So, the effects of ultrasound on meat texture could be linked to the intensification of NaCl transport, which provoked structural changes in meat proteins. Lee and Feng (2011) reported that the texture of ultrasound-treated food is influenced by protein changes during sonication, as well as Siró et al., (2009), who linked the hardening of meat tissue to the high ultrasonic intensities applied. Sanchez et al., (2001) showed that US application in the brining of Mahon cheese increased the sample hardness due to the improvement of proteolysis and lipolysis reactions.

Raw and brined CONTROL and US pork loin previously characterized from instrumental texture were studied by Cryo-SEM and SEM techniques in order to contribute to a better understanding of the effects produced by ultrasound application, being this fact analyzed in the following section.

3.4. Microstructure

3.4.1. Cryo-scanning electron microscopy (Cryo-SEM)

First of all the microstructure of raw pork loin was characterized. Fig. 5A shows a cross section of the raw pork loin, where cells are surrounded by the membrane or sarcolemma (Fig. 5A, S). These cells are interconnected by endomysial connective tissue (Fig. 5A, EC), which keeps the muscle fibers tightly attached. In addition, the myofibrils inside the muscle cell can be observed, which are fundamental components of the cell's contractile apparatus (Fig. 5A, M).

Intercellular spaces appear full of typical eutectic artifacts in brined samples (Figs. 5B, C and D) due to solute aggregation after water sublimation provoked by Cryo-SEM technique (Pérez-Munuera et al., 2008). The accumulation of solutes in the intercellular spaces can be linked to both the penetration of the NaCl and the strong solubilization and dehydration in muscle tissue. The greater the brining NaCl concentration, the greater the solute accumulation and the more compact the eutectic artifacts (Larrea et al., 2007). The bundles of muscle fibers in CONTROL samples brined at 280 kg NaCl/m^3 (Fig. 5D) seem to be more compact, showing the more intense sample dehydration linked to the "salting-out" phenomenon. The denaturation and precipitation of proteins involves progressive structural shrinkage and less space for water (Vestergaard et al., 2005).

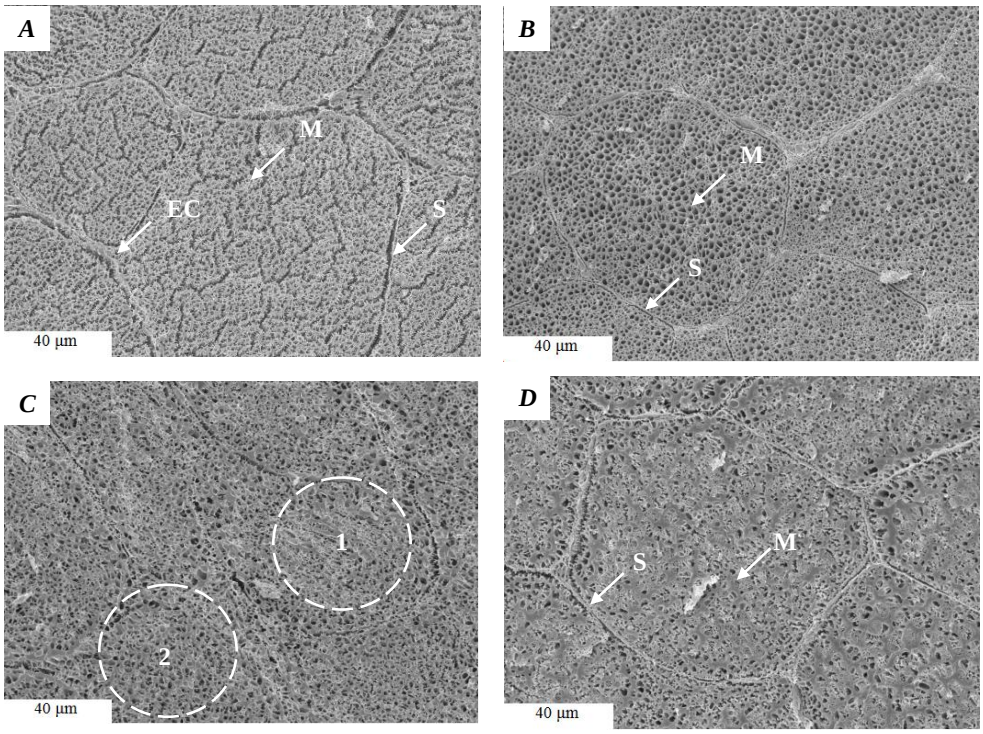

Fig. 5 Cross-section of *Longissimus dorsi* muscle of pork meat observed by Cryo-SEM (x 750). Raw meat (A), meat brined for 120 min in 50 kg NaCl/m^3 (B), 200 kg NaCl/m^3 (C) and 280 kg NaCl/m^3 (D). S: sarcolemma, EC: endomysial connective tissue, M: myofibrills, 1: "salting-out effects", 2: "salting-in effects".

These effects are widely related with the hardening observed in the textural analysis of meat brined at the highest NaCl concentration (280 kg NaCl/m^3) (Table 3). In samples brined at the lowest NaCl concentration (50 kg NaCl/m^3, Fig. 5B), however, may be observed an expansion of myofibrils coupled with the protein solubilization that is related with the "salting-in" phenomena (Graiver et al., 2006). Some authors have already reported that an increase in water binding and hydration in the muscle fibers of brined meat at low brine concentrations (< 50 kg NaCl/m^3) is ascribed to enhanced electrostatic repulsion between myofibril filaments causing the filament lattice to expand for water entrapment (Graiver et al., 2009; Cheng and Sun, 2008). These phenomena in meat proteins can explain the hydration of samples brined at low NaCl concentrations (Fig. 3) and the meat softening observed in the textural analysis (Table 3). Samples brined with 200 kg NaCl/m^3 (Fig. 5C), showed a mixed effect. Some parts of the sample show structural dehydration due to a high NaCl

concentration (Fig. 5C, 1), whereas in other parts of the sample, the opposite phenomena (hydration) can be observed in the myofibrillar structure (Fig. 5C, 2). As mentioned before (Fig. 3), no net transport of moisture was identified at 200 kg NaCl/m^3, which can be linked to the combined effect of hydration-dehydration observed in the meat microstructure (Fig. 5C).

From micrographs obtained with Cryo-SEM, no effects of ultrasound in the meat structure were found. Thus, the Cryo-SEM microstructural analysis was completed with SEM observations.

3.4.2. Scanning electron microscopy (SEM) with combined dispersion X-ray analysis (SEM-EDX)

CONTROL samples brined with the lowest NaCl concentration tested (50 kg NaCl/m^3, Fig. 6B) showed a swelling of muscle fibers (width 87.6±7.3 μm) compared to raw meat (width 72.5±9.1 μm) (Fig. 6A). The swelling of muscle fibers could be mainly ascribed to the "salting-in" phenomena. Samples brined at higher NaCl concentrations (280 kg NaCl/m^3) behaved in the opposite way and presented a dehydration of muscle fibers and an accumulation of NaCl; these effects may be observed in Figs. 7A, C, E.

The SEM technique also allowed the effect brought about by high intensity ultrasound in meat structure to be observed, this effect mainly focusing on myofibrils (Figs. 7B, D, F). The micrograph of the US sample brined at 50 kg NaCl/m^3 (Fig. 7B) shows the disruption and the dispersion of the connective tissue of the fibers caused by US application. In Fig. 7F the rupture of a myofibril provoked by the acoustic energy was identified. The aforementioned myofibrillar changes could be explained by the alternating compressions and decompressions induced by US in solid materials ("sponge effect"). Another important effect produced by high intensity ultrasound in liquid media is cavitation, which may be observed in Fig. 7D, where the erosion of meat fiber produced by cavitation is shown. The asymmetric implosion of bubbles near the solid surface could produce violent microjets that collide with the samples, which can improve mass transfer by disturbing the boundary layer and producing changes in the meat structure. These results coincide with those found by several

authors that related the application of high power ultrasound with the physical disruption of cellular and sub-cellular components (Reynolds et al., 1978), the degradation of collagen macromolecules (Nishira and Doty, 1958), and the creation of micro channels (Muralidhara et al., 1985).

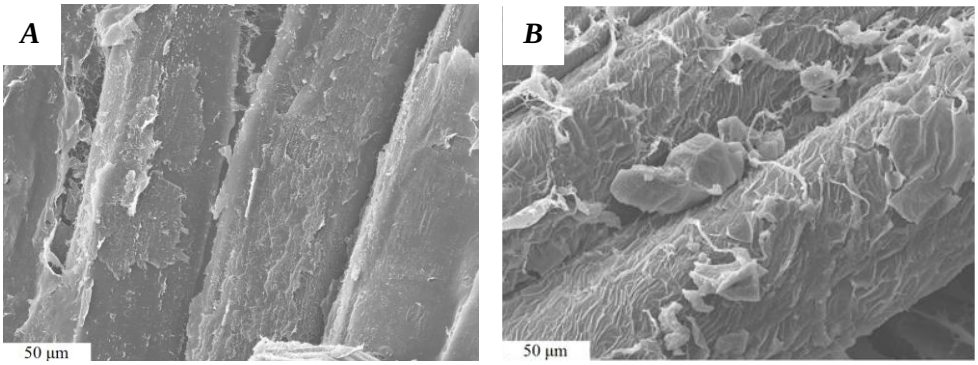

Fig. 6 Longitudinal section of *Longissimus dorsi* muscle of pork meat observed by SEM (x500). Raw meat (A) and meat brined in 50 kg NaCl/m^3 for 120 min (B).

The obtained SEM-EDX mapping images confirmed the presence of NaCl in meat after brining, which is shown up by the red (Cl^-) and green (Na^+) dots in the micrographs. As can be observed in Fig. 8, the NaCl concentration in US samples (Figs. 8B, D and F) was higher than those observed in CONTROL samples (Figs. 8A, C and E), as manifested by a higher number of dots in the micrographs. In CONTROL samples (Figs. 8A, C and E), NaCl molecules are mainly located around the myofibrils. However, the US brined samples (Figs. 8B, D and F) showed a more homogeneous NaCl dispersion due to the collapse of myofibrillar structure caused by the effects of high power ultrasound, permitting a higher NaCl penetration in the meat. The obtained SEM-EDX images showed the intensification of NaCl transport brought about by US application and the increase in NaCl content, which confirms the results provided by modeling and textural tools.

Therefore, ultrasound application could improve the brining process by reducing the brining time and ensuring a faster and more uniform distribution of sodium chloride. In this sense, this technology could be an interesting alternative to reduce NaCl levels in cured meat foods.

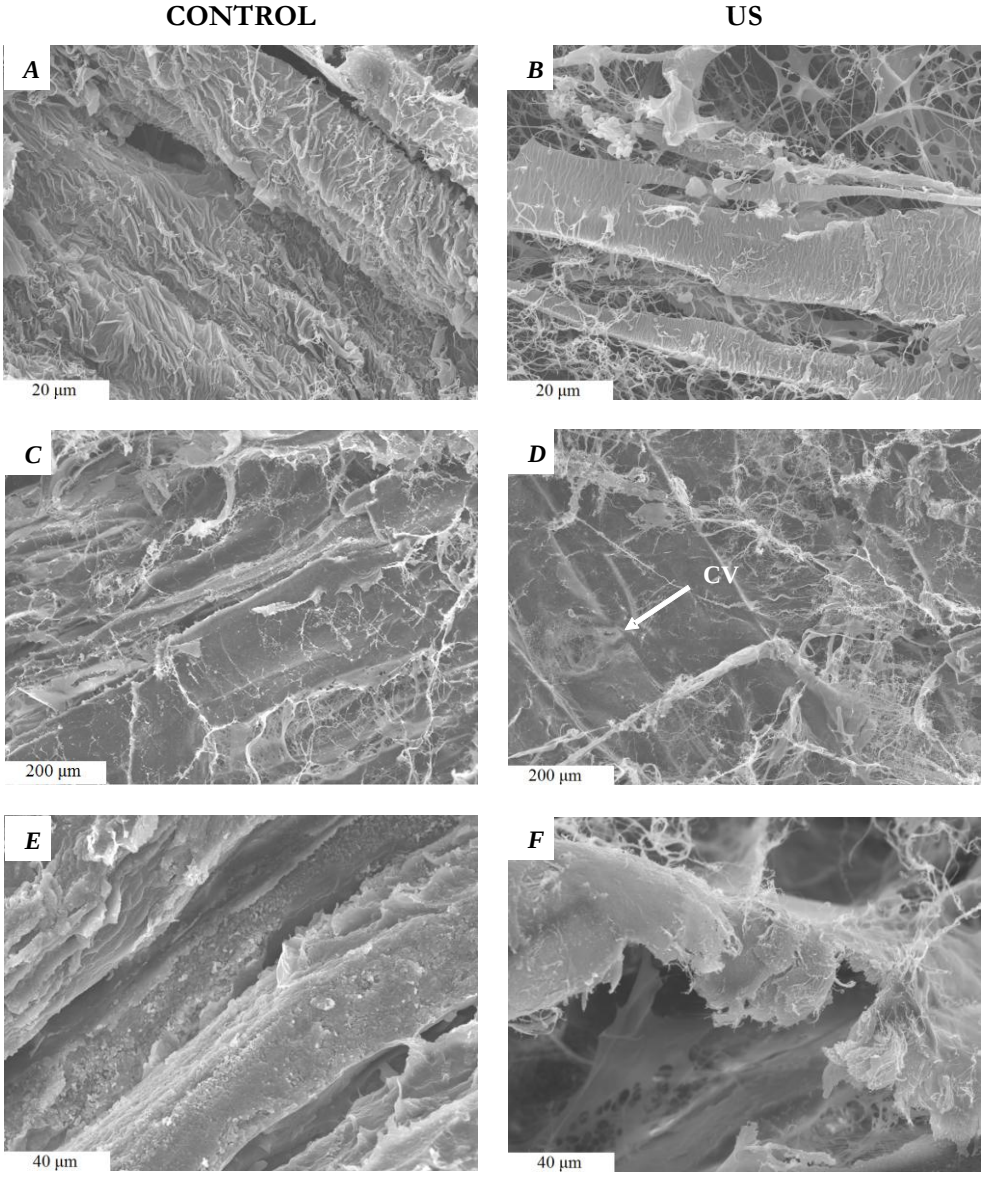

Fig. 7 Longitudinal section observed by SEM of *Longissimus dorsi* muscle of pork meat brined for 120 min in 50 kg NaCl/m³ (A, B: x1500), 200 kg NaCl/m³ (C, D: x150) and 280 kg NaCl/m³ solution (E, F: x750) without (CONTROL: A, C and E) and with (US: B, D and F) ultrasound application (40 kHz, 37.5 W/dm³). CV: impact of cavitation bubble implosion on myofibrill.

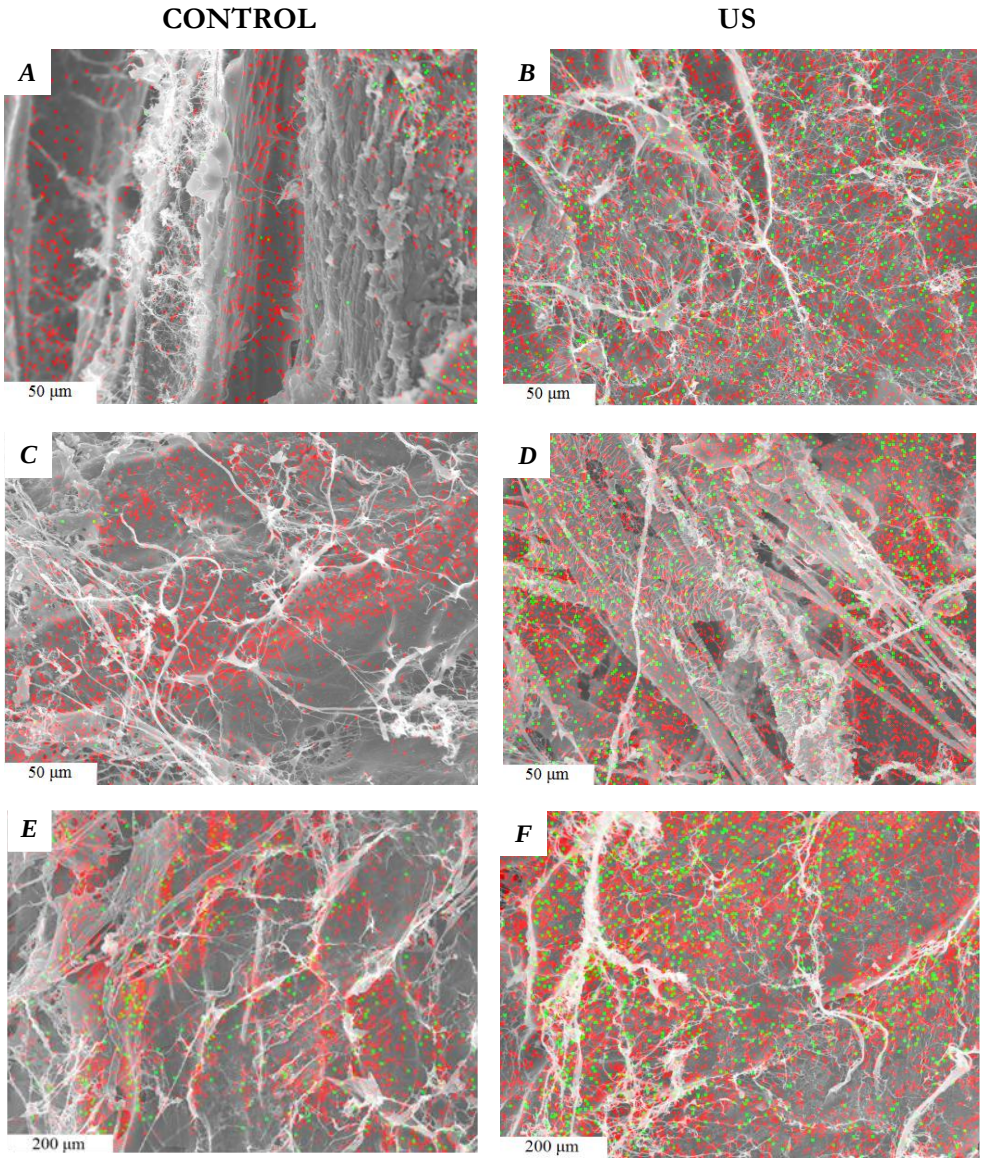

Fig. 8 Effect of ultrasound application on NaCl dispersion. Longitudinal section observed by SEM-EDX of Longissimus dorsi of pork meat brined for 120 min in 50 kg NaCl/m³ (A, B: x500), 200 kg NaCl/m³ (C, D: x500) and 280 kg NaCl/m³ (E, F: x150) without (CONTROL: A, C and E) and with (US: B, D and F) ultrasound application (40 kHz, 37.5 W/dm³).

4. Conclusions

The NaCl concentration in the brine solution significantly ($p<0.05$) affected moisture and NaCl transport during meat brining. At NaCl concentrations lower than 200 kg NaCl/m^3, the meat was hydrated while, dehydration took place at concentrations higher than 200 kg NaCl/m^3. As for the NaCl transport, the more concentrated the brine, the greater the NaCl sample gain. Ultrasound application intensified the brining kinetics, increasing both moisture effective and NaCl diffusivities. The NaCl gain promoted changes in meat texture, high NaCl contents leading to harder samples. Microstructural analyses showed that the application of high intensity ultrasound during brining brought about relevant effects on meat microstructure, such as a more homogeneous NaCl distribution in meat. Therefore, ultrasound could be considered a potential technology with which to accelerate the brining process.

Acknowledgments

This work is financed by project CARNISENUSA (CSD2007-00016) included in the CONSOLIDER-INGENIO-2010.

Nomenclature

W_{eq}	Equilibrium moisture content, kg water/kg initial d.m.
W_0	Initial moisture content, kg water/kg initial d.m.
S_{eq}	Equilibrium sodium chloride content, kg NaCl/kg initial d.m.
S_0	Initial sodium chloride content, kg NaCl/kg initial d.m.
D_S	Effective NaCl diffusivity (m^2/s)
D_W	Effective moisture diffusivity (m^2/s)
L	Half length, m

References

Asociación de industrias de la carne de España (AICE), available online http://www.aice.es. Accesed on November 01, 2011.

Association of Official Analytical Chemists. Official Methods of Analysis; AOAC: Washington, DC, 1997.

Barat, J.M., Grau, R., Ibáñez, J.B., Pagán, M.J., Flores M., Toldrá F., & Fito P. (2006). Accelerated processing of dry-cured ham. Part I. Viability of the use of brine thawing/salting operation. *Meat Science*, 72 (4), 757-765.

Cárcel, J.A., Benedito, J., Roselló, C., & Mulet, A. (2007a). Influence of ultrasound intensity on mass transfer in apple immersed in a sucrose solution. *Journal of Food Engineering*, 78 (2), 472-479.

Cárcel, J.A., Benedito, J., Bon, J., & Mulet A. (2007b). High intensity ultrasound effects on meat brining. *Meat Science*, 76 (4), 611-619.

Cheng, Q., & Sun, D.-W. (2008). Factors affecting the water holding capacity of red meat products: a review of recent research advances. *Critical Reviews in Food Science and Nutrition*, 48 (2), 137-159.

Crank, J. (1975). *The Mathematics of Diffusion*. London: Oxford University Press.

Gabaldón-Leyva, C. A., Quintero-Ramos, A., Barnard, J., Balandrán-Quintana, R. R., Talamás-Abbud, R. T., & Jiménez-Castro, J. (2007). Effect of ultrasound on the mass transfer and physical changes in brine bell pepper at different temperature. *Journal of Food Engineering*, 81(2), 374–379.

Gou, P., Comaposada, J., & Arnau, J. (2003). NaCl content and temperature effects on moisture diffusivity in the *Gluteus medius* muscle of pork ham. *Meat Science*, 63 (1), 29-34.

Graiver, N., Pinotti, A., Califano, A., & Zaritzky, N. (2006). Diffusion of sodium chloride in pork tissue. *Journal of Food Engineering*, 77 (4), 910–918.

Graiver, N., Pinotti, A., Califano, A., & Zaritzky, N. (2009). Mathematical modeling of the uptake of curing salts in pork meat. *Journal of Food Engineering*, 95 (4), 533-540.

Grote, M. & Georg, H. (1984) Determination of element concentrations in fresh and processed vegetables by quantitative X-ray microanalysis. *Food Microstructure*, 3 (1), 49–54.

Jayasooriya S.D., Torley P.J., D'Arcy B.R. & Bhandari B.R. (2007). Effect of high power ultrasound and ageing on the physical properties of bovine *Semitendinous* and *Longissimus* muscles. *Meat Science*, 75 (4), 628-639.

Larrea, V., Pérez-Munuera, I., Hernardo, I., Quiles, A., Llorca, E., & Lluch, M.A. (2007). Microstructural changes in Teruel dry-cured ham during processing. *Meat Science*, 76 (3), 574-582.

Lee, H. & Feng, H. (2011). Effect of power ultrasound on food quality. In Feng, H., Barbosa-Cánovas, G.M. & Weiss, J. (Eds.), *Ultrasound Technologies for Food and Bioprocessing* (pp. 559–582). London: Springer.

Leighton, T. G. (1998). The principles of cavitation. In M. J. W. Povey & T. J. Mason (Eds.), *Ultrasound in Food Processing* (pp. 151–182). London: Chapman & Hall.

Llorca, E., Puig, A., Hernando, I., Salvador, A., Fiszman S., & Lluch, M.A. (2001). Effect of fermentation time on texture and microstructure of pickled carrots. *Journal of the Science of Food and Agriculture,* 81 (15), 1553–1560.

Mason, T. J., & Lorimer, J. P. (2002). Applied sonochemistry. *The uses of power ultrasound in chemistry and processing*. Weinheim: Wiley-VCH.

Muralidhara, H. S., Ensminger, D., & Putnam, A. (1985). Acoustic dewatering and drying (low and high frequency): State of the art review. *Drying Technology*, *3*(4), 529–566.

Nguyen, M.V., Arason, A., Thorarinsddottir, K.A., Thorkelsson, G. & Gudmundsdóttir, A. (2010). Influence of salt concentration on the salting kinetics of cod loin (*Gadus morhua*) during brine salting. *Journal of Food Engineering*, 100 (2), 225-231.

Nishira, T., & Doty, P. (1958). The sonic fragmentation of collagen macromolecules. *Proceedings of the National Academy of Sciences of the United States of America*, 44(5), 411-417.

Offer, G. & Trinick, J. (1983). On the mechanism of water holding in meat: The swelling and shrinking of myofibrils. *Meat Science*, 8 (4), 245-281.

Pérez-Munuera, I., Larrea, V., Quiles, A., & Lluch, M.A. (2008). Microstructure of muscle foods. In L.M.L., Nollet & F. Toldrá (Eds.), Handbook of muscle food analysis (pp. 335-352). Boca Raton FL: CRC Press Taylor & Francis Group.

Pohlman, F.W, Dikeman M.E., & Kropf D.H. (1997). Effects of high intensity ultrasound treatment, storage time and cooking method on shear, sensory, instrumental color and cooking properties of packaged and unpackaged beef pectoralis muscle. *Meat Science*, 46 (1), 89–100.

Rastogi, N.K., Raghavarao, K.S.M.S., Niranjan, K., & Knorr, D. (2002). Recent developments in osmotic dehydration: methods to enhance mass transfer. *Trends in Food Science & Technology*, 13 (2), 48-59.

Reynolds, J.B., Anderson D.B., Schmidt, G.R., Theno, D.M., & Siegel D.G. (1978). Effects of ultrasonic treatment on binding strength in cured ham rolls. *Journal of Food Science*, 43 (3), 866-869.

Ruiz-Ramírez, J., Arnau, J., Serra, X., & Gou, P. (2005). Relationship between water content, NaCl content, pH and texture parameters in dry-cured muscles. *Meat Science*, 70 (4), 579-587.

Sanchez, E. S., Simal, S., Femenía, A., Benedito, J. & Roselló, C. (2001). Effect of acoustic brining on lipolysis and on sensory characteristics of Mahon cheese. *Journal of Food Science*, 66(6), 892-896.

Schmidt, F.C., Carciofi, B.A.M. & Laurindo, J. B. (2008). Salting operational diagrams for chicken breast cuts: Hydration-dehydration. *Journal of Food Engineering*, 88 (1), 36-44.

Shi J. & Le Maguer M. (2002). Osmotic dehydration of foods: mass transfer and modelling aspects. *Food Reviews International*, 18(4), 305-335.

Siró, I., Vén, C., Balla, C., Jónás, G., Zeke, I., & Friedrich, L. (2009). Application of an ultrasonic assisted curing technique for improving the diffusion of sodium chloride in porcine meat. *Journal of Food Science*, 91 (2), 363-362.

Vercet, A., Sánchez, C., Burgos, J., Montañés, L., & Buesa, P. L. (2002). The effects of manothermosonication on tomato pectic enzymes and tomato paste rheological properties. *Journal of Food Engineering*, 53 (3), 273–278.

Vestergaard, C., Lohmann Andersen, B., & Adler-Nissen, J. (2007). Sodium diffusion in cured pork determined by ^{22}Na radiology. *Meat Science*, 76 (2), 258–265.

Vestergaard, C., Risum, J., & Adler-Nissen, J. (2005). ^{23}Na-MRI quantification of sodium and water mobility in pork during brine curing. *Meat Science*, 69 (4), 663-672.

Wu, H., Hulbert, G. J., & Mount, J. R. (2000). Effects of ultrasound on milk homogenization and fermentation with yogurt starter. *Innovative Food Science and Emerging Technologies*, 1 (13), 211–218.

CHAPTER 2

Cod Desalting

LWT- Food Science and Technology (Submitted)

Ultrasonically Enhanced Desalting of Cod (*Gadus morhua*). Mass Transport Kinetics and Structural Changes

César Ozuna[a], Ana Puig[b], Jose V. García-Pérez[a] and Juan A. Cárcel[a,]*

[a] Grupo de Análisis y Simulación de Procesos Agroalimentarios. Departamento de Tecnología de Alimentos. Universitat Politècnica de València.

Camino de Vera. s/n. E46022. Valencia, Spain

[b] Grupo de Microestructura y Química de Alimentos. Departamento de Tecnología de Alimentos. Universitat Politècnica de València.

Camino de Vera. s/n. E46022. Valencia, Spain

Abstract

The search for an alternative means for reconstituting dried and salted products prior to consumption is of relevance for the food industry. New techniques should speed up the process while causing minimum impact on product quality. Thereby, the aim of this work was to evaluate the effect of high-intensity ultrasound application on the desalting kinetics of cod, as well as the changes in its textural and microstructural properties. Moisture and NaCl transport was studied separately by taking the diffusion theory into account. The evolution in the swelling and hardness of cod during desalting was determined and modeled by assuming a first-order kinetic. A microstructural analysis of raw salted and desalted cod was also carried out by means of light microscopy and SEM techniques. Ultrasound application significantly ($p<0.05$) affected both moisture and NaCl transport, increasing both effective diffusivities (from 24% to 103%). The desalting process induced the swelling and the softening of the cod tissue, both of which are phenomena that are intensified by ultrasound application. From the microstructural observations, it was shown that the application of high-intensity ultrasound modified the cod structure, e.g. the increase in the fiber width.

Keywords:
Ultrasonic, Modeling, Diffusivity, Texture, Light microscopy, SEM.

1. Introduction

Salted cod (*Gadus morhua*) is one of the most widely-consumed heavy-salted products in southern European countries and Latin America (Martínez-Alvarez & Gómez-Guillén, 2013; Oliveira, Pedro, Nunes, Costa, & Vaz-Pires, 2012). Due to the unpalatably high salt concentration in the fish muscle, salted cod must be desalted before consumption (Barat, Rodríguez-Barona, Andrés, & Visquert, 2004a). This process is traditionally carried out by immersing the salted cod in stagnant water over a period of 24–48 h. Thus, desalting is accomplished not only through the loss of salt but also as a result of sample rehydration (Barat, Rodríguez-Barona, Andrés & Ibañez, 2004b). The combined effect of water gain and salt loss on the protein matrix (Thorarinsdottir et al., 2011) modifies the product's structure. Protein rehydration involves a decrease in firmness (Barat et al., 2004a,b). Moreover, the reduction in NaCl content improve the water holding capacity, which, in turn, increases the water absorption, thus contributing to the total weight gain (Oliveira et al., 2012).

The main problems of industry-scale cod desalting are linked to the final product quality and long processing times (Pedro et al., 2002; Lorentzen, Ytterstad, Olsen, & Skjerdald, 2010). For this reason, recent research has gone into finding new cod desalting methods in order to improve the mass transfer process. In this sense, tumbling technology allows the processing time to be reduced by 70-90% (Skjerdal, Pedro, & Serra, 2002). However, it not only provides a product with an uneven salt content distribution but also physically damaged as a result of the product hitting (Bjørkevoll, Olsen, & Olsen, 2004). Andrés, Rodríguez-Barona, and Barat (2005) improved the mass transport by applying vacuum pulses (50 mbar); the effectiveness of this technology was highly dependent on the size and shape of the cod pieces. Recently, Salvador, Saraiva, Fidalgo and Delgadillo (2013) have applied high pressures (50-300 MPa), obtaining a significantly shorter process time. There has been no reported process influence on the final product quality in this study.

High-intensity ultrasound (**US**) is being used as a novel food process intensification technique (Tao & Sun, 2013; Chemat, Zill-e-Huma, & Khan, 2011). In liquid media, US enhances mass transfer mainly by inducing cavitation (Ozuna, Puig, García-Pérez, Mulet, & Cárcel, 2013). In addition, some other mechanical phenomena, such as the "sponge effect" (Cárcel, Benedito, Rosselló, & Mulet, 2007a), the generation of microchannels in the solids or microstirring at the solid-liquid interfaces, could also

affect both the external and internal mass transfer resistance (Fernandes, Gallão, & Rodrigues, 2008). Moreover, the mechanical stress that US cause in the product may modify both structural and textural properties (Deng & Zhao, 2008; Gabaldón-Leyva et al., 2007). Ultrasonic baths (Ozuna et al., 2013; Stadnik, Dolatowski, & Baranowska, 2008; Gabaldón-Leyva et al., 2007) and probes (Pananun, Montalbo-Lomboy, Noomhorm, Grewell, & Lamsal, 2012; Siró et al., 2009; Tiwari, Muthukumarappan, O'Donnell, & Cullen, 2008) are the devices most commonly used to apply US in liquid media. The effectiveness of applying US is directly linked to the actual acoustic energy introduced into the medium (Kulkarni & Rathod, 2013). This fact mainly depends on the emitter-liquid-product coupling, which should be experimentally determined in each specific application (Ahmad-Qasem et al., 2013; Cárcel, Benedito, Bon, & Mulet, 2007b).

US has been used to improve meat and cheese salting processes (Ozuna et al., 2013; Siró et al., 2009; Cárcel et al., 2007b; Sánchez, Simal, Femenia, Benedito, & Rosselló, 1999) but, as far as we are concerned, there is no previous literature on the use of US to improve the desalting of foodstuffs. Therefore, the aim of this work was to evaluate the feasibility of using US in cod desalting. For that purpose, mass transport kinetics was analyzed and research was carried out into whether any changes occur in microstructure and texture.

2. Materials and methods

2.1. Raw material and sample preparation

Salted cod (*Gadus morhua*) was provided by a local supplier (Carmen Cambra S. L., Spain) to ensure the homogeneity of the raw material. According to supplier specifications, cod fish were caught in high seas and processed immediately in the fishing boat (bled, gutted, beheaded, split and salted). The weight of the salted cod pieces was 1.50±0.25 kg. Parallelepiped-shaped samples (50 x 30 x 5 mm) were obtained from the central part of the cod loin using a sharp knife, wrapped in plastic waterproof film and kept refrigerated at 2±0.5 ºC (maximum storage time 120 h) until the desalting experiments.

2.2. Ultrasonic equipment

The desalting treatments were carried out in an ultrasonic bath (71 L, 40 kHz; ATU Ultrasonidos, Spain), equipped with a cooling jacket (Fig 1, F). The equipment allows the applied ultrasonic power to be modulated (up to 1500 W) (Fig. 1, L). For the temperature control, a glycol solution was pumped (1-38023 CLES, EBARA, Italy) (Fig. 1, D) from a reservoir tank (Fig. 1, E) into the cooling jacket. Afterwards, the glycol solution was cooled down in a plate heat exchanger connected to a chiller unit (Fig. 1, A). The temperature in the bath was measured using seven type K thermocouples (Fig. 1, H), placed in different positions and connected to a data logger (HP Data Logger 34970 A, Hewlett-Packard S.A., Spain) (Fig. 1, K), and recorded on a computer (Fig. 1, M).

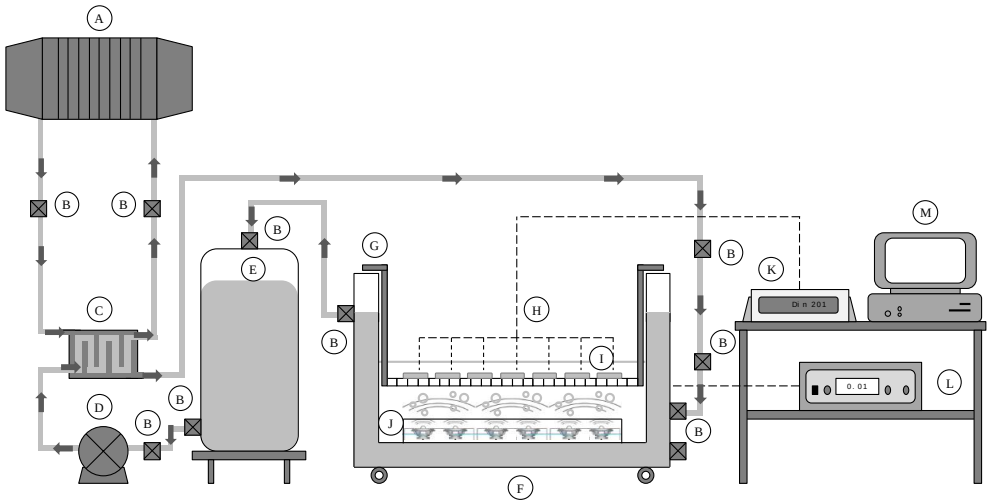

Fig. 1 Desalting set-up. A) Chiller B) Valve C) Plate heat exchanger D) Pump E) Cooling reservoir F) Ultrasonic bath G) Sample holder H) Thermocouples I) Salted cod samples J) Ultrasonic transducers K) Data logger L) Ultrasonic generator M) Computer.

2.3. Characterization of acoustic field

The electrical power supplied to the ultrasonic bath is frequently used as a rough estimation of the ultrasonic power applied. However, some facts, such as the electric/mechanical energy conversion factor or the medium attenuation, can affect the actual acoustic energy (Kulkarni & Rathod, 2013; Mulet, Cárcel, Benedito, Rosselló, & Simal, 2003). In this work, two different techniques were used to estimate the ultrasonic energy applied: calorimetry and acoustic pressure determination. The measurements were carried out at a depth of 100 mm from the water-air interface, where samples were placed during treatment. This depth corresponded to a maximum pressure plane detected through the erosion planes produced by cavitation on a piece of aluminum foil.

The calorimetric method consisted of recording the temperature, each second, for the first 1 min of US application (Cárcel et al., 2007b) at 7 different points (Fig. 1, H). Moreover, at least five replicates were carried out for each measurement. The slope of the temperature vs. time curve gave an estimation of the average ultrasonic power in the medium.

For the acoustic pressure measurement, a hydrophone (TC4013, Reson A/S, Denmark) was connected to a digital oscilloscope (Tektronix TDS 420 A, Tektronix Inc., USA) for signal digitalization. The output voltage level from the hydrophone (average of 100 signal acquisitions) was converted to the equivalent acoustic pressure (bar) by using the known sensitivity of the hydrophone. For the measurement, 2D scans were performed parallel to the length (X-axis) and perpendicular to the width (Y-axis) of the ultrasonic bath. The hydrophone was stepped in 30 mm increments in both X and Y-directions. In such a way, the surface of the ultrasonic bath (length 600 and width 300 mm) was mapped by measuring the acoustic pressure in a rectangular mesh of 171 nodes. These measurements allowed the acoustic field distribution to be determined thus, making it possible to identify the location of points with minimum and maximum energy levels.

2.4. Desalting experiments

For each desalting experiment, 28 samples were immersed in distilled water for 20 s to remove the superficially adhered salt. Then samples were blotted and weighed (PB3002-S/PH, J.P., Mettler Toledo, Spain). Afterwards, they were placed in a sample holder (Fig. 1, G) and introduced into the ultrasonic bath containing 27 L of low-mineral content water (Cortes, S.A., Spain). The ratio of salted cod/water was 0.01 kg cod/kg water, assuming no significant changes in the NaCl concentration of water occur during the desalting experiments. These were carried out without (CONTROL) and with US application. US was continuously applied using two electric powers: 1500 W (US-1500) and 750 W (US-750). At least 3 replicates were made for each treatment tested.

In order to determine the mass transport kinetics, four samples were randomly taken out from the bath at preset times (15, 30, 45, 60, 90, 120 and 180 minutes). Afterwards, samples were blotted, wrapped in plastic waterproof film and frozen (-18 ± 0.5 ºC) until moisture (method No. 950.46 AOAC, 1997) and NaCl (Cárcel et al., 2007b) were determined; this was carried out in triplicate in each case.

The thickness of each sample was measured before (T_0) and after (T) desalting with a Vernier caliper and the thickness ratio (TR) (Eq. (1)) was estimated as an index of swelling.

$$TR = \frac{T}{T_0} \tag{1}$$

Hardness (H), characterized as the maximum penetration force, was also evaluated in desalted cod samples at different times using a Texture Analyzer (TAX-T2®, Stable Micro System, United Kingdom). Penetration tests were conducted with a 2 mm flat cylinder probe (SMS P/2N), at a crosshead speed of 1 mm/s and a strain of 70% (penetration distance 3.5 mm). In each cod sample, a preset pattern was followed to carry out penetration tests at, at least, 12 different points.

2.5. Mathematical modeling

2.5.1. Moisture and NaCl transport

A mathematical model based on Fick's 2nd law (Cranck 1975) was used to describe the evolution of moisture and NaCl content in the samples during desalting separately. Samples were assumed to behave as infinite slabs; thus, mass transfer was simplified as one-dimensional. Constant effective diffusivities (D_{NaCl} and D_W), negligible changes in temperature and sample volume, solid symmetry, homogeneous initial NaCl and moisture contents and negligible external resistance (Barat et al., 2004a) were assumed. Eqs. (2) and (3) show the solution of the diffusion model in terms of the average moisture and NaCl content, respectively (Ozuna et al., 2013).

$$W = W_{eq} + (W_0 - W_{eq})\left[2\sum_{n=0}^{\infty}\frac{1}{\lambda_n^2 L^2}e^{-D_W\lambda_n^2 t}\right] \quad (2)$$

$$NaCl = NaCl_{eq} + \left(NaCl_0 - NaCl_{eq}\right)\left[2\sum_{n=0}^{\infty}\frac{1}{\lambda_n^2 L^2}e^{-D_{NaCl}\lambda_n^2 t}\right] \quad (3)$$

where, λ_n are the eigenvalues that are calculated by $\lambda_n L = (2n+1)\frac{\pi}{2}$.

The equilibrium moisture (W_{eq}) and NaCl ($NaCl_{eq}$) contents were determined by means of the desalting of cod samples for at least 24 h; this was the time established from previous experiments.

2.5.2. Hardness and swelling evolution

First-order reaction models, widely used to describe the kinetics of structural changes in processed foods (Blasco, Esteve, Frígola, & Rodrigo, 2004; Baik & Mittal, 2003), were considered to study the evolution of hardness and swelling in the salted cod during desalting. Thus, experimental data on the thickness ratio (TR) and hardness (H) was modeled following Eq. (4) and Eq. (5), respectively.

$$TR = TR_{eq} + (TR_0 - TR_{eq})e^{(-k_{TR}\cdot t)} \quad (4)$$

$$H = H_{eq} + (H_0 - H_{eq})e^{(-k_H\cdot t)} \quad (5)$$

2.5.3. Model fitting

The parametric identification of the first order kinetics (k_{TR}, TR_{eq}, k_H and H_{eq}) and the diffusion models (D_{NaCl}, D_W) was carried out by using an optimization procedure that minimized the sum of the squared differences between the experimental and calculated data. For that purpose, the non-linear optimization algorithm of the Generalized Reduced Gradient (GRG), available in Microsoft Excel™ spreadsheet from MS Office 2010 (Microsoft Corporation, USA), was used. The goodness of the fit was determined by assessing the percentage of explained variance, VAR (%) (Eq. (6)).

$$VAR(\%) = \left[1 - \frac{S_{xy}^2}{S_y^2} \right] \cdot 100 \quad (6)$$

2.6. Microstructure

2.6.1. Scanning electron microscopy (SEM) with combined dispersion X-ray analysis (SEM-EDX)

Cubic samples (side 3 mm) of salted and desalted cod (CONTROL, US-750 and US-1500 after 180 min of desalting) were immersed in liquid nitrogen and then freeze-dried at 1 Pa for 3 days (LIOALFA-6, Telstar, Spain). Then the samples were vacuum sealed in vials in the same freeze-drier so that they would remain stable (Hernando, Llorca, Puig, & Lluch, 2011). After that, they were individually placed on SEM slides with the aid of colloidal silver and then gold-coated with carbon (SCD005, Baltec, Germany) at 10^{-2} Pa and an ionization current of 40 mA. The samples were observed through a scanning electron microscope (JSM-5410, Jeol, Japan) equipped with an X-ray detector and LINK data-processing system (INCA 4.09, Oxford Instruments, England) at an acceleration voltage of 10-20 kV, which provides internal information about the standards of the energy dispersive X-ray spectra of the elements analyzed (Na^+ and Cl^-). This technique is an analytical tool that allows the Cl^- and Na^+ ions inside the samples to be identified (Ozuna et al., 2013). For the EDX (energy-dispersive X-ray) analysis, the samples were carbon-coated (CEA035, Baltec, Germany). Mapping images of Cl^- and Na^+ distribution in cod samples were taken using a voltage of 20 kV and at a working distance of 15 mm.

2.6.2. Light microscopy (LM)

For LM observation, cryostat sections (200 μm) were obtained from frozen desalted cod (CONTROL, US-750 and US-1500 after 180 min of desalting) using a CM1950 microtome (Leica Biosystems, Germany). The sections were transferred to coated glass slides, which had previously been placed inside the cryo chamber to achieve an improved adherence of the tissue sections (Thorarinsdottir et al., 2011). The cryostat section samples were examined under a light microscope (Nikon Eclipse E800, Japan).

The fiber thickness was measured from micrographs obtained by both light microscopy and SEM-EDX using the ImageJ 1.44d software (Wayne Rasband, National Institute of Health, USA). All the measurements were assessed from at least six randomly acquired images.

2.7. Statistical analysis

In order to identify if US application significantly ($p<0.05$) influenced both the mass transport kinetics and the hardness and swelling of the samples during the desalting process, an analysis of variance (ANOVA) ($p<0.05$) was carried out and the least significant difference (LSD) intervals were identified using the Statgraphics Plus 5.1. statistical package (Statistical Graphics Corp., USA).

3. Results and discussion

3.1. Acoustic field characterization

The acoustic field characterization was carried out at two different levels of electric power applied to the bath: 750 W (US-750) and 1500 W (US-1500). From the calorimetric measurements, it was obtained that the average volumetric energy available in the medium was 18.7±5.0 kW/m^3 and 37.9±5.2 kW/m^3 for US-750 and US-1500, respectively. The calorimetric/electric yields were close to 70%. As can be seen, doubling the electric energy supplied to the ultrasonic transducer also doubles the acoustic energy measured in the medium.

The acoustic pressure measurements showed a very irregular acoustic field distribution in the bath (Fig 2, A and B). In addition, the acoustic field pattern for US-750 was quite different from that for US-1500. The reflections of ultrasonic waves at the

moving air-water interface or the bath walls (Kulkarni & Rathod, 2013) and the implosions of cavitation bubbles (Mulet et al., 2003) can generate this heterogeneous ultrasonic field. For US-1500, the integrated average acoustic pressure was 0.51±0.10 bar (Fig. 2, B; range 0.25-0.75 bar), while for US-750 it was 0.39±0.13 bar (Fig. 2, A; range 0.13-0.70 bar). Thereby, doubling the supply of electric power does not lead to there being twice the acoustic pressure in the medium; this differs from what was observed from the calorimetric measurements.

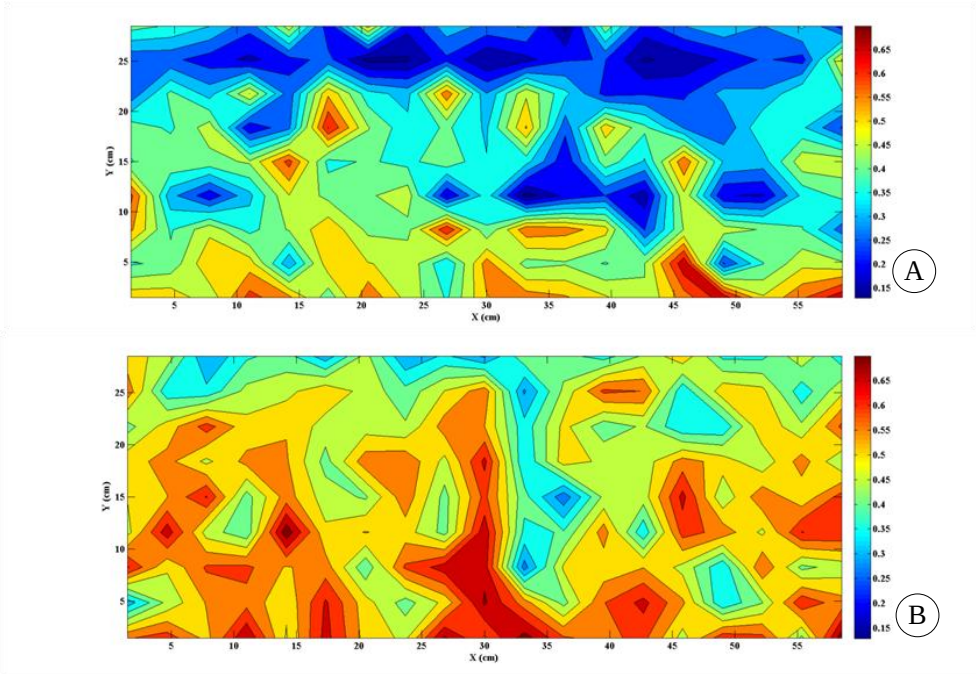

Fig. 2 Distribution of acoustic pressure (bar) measured by a hydrophone in the ultrasonic bath with an applied electric power of 750 W (A) and 1500 W (B). Measurements carried out in a horizontal section at 100 mm from the water (27 L) surface.

The calorimetric method provided a measurement of the amount of acoustic energy converted into heat, while the hydrophone provided a direct measurement of the acoustic pressure present in the bath. The interaction between waves of different directions produced by reflections or cavitation can partially neutralize them, which produces a conversion of acoustic energy into heat. Therefore, the acoustic pressure method is a more accurate means of measuring the actual level of applied ultrasonic energy than the calorimetric.

3.2. NaCl and water transport

3.2.1. NaCl and water content

Salted cod loin showed an initial NaCl content of 0.63±0.20 kg NaCl/kg SFS (salt-free solids). The immersion of samples in water produced a decrease in NaCl content, which was greater when US was applied (Fig. 3, A). Thus, after 180 min of desalting, the NaCl content in the US-1500 (0.114±0.015 kg NaCl/kg SFS) was 32% lower than that measured in CONTROL samples (0.167±0.037 kg NaCl/kg SFS). In terms of treatment time, US-1500 samples needed approximately 50% less time than CONTROL ones to reach the same NaCl content. US-750 was found to need an intermediate treatment time, in which case the US influence depended on the acoustic power applied (Fig. 3, A).

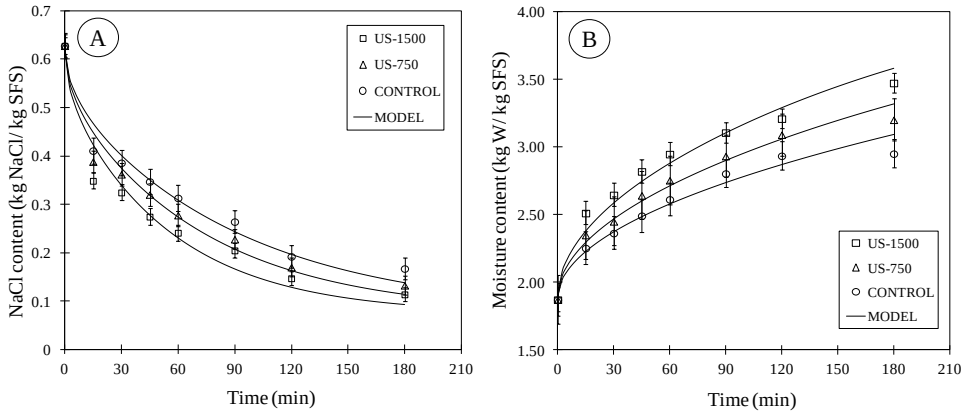

Fig. 3 Experimental NaCl (A) and moisture (B) transport kinetics of salted cod slices (thickness 5 mm) desalted with (US, 40 kHz, 750 and 1500 W) and without ultrasound application (CONTROL). Each point represents the average of 12 measurements: four independently desalted samples analyzed in triplicate. Average values ± LSD intervals ($p<0.05$) are plotted.

As regards the moisture content, the cod loin's initial content of 1.87±0.22 kg water/kg SFS salted increased during the experiments. The US application also significantly ($p<0.05$) accelerated the water transport (Fig. 3, B). For example, the moisture content of CONTROL after 180 min of treatment (2.95±0.38 kg water/kg SFS) was achieved for US-1500 in only 63 min (65 % reduction in treatment time). As

in the case of NaCl transport, the water gain was dependent on the acoustic power applied.

3.2.2. Modeling transport kinetics

The fit of the proposed diffusion models to the experimental data provided percentages of explained variance ranging from 93 to 95% for NaCl and 95 to 97% for moisture kinetics (Table 1). These low values can be attributed to the great variability of the raw material and the complexity of the desalting process (Oliveira et al., 2012; Barat et al., 2004 a,b). However, the fact that the trend observed between the calculated and experimental data was similar (Fig. 3), showed the goodness of the model.

Table 1 Effective diffusivity of moisture (D_W) and NaCl (D_{NaCl}) identified from modeling of mass transport in cod desalting (4±1 ºC) with (US, 40 kHz, 750 and 1500 W) and without US application (CONTROL) and percentage of explained variance by the model (VAR (%)). ΔD_W and ΔD_{NaCl} (%) are the increases in effective diffusivity produced by ultrasound application. Average ± confidence intervals of the estimation (significance level 95%) are shown.

	NaCl transport			Water transport		
	D_{NaCl} (10^{-10}) [m^2/s]	ΔD_{NaCl} (%)	VAR (%)	D_W (10^{-10}) [m^2/s]	ΔD_W (%)	VAR (%)
CONTROL	4.57 ± 0.81	-	95.0	1.09 ± 0.17	-	95.0
US-750	5.71 ± 1.01	24.9	95.7	1.54 ± 0.18	41.3	97.2
US-1500	7.40 ± 1.08	61.9	93.3	2.21 ± 0.32	102.8	95.0

The D_{NaCl} values identified for CONTROL (4.57 x 10^{-10} m^2/s) were in the same order of magnitude as others found in literature. Barat et al. (2006 and 2004b) reported values of 5.69 x 10^{-10} and 2.33 x 10^{-10} m^2/s for cod desalting at 4 and 5 ºC, respectively. The US application during desalting produced a significant ($p<0.05$) increase in D_{NaCl}, which depended on the power applied. Thus, D_{NaCl} was 25% higher for US-750 and 62% higher for US-1500 than that identified for CONTROL experiments (Table 1). In this sense, Siró et al. (2009) found increases of 96% in D_{NaCl} when US was applied during meat brining (5 ºC, 4% NaCl), and Gabaldón-Leyva et al.

(2007) stated an improvement of 190% in the total solid diffusion coefficients during the brining of bell pepper (55 ºC, 13.51% NaCl). No accurate measurement of the acoustic pressure introduced into the medium was reported in these papers. Comparing US-750 and US-1500 experiments, it can be observed that the 30% increase in the acoustic pressure (from 0.39 bar in US-750 to 0.51 bar in US-1500) produced the 30% increases in D_{NaCl} (from 5.71 x 10^{-10} m^2/s in US-750 to 7.40 x 10^{-10} m^2/s in US-1500). Taking into account the power value determined by calorimetry (18.7 kW/m^3 in US-750 to 37.9 kW/m^3 in US-1500), an effective diffusivity increase of 103% will be expected. However, it must be highlighted that during desalting experiments, the temperature was held at 4 ºC. Therefore, the US influence on mass transport was not due to thermal effects, but just to mechanical effects. In this sense, the calorimetric measurements included thermal effects, but the acoustic pressure measurements only provided a measurement of the acoustic field with the capacity to produce mechanical effects.

In the case of moisture transport, the increase in D_W brought about by US application was close to 41% for US-750 and 103% for US-1500 as compared to CONTROL experiments. Ozuna et al. (2013) reported increases in D_W of around 101% when US was applied in meat brining (5 ºC, 28% NaCl) and Cárcel et al. (2007a) found increases of 117% in moisture transport during the osmotic dehydration of apple (30 ºC, 30 ºBrix). As in the case of D_{NaCl}, the observed increase in D_W was also well correlated with the acoustic pressure measured in the medium.

The identified effective diffusivities (D_{NaCl} and D_W) are global mass transport parameters which include not only pure diffusion mechanisms but also other phenomena affecting convective flow (Tao & Sun, 2013). Therefore, the influence of US can be attributed to phenomena that affect diffusion, like the "sponge effect" or the generation of microchannels, and to those that influence the convective flow, such as pressure variations, oscillating velocities or microstreaming (Chemat et al., 2011; Fernandes et al., 2008). As previously explained, temperature control avoids any improvement linked to thermal energy.

3.3. Swelling evolution

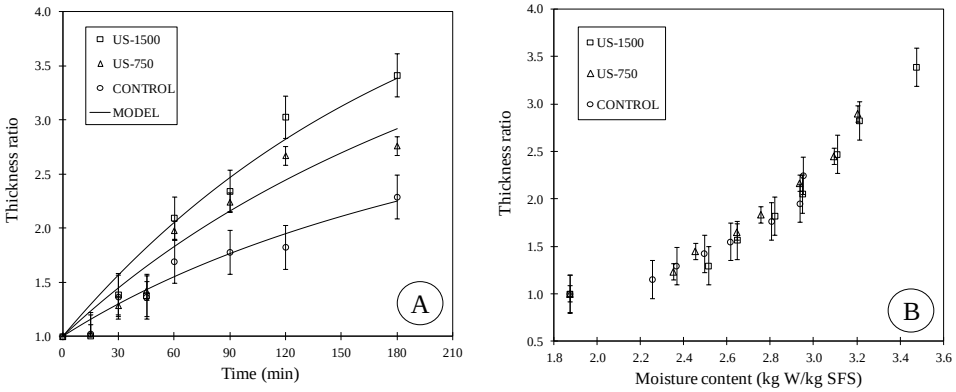

Fig. 4 Evolution of thickness ratio vs time (A) and vs moisture content (B) during desalting of salted-cod with (US, 40 kHz, 750 and 1500 W) and without ultrasound application (CONTROL). Each point represents the average of 8 measurements. Average values ± LSD intervals ($p<0.05$) are plotted.

Sample swelling during the desalting process was followed from the evolution of the thickness ratio (TR), (Eq. 1). The application of US increased the TR and this increase depended on the level of acoustic power applied (Fig. 4, A). Thus, after 180 min desalting, while US-750 samples showed a TR value (2.76±0.10) which was 22% higher than that of CONTROL (2.25±0.41), this increase was of 50% for US-1500 (3.38±0.28).

Table 2 First-order kinetic parameters for thickness ratio (TR_{eq}, K_{TR}) and evolution of hardness (H_{eq}, K_H) during cod desalting (4±1 ºC) with (US, 40 kHz, 750 and 1500 W) and without US application (CONTROL). Average ± confidence intervals of the estimation (significance level 95%) are shown.

	Swelling evolution			Hardness evolution		
	TR_{eq}	k_{TR} (10^{-3}) [min^{-1}]	VAR (%)	H_{eq} (N)	k_H [min^{-1}]	VAR (%)
CONTROL	3.07±0.20	5.14±2.12	94.4	1.26±0.08	0.056±0.024	99.1
US-750	4.14±0.43	5.17±0.98	92.9	1.14±0.06	0.121±0.025	99.6
US-1500	4.87±0.38	5.20±1.07	92.7	1.15±0.09	0.167±0.073	99.2

Considering the experimental variability, the first order kinetic (Eq. (4)) provided an adequate estimation of the TR (VAR close to 93%). The rate constant (k_{TR}), which is related with the rate of swelling during desalting, was not significantly ($p<0.05$) increased by US application (Table 2). As can be observed in Fig. 4, B, there was no direct kinetic effect on the swelling itself produced by applying US, but the influence observed in the experimentally measured swelling can be just linked to the fact that US application intensified water transport.

3.4. Evolution of hardness

The measurement of the maximum penetration force was used to monitor the evolution of cod hardness during desalting. The initial degree of hardness of the salted cod (3.62±0.35 N) reduced as the desalting process progressed (Fig. 5). Major hardness changes took place in the first 45 min and an asymptotic value was found after approximately 60 min of desalting (Fig. 5, A). The softening of cod samples can mainly be ascribed to the rehydration of the protein matrix and fast salt dissolution (Barat et al., 2004a).

US application accelerated the reduction of hardness (Fig. 5, A). The greatest differences between CONTROL and US experiments were observed at the beginning of desalting. Unlike what was observed in the case of swelling, the influence of US on the evolution of hardness can be attributed not only to the ultrasonic intensification of mass transport but also to some textural effects (Stadnik et al., 2008), since, at a similar water content (Fig. 5, B), US samples exhibited a lower hardness value than CONTROL. As far as the applied ultrasonic power is concerned, there were no differences observed between US-750 and US-1500.

The ability of US to induce structural effects has already been reported (Ozuna et al., 2013). Deng and Zhao (2008) and Gabaldón-Leyva et al. (2007) reported a softening of vegetable samples during osmotic treatments when US was applied, due to the disruption of the cell walls. The compressions and expansions produced by US induced mechanical stress on the protein structure and the constituents of the connective tissue that can lead to softening (Fig. 5, B).

The first-order kinetic model (Eq. 5) accurately described the hardness changes during desalting (Fig. 5, A) providing a VAR of over 99% (Table 2). Both model parameters (k_H and H_{eq}) were significantly ($p<0.05$) affected by US application. However, no

significant differences were found between the two acoustic powers tested. The rate constant (K_H) significantly ($p<0.05$) increased when acoustic energy was applied according to the faster drop in hardness when US was applied (Fig. 5, B). The equilibrium hardness (H_{eq}) was lower for US treatments than CONTROL, which may be ascribed to the abovementioned structural effects of US.

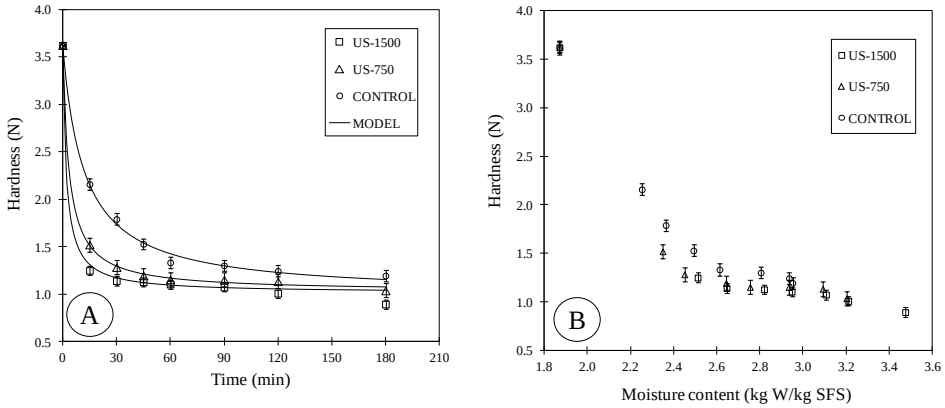

Fig. 5 Evolution of hardness vs time (A) and vs moisture content (B) during desalting of salted-cod with (US, 40 kHz, 750 and 1500 W) and without ultrasound application (CONTROL). In this figure, each point represents the average of 30 measurements. Average values ± LSD intervals ($p<0.05$) are plotted.

3.5. Microstructure

The microstructure of salted cod was studied from micrographs obtained by means of SEM (Fig. 6). Fig 6, A shows a longitudinal section of salted cod, where three fibers can be observed covered by salt deposits. Salted cod fibers show an intense dehydration and compaction with a total degradation of connective tissue. Fig. 6, B shows a cross section of salted cod tissue, where the presence of salt makes the etching of the sample for observation difficult and masks the underlying structures.

During desalting, important changes in the structural properties of salted cod take place as a consequence of cell rehydration. After 180 min of treatment, samples showed a significant swelling of muscle fibers (Fig. 7, A, B and C) compared to salted cod (Fig. 6). Thus, the average width increased from 64.40±9.18 μm of salted cod fibers to 84.13±11.73 μm in CONTROL samples. This increase was even greater when US was applied (Figs. 7, B and C). In this sense, US-1500 fibers (Fig. 7, C) were, on average, 27% wider (106.71±11.48 μm) than CONTROL. The fiber width increase

was also observed in LM micrographs. In this case, the measured fiber width increased from 90.36±4.41 μm in CONTROL (Fig. 7, D) to 108.77±13.18 and 139.39±11.66 μm in US-750 (Fig. 7, E) and US-1500 (Fig. 7, F), respectively. The differences between LM and SEM measurements can be attributed to the differences in sample preparation.

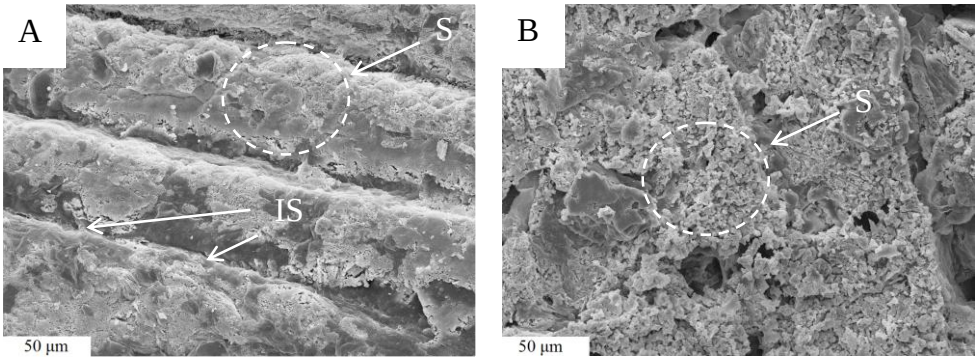

Fig. 6 Longitudinal (A) and transversal (B) section of salted cod (*Gadus morhua*) fibers observed by SEM (x500). S: NaCl deposits, IS: Interfibrillar space.

The fiber width increase explains the macroscopic swelling already described in Fig. 4. In addition, the US application increased the interfibrillar spaces (IS) in cod tissue (Figs. 7, B and C) that can also contribute to the softening of US samples (Fig. 5). The SEM-EDX technique confirmed the presence of residual NaCl in samples after desalting (180 min). US application intensified the NaCl leakage (Figs. 7, B and C), which was manifested by a lower number of dots in micrographs than in CONTROL (Fig. 7, A).

The damage to desalted cod fibers brought about by the salting process (Fig. 7, D) and the mechanical effects of acoustic energy during the desalting process (Figs. 7, E and F) were also observed by LM. The US samples showed greater fiber and connective tissue degradation (Figs. 7, E and F) than CONTROL (Fig. 7, D). This fact can be attributed to violent microjets produced by the asymmetric implosion of bubbles near the solid surface. These results coincide with those found by other authors who related the application of US with the physical disruption of the myofibril structure (Ozuna et al., 2013), the degradation of collagen macromolecules, or the creation of micro-channels (Jayasooriya, Bhandari, Torley, & D'Arcy, 2004).

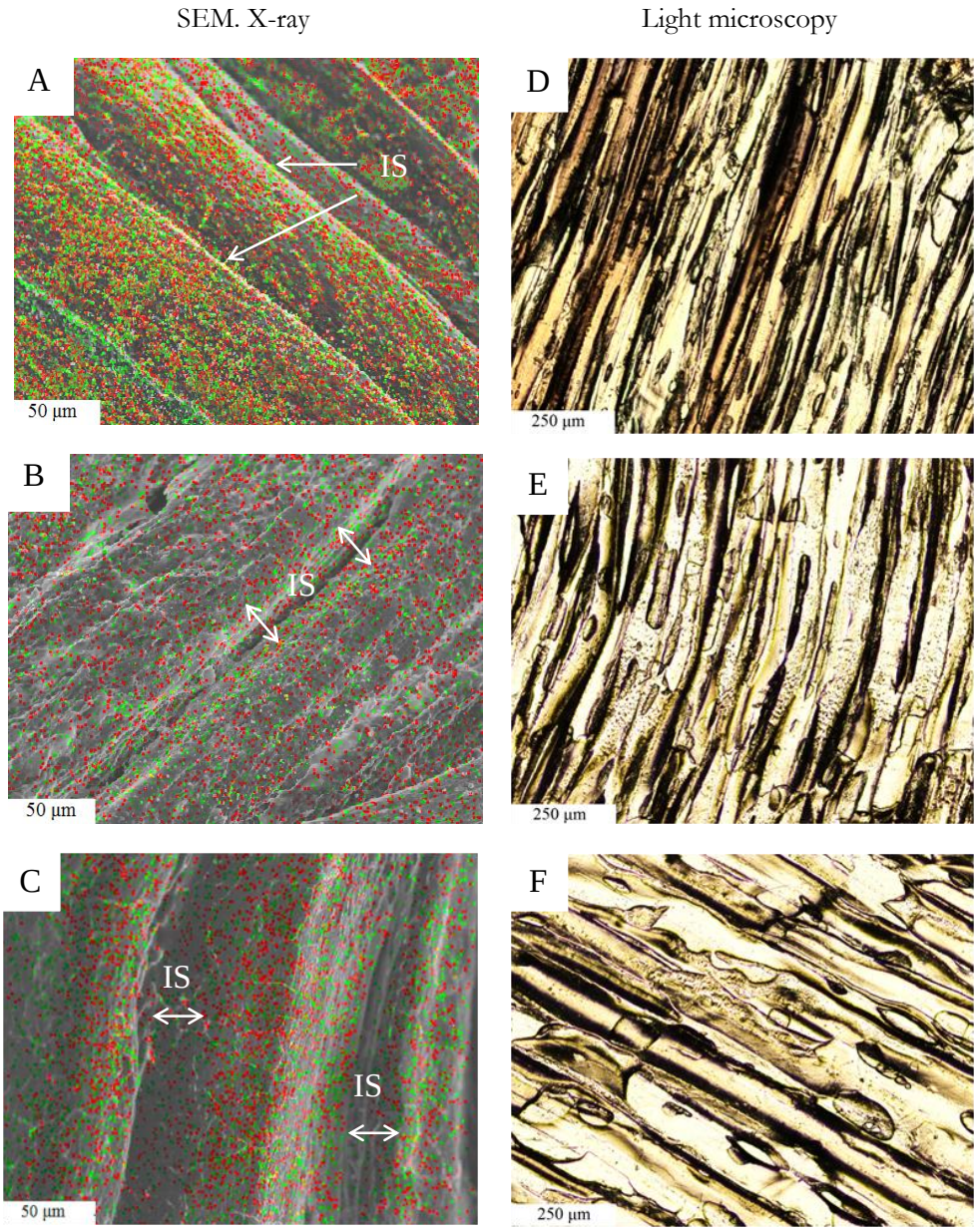

Fig. 7 Longitudinal section observed by SEM-EDX (A, B and C; x500) and LM (D, E and F; x4) of cod loin desalted for 180 min without (CONTROL, A, D), and with US at 750 (B, E) and 1500 W (C, F). IS: Interfibrillar space.

4. Conclusions

The application of high-intensity ultrasound improved cod desalting, increasing both moisture and NaCl effective diffusivities up to 103 and 62%, respectively. The desalting process induced both tissue swelling and hardness decrease in the samples, both of which were intensified by ultrasound application. Microstructural analyses showed that cod fibers were significantly affected by ultrasound application. These facts coincide with the intensification of mass transport and the observed enhancement of both swelling and hardness decrease. Therefore, high-intensity ultrasound could be considered a non-thermal technology, suitable as a means of intensifying the desalting process.

Acknowledgments

The authors acknowledge the financial support of the Spanish Ministerio de Economía y Competitividad and FEDER (Ref. DPI2013-37466-C03-03). The author César Ozuna thanks Universitat Politècnica de València for an FPI grant (Ref. 2009-02). The author also wishes to thank Carmen Cambra S.L. for providing the homogeneous raw material.

Nomenclature

SFS	Salt-free solids
W_0	Initial moisture content, kg water/kg SFS
W_{eq}	Equilibrium moisture content, kg water/kg SFS
$NaCl_0$	Initial sodium chloride content, kg NaCl/ kg SFS
$NaCl_{eq}$	Equilibrium sodium chloride content, kg NaCl/kg SFS
t	Time, s
D_{NaCl}	Effective NaCl diffusivity, m^2/s
D_W	Effective moisture diffusivity, m^2/s
ΔD_{NaCl}	Increment of effective NaCl diffusivity by ultrasound application, %
ΔD_W	Increment of effective moisture diffusivity by ultrasound application, %
L	Half length, m
λ_n	Eigenvalues
T_0	Initial sample thickness, m
T	Thickness after a certain time of treatment, m
TR_0	Initial thickness ratio
TR_{eq}	Equilibrium thickness ratio
H_0	Initial equilibrium, N
H_{eq}	Equilibrium hardness, N
k_{TR}	Rate constant of thickness ratio, 1/s
k_H	Rate constant of hardness, N/s
S_y	Standard deviation of the sample
S_{yx}	Standard deviation of the estimation

References

Ahmad-Qasem, M. H., Cánovas, J., Barrajón-Catalán, E., Micol, V., Cárcel, J. A., & García-Pérez, J. V. (2013). Kinetic and compositional study of phenolic extraction from olive leaves (var. Serrana) by using power ultrasound. *Innovative Food Science & Emerging Technologies*, 17, 120-129.

Andrés, A., Rodríguez-Barona, S., & Barat, J.M. (2005). Analysis of some cod-desalting process variables. *Journal of Food Engineering*, 70, 67-72.

Association of Official Analytical Chemists. Official Methods of Analysis; AOAC: Washington, DC, 1997.

Baik, O. D., & Mittal, G. S. (2003). Kinetics of tofu color changes during deep-fat frying. *LWT-Food Science and Technology*, 36, 43-48.

Barat, J. M., Gallart-Jornet, L., Andrés, A., Akse, L., Carlehög, M., & Skjerdal, O. T. (2006). Influence of cod freshness on the salting, drying and desalting stages. *Journal of Food Engineering*, 73, 9-19.

Barat, J.M., Rodríguez-Barona, S., Andrés, A. & Visquert, M. (2004a). Mass transfer analysis during the cod desalting process. *Food Research International*, 37, 203-208.

Barat, J. M., Rodríguez-Barona, S., Andrés, A., & Ibáñez, J. B. (2004b). Modeling of the cod desalting operation. *Journal of Food Science*, 69, FEP183-FEP189.

Bjørkevoll, I. Olsen, J., & Olsen, R.L. (2004). Rehydration of salt-cured cod using injection and tumbling technologies. *Food Research International*, 37, 925-931.

Blasco, R., Esteve, M. J., Frígola, A., & Rodrigo, M. (2004). Ascorbic acid degradation kinetics in mushrooms in a high-temperature short-time process controlled by a thermoresistometer. *LWT-Food Science and Technology*, 37, 171-175.

Cárcel, J.A., Benedito, J., Rosselló, C., & Mulet, A. (2007a). Influence of ultrasound intensity on mass transfer in apple immersed in a sucrose solution. *Journal of Food Engineering*, 78, 472-479.

Cárcel, J. A., Benedito, J., Bon, J., & Mulet, A. (2007b). High intensity ultrasound effects on meat brining. *Meat science*, 76, 611-619.

Chemat, F., Zill-e-Huma, & Khan, M.K. (2011). Applications of ultrasound in food technology: processing, preservation and extraction. *Ultrasonics Sonochemistry*, 18, 813–835.

Crank, J. (1975). *The Mathematics of Diffusion*. London: Oxford University Press.

Deng, Y., & Zhao, Y. (2008). Effects of pulsed-vacuum and ultrasound on the osmodehydration kinetics and microstructure of apples (Fuji). *Journal of Food Engineering*, 85, 84-93.

Fernandes, F. A. N., Gallão, M. I., & Rodrigues, S. (2008). Effect of osmotic dehydration and ultrasound pre-treatment on cell structure: melon dehydration. *LWT-Food Science and Technology*, 41, 604-610.

Gabaldón-Leyva, C. A., Quintero-Ramos, A., Barnard, J., Balandrán-Quintana, R. R., Talamás-Abbud, R., & Jiménez-Castro, J. (2007). Effect of ultrasound on the mass transfer and physical changes in brine bell pepper at different temperature. *Journal of Food Engineering*, 81, 374–379.

Hernando, I., Llorca, E., Puig, A. & Lluch, M.A. (2011). Microstructure. In L.M.L., M.L. Leo & F. Toldra (Eds.), Handbook of Seafood and Seafood Products Analysis (pp. 139-151). Boca Raton FL: CRC Press Taylor & Francis Group.

Jayasooriya, S. D., Bhandari, B. R., Torley, P., & D'Arcy, B. R. (2004). Effect of high power ultrasound waves on properties of meat: a review. *International Journal of Food Properties*, 7, 301-319.

Kulkarni, V. M., & Rathod, V. K. (2013). Mapping of an ultrasonic bath for ultrasound assisted extraction of mangiferin from *Mangifera indica* leaves. *Ultrasonics Sonochemistry*. http://dx.doi.org/10.1016/j.ultsonch.2013.08.021.

Lorentzen, G., Ytterstad, E., Olsen, R.L., & Skjerdald, T. (2010). Thermal inactivation and growth potential of *Listeriainnocua* in rehydrated salt-cured cod prepared for ready-to-eat products. *Food Control*, 21, 1121-1126.

Martínez-Alvarez, O., & Gómez-Guillén, C. (2013). Influence of mono- and divalent salts on water loss and properties of dry salted cod fillets. *LWT-Food Science and Technology*, 53, 387-394.

Mulet, A., Cárcel, J. A., Benedito, J., Rosselló, C. & Simal, S. (2003). Ultrasonic mass transfer enhancement in food processing. In: Transport Phenomena in Food Processing. Welti-Chanes, J., Vélez-Ruiz, J. & Barbosa-Cánovas, G (Eds). CRC Press. Boca Raton. USA. 265-277.

Oliveira, H. , Pedro S., Nunes, M. L., Costa, R., & Vaz-Pires, P. (2012). Processing of salted cod (*Gadus* spp.): a review. *Comprehensive Reviews in Food Science and Food Safety*, 11, 546-564.

Ozuna, C., Puig, A., García-Pérez, J.V., Mulet, A., & Cárcel, J.A. (2013). Influence of high intensity ultrasound application on mass transport, microstructure and textural properties of pork meat (*Longissimus dorsi*) brined at different NaCl concentrations. *Journal of Food Engineering*, 119, 84-93.

Pananun, T., Montalbo-Lomboy, M., Noomhorm, A., Grewell, D., & Lamsal, B. (2012). High-power ultrasonication-assisted extraction of soybean isoflavones and effect of toasting. *LWT-Food Science and Technology*, 47, 199-207.

Pedro, S., Magalhães, N., Albuquerque, M.M., Batista, I., Nunes, M.L., & Bernardo, F. (2002). Preliminary observations on spoilage potential of flora from desalted cod (*Gadus morhua*). *Journal of Aquatic Food Product Technology*, 11, 143-150.

Salvador, Â. C., Saraiva, J. A., Fidalgo, L. G., & Delgadillo, I. (2013). Effect of high pressure on cod (*Gadus morhua*) desalting. *High Pressure Research*, 33, 432-439.

Sánchez, E. S., Simal, S., Femenia, A., Benedito, J., & Rosselló, C. (1999). Influence of ultrasound on mass transport during cheese brining. *European Food Research and Technology*, 209, 215-219.

Siró, I., Vén, C., Balla, C., Jónás, G., Zeke, I., & Friedrich, L. (2009). Application of an ultrasonic assisted curing technique for improving the diffusion of sodium chloride in porcine meat. *Journal of Food Engineering*, 91, 353-362.

Skjerdal, O.T., Pedro, S. & Serra, J.A. Improved quality and shelf life of desalted cod– an easy-to-use product of salted cod. Final Report to the European Commission. FAIR Project CT98-4179.

Stadnik, J., Dolatowski, Z. J., & Baranowska, H. M. (2008). Effect of ultrasound treatment on water holding properties and microstructure of beef (*m. semimembranosus*) during ageing. *LWT-Food Science and Technology*, 41, 2151-2158.

Tao, Y., & Sun, D. (2013). Enhancement of food processes by ultrasound: a review. *Critical Reviews in Food Science and Nutrition*. http://dx.doi.org/10.1080/10408398.2012.667849.

Thorarinsdottir, K. A., Arason, S., Sigurgisladottir, S., Gunnlaugsson,V. N. Johannsdottir, J., & Tornberg, E. (2011). The effects of salt-curing and salting procedures on the microstructure of cod (*Gadus morhua*) muscle. *Food Chemistry*, 126, 109-115.

Tiwari, B. K., Muthukumarappan, K., O'Donnell, C. P., & Cullen, P. J. (2008). Colour degradation and quality parameters of sonicated orange juice using response surface methodology. *LWT-Food Science and Technology*, 41, 1876-1883.

CHAPTER 3

Low-Temperature Drying

Innovative Food Science & Emerging Technologies (Submitted)

Low-Temperature Drying of Salted Cod (*Gadus morhua*) Assisted by High Power Ultrasound: Kinetics and Physical Properties

César Ozuna[a], Juan A. Cárcel[a], Per M. Walde[b], Jose V. Garcia-Perez[a,]*

[a] Grupo de Análisis y Simulación de Procesos Agroalimentarios.
Departamento de Tecnología de Alimentos.
Universitat Politècnica de València.

Camino de Vera. s/n. E46022. Valencia, Spain

[b] Aalesund University College,

N-6025 Ålesund, Norway

Abstract

Low-temperature convective drying could be considered an affordable alternative to conventional freeze-drying for foodstuffs. The process intensification should be based on non-thermal technologies, such as power ultrasound. Thereby, the aim of this work was to evaluate the air-borne application of power ultrasound on the low-temperature drying of salted cod, quantifying its influence on the drying kinetics and physical properties of the final dried product. For that purpose, drying experiments were carried out at -10, 0, 10 and 20 °C on salted cod slabs (length 50 mm, width 30 mm and thickness 5 mm) at constant air velocity (2 ± 0.1 m/s) and relative humidity (9 ± 4%) with (AIR+US, 20.5 kW/m^3) and without ultrasonic application (AIR). In the dried-salted cod, its rehydration capacity (27 h, 4 ºC) was analyzed, as were the microstructural, textural and color changes. Diffusion and empirical models were used in order to quantify the influence of the ultrasound application and the drying temperature on drying and rehydration kinetics, respectively. At every temperature tested, ultrasound application increased the drying rate; thus, an average increase of 74% was observed in the effective moisture diffusivity. AIR+US dried samples were softer and exhibited a higher rehydration capacity than AIR ones, which was linked to the microstructural changes produced by ultrasound. In addition, significant ($p<0.05$) color changes were induced by ultrasound application.

Industrial relevance: Nowadays, low-temperature convective drying represents a promising alternative for the production of high-quality dried products. However, this technology is mostly limited by the low drying rate, which retards the dehydration process and directly increases the processing costs. Power ultrasound, a non-thermal technology, represents an interesting alternative means of improving low-temperature convective drying due to the fact that acoustic (mechanical) waves may affect water removal during drying with a low heating capacity. Thereby, the ultrasonically enhanced low-temperature convective drying could constitute an affordable alternative to lyophilization (or freeze-drying), which is mainly restricted to high quality food commodities.

Keywords:
Ultrasonic; non-thermal processing, dehydration; rehydration; microstructure; texture; color.

1. Introduction

Dried-salted cod (*Gadus morhua*) or klipfish has long been highly appreciated due to its high nutritional value and specific sensory properties (Walde, 2003). Although, dried-salted cod presents a water content of under 45% (wet basis), its salt content may reach 20% (wet basis) (Barat, Rodríguez-Barona, Andrés, & Fito, 2003). The processing includes the following steps: salting, washing, pre-drying by keeping the green salted cod for several days in piles outside the drying chambers, drying, grading and packaging (Oliveira, Pedro, Nunes, Costa, & Vaz-Pires, 2012). The drying of salted cod is performed at temperatures of around 20 ºC and at relative humidities of under 70% (Walde, 2003). Two main products can be found on the market depending on the intensity of the drying process: semi-dried or extra-dried cod.

The quality of dried-salted cod is greatly influenced by the salting and drying operation (Kilic, 2009). Salting induces changes in the muscle protein, generating modification in the texture, weight and water holding capacity (Oliveira et al., 2012). As far as drying is concerned, the use of high temperatures entails chemical and microbiological changes (Ortiz et al., 2013), structural, physical and mechanical modifications (Duan, Jiang, Wang, Yu, & Wang, 2011), crust formation on the surface (Bellagha, Sahli, Farhat, Kechaou, & Glenza, 2007) and the reduction of the hydration capacity of proteins (Brás & Costa 2010).

The use of low-temperature convective drying constitutes an interesting alternative means of improving the quality of the dried-salted cod due to the fact that it provides products with similar quality characteristics than conventional freeze-drying at lower cost (Kilic, 2009). The term "low temperature" makes reference to the use of air temperatures below standard room conditions, which includes figures below or close to the product's freezing point. Despite its great potential, the use of low-temperatures in convective drying is mostly limited by the low drying rate, which retards the dehydration process and directly increases the processing costs (Walde, 2003). In this regard, it is of great interest to deal with the process intensification in order to improve the drying rate. For that purpose, coupling non-thermal technologies, such as power ultrasound (Ortuño, Martínez-Pastor, Mulet, & Benedito, 2012), to convective drying so as to achieve a higher yield, a lower energy use and high product quality and processing safety (Garcia-Perez, Carcel, Riera, Rosselló, & Mulet, 2012a) is worth exploring.

The application of power ultrasound may be accomplished by direct-contact or air-borne transmission (Schössler, Jäger, & Knorr, 2012a; Ozuna, Cárcel, García-Pérez, & Mulet, 2011). In direct-contact applications, there is an intimate contact between ultrasonic source and product, while in air-borne applications, ultrasound is transmitted through the air. Despite air-borne applications are less efficient than direct-contact ones in terms of energy yield, its lower heating effect and better adaptability to convective driers have largely contributed to its development. The feasibility of the ultrasonic application should be evaluated considering both kinetic and quality issues (Ozuna, Puig, García-Pérez, Mulet, & Cárcel, 2013; Vilkhua, Mawsona, Simonsa, & Bates, 2008).

Air-borne ultrasound applications have been reported to assist conventional hot-air drying (Ozuna et al., 2011; Garcia-Perez, Ortuño, Puig, Carcel, & Perez-Munuera, 2012b) and, more recently, for the convective freeze-drying (Bantle & Eikevik, 2011; Garcia-Perez et al., 2012a). Previous results have shown that air-borne ultrasound application during drying may greatly accelerate water removal. However, the effectiveness of ultrasound greatly depends on the process and product variables, such as temperature, air velocity, acoustic power applied, and product porosity (Cárcel, García-Pérez, Benedito, & Mulet, 2012). In addition, as far as we are concerned, the most recent air-borne applications have been focused on the drying of fruits and vegetables and few works have addressed the treatment of protein matrices, such as meat or fish products (Nakagawa, Yamashita, & Miura, 1996).

According to literature, ultrasound is able to produce modifications in food quality parameters such as texture, color, flavor and nutrients (Pingret, Fabiano-Tixier, & Chemat, 2013). To understand the effect of high power ultrasound on food quality, it is important to know the interactions between acoustic energy and the food structure (Jaeger, Reineke, Schoessler, & Knorr, 2012). Although several papers have focused on the quality changes brought about by ultrasonic applications in liquid media (Ahmad-Qasem et al., 2013 Wu, Hulbert, & Mount, 2000), few references have addressed this issue in gas media applications. In hot air drying and direct-contact ultrasonic application, Soria et al. (2010) and Schössler, Thomas, and Knorr (2012b) have studied the changes in chemical and physical quality parameters induced by a direct-contact ultrasonic application during the dehydration of carrot (20, 40 and 60 ºC, 1.2 m/s) and potato (70 ºC), respectively. Garcia-Perez et al. (2012b) and Puig, Perez-Munuera, Carcel, Hernando, and Garcia-Perez (2012) reported that the

application of ultrasound during drying (40 ºC and 1 m/s) of orange peel and eggplant, respectively, could contribute to a better preservation of the quality (internal food structure) due to the shortening of the drying time. Schössler, Jager, and Knorr (2012c) reported that bulk density, color, ascorbic acid content and rehydration characteristics of red bell pepper was not affected by an ultrasonically (direct-contact) accelerated freeze-drying .

The main aim of this work was to evaluate the air-borne application of power ultrasound on the low-temperature drying of salted cod, quantifying its influence on the drying kinetics and on the physical properties of the final dried product.

2. Materials and methods

2.1. Raw material and shaping samples

Salted cod (*Gadus morhua*) was provided by a local supplier (Carmen Cambra S. L., Spain), to better ensure the homogeneity of the raw material. According to supplier specifications, cod fish were caught in high seas and processed immediately in the fishing boat (bled, gutted, beheaded, split and salted). On average, the pieces of salted cod weighed 1.5±0.25 kg.

Parallelepiped-shaped samples (length 50 mm, width 30 mm and thickness 5 mm) were obtained from the central part of the salted cod loin using a sharp knife. The samples were wrapped in plastic waterproof film and stored at -18 ± 0.5 ºC until the drying experiments were carried out (maximum storage time 120 h). The initial moisture and the NaCl content were measured following standard methods 950.46 and 971.27, respectively (AOAC, 1997).

2.2. Drying experiments

The drying experiments of salted cod slabs were conducted in a convective drier with air recirculation and temperature and air velocity control. Air temperature and velocity are controlled using a PID algorithm. A cooper tube heat exchanger (Frimetal, Spain), installed in the air duct, cooled down the air to temperatures close to -20 ºC, which was subsequently heated using electrical devices (3000 W). The air temperature and relative humidity were measured at three points in the air duct using a combined sensor (KDK, Galltec+Mela, Germany).

The drier includes an ultrasonically activated drying chamber, already described in literature (Garcia-Perez et al., 2012a). The air-borne ultrasound application system consisted of a cylindrical radiator (internal diameter 100 mm, height 310 mm, thickness 10 mm) driven by a power ultrasonic transducer (frequency 21.9 kHz, impedance 369 Ω, power capacity 90 W). The ultrasonic system provided an average sound pressure level in the drying chamber of 155 dB. A resonance dynamic controller was connected to a PC by the RS-232 interface to adequately monitor the main electric parameters of the system during the air-borne ultrasonic application (power, intensity, voltage, phase, frequency and impedance).

The cod samples were weighed at preset times using an industrial weighing module (6000±0.01 g; VM6002-W22, Mettler-Toledo, USA). An application was developed using LabVIEW 2011 programming code (National Instruments, USA) to provide overall control and monitoring of the ultrasonically intensified drying process, integrating information on the air flow, the sample and the ultrasonic parameters.

Air-drying (AIR) and ultrasonically assisted air-drying (AIR+US) experiments were conducted at -10, 0, 10 and 20 ± 1 °C, 2 ± 0.1 m/s and an average relative humidity of 9 ± 4%. In the AIR+US experiments, an acoustic power density of 20.5 kW/m^3 was applied (Ozuna et al., 2011). Prior to the drying experiments, the sealed samples (9 slabs per experiment) were tempered at the drying temperature for 24 h. Then, the cod slabs were unwrapped and placed on the sample holder, which consists of a metallic frame where samples are suspended to allow free airflow around the slabs, and introduced into the drying chamber. The sample weight was automatically measured and recorded at regular time intervals (15 min). The drying experiments were replicated at least three times for each condition tested and extended until the samples lost 20% of the initial weight, which is a usual figure for klipfish (Oliveira et al., 2012).

2.3. Rehydration experiments

Rehydration experiments of dried-salted cod (AIR and AIR+US at -10, 0, 10 and 20 °C) were carried out by immersing the samples in distilled water at 4 ± 1 ºC for 27 h. The ratio of cod and water volume was kept as 1:20. In this study, the rehydration kinetics were studied globally from the evolution of the net sample weight that includes both moisture and salt transport, since samples both gained water and

lost salt. For that purpose, samples were taken at regular time intervals, superficially drained with absorbent paper to remove surface water and weighed. Thus, the net weight change was monitored (Eq. 1).

$$\Delta M^{0}_{t} = \frac{M_t - M_0}{M_0} \tag{1}$$

For each drying condition tested, a minimum of 6 rehydration experiments were carried out.

2.4. Modeling

2.4.1. Drying

A diffusion model, based on Fick's law, was used to mathematically describe the drying kinetics (AIR and AIR+US) of cod samples. The differential equation of diffusion is obtained by combining Fick's law and the microscopic mass balance. For infinite slab geometry, the diffusion equation is shown in Eq. 2, assuming the effective moisture diffusivity as constant and the solid to be isotropic.

$$\frac{\partial W_p(x,t)}{\partial t} = D_W\left(\frac{\partial^2 W_p(x,t)}{\partial x^2}\right) \tag{2}$$

In order to solve Eq. 2, some further assumptions were considered: solid symmetry, a uniform initial moisture content and temperature, constant shape during drying and a negligible external resistance to water transfer. Taking these assumptions into account, the analytical solution of the diffusion equation is expressed in terms of the average moisture content in Eq. 3 (Crank, 1975).

$$W = W_{eq} + (W_0 - W_{eq})\left[2\sum_{n=0}^{\infty}\frac{1}{\lambda_n^2 L^2}e^{-D_W\lambda_n^2 t}\right] \tag{3}$$

where, λ_n are the eigenvalues calculated as $\lambda_n L = (2n+1)\frac{\pi}{2}$

The equilibrium moisture data were obtained from the desorption data of salted cod at 25 ºC reported by Walde (2003).

2.4.2. Rehydration

The evolution of sample weight during rehydration was modeled by means of Peleg's empirical equation (Peleg, 1988) (Eq. 4).

$$M_t = M_0 + \frac{t}{k_1 + k_2 t} \tag{4}$$

where $1/k_1$ and $1/k_2$ are the model's parameters. The rate constant, $1/k_1$, is related to the weight gain rate at the very beginning, $t = t_0$, and represents the initial rehydration rate (Eq. 5).

$$\frac{dM(t = t_0)}{dt} = \frac{1}{k_1} \tag{5}$$

The capacity constant, $1/k_2$, is related to the equilibrium weight (M_e). Thus, when rehydration time is very long, Eq. 4 becomes Eq. 6, giving the relationship between M_e and $1/k_2$.

$$M_e = M_0 + \frac{1}{k_2} \tag{6}$$

2.5. Model fitting

The model parameters (D_W of diffusion model and $1/k_1$ and $1/k_2$ of Peleg model) were identified by using an optimization procedure that minimized the sum of the squared differences between the experimental and calculated average data. For that purpose, the non-linear optimization algorithm of the Generalized Reduced Gradient (GRG), available in Microsoft Excel™ spreadsheet from MS Office 2010 (Microsoft Corp., USA), was used. The goodness of the fit was determined by the percentage of explained variance, %VAR (Eq. 7).

$$\%VAR = \left[1 - \frac{S_{xy}^2}{S_y^2}\right] \cdot 100 \tag{7}$$

2.6. Texture

Hardness, characterized as the maximum penetration force, was evaluated in the dried and rehydrated samples using a Texture Analyzer (TAX-T2®, Stable Micro System, United Kingdom). Penetration tests were conducted with a 2 mm flat cylinder probe (SMS P/2N), at a crosshead speed of 1 mm/s and a strain of 70% (penetration distance 3.5 mm). In each sample, penetration tests were carried out at 12 points following a preset pattern.

2.7. Microstructure. Scanning electron microscopy (SEM)

Cubes (side 3 mm) from samples dried at 0 ºC with and without ultrasound application were immersed in liquid N_2 and then freeze-dried at 1 Pa for 3 days (LIOALFA-6, Telstar, Spain). Then, samples were vacuum sealed in vials in the same freeze-drier, so that they would remain stable (Ozuna et al., 2013). After that, they were individually placed on SEM slides with the aid of colloidal silver and then gold-coated with carbon (SCD005, Baltec, Germany) at 10^{-2} Pa and an ionization current of 40 mA. The samples were observed in a scanning electron microscope (JSM-5410, Jeol, Japan) equipped with a LINK data-processing system (INCA 4.09, Oxford Instruments, England) at an acceleration voltage of 10-20 kV.

2.8. Color

The color of dried-salted cod was measured by computing the CIE L*a*b* color coordinates using a colorimeter (Minolta CR-200, Konica Minolta Optics, Inc., Japan). In each slice, color test was conducted at 6 points following a preset pattern. According to CIE L*a*b* system, L^* measures the lightness on a 0 to 100 scale from black to white; a^*, (+) red or (-) green; and b^*, (+) yellow or (-) blue (Bai, Sun, Xiao, Mujumdar, & Gao, 2013). The overall color differences (ΔE) between AIR and AIR+US samples were also determined by Eq. 8.

$$\Delta E = \sqrt{\Delta L^{*2} + \Delta a^{*2} + \Delta b^{*2}} \quad (8)$$

2.9. Statistical analysis

In order to identify whether ultrasound and the air temperature significantly ($p<0.05$) influenced the drying, rehydration properties and the texture and color of dried-salted cod, analysis of variance (ANOVA) ($p<0.05$) was carried out and the least significant difference (LSD) intervals were identified using the Statgraphics Plus 5.1. statistical package (Statistical Graphics Corp., USA).

3. Results and discussion

3.1. Experimental drying kinetics

The experimental drying kinetics (AIR, AIR+US) of salted cod slabs at -10, 0, 10 and 20 ºC are shown in Fig. 1. The average initial moisture and NaCl contents of salted cod were 1.23±0.07 kg W/kg dry matter and 0.41±0.03 kg NaCl/kg dry matter, respectively. Both the fact that the raw matter used constitutes a partially-dried material and also the high concentration of NaCl in cod flesh limits the presence of free water. For this reason, no constant rate drying period was observed and drying occurred in the falling rate period (Bellagha et al., 2007). Thus, the initial moisture content was considered as the critical one for modeling purposes.

As stated in Section 2.2, drying experiments were extended until the weight loss reached 20% of the initial weight. Thereby, dried-salted samples presented final moisture and NaCl contents of 0.77±0.04 kg W/kg dry matter and 0.41±0.02 kg NaCl/kg dry matter, respectively. The results obtained for the AIR experiments showed that the air temperature affected drying kinetics, shortening the drying time. For example, the drying time for the lowest temperature tested, -10 ºC, was over 14 h, while at 20 ºC, it was only 5 h. Air temperature was found to have a similar influence in AIR+US experiments.

The application of power ultrasound sped up the drying kinetics, as can be observed if the AIR and AIR+US experiments are compared (Fig. 1). Ultrasound application led to a shortening of the drying time of between 35 and 54% as compared to AIR experiments. The greatest time reduction under ultrasound application was found at the lowest and the highest temperatures tested (-10 and 20 ºC). Using the same ultrasonic set-up and under similar experimental conditions, Garcia-Perez et al. (2012a) found drying time reductions of 68 and 70% in the drying of carrot and

eggplant cubes (-14 ºC and 2 m/s), respectively. When drying green peas at -3 ºC, Bantle and Eikevik (2011) showed that, with ultrasound application (20 kHz; DN 20/2000, Sonotronic), there was a maximum reduction in the drying time of around 10%. On the other hand, drying surimi slabs at 20 ºC and 2.8 m/s, Nakagawa et al. (1996) observed that the drying time was 80% shorter when acoustic waves (155.5 dB, 19.5 kHz) were applied.

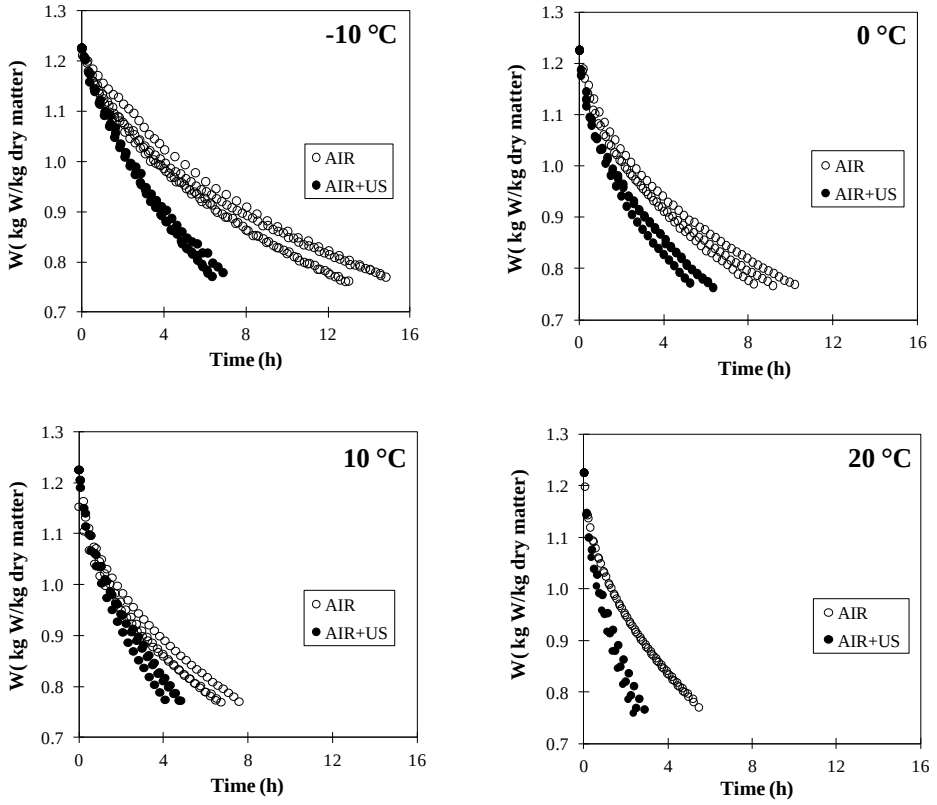

Fig. 1 Drying kinetics of salted cod slabs (length 50 mm, width 30 mm and thickness 5 mm) at -10, 0, 10 and 20 ºC (2 m/s) with (AIR+US, 20.5 kW/m³) and without (AIR) ultrasound application.

3.2. Modeling drying kinetics

In order to quantify the influence of power ultrasound application and temperature on the drying kinetics of salted cod slabs, the proposed diffusion model (Eq. 3) was fitted to the experimental data.

The diffusion model provided a percentage of explained variance (%VAR) close to 99% for AIR and AIR+US experiments at 0, 10 and 20 ºC (Table 1). This fact suggests that, in these cases, the drying process followed a clear diffusion pattern. In the case of AIR+US experiments at -10 ºC, the explained variance achieved by the model was much lower (95.4%) than at other temperatures, and also lower than that found in AIR experiments at the same temperature (98.3%). This indicates that there is some influence of ultrasound on the mass transfer control mechanisms and diffusion was not the only significant mechanism controlling water transport. In this regard, Garcia-Perez et al., (2012a) observed the same behavior when analyzing the low-temperature drying (-14 ºC, 2 m/s) of carrot and highlighted that, under such particular conditions, ultrasound application led to a larger improvement in the diffusion coefficient (407-428%) than it did in the mass transfer coefficient (96-170%). Therefore, the application of power ultrasound reduced the internal resistance to mass transfer more than the external, which means that diffusion does not prevail as the most significant ($p<0.05$) water transfer controlling mechanism and convection grows in importance.

Table 1 Average values and standard deviation of effective diffusivity, D_W, on salted cod drying. Increase in effective moisture diffusivity, ΔD_W (%), produced by ultrasound application and percentage of explained variance, VAR (%). The superscripts a, b, c, d and e show homogeneous groups established from LSD (least significance difference) intervals ($p<0.05$).

T (°C)		D_W (10^{-10} m²/s)	VAR (%)	ΔD_W (%)
-10	AIR	$0.14 \pm 0.01_a$	98.3	-
	AIR+US	$0.25 \pm 0.02_b$	95.4	85.5
0	AIR	$0.21 \pm 0.02_b$	99.8	-
	AIR+US	$0.33 \pm 0.03_c$	99.6	57.3
10	AIR	$0.28 \pm 0.02_{b,c}$	99.6	-
	AIR+US	$0.40 \pm 0.04_d$	99.4	42.4
20	AIR	$0.35 \pm 0.01_{c,d}$	99.6	-
	AIR+US	$0.74 \pm 0.04_e$	99.9	110.1

In AIR experiments, D_W values ranged from 0.14 x 10^{-10} to 0.35 x 10^{-10} m^2/s. Temperature affected the effective moisture diffusivity, so, the higher the temperature applied, the greater the identified effective moisture diffusivity (Table 1). The effective moisture diffusivities identified for the AIR experiments are close to other reported values. Park (1998) obtained values of around 0.87-1.61 x 10^{-10} m^2/s for salted fish muscle dried at 20-40 ºC. In a data compilation of the moisture diffusivity of foodstuffs, Zogzas, Maroulis, and Marinos-Kouris (1996) reported D_W values ranging between 0.13 x 10^{-10} and 3.1 x 10^{-10} m^2/s for the drying of unsalted fish muscle (30 ºC).

The application of high power ultrasound significantly increased ($p<0.05$) the effective moisture diffusivity at every temperature tested. The increase in this parameter (ΔD_W) ranged from 110% at the highest temperature tested, 20 ºC, to 42% at 0 ºC (Table 1). The improvement in the D_W values is mainly linked with the mechanical effects brought about by applying ultrasound to the material being dried (Puig et al., 2012). Ultrasound introduces a series of rapid and cyclic compressions and expansions of the material that can be compared to a sponge being squeezed and released repeatedly, thus improving the water diffusion in the particle. Moreover, acoustic energy also introduces pressure variations, oscillating velocities, and microstreaming on the solid-gas interfaces, reducing boundary layer thickness and, therefore, improving the water transfer rate from the solid surface to the air medium (Cárcel et al., 2012).

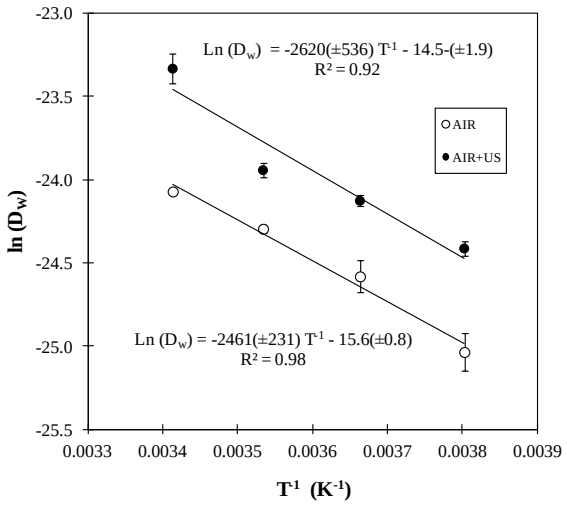

Fig. 2 Influence of drying air temperature on the average effective moisture diffusivities identified for salted cod drying with (AIR+US, 20.5 kW/m^3) and without (AIR) ultrasound application.

The influence of air temperature on D_W identified for AIR and AIR+US experiments followed an Arrhenius type relationship (Fig. 2) (Bai et al., 2013). A similar activation energy of 20.46 and 21.79 kJ/mol was obtained for AIR and AIR+US drying experiments, respectively. In such a way, the energy needed for water removal was not affected by ultrasound application. The activation energy figures are similar to those proposed by other authors for fish drying. Thus, Jason (1958) reported an activation energy of 30 kJ/mol for cod muscle (unsalted) and Park (1998) a value of 21.94 kJ/mol for the drying of salted shark muscle.

From Fig. 2, the D_W values for AIR and AIR+US experiments are easily compared. It may be observed that the D_W for AIR+US experiments at -10 ºC was similar to the figure found in AIR experiments at 0 ºC. Similar values were also found for AIR+US and AIR experiments at 0 and 20 ºC, respectively. This fact suggests that the increase in D_W produced by US application could be equivalent to a temperature rise of between 10 and 20 ºC.

3.3. Rehydration kinetics

Samples dried under the different conditions tested were rehydrated in distilled water at 4 ºC. The net weight change was used to monitor the process kinetics (ΔM^0_t), in which a coupled water and salt transfer exists. The experimental data showed that the drying air temperature influenced the rehydration kinetics (Fig. 3). For example, after 27 h of rehydration, AIR samples dried at 20 ºC gained 38% more weight than that observed in samples dried at -10 °C. Duan, Jiang, Wang, Yu, and Wang (2011) reported that the rehydration ratio of dried tilapia fish fillets increased with the rise in drying temperature. Likewise, Russo, Adiletta, and Di Matteo. (2013) connected the drying temperature with a marked influence on the microstructure of dried products; high drying temperatures led to an increase in porosity and the collapse of the structure, causing a rise in the initial water uptake during rehydration.

The application of ultrasound during drying affected the rehydration ability of dried-salted cod samples. The AIR+US samples exhibited a higher final weight gain than AIR ones (Fig. 3) and, therefore, a higher final water content (Table 2). As regards the final NaCl content, no significant ($p>0.05$) changes were observed between AIR and AIR+US samples.

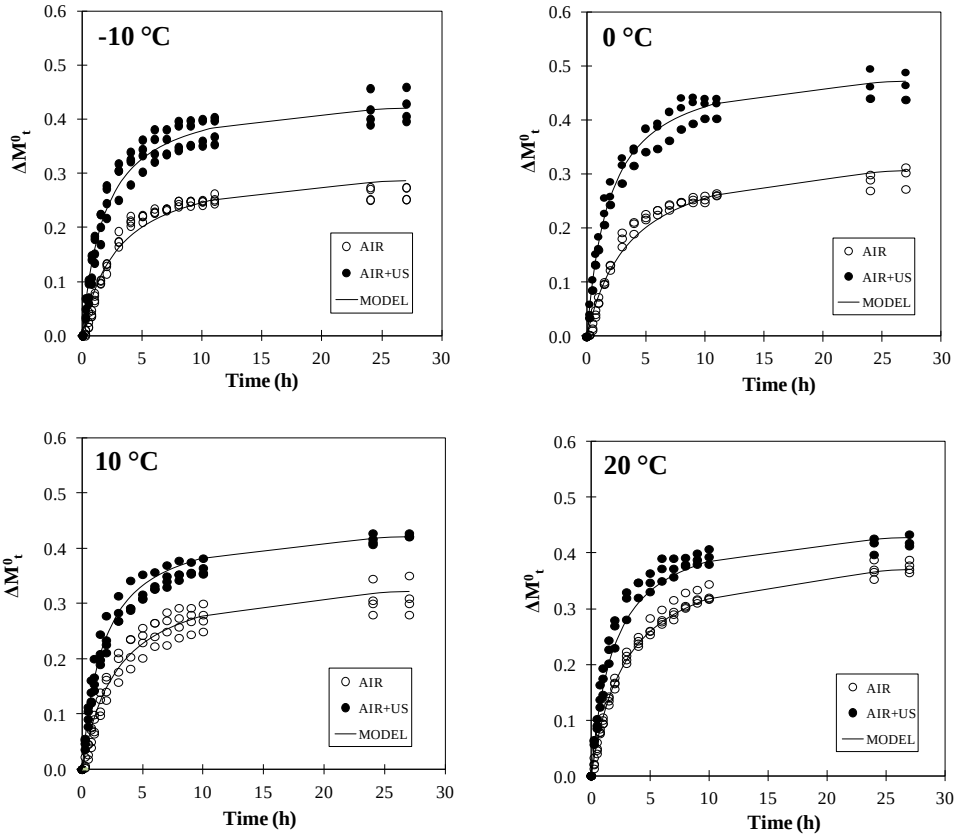

Fig. 3 Rehydration kinetics (4 °C) of salted cod slabs (length 50 mm, width 30 mm and thickness 5 mm) dried at -10, 0, 10 and 20 ºC (2 m/s) with (AIR+US, 20.5 kW/m^3) and without (AIR) ultrasound application.

The higher water gain in AIR+US dried samples could be linked to changes produced by ultrasound in the microstructure during drying (Fig. 4). According to the SEM micrograph obtained from the longitudinal section of salted cod dried at 0 ºC, AIR+US samples (Figs. 4 D and E) showed a more damaged and collapsed structure than AIR ones (Figs. 4 A and B). Ultrasound application provoked ruptures in the cod fibers (Fig 4 E) and a greater migration of salt to the fiber surface (Fig. 4 D). In addition, micrographs obtained from a cross section of AIR+US dried-salted cod exhibited the formation of wider spaces between myofibrils and a more intense salt redistribution on the surface (Fig. 4 F). Hence, these structural differences which are induced by mechanical effects linked to ultrasound can explain the greater weight gain of AIR+US samples during rehydration. In addition, the fact that ultrasound

application leads to a shorter drying time can lessen the damage to the protein structure (denaturation), contributing to a greater water holding capacity, thereby increasing the rehydration capacity of AIR+US samples (Barat, Rodríguez-Barona, Andrés, & Visquert, 2004; Brás & Costa, 2010).

Table 2 Experimental moisture and NaCl content of rehydrated (27 h) dried salted cod at -10, 0, 10 and 20 ºC with (20.5 kW/m^3, AIR+US) and without (AIR) ultrasound application. Average ± standard deviations are shown. The superscripts a, b and c (in moisture) and x (in NaCl) show homogeneous groups established from LSD (least significance difference) intervals ($p<0.05$).

T (ºC)		W (kg W/kg dry matter)	NaCl (kg NaCl/kg dry matter)
-10	AIR	$3.38 \pm 0.11_a$	$0.037 \pm 0.004_x$
	AIR+US	$3.80 \pm 0.20_c$	$0.036 \pm 0.004_x$
0	AIR	$3.37 \pm 0.19_a$	$0.041 \pm 0.005_x$
	AIR+US	$3.81 \pm 0.17_c$	$0.040 \pm 0.007_x$
10	AIR	$3.39 \pm 0.15_a$	$0.040 \pm 0.007_x$
	AIR+US	$3.76 \pm 0.12_c$	$0.040 \pm 0.005_x$
20	AIR	$3.00 \pm 0.13_b$	$0.040 \pm 0.009_x$
	AIR+US	$3.37 \pm 0.18_a$	$0.041 \pm 0.003_x$

3.4. Modeling rehydration kinetics

The Peleg model was used to analyze and quantify the influence of both drying temperature and ultrasound application on the net weight gain (ΔM^0_t) of dried-salted cod slabs during rehydration. As can be observed in Table 3, the model adequately described the rehydration kinetics, providing percentages of explained variance ranging between 96.8 and 99.3%.

The identified Peleg parameters, related to the initial mass transfer rate ($1/k_1$) and the equilibrium weight ($1/k_2$), are shown in Table 3. As far as the effect of the drying temperature is concerned, the identified model parameters for AIR samples slightly increased when the temperature rose (Table 3). However, these increases were only significant ($p<0.05$) for the equilibrium constant, $1/k_2$. Air temperature was also observed to have a similar effect on AIR+US samples.

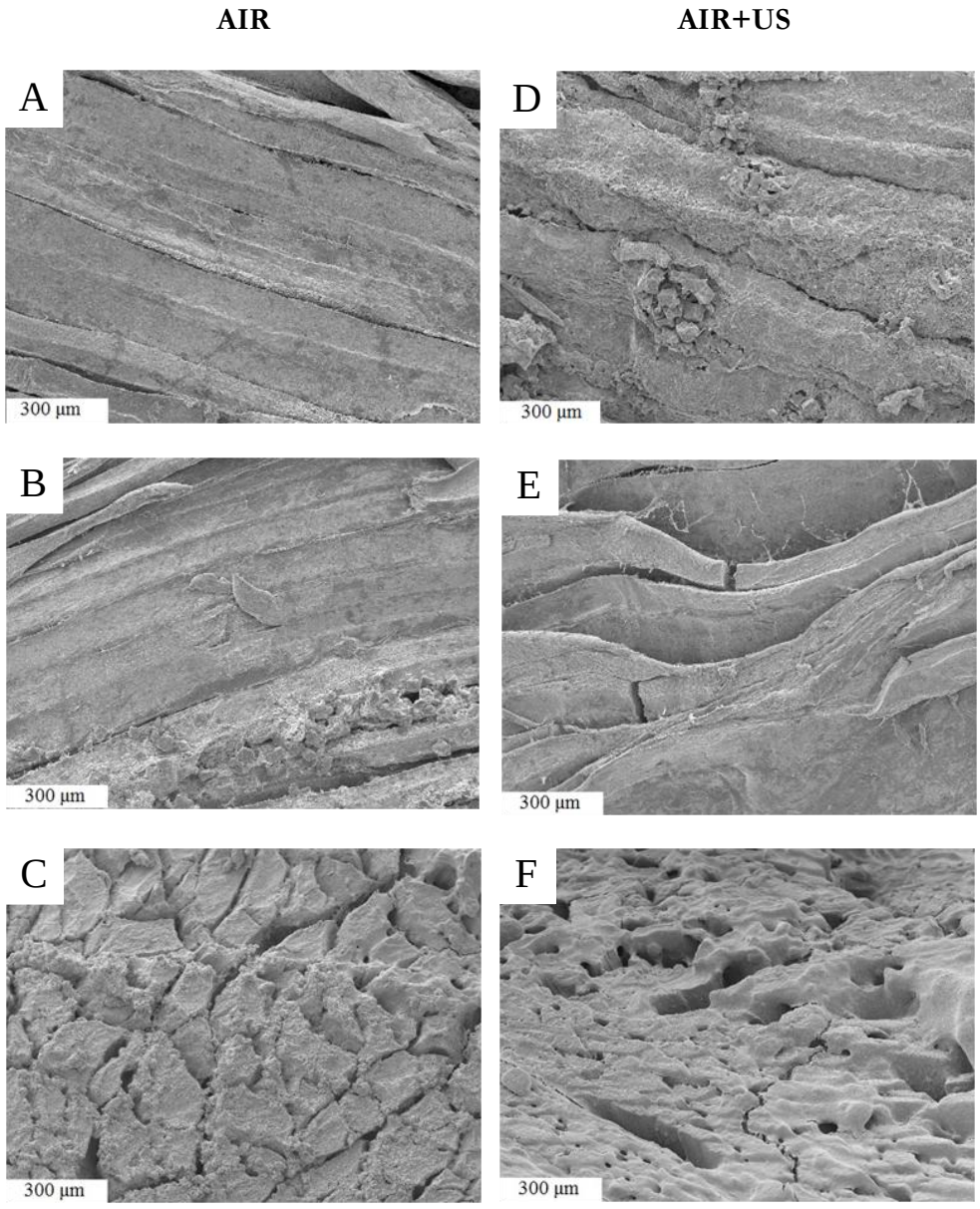

Fig. 4 Longitudinal and cross-section (x100) observed by SEM. Dried salted cod at 0 °C and 2 m/s with (AIR+US, 20.5 kW/m^3: D, E and F) and without ultrasound application (AIR: A, B and C).

Table 3 Modeling of the net weight gain, ΔM0t, by means of the Peleg model during rehydration of dried salted cod at -10, 0, 10 and 20 ºC with (20.5 kW/m^3, AIR+US) and without (AIR) ultrasound application. Increase in Peleg parameters, $\Delta 1/k_1$ and $\Delta 1/k_2$ (%), produced by ultrasound application and percentage of explained variance, VAR (%). The superscripts x and y (in $1/k_1$) and a, b, c, d and e (in $1/k_2$) show homogeneous groups established from LSD (least significance difference) intervals ($p<0.05$).

T (ºC)		$1/k_1$ (10^{-3} g W/g dry matter × s)	$1/k_2$ (g)	VAR (%)	$\Delta 1/k_1$ (%)	$\Delta 1/k_2$ (%)
-10	AIR	$1.8 \pm 0.2_x$	$0.32 \pm 0.01_a$	96.8	-	-
	AIR+US	$4.2 \pm 0.9_y$	$0.45 \pm 0.01_d$	98.8	133.0	41.8
0	AIR	$1.8 \pm 0.3_x$	$0.35 \pm 0.01_b$	97.7	-	-
	AIR+US	$4.4 \pm 0.4_y$	$0.51 \pm 0.02_e$	98.6	151.8	46.6
10	AIR	$2.2 \pm 0.3_x$	$0.36 \pm 0.02_b$	98.6	-	-
	AIR+US	$4.4 \pm 0.8_y$	$0.45 \pm 0.02_d$	99.3	104.1	25.8
20	AIR	$2.4 \pm 0.2_x$	$0.41 \pm 0.03_c$	98.7	-	-
	AIR+US	$4.1 \pm 0.7_y$	$0.46 \pm 0.03_d$	99.1	70.6	11.4

The application of ultrasound during drying significantly modified ($p<0.05$) the Peleg parameters at every drying air temperature tested. There was a faster and more substantial rehydration of AIR+US samples than AIR samples, which could be observed in the increase in both $1/k_1$ and $1/k_2$ parameters. Thereby, when comparing the rehydration patterns of AIR and AIR+US samples, the changes observed should be related to the structural changes brought about by ultrasound and depicted in Section 3.3. As can be observed in Table 3, ultrasound had a greater effect on Peleg parameters, $\Delta 1/k_1$ and $\Delta 1/k_2$, at the lowest temperatures tested (-10 and 0 ºC) than at the highest ones (10 and 20 ºC). This fact could be linked to the length of time samples are exposed to the ultrasonic energy. While drying experiments carried out at the lowest temperatures (-10 and 0 ºC) lasted approximately 6 to 8 h, at the highest temperatures (10 and 20 ºC), the drying time was reduced by almost half (Fig. 1). Therefore, the longer the exposure time to ultrasound application, the more intense the ultrasound effects on the cod structure (Fig. 4).

3.5. Texture

The hardness of dried and rehydrated cod was evaluated by computing the maximum penetration force. The initial hardness value of salted cod was 3.62 ± 0.35 N, thus, the drying process provoked a hardening of the samples (Table 4). The measurements taken from AIR samples showed that the sample hardness was dependent on the drying air temperature used (Table 4); the higher the air temperature applied, the harder the dried cod. Thus, AIR samples dried at 10 and 20 °C were significantly ($p<0.05$) harder than those dried at 0 and -10 °C. The temperature rise could induce a greater denaturation of the connective tissues and the myofibrillar proteins (myosin and actin) promoted by NaCl, leading to the sample hardening. (Ortiz et al., 2013; Brás & Costa, 2010).

As is shown in Table 4, AIR+US dried samples were significantly ($p<0.05$) softer than AIR ones. This fact could be linked to the mechanical effects caused by ultrasound application on salted cod fibers (Figs. 4 D, E and F). The fact that the structure of the AIR+US samples is more collapsed and porous than the AIR samples (Figs. 4 A, B and C) explains the low degree of hardness found. In addition, the application of ultrasound is linked to a reduction in the drying time which could contribute to some mild damage in the protein structure, causing a lesser degree of hardening (Oliveira et

al., 2012; Kilic, 2009). Moreover, the hardness of AIR+US samples was not affected by the drying air temperature (Table 4).

Table 4 Hardness (average ± standard deviations) of dried and dried+rehydrated-salted cod samples at -10, 0, 10 and 20 ºC with (20.5 kW/m^3, AIR+US) and without (AIR) ultrasound application. The superscripts a, b and c (in dried) and x, y and z (in dried+rehydrated) show homogeneous groups established from LSD (least significance difference) intervals ($p<0.05$).

T (°C)		Dried	Dried+Rehydrated
		Hardness (N)	Hardness (N)
-10	AIR	$9.93 \pm 0.80_a$	$1.13 \pm 0.13_x$
	AIR+US	$7.65 \pm 0.48_b$	$0.89 \pm 0.09_y$
0	AIR	$9.93 \pm 0.70_a$	$1.12 \pm 0.11_x$
	AIR+US	$7.30 \pm 0.61_b$	$0.88 \pm 0.10_y$
10	AIR	$11.58 \pm 0.50_c$	$1.17 \pm 0.16_x$
	AIR+US	$7.31 \pm 0.55_b$	$0.88 \pm 0.10_y$
20	AIR	$12.4 \pm 0.96_c$	$2.38 \pm 0.20_z$
	AIR+US	$8.25 \pm 0.57_b$	$1.19 \pm 0.17_x$

The hardness was also measured in rehydrated samples (4 ºC, 27 h). As can be observed in Table 4, the rehydration produced a softening of dried-salted samples. After rehydration, AIR samples dried at -10, 10 and 0 ºC were significantly ($p<0.05$) softer than those dried at 20 ºC. This fact suggests that drying at 20 ºC affected the structure of the dry material, limiting the softening of rehydrated samples. At every temperature tested, AIR+US rehydrated samples were softer than AIR ones, which is consistent with the effect observed in rehydration kinetics (Fig. 3, Table 2) produced by structural changes (Fig. 4).

3.6. Color

The color of dried-salted cod is generally considered to be one of the most relevant quality traits. In order to analyze the influence of ultrasound application and drying temperature on the color changes of dried-salted cod, CIE L*a*b* color coordinates were measured directly on dried samples under different conditions (AIR and

AIR+US at -10, 0, 10 and 20 ºC). The average values of chromatic coordinates (L*, a*, b*) for raw salted cod were L*=58.93±2.00, a*=-3.66±0.49 and b*=4.86±1.50. Thus, as observed in Fig. 5, the drying process provoked changes in the color of fish muscle. In general terms, L*, a* and b* increased, which indicates that the drying process caused both the yellowing (higher b*) of the samples and the decrease in their lightness index (higher L*) (Brás & Costa, 2010, Lauritzen et al., 2004).

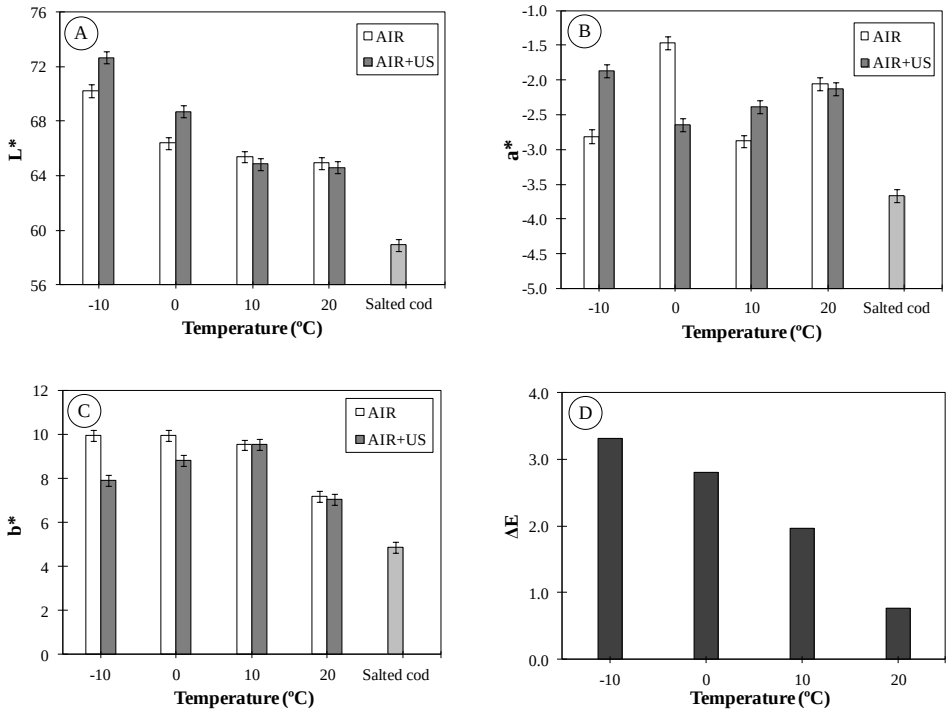

Fig. 5 CIELAB coordinates (L*, a*, b*) of salted cod (length 50 mm x width 30 mm x thickness 5 mm) dried at -10, 0, 10 and 20 ºC with (20.5 kW/m^3, AIR+US) and without (AIR) ultrasound application. ΔE represents the overall color change between AIR+US and AIR samples. Average values ± LSD intervals at a confidence level of 95% are plotted.

In AIR samples, L* and b* coordinates values were significantly ($p<0.05$) affected by the drying air temperature; the higher the temperature applied, the lower the values of L* and b* (Figs. 5 A, C). This may be explained by the fact that a temperature rise induces, in the cod muscle, the contraction of myotomes due to protein aggregation (Fernandez-Segovia, Martinez-Navarrete, Escriche, & Chiralt, 2003), the oxidation of phospholipids and reactions which stem from the presence of other ions in the salt

composition (Oliveira et al., 2012). This leads to an increase in the opacity of the fish tissue (Lauritzsen et al., 2004) and contributes to the color degradation of dried-salted cod samples. The experimental measurements obtained coincide with those reported by Ortiz et al. (2013), who studied the influence of drying air temperature on the color of dried salmon (*Salmo salar* L.) fillets and found a significant ($p<0.05$) increase in L* and b* values when comparing samples dried at 40 and 60 ºC. On the contrary, the a* value for AIR samples did not show any significant ($p<0.05$) temperature-linked trend (Fig. 5 B).

As observed in Fig. 5 D, there were found to be changes between the color (ΔE) of AIR+US and AIR samples, which were dependent on the drying temperature; thus, the lower the drying temperature, the greater the color differences between AIR and AIR+US samples. These differences are obviously linked to specific changes in chromatic coordinates (L*, b* and a*), although no common pattern was found. As regards L* and b* coordinates, AIR+US samples dried at -10 and 0 ºC exhibited higher lightness (L*) and lower yellowness (b*) values in comparison to AIR samples, which could be interesting for the cod industry which requires products with high whiteness values (Oliveira et al., 2012). Moreover, AIR+US samples dried at 10 and 20 ºC did not show significant ($p<0.05$) changes in L* and b* coordinates compared to AIR samples (Figs. 5 A, C). According to the a* coordinate (Fig. 5 B), there was a significant ($p<0.05$) effect of ultrasound on samples dried at -10, 0 and 10 ºC; however, this effect did not exhibit a significant temperature-linked trend.

4. Conclusions

The application of power ultrasound during the drying of salted cod improved the drying rate, shortening the drying time by an average of 35-50%. Water removal at 0, 10 and 20 ºC showed a diffusion pattern, while at -10 ºC convection was also significant, especially when ultrasound was applied. Microstructural analyses showed that the application of ultrasound during drying brought about changes in cod fibers, which led to a higher rehydration capacity and softer samples. Ultrasound also promoted changes in dried-salted cod, particularly an increase in lightness (L*) at low temperatures. Therefore, the feasibility of power ultrasound, a non-thermal technology, to improve the low-temperature drying of salted cod has been highlighted and further studies should address whether the kinetic improvement is coupled to an

energy reduction, which could bring this technology closer to a potential industrial use.

Acknowledgements

The authors acknowledge the financial support both from the Ministerio de Economía y Competitividad (Ref. DPI2012-37466-C03-03) and Carmen Cambra S.L. for their technical support with the selection of the raw material. César Ozuna was the recipient of a fellowship from the Universitat Politècnica de València for his research stay in Aalesund University College.

Nomenclature

D_W	Effective moisture diffusivity, m^2/s
ΔD_W	Increase in effective moisture diffusivity produced by ultrasound application, %
L	Half thickness, m
x	Characteristic coordinate in slab geometry, m
λ_n	Eigenvalues
S_y	Standard deviation of the sample
S_{yx}	Standard deviation of the estimation
t	Time, s
M_0	Initial weight, g
M_t	Weight at time t, g
M_e	Equilibrium weight, g
ΔM^0_t	Net weight change, g
W	Average moisture content, kg water/kg dry matter
W_0	Initial moisture content, kg water/kg dry matter
W_p	Local moisture content, kg water/kg dry matter
W_{eq}	Equilibrium moisture content, kg water/kg dry matter
$1/k_1$	Peleg rate constant, g water/g dry matter × s
$1/k_2$	Peleg capacity constant, g
$\Delta 1/k_1$	Increase in Peleg rate constant produced by ultrasound application, %
$\Delta 1/k_2$	Increase in Peleg capacity constant produced by ultrasound application, %
L*	Chromatic coordinate, lightness 0 (black) to 100 (white)
a*	Chromatic coordinate, (+) red or (-) green
b*	Chromatic coordinate, (+) yellow or (-) blue

References

Ahmad-Qasem, M. H., Cánovas, J., Barrajón-Catalán, E., Micol, V., Cárcel, J. A., & García-Pérez, J. V. (2013). Kinetic and compositional study of phenolic extraction from olive leaves (var. Serrana) by using power ultrasound. *Innovative Food Science & Emerging Technologies*, 17, 120-129.

AOAC. (1997). Official Methods of Analysis. Association of Official Analytical Chemists: (Virginia, USA).

Bai, J.-W., Sun, D.-W., Xiao, H.-W., Mujumdar, A.S., & Gao, Z.-J. (2013). Novel high-humidity hot air impingement blanching (HHAIB) pretreatment enhances drying kinetics and color attributes of seedless grapes. *Innovative Food Science & Emerging Technologies*, in press, DOI: 10.1016/j.ifset.2013.08.011.

Bantle, JM., & Eikevik, T. M. (2011). Parametric study of high-intensity ultrasound in the atmospheric freeze drying of peas. *Drying Technology*, 29, 1230-1239.

Barat, J.M., Rodriguez-Barona, S., Andrés, A., & Fito, P. (2003). Cod salting manufacturing analysis. *Food Research International*, 36, 447-453.

Bellagha, S., Sahli, A., Farhat, A., Kechaou, N., & Glenza, A. (2007). Studies on salting and drying sardine (Sardinella aurita): Experimental kinetics and modeling. *Journal of Food Engineering*, 78, 947-952.

Brás, A., & Costa, R. (2010). Influence of brine salting prior to pickle salting in the manufacturing of various salted-dried fish species. *Journal of Food Engineering*, 100, 490–495.

Cárcel, J.A., García-Pérez, J.V., Benedito, J., & Mulet, A. (2012). Food process innovation through new technologies: use of ultrasound. *Journal of Food Engineering*, 110, 200-207.

Crank, J. (1975). The mathematics of diffusion. Oxford university press.

Duan, Z., Jiang, L., Wang, J., Yu, X., & Wang, T. (2011). Drying and quality characteristics of tilapia fish fillets dried with hot air-microwave heating. *Food and Bioproducts Processing*, 89, 472-476.

Fernandez-Segovia, I., Camacho, M.M., Martinez-Navarrete, N., Escriche, I., & Chiralt, A. (2003). Structure and color changes due to thermal treatments in desalted cod. *Journal of Food Processing Preservation*, 27, 465-474.

Garcia-Perez, J.V., Carcel, J.A., Riera, E., Rosselló, C., & Mulet, A. (2012a). Intensification of low-temperature drying by using ultrasound. *Drying Technology*, 30, 1199-1208.

Garcia-Perez, J.V., Ortuño, C., Puig, A., Carcel J.A., & Perez-Munuera, I. (2012b). Enhancement of water transport and microstructural changes induced by high-intensity ultrasound application on orange peel drying. *Food and Bioprocess Technology*, 5, 2256-2265.

Jaeger, H., Reineke, K., Schoessler, K., & Knorr, D. (2012). Effects of emerging processing technologies on food material properties. In B.R. Bhandari, & Y.H. Roos (Eds), Food Materials Science and Engineering, (pp. 222-254). Blackbell Publishing Ltd.

Jason, A.C. (1958). A study of evaporation and diffusion processes in the drying of fish muscle. In Fundamental Aspects of the Dehydration of Foodstuffs (pp. 103-155). Aberdeen: The Society of Chemical Industry.

Kilic, A. (2009). Low temperature and high velocity (LTHV) application in drying: characteristics and effects on the fish quality. *Journal of Food Engineering*, 91, 173-182.

Lauritzsen, K., Akse, L., Johansen, A., Joensen, S., Sørensen, N.K., & Olsen, RL. (2004). Physical and quality attributes of salted cod (Gadus morhua L.) as affected by the state of rigor and freezing prior to salting. *Food Research International*, 37, 677–688.

Nakagawa S., Yamashita T., & Miura H. (1996). Ultrasonic drying of walleye pollack surimi. *Journal of the Japanese Society for Food Science and Technology*, 43, 388-394.

Oliveira, H., Pedro S., Nunes, M.L., Costa, R., & Vaz-Pires, P. (2012). Processing of salted cod (Gadus spp.): a review. *Comprehensive Reviews in Food Science and Food Safety*, 11, 546-564.

Ortiz, J., Lemus-Mondaca, R., Vega-Gálvez, A., Ah-Hen, K., Puente-Diaz, L., Zura-Bravo, L., & Aubourg, S. (2013). Influence of air-drying temperature on drying kinetics, colour, firmness, and biochemical characteristics of Atlantic salmon (Salmo salar L.) fillets. *Food Chemistry*, 139, 162-169.

Ortuño, C., Martínez-Pastor, M. T., Mulet, A., & Benedito, J. (2012). An ultrasound-enhanced system for microbial inactivation using supercritical carbon dioxide. *Innovative Food Science & Emerging Technologies*, 15, 31-37.

Ozuna, C., Puig, A., García-Pérez, J.V., Mulet, A., & Cárcel, J.A. (2013). Influence of high intensity ultrasound application on mass transport, microstructure and textural properties of pork meat (*Longissimus dorsi*) brined at different NaCl concentrations. *Journal of Food Engineering*, 119, 84-93.

Ozuna, C., Cárcel, J.A., García-Pérez, J.V., & Mulet, A. (2011). Improvement of water transport mechanisms during potato drying by applying ultrasound. *Journal of the Science of Food and Agriculture*, 91, 2511–2517.

Park, K.J. (1998). Diffusional model with and without shrinkage during salted fish muscle drying. *Drying Technology*, 16, 889-905.

Peleg, M. (1988). An empirical model for the description of moisture sorption curves. *Journal of Food Science*, 53, 1216-1217.

Pingret, D., Fabiano-Tixier, A. S., & Chemat, F. (2013). Degradation during application of ultrasound in food processing: a review. *Food Control*, 31, 593-606.

Puig, A., Perez-Munuera, I., Carcel, J.A., Hernando, I., & Garcia-Perez, J.V. (2012). Moisture loss kinetics and microstructural changes in eggplant (Solanum melongena L.) during conventional and ultrasonically assisted convective drying. *Food and Bioproducts Processing*, 90, 624-632.

Russo, P., Adiletta, G., & Di Matteo, M. (2013). The influence of drying air temperature on the physical properties of dried and rehydrated eggplant. *Food and Bioproducts Processing*, 91, 249-256.

Schössler, K., Jäger, H., & Knorr, D. (2012a). Effect of continuous and intermittent ultrasound on drying time and effective diffusivity during convective drying of apple and red bell pepper. *Journal of Food Engineering*, 108, 103-110.

Schössler, K., Thomas, T., Knorr, D. (2012b). Modification of cell structure and mass transfer in potato tissue by contact ultrasound. *Food Research International*, 49, 425-431.

Schössler, K., Jager, H., Knorr, D. (2012c). Novel contact ultrasound system for the accelerated freeze-drying of vegetables. *Innovative Food Science and Emerging Technologies*, 16, 113-120.

Soria, A.C., Corzo-Martinez, M., Montilla, A., Riera, E., Gamboa-Santos, J., & Villamiel, M. (2010). Chemical and physicochemical quality parameters in carrots dehydrated by power ultrasound. *Journal of Agricultural and Food Chemistry*, 58, 7715-7722.

Vilkhu, K., Mawson, R., Simons, L., & Bates, D. (2008). Applications and opportunities for ultrasound assisted extraction in the food industry-A review. *Innovative Food Science & Emerging Technologies*, 9, 161-169.

Walde, P. M. (2003). Transport Phenomena in Dehydration of Fish Muscle (Doctoral dissertation, Norwegian University of Science and Technology).

Wu, H., Hulbert, G. J., & Mount, J. R. (2000). Effects of ultrasound on milk homogenization and fermentation with yogurt starter. *Innovative Food Science & Emerging Technologies*, 1, 211-218.

Zogzas, N. P., Maroulis, Z. B., & Marinos-Kouris, D. (1996). Moisture diffusivity data compilation in foodstuffs. *Drying technology*, 14, 2225-2253.

CHAPTER 4

Hot-Air Drying

Journal of the Science of Food and Agriculture, 2011, 91, 2511-2517

Improvement of Water Transport Mechanisms during Potato Drying by Ultrasonic Application

César Ozuna, Juan A Cárcel, José V García-Pérez[*]*, Antonio Mulet*

Grupo de Análisis y Simulación de Procesos Agroalimentarios, Departamento de Tecnología de Alimentos. Universidad Politécnica de Valencia

Camino de Vera. s/n. E46022. Valencia, Spain

Abstract

Background: Drying rate of vegetables is limited by the internal moisture diffusion and convective transport mechanisms. The increase of drying air temperature leads to faster water mobility; however it provokes quality loss in the product and presents a higher energy demand. Therefore, the search of new strategies to improve water mobility during convective drying constitutes a topic of relevant research. The aim of this work was to evaluate the use of power ultrasound to improve convective drying of potato and quantify the influence of the applied power in the water transport mechanisms.

Results: Drying kinetics of potato cubes were sped up by the ultrasonic application. The influence of power ultrasound was dependent on the ultrasonic power (from 0 to 37 kW m^{-3}), the higher the applied power, the faster the drying kinetic. The diffusion model considering external resistance to mass transfer provided a good fit of drying kinetics. From modeling, it was observed a proportional and significant ($p<0.05$) influence of the applied ultrasonic power on the identified kinetic parameters: effective moisture diffusivity and mass transfer coefficient.

Conclusions: The ultrasonic application during drying represents an interesting alternative to traditional convective drying by shortening drying time, which may involve an energy saving concerning industrial applications. In addition, the ultrasonic effect in the water transport is based on mechanical phenomena with a low heating capacity, which is highly relevant for drying of heat sensitive materials and also for obtaining high quality dry products.

Keywords:
dehydration, energy efficiency, modeling, diffusion

1. Introduction

Nowadays, global consumption is shifting from fresh to value-added processed products (FAO (www.potato2008.org)). In this context, the dehydration process constitutes an alternative for producing high quality products at a competitive cost; furthermore, it provides longer shelf-life, lighter weight for transportation and smaller space for storage. [1] However, drying process can affect sensory and nutritional attributes due to textural and biochemical changes that occur mainly by the high temperatures applied in the process [2] and the long drying times.

Drying is a complex process, involving simultaneously coupled heat and mass transfer phenomena [3] with external and internal transport. [4] During drying of vegetables, drying rate may be affected by both diffusion and convective water transports. [5] Drying rate could be sped up by adequately combining other energy sources, such as, microwave, infrared radiation, radio frequency and power ultrasound. [6] In comparison to those technologies, ultrasound assisted convective drying represents an interesting way to improve dehydration rate due to a low heating effect, which limits the quality loss in the product. [7, 8]

Literature reports that the application of efficient ultrasonic energy involves the improvement of drying rate [8, 9, 10, 11] due to the mechanical effects associated to the ultrasonic wave. Ultrasound brings about the reduction of boundary layer thickness by pressure variations, oscillating velocities and microstreaming that affects the solid-gas interfaces. In addition, ultrasound may also affect internal water transfer by alternating expansions and compressions waves produced in the material ("sponge effect"). [12] This alternating stress creates microscopic channels that involve an easier moisture removal. In addition, high-intensity acoustic waves could produce cavitation in the moisture phase inside the solid matrix, which may be beneficial for the removal of the strongly attached water molecules. [13] Therefore, the ultrasonic effects could contribute to reduce the external and internal resistance to mass transfer during drying.

The application of power ultrasound in gas systems may be more difficult than in liquid medium due to both, the high impedance mismatch between the application systems and air, and the high acoustic energy absorption of this medium. [14] Ultrasound-assisted drying has been mainly addressed by using two different strategies: air-borne and direct contact applications. [12] The direct contact between

samples and the vibrating element facilitates the acoustic energy transfer, resulting in a high efficiency of the ultrasound application. [8] In the last years, advances in the design and development of efficient air-borne ultrasonic transducers have allowed a better energy transfer achieving a low impedance mismatch with the air, large amplitudes of vibration, high directionality, high power capacities and large radiating areas. [9, 14, 15]

Ultrasound assisted convective drying techniques have been applied to accelerate the drying of several products including, carrot, [7,11] onion, [16] wheat and corn, [17] rice, [18] persimmon, [10] eggplant, [19] olive leaves, [20] lemon peel [11] and surimi. [21] Despite all these works showed a significant ultrasonic effect on the water transport during drying, it should be remarked that the ultrasonic application becomes more o less efficient depending on the process variables, such as, air velocity, [10, 22] temperature [23] or, applied ultrasonic power. [11] In addition, product characteristics also affect the ultrasonic influence on drying processes. [10] Thus, high porosity products are more prone to the mechanical stress (sponge effect) produced by the ultrasonic wave due to their low mechanical resistance, [11] which increases the ultrasonic effects on drying rate.

Therefore, it results very difficult to predict the efficiency of the ultrasonic application on a target product due to the effect of both the process and the product variables. The study of the ultrasonic effect on the mass transport process should be carried out when an ultrasonic application is designed for a specific product not previously addressed. For this purpose, modeling is a useful tool not only to quantify the influence of ultrasound on the drying kinetics but also to gain insight into the effects over the mass transfer process and separate it on external and internal mechanisms. [4, 10] Thereby, the aim of this work was to evaluate the use of air-borne power ultrasound on convective drying of potato establishing the ultrasonic influence on water transport mechanisms.

2. Materials and methods

2.1. Raw material

Drying experiments were conducted with cubic samples (side 8.7 mm) of potato (*Solanum tuberosum* var. Monalisa) purchased in a local market. Samples were obtained using a household tooI, sealed in plastic films to avoid moisture loss, and stored at

4±1 ºC until processing. Initial moisture content was determined by keeping the samples at 70 ºC and 200 mmHg until constant weight according to the AOAC method Nº 934.06. [24]

2.2. Drier assisted by power ultrasound

The convective drier assisted by power ultrasound has already been described in previous works (Fig. 1). [10, 11, 19, 23] The equipment consists of a pilot scale convective drier with an aluminium cylindrical vibrating element (internal diameter 100 mm, height 310 mm and thickness 10 mm) working as an air-borne ultrasonically activated drying chamber. The cylinder is driven by a piezoelectric composite transducer (21.8 kHz), thus, the ultrasonic system is able to generate a high-intensity ultrasonic field with an average sound pressure of 154.3 dB (measured using an ultrasonic power of 31 kW m^{-3} and air stagnant conditions). In order to supervise and monitor the behavior of the ultrasonic device, some electric parameters of the electrical signal (voltage, intensity, frequency, power, and phase) were measured using a digital power meter (WT210, Yokogawa, Japan) and logged using an application developed in LabVIEW™ (National Instruments, Austin, Texas, USA). The drier operates automatically and a PC supervises the whole process; the air velocity and temperature were controlled using a PID algorithm. A balance allowed the samples to be weighed at preset times by using two pneumatic moving arms.

2.3. Drying kinetics

Drying experiments were carried out at 40 ºC and 1 m s^{-1} using an initial mass load density of 12 kg m^{-3}, these values were chosen according to previous results. [9, 10] Experiments were conducted applying seven different ultrasonic power levels (UP): 0, 6, 12, 19, 25, 31 and 37 kW m^{-3}. For each one of the different ultrasonic powers tested, experiments were conducted at least in triplicate.

Before starting the experiments, the sealed samples were warmed for 15 min at the drying temperature. Then, the samples were unwrapped and placed on the trays of the drying chamber. Samples weight was measured every 5 minutes until 70 % loss of the initial weight.

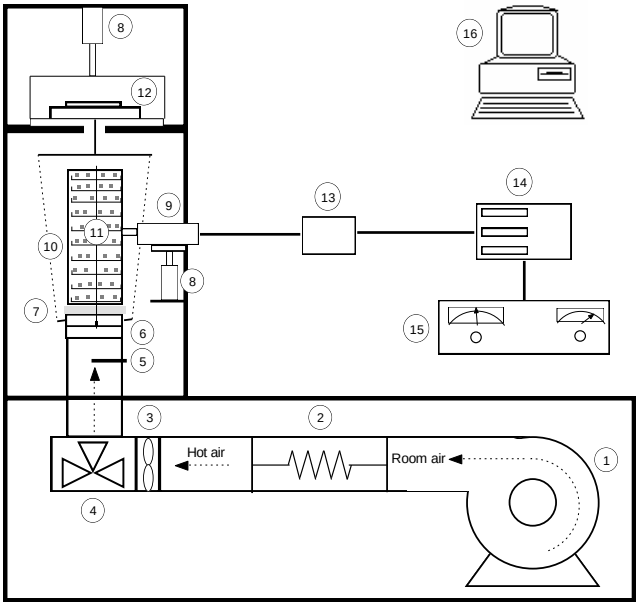

Fig. 1 Diagram of the ultrasonic assisted convective drier. [27] 1. Fan, 2. Heating unit, 3. Anemometer, 4. 3-way valve, 5. Thermocouple, 6. Sample loading chamber, 7. Coupling material, 8. Pneumatic moving arms, 9. Ultrasonic transducer, 10. Vibrating cylinder, 11. Trays, 12. Balance, 13. Impedance matching unit, 14. Digital power meter, 15. High power ultrasonic generator, 16. PC.

2.4. Modeling

Drying kinetics of potato cubes were modeled according to the diffusion theory. The governing equation of the mass transfer process for a cubic geometry, considering the material as isotropic and homogeneous and the average effective moisture diffusivity (D_e) constant, is shown in Eq. 1.

$$\frac{\partial W_p(x,y,z,t)}{\partial t} = D_e\left(\frac{\partial^2 W_p(x,y,z,t)}{\partial x^2} + \frac{\partial^2 W_p(x,y,z,t)}{\partial y^2} + \frac{\partial^2 W_p(x,y,z,t)}{\partial z^2}\right) \quad \text{(Eq. 1)}$$

Where W_p is the local moisture content (dry basis, kg W kg dry matter^{-1}), D_e is the average effective moisture diffusivity (m^2 s^{-1}), t time (s) and x, y, z represent characteristic coordinates of cubic geometry.

For modeling, it was considered the initial moisture content uniform (Eq. 2), the product temperature constant and the shrinkage negligible during drying and the solid symmetry (Eq. 3). The external resistance to mass transfer was also considered (Eq. 4 to 6) due to previous works have pointed out a significant effect of the flow characteristics when a low figure of the air velocity is used (1 m s^{-1}). [10]

$$W_p(x,y,z,0) = 0 \qquad \text{(Eq. 2)}$$

$$\frac{\partial W_p(0,y,z,t)}{\partial x} = 0 \qquad \frac{\partial W_p(x,0,z,t)}{\partial y} = 0 \qquad \frac{\partial W_p(x,y,0,t)}{\partial z} = 0 \qquad \text{(Eq. 3)}$$

$$t > 0 \qquad x = L \qquad -D_e \rho_{ds} \frac{\partial W_p(L,y,z,t)}{\partial x} = k\left(\varphi_e\left(W_p,T\right) - \varphi_{air}\right) \qquad \text{(Eq. 4)}$$

$$t > 0 \qquad y = L \qquad -D_e \rho_{ds} \frac{\partial W_p(x,L,z,t)}{\partial y} = k\left(\varphi_e\left(W_p,T\right) - \varphi_{air}\right) \qquad \text{(Eq. 5)}$$

$$t > 0 \qquad z = L \qquad -D_e \rho_{ds} \frac{\partial W_p(x,y,L,t)}{\partial z} = k\left(\varphi_e\left(W_p,T\right) - \varphi_{air}\right) \qquad \text{(Eq. 6)}$$

Where L represents the half length of the cubic side (m), ρ_{ds} is the dry solid density (kg dry matter m^{-3}), k the mass transfer coefficient (kg W m^{-2} s^{-1}), T the temperature (K) and φ_{air} the relative humidity of drying air. The water activity in the surface of the material ($\varphi_e\left(W_p,T\right)$) was obtained from the literature data reported by McMinn and Magee [25] about sorption isotherms of potato.

These boundary conditions make difficult to find an analytical solution of the model. For that reason, an implicit finite difference numerical method was used for solving the model considered. The set of implicit equations for the whole sub volume net was solved by programming a series of functions in Matlab® 7.1 SP3 (The MathWorks, Inc., Natick, MA, USA). The program provided the local moisture distribution inside the solid and the average moisture content (W) of the solid, both as functions of the drying time, the characteristic dimension (L), the effective moisture diffusivity (D_e) and the mass transfer coefficient (k). The effective moisture diffusivity and the mass transfer coefficient were simultaneously identified by fitting the model to the

experimental data using the SIMPLEX method (*fminsearch function*). The objective function (OF) to be minimized was the sum of the squared differences between the experimental and the calculated average moisture content (Eq. 7).

$$OF = \sum_{i=1}^{N} \left(W_{ei} - W_{ci} \right)^2 \qquad \text{(Eq. 7)}$$

Where W_{ei} and W_{ci} are the experimental and calculated average moisture content.

The explained variance (Eq. 8) and the mean relative error (Eq. 9) were computed to determine the fitting ability of the model to the experimental data.

$$VAR = \left[1 - \frac{S_{tW}^2}{S_W^2} \right] \cdot 100 \qquad \text{(Eq. 8)}$$

$$MRE = \frac{100}{N} \left[\sum_{i=1}^{N} \frac{\left| W_{ei} - W_{ci} \right|}{W_{ei}} \right] \qquad \text{(Eq. 9)}$$

Where S^2_w and S^2_{tw} are the variance of the sample and the estimation respectively and N the number of experimental data.

The analysis of variance (ANOVA) was carried out and the Tukey HSD (Honestly Significant Difference) intervals were determined in order to evaluate the significance ($p<0.05$) of the differences among the identified kinetic parameters. The statistical analysis was carried using Statgraphics Plus 5.1 software package (Statistical Graphics Corp., Herdorn, Virginia, USA).

3. Results and discussion

3.1. Experimental drying data

Experimental drying kinetics of potato cubes are plotted in Fig. 2. The average initial moisture content of potato was 4.59±0.14 (dry basis); this value was considered as the critical moisture content due to only the falling rate period was found at these experimental conditions, which is the usual behavior for agro-food products. [5, 26]

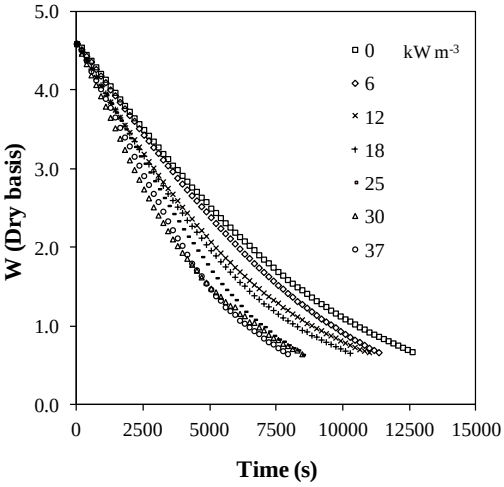

Fig. 2 Evolution of moisture content during drying of potato cubes (1 m s^{-1}, 40 ºC) applying different ultrasonic power levels. Experimental points are the average of the three replicates.

The effect of power ultrasound on experimental drying kinetics can be observed in Fig. 2. The drying kinetics were sped up by the ultrasonic application, increasing the ultrasonic effects with the applied ultrasonic power. Thus, the experiments carried out at the highest ultrasonic power tested (37 kW m^{-3}) reduced the drying time by approximately 40% in comparison to experiments without ultrasound application (0 kW m^{-3}).

Because the efficiency of the ultrasonic application is very dependent on the characteristics of the vibrating element which transfers the acoustic waves to the air medium, it results complicated to compare the effects brought about by different ultrasonic devices. Thus, Gallego-Juárez et al. [14] using a direct contact technique with stepped plate transducers (21 kHz, 100 W and 55 ºC) found an approximated time reduction of 58.3 % for carrot, 300 % for apple and 62.5% for mushroom slices. Nakagawa et al. [21] working on surimi slabs drying observed an increase of drying rate from 600% (155.5 dB, 19.5 kHz, 30 ºC) to 250% (155 dB, 19.5 kHz, 50 ºC). These authors used vibrating plates activated by an exponential horn. In the case of air-borne applications, García-Pérez et al., [11] found drying time reductions of 32% in carrot cubes and 53% in lemon peel slabs, Cárcel et al., [10] 40% in persimmon cylinders, and Ortuño et al., [19, 27] 72% in eggplant cylinders and 49% in orange peel slabs. It is observed that the effects of the ultrasonic application are dependent on the material

being dried. If it is compared the reduction of drying time for the different products, potato and carrot (low porosity products) may be considered a less sensitive material to be affected by the ultrasonic application than eggplant (high porosity product) [11].

Regarding the use of other additional energy sources to accelerate drying rate, Chua and Chou [28] found a time saving of 42% for potato and 31% for carrot slabs (thick, 4 mm x long, 20 mm x wide, 20 mm) by combining hot air (40 ºC) and microwave power (100 W). It should be remarked that the microwave power (100 W) was chosen to minimize the temperature increase avoiding the burning of the samples, being the high heating effect of microwave a key issue for drying of heat sensitive materials. The heating effect is also the main factor on the application of infrared ration. Hebbar et al. [29] found drying times reduction by nearly 48% in carrot slices (25 mm diameter x 5 mm) and potato cubes (17 mm x 17 mm x 5 mm) using a combination of infrared radiation (17 kW) and hot air (80 ºC and 1 m s^{-1}). As can be observed, the application of power ultrasound involved similar saving times than microwave and infrared radiation but presents the advantage of producing low heating of samples that could provide dry products with better quality due to water mobility is increased using mechanical (acoustic) waves and not just by heating.

3.2. Drying kinetic modeling

For quantifying the influence of power ultrasound application on the drying rate of potato cubes it is convenient to consider modeling.

Modeling is a useful tool to predict the behaviour of the drying process under different experimental conditions, and also it can be used to evaluate the application of ultrasound. [30] In this work, the diffusion model considered was adequate for describing the drying kinetics of potato cubes at the different experimental condition tested, achieving percentages of explained variance over 98% and mean relative errors under 6% in all cases (Table 1). Figure 3 shows the high agreement between experimental and calculated data, being similar the tendency found. Therefore, the assumptions considered in the model seem to be adequate to describe the behavior of experimental potato drying.

Table 1 Identified effective diffusivity (D_e) and mass transfer coefficient (k), and calculated percentage of explained variance (% VAR) and mean relative error (% MRE). Subscrips (a,b,c) and (x,y,z) shows homogeneous group established from Tukey intervals ($p<0.05$).

UP (kW m^{-3})	D_e (10^{-10} m^2 s^{-1})	k (10^{-4} kg W m^{-2} s^{-1})	VAR (%)	MRE (%)
0	$4.58\pm0.03_a$	$2.03\pm0.36_x$	99.50±0.29	4.29±0.72
6	$5.23\pm0.18_{ab}$	$2.09\pm0.15_x$	99.08±0.14	4.47±0.79
12	$5.43\pm0.25_{ab}$	$2.32\pm0.12_{xy}$	99.35±0.18	3.63±0.99
19	$6.09\pm0.37_{abc}$	$2.52\pm0.16_{xyz}$	99.17±0.49	5.66±1.98
25	$6.46\pm0.86_{bc}$	$2.68\pm0.01_{xyz}$	98.69±0.31	5.92±1.03
31	$6.06\pm0.34_{bc}$	$3.19\pm0.42_z$	99.25±0.51	4.15±1.65
37	$7.51\pm0.34_c$	$3.21\pm0.35_{yz}$	98.84±0.36	4.84±1.35

The identified effective moisture diffusivity (4.58±0.03 x 10^{-10} m^2 s^{-1}) in the experiments without power ultrasound application (0 kW m^{-3}) is in the same order that others reported in the literature for convective drying of potato at similar temperatures (40-50 ºC). Thus, Hassini et al. [31] found values in the range of 4.30 x 10^{-10} – 3.60 x 10^{-10} m^2 s^{-1}, Zogzas & Maroulins [32] reported a range from 5.3 x10^{-9} to 2.8 x10^{-10} m^2 s^{-1}, Pavón-Melendez et al. [33] showed values between 2.2 x10^{-10} to 9.4 x10^{-10} m^2 s^{-1} and Ronald et al., [34] values between 8.8 x 10^{-10}-1.2 x 10^{-9} m^2 s^{-1}. The application of power ultrasound during drying produced the increase of the identified effective diffusivity (Table 1). Thus, for the maximum ultrasonic power level tested (37 kW m^{-3}), the increase of the effective moisture diffusion coefficient was 64 % regarding the experiments without power ultrasound application (0 kW m^{-3}). The ultrasonic effects were dependent on the applied power, the higher the ultrasonic power, the higher the identified effective diffusivity values. In the range of the ultrasonic power level (UP) used in this work (0-37 kW m^{-3}), a significant linear relationship ($p<0.05$) between the UP and the effective moisture diffusivity (D_e) was found $\left(D_e\left(10^{-10}\ m^2 s^{-1}\right) = 0.03\ UP\left(kW\ m^{-3}\right) + 4.68, \quad \text{Fig. 4}\right)$.

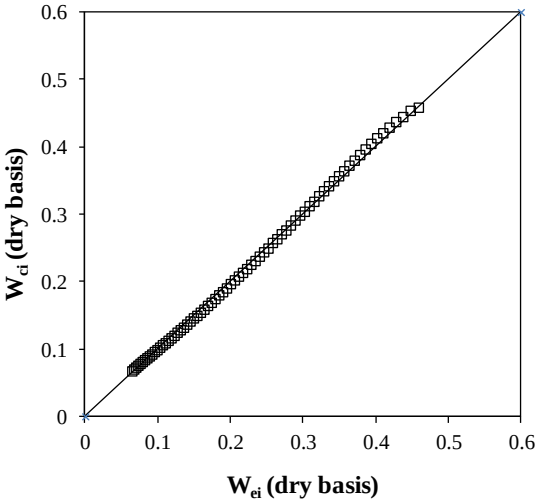

Fig. 3 Experimental versus calculated moisture content of potato cubes dried without applying ultrasound (one replicate at 0 kW m^{-3})

The easiest way to improve internal water mobility is by increasing air temperature, thus, the improvement of the D_e achieved in this work by the ultrasonic application was compared with the effect of the drying air temperature using the activation energy reported by Bon et al. [35] for convective drying of potato. As already mentioned, the application of the maximum ultrasonic power (37 kW m^{-3}) at 40 ºC involved an increase (64%) of D_e from 4.58 to 7.51 10^{-10} m^2s^{-1} (Table 1). In order to reach that improvement just by heating, an increase of the air drying temperature from 40 to 65 ºC should be necessary, which could involve the degradation of heat sensitive compounds. The increase of the D_e produced by ultrasound is mainly associated to mechanical effects and particularly to the "sponge effect". The samples were subbmitted to alternating expansions and contractions, which accelerate the water reaching the solid surface thus reducing the internal resistance to mass transfer. High porosity products present a low internal resistance due to large intercellular spaces; as a consequence, the mechanical effects associated to the acoustic energy are more intense than in low porosity products. [11, 22] Thereby, Ortuño et al., [19] found an increase of 211% in D_e of ultrasonic assisted drying (37 kW m^{-3}) of eggplant compared to a conventional air drying process and García-Pérez et al., [11] reported an increase of 40% for carrot drying. In this sense, the influence of ultrasound on potato drying rate was interesting due to it could be considered as a low porosity product.

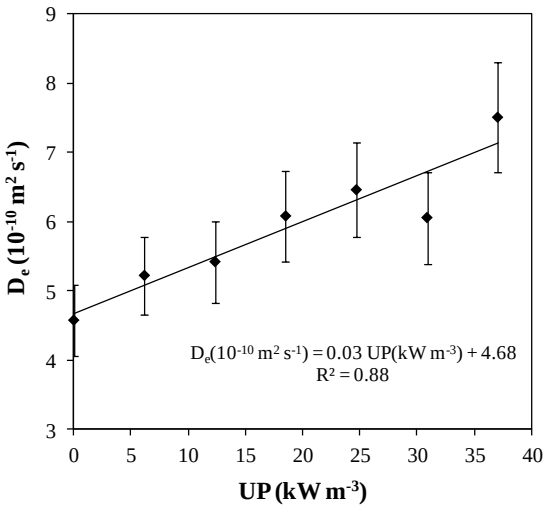

Fig. 4 Influence of the applied ultrasonic power level on the identified effective moisture diffusivity. Average values ± Tukey intervals ($p<0.05$).

Comparing the effects of combining other energy sources to increase drying rate, Tang and Cenkowski, [36] using superheated steam and hot air (125 ºC) on drying of cylindrical potato samples (5 mm diameter and 30 mm length) reported similar diffusivity values ($7 \times 10^{-10} - 9 \times 10^{-10}$ m^2 s^{-1}) than the identified at the maximum ultrasonic power tested in this work (37 kW m^{-3}). Afzal and Abe [37] found effective moisture diffusivity values for far infrared radiation drying (0.125 W cm^{-2} - 0.500 W cm^{-2} and 30 ºC) of slab potatoes (40 x 40 mm and different thickness) ranged between 5.93×10^{-11} and 1.73×10^{-9} m^2 s^{-1}. McMinn et al. [38] combining microwave (250 W) and convective drying (1.5 m s^{-1} and 30 ºC) of slab (13.5 mm radius, thickness 3.5 mm) and cylinder (radius 13.5 mm, length-to-radial ratio 4:1) potato samples showed D_e values from 0.13×10^{-8} to 3.73×10^{-8} m^2 s^{-1}, and from 2.90×10^{-8} to 24.22×10^{-8} m^2 s^{-1}, respectively. In the case of microwave, it should be remarked that at high power levels the biomaterial dries so fast that the steam or other vapours could not escape quickly enough, leading to internal pressure build up, which could rupture the material. [39] As already mentioned, infrared radiation and microwave involve a high heating effect in comparison to the acoustic energy, which mainly involves mechanical effects. [12]

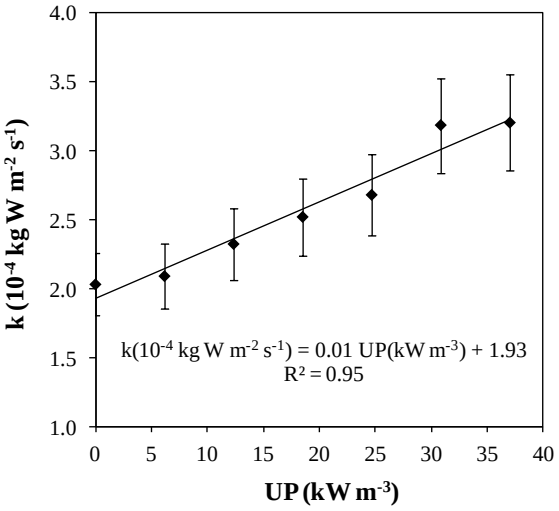

Fig. 5 Influence of the applied ultrasonic power level on the identified mass transfer coefficient. Average values ± Tukey intervals ($p<0.05$).

The external resistance to water transport was also affected by power ultrasound application during drying. The mass transfer coefficient (k) was increased by 58% by the application of power ultrasound (37 kW m^{-3}) in comparison with the conventional drying experiments (0 kW m^{-3}) (Table 1). As in the case of D_e, the ultrasonic effect on k was dependent on the applied power, the higher the ultrasonic power, the higher the mass transfer coefficient. A significant ($p<0.05$) linear relationship between the applied ultrasonic power level (UP) and the mass transfer coefficient (k) was also found $\left(k\left(10^{-4}\ \text{kg W m}^{-2}\ \text{s}^{-1}\right)= 0.01\ \text{UP}\left(\text{kW m}^{-3}\right) + 1.93,\ \text{Fig. 5}\right)$. Then, in the range of ultrasonic power tested, the ultrasonic effects were proportional to the energy supplied to the medium. This fact suggests a high interest in designing and developing more efficient ultrasonic devices of high power in order to deeply affect the mass transfer processes during drying.

A similar behaviour about the influence of ultrasound in the mass transfer coefficient has been previously observed [10]. In the case of persimmon drying, Cárcel et al. [10] analyzed the influence of drying air velocity on the ultrasonic application. These authors found an improvement on the mass transfer coefficient of 34.5% at 1 m s^{-1} and 31 kW m^{-3} and concluded that power ultrasound increased the drying rate only at the lowest air velocities tested, affecting both external and internal resistance to mass

transfer. The increase of the mass transfer coefficient can be linked to the reduction on the boundary layer thickness produced by pressure variations, oscillating velocities and microstreaming generated by ultrasound on the solid-gas interfaces. The aforementioned effects could reduce the boundary layer of diffusion and improve the water transfer rate from the solid surface to the air medium. [40]

From the results obtained in this work, it can be observed that the ultrasonic application during drying represents an interesting alternative to traditional drying, accelerating internal and external water transfer mechanisms and shortening drying times, which could be very promising in order to fully develop this technology at industrial scale taking energy saving into account. In addition, the low heating effect of ultrasound will permit to achieve products with a better quality reducing the impact of high temperatures on heat sensitive compounds.

4. Conclusions

Power ultrasound application represents a real alternative for improving water transport in convective drying process in order to reduce drying time. Drying kinetics of potato cubes were significantly ($p<0.05$) sped-up by the application of power ultrasound shortening the drying time. Experimental drying kinetics were well described by a diffusion model considering external resistance to mass transfer. Both kinetic parameters, the effective moisture diffusivity and the mass transfer coefficient, were significantly ($p<0.05$) increased by the application of power ultrasound. Therefore, the ultrasound application involved the reduction of both internal and external resistance to mass transfer.

Acknowledgements

The authors acknowledge the Ministerio de Ciencia e Innovación the financial support from the project DPI2009-14549-C04-04.

References

1. Ertekin C. & Yaldiz O., Drying of eggplant and selection of a suitable thin layer drying model. *J Food Eng* **63**:349-359 (2004).
2. Watson E. L., & Harper J.C. In: *Elements of food engineering (2nd ed.)*. New York: AVI. (1988).
3. Hernández J.A., Pavón G., García M.A., Analytical solution of mass transfer equation considering shrinkage for modelling food-drying kinetics. *J Food Eng* **45**:1-10 (2000).
4. Simal S., Femenia A., García-Pascual P., Rosselló C., Simulation of the drying curves of a meat-based product: effect of the external resistance to mass transfer., *J Food Eng* **58**:193-199 (2003).
5. Mulet A., Blasco M., Garcia-Reverter J., García-Pérez J.V., Drying kinetics of *Curcuma longa* rhizomes. *J Food Sci* **70**:e318-e322 (2005).
6. Mulet A., Cárcel J.A., Sanjuan N. and García-Pérez J.V., Food dehydration under forced convection conditions. In: *Current Trends in Chemical Engineering*, ed. by Delgado J., Studium Press LLC, Houston, TX, USA. pp. 153-177 (2010).
7. Gallego-Juárez, J.A., Some applications of power ultrasound to food processing. In: *Ultrasound in food processing* ed. by Povey M.J.W. Mason T.J., Blackie Academic & Professional, Glasgow, UK. (1998).
8. De la Fuente S., Riera E., Acosta V.M., Blanco A. and Gallego-Juárez J.A., Food drying process by power ultrasound. *Ultrasonics* **44**: e523-e527 (2006).
9. García-Pérez J.V., Cárcel J.A., De la Fuente S. and Riera E., Ultrasonic drying of foodstuff in a fluidized bed. Parametric study. *Ultrasonics* **44**: e539-e543 (2006).
10. Cárcel J.A., García-Pérez, J.V., Riera E. and Mulet, A., Influence of high intensity ultrasound on drying kinetics of persimmon. *Dry Technol* **25**: 185-193 (2007).
11. García-Pérez J.V., Cárcel J.A., Riera E. and Mulet, A., Influence of the applied acoustic energy on the drying of carrots and lemon peel. *Dry Technol* **27**:281-287 (2009).
12. Gallego-Juárez, J.A., High power ultrasound processing: recent developments and prospective advances. *Physics Procedia* **3**: 35-47 (2010).
13. Mulet A., Cárcel J.A., Sanjuan N., Bon J., New food drying technologies-use of ultrasound. *Food Sci Tech Int* **9**:0215-8 (2003).

14. Gallego-Juárez J.S., Rodriguez-Corral G., Galvez-Moraleda J.C. and Yang T.S., A new high intensity ultrasonic technology for food dehydration. *Dry Technol* **17**: 597-608 (1999).
15. Gallego-Juárez J. A., Rodriguez G., Acosta V. and Riera E., Power ultrasonic transducers with extensive radiators for industrial processing. *Ultrason Sonochem* **17**: 953-964 (2010).
16. Da-Mota V.M., & Palau E., Acoustic drying of onion. *Dry Technol* **17**: 855-867 (1999).
17. Huxsoll C.C., & Hall C.W., Effects of sonic irradiation on drying rates of wheat and shelled corn. *Transactions of the ASAE* **13**: 21-24 (1970).
18. Muralidhara, H.S., & Ensminger, D., Acoustic drying of green rice. *Dry Technol* **4**: 137-143 (1986).
19. Ortuño C., García-Pérez J.V., Cárcel J.A., Femenia A., Mulet, A., Modelling of ultrasonically assisted convective drying of eggplant, 17th International Drying Simposium (IDS 2010), Magdeburg, Germany (2010).
20. Cárcel J.A., Nogueira R.I., García-Pérez J.V., Sanjuan N., Riera E. Ultrasound effects on the mass transfer during drying kinetic of olive leave (olea europea, var. serrana). *Deffect Diffus Forum* **297-301**: 1083-1090 (2010).
21. Nakagawa S., Yamashita T., Miura H., Ultrasonic drying of walleye pollack surimi. *Nippon Shokuhin Kagaku Kaishi* **43**: 388-394 (1996).
22. García-Pérez J.V., Cárcel J.A., Benedito J. and Mulet A., Power ultrasound mass transfer enhancement in food drying. *Food and Bioprod Procces* **85**: 247-254 (2007).
23. García-Pérez J.V., Roselló C., Cárcel, J.A., De la Fuente S. and Mulet A., Effect of air temperature on convective drying assisted by high power ultrasound, *Deffect Diffus Forum* **258-260**: 563-74 (2006).
24. AOAC. Official methods of analysis, Association of Official Analytical Chemist, Arlington, Virginia, USA (1997).
25. McMinn, W.A.M. & Magee T.R.A., Thermodynamic properties of moisture sorption of potato, *J Food Eng* **60**: 157-165 (2003).
26. Garau M.C., Simal S., Femenia A., Roselló C., Drying of orange skin: drying kinetics modelling and functional properties. *J Food Eng* **75**: 288-295 (2006).
27. Ortuño C., Perez-Munuera I., Puig A., Riera E., García-Pérez J.V., Influence of power ultrasound application on mass transport and microestructure of orange peel during hot air drying. *Physics Procedia* **3**: 153-159 (2010).

28. Chua K.J. & Chou S.K., A comparative study between intermittent microwave and infrared drying of bioproducts. *Int J Food Sci and Tech* **40**: 23-39 (2005).
29. Hebbar H.U., Vishwanathan K.H., Ramesh M.N., Development of combined infrared and hot air dryer for vegetables. *J Food Eng* **65**: 557-563 (2004).
30. Mulet A., Drying modelling and water diffusivity in carrots and potatoes. *J Food Eng* **22**:329-348 (1994).
31. Hassini L., Azzouz S., Peczalski R., Belghith A., Estimation of potato moisture diffusivity from convective drying kinetics with correction for shrinkage. *J. Food Eng* **79**: 47-56 (2007).
32. Zogzas N.P., Maroulis Z.B, Marinos-Kouris D. Moisture diffusivity methods of experimental determination: A review. *Dry Technol* **12(3)**: 483-515 (1994).
33. Pavón-Melendez G., Hernández J.A., Salgado M.A, García M.A. Dimensionnels analyisis of simultaneous heat and mass transfer in food drying. *J Food Sci* **51**: 347-353 (2002).
34. Ronald T., Magee A., Wilkinson C., Influence of process variables on the drying of potato slices. *J Food Sci Tech* **27**: 541-549 (1992).
35. Bon J., Simal S., Roselló C., Mulet A. Drying characteristics of hemispherical solids. J Food Eng **34**: 109-122 (1997).
36. Tang Z. & Cenkowski S., Dehydration dynamics of potatoes in superheated steam and hot air. *Can Agr Eng* **42-1**: 6.1-6.13 (2000).
37. Afzal T.M & Abe T. Diffusion potato during far infrared radiation drying. *J Food Eng* **37**: 353-365 (1998).
38. McMinn W.A.M., Khraisheh M.A.M., Magee T.R.A., Modelling the mass transfer during convective, microwave and combined microwave-convective drying of solid slabs and cylinders. *Food Res Int* **36**: 977-983 (2003).
39. Shiffmann R.F. Microwave and dielectric drying, in: *Handbook of Industrial Drying,* ed. by Mujumdar A.S, Marcel Dekker Inc., New York, USA pp. 345-372 (1995).
40. Gallego-Juárez J.A., Riera E., De la Fuente S., Rodríguez-Corral G., Acosta-Aparicio V.M., Blanco, A. Application of high-power ultrasound for dehydration of vegetables: processes and devices. *Dry Tech* **25**:1893-1901 (2007).

Drying Technology, 2011, 29, 1499-1509

Modeling Ultrasonically Assisted Convective Drying of Eggplant

José V. García-Pérez[*]*, César Ozuna, Carmen Ortuño,*
Juan A. Cárcel and Antonio Mulet

Grupo ASPA (Análisis y Simulación de Procesos Agroalimentarios). Departamento de Tecnología de Alimentos. Universidad Politécnica de Valencia.

Camino de Vera. s/n. E46022. Valencia, Spain

Abstract

Modeling constitutes a fundamental tool with which to analyze the influence of ultrasound on mass transfer phenomena during drying. In this work, the study of the effect of power ultrasound application on the drying kinetics of eggplant was addressed by using different models based on theoretical (diffusion) or empirical approaches. Drying kinetics of eggplant cylinders (height 20 mm and diameter 24 mm) were carried at 40 ºC and 1 m/s applying different ultrasonic powers: 0, 6, 12, 19, 25, 31 and 37 kW/m^3. The experiments were carried out at least three times at each different ultrasonic power. Shrinkage and sorption isotherms were also addressed in order to attain an optimal description of eggplant drying.

Applying ultrasound sped up the drying kinetics. The ultrasonic power was identified as having a significant ($p<0.05$) influence on both the effective moisture diffusivity and the mass transfer coefficient; which was well explained by linear relationships. The most complex model, which considered both external resistance and shrinkage to be significant phenomena, provided the best agreement with experimental data, giving percentages of explained variance of over 99.9 % and mean relative errors of under 1.2 % in every case. According to these results, ultrasound technology could have the potential to improve the convective drying of eggplant at industrial scale.

Keywords:
dehydration, ultrasound, mass transfer, diffusion, shrinkage.

1. Introduction

The energy consumed by food processing industries represents one of the largest production costs, pushing up the product price and provoking a negative environmental impact. In developed countries, around 12-25 % of the overall industrial energy consumption is ascribed to the drying industry.[1] On an industrial scale, air-forced or convective drying is the most common dehydration method. Drying operations are limited by the slow kinetic during the falling rate period, which leads to high energy consumption,[2] and a loss of quality in the final product due to the high temperatures employed.[3] Convective drying affects the biochemical properties of foodstuffs, provoking the deterioration of aroma compounds,[4] the degradation of nutritional substances,[5] the browning reaction and the color loss.[6] Other effects are linked to the variation of the sample volume or shrinkage, which depends on the volume of removed water, the mobility of the solid matrix and the drying rate.[7] Drying is also responsible for the main changes in the mechanical properties of the product, such as texture and rehydration capability.[8]

The food industry is seeking new technologies with the aim of improving both the energy efficiency in drying operations and the quality of the dried products.[2] In this sense, combining traditional methods with non-conventional energy sources seems to be a sound way of improving drying processes. One advantage power ultrasound has over other technologies, such as microwave, infrared radiation and radio frequency, is that the drying rate increases but the effect of the heating is slight. Thus, the influence on mass transfer is related with mechanical, not heating, mechanisms.[9,10] Literature reports that the application of power ultrasound during convective drying influences the external and/or internal resistance to mass transfer.[11] Ultrasound brings about the reduction of the boundary layer through mechanical effects, such as pressure variations, oscillating velocities and microstreaming that the ultrasonic waves introduce at the solid-gas interfaces. In addition, the application of ultrasound may also affect internal water transfer by provoking the well-known "sponge effect",[9,12] which is the alternating expansion and compression waves induced in the material that create micro-channels suitable for liquid movement.[12] In addition, the effects linked to the ultrasonic waves, like the cavitation,[9,10] may facilitate the removal of strongly attached water molecules in the solid matrix.

It is less frequent to apply power ultrasound in solid-gas processes than in solid-liquid ones due to the high impedance mismatch between the application systems and air, and the high acoustic energy absorption of this medium.[12] Recent developments in the design and construction of new air borne ultrasonic transducers have created a great deal of interest in its use in convective drying.[11] These transducers transfer energy efficiently due to a low impedance mismatch with the air, large amplitudes of vibration, high directionality, high power capacities and large radiating areas.[9] Previous studies into carrot and lemon peel[11] have related the efficiency of the ultrasonic application with the properties of the raw material to be dried. In this sense, it would be interesting to study the application of ultrasound to a product with a highly unconsolidated porous structure, like eggplant, in order to compare the results with those observed in products with a closer structure (denser) than eggplant. Therefore, in order to properly evaluate and design an ultrasonic application for eggplant, it is convenient to analyze the influence of ultrasound on the drying kinetics thoroughly.[11]

Modeling constitutes an approach to drying process analysis; both the water equilibrium and the kinetics should be addressed. The water sorption isotherm shows the relationship between the water activity and the equilibrium moisture content for a constant temperature. A proper mathematical description of the isotherms is needed in order to thoroughly address the drying kinetic modeling and, to this end, the GAB model is the most widely used equation.[13] Empirical and theoretical approaches may be used to analyze drying kinetics. Empirical models do not provide a physical description of the process but rather give an outline of what happens and allow the identification of the most relevant kinetic variables.[14] In this sense, the Weibull model[15] has been used for modeling the drying kinetics of different kinds of foods.[16,17] Theoretical models look for a better description of the water removal mechanisms and the most popular is the diffusion theory, which is based on Fick's law.[18] Diffusion models are built according to some assumptions which establish the degree of complexity for the resolution. The most common assumptions to consider are related to the effective moisture diffusivity,[19] the external resistance to mass transfer[20] and the food shrinkage.[7] Although the influence of the assumptions related to effective diffusivity or external resistance on model behavior is often analyzed, shrinkage is seldom considered. The importance of including food shrinkage as a significant phenomenon in modeling has been widely discussed in literature.[21,22]

Shrinkage, which is linearly related to water content in the early stages of drying, is extremely important in diffusion mechanisms during drying because it leads to a reduction of the distance for molecular diffusion.[23] This phenomenon should be included in the development of a model in order to improve the physical representation of the process and to increase the validity of the effective diffusion coefficient.[21] Due to its high moisture content and weak structure, eggplant should be expected to shrink greatly during drying and, therefore, it should be addressed in order to give consistency to the modeling results.[24]

The main aim of this work was to model the ultrasonic assisted drying kinetics of eggplant under different experimental conditions by considering different models based on theoretical (diffusion) or empirical approaches. Modeling the drying process will not only allow insight to be gained into the effects that power ultrasound has on it, but will also permit those effects to be quantified.

2. Materials and methods

2.1. Ultrasonic assisted drying kinetics

Drying experiments were carried out on eggplants (*Solanum melongena* var Black Enorma) purchased from a local market. For drying, cylinders (height 20 mm and diameter 24 mm) were taken from eggplant flesh using a household tool. The experiments were conducted at 40 ºC and 1 m/s applying seven ultrasonic power levels (UP): 0, 6, 12, 19, 25, 31, 37 kW/m^3 until sample lost 75 % of its initial weight. The ultrasonic power was defined as the electric power supplied to the ultrasonic transducer divided by the drying chamber volume, thus representing a power density. For each condition tested, the drying experiments were carried out at least three times. Drying kinetics were determined from the sample weight lost during drying and the initial moisture content (AOAC method Nº 934.06).[25]

For this purpose, a convective drier assisted by power ultrasound was used, as already described in previous works.[26] The drying chamber consists of an aluminum vibrating cylinder (internal diameter 100 mm, height 310 mm and thickness 10 mm) driven by a piezoelectric composite transducer (21.8 kHz). The ultrasonically activated drying chamber is able to generate a high-intensity ultrasonic field in its interior, reaching an average sound pressure of 154.3 dB (measured applying an electrical power of 75 W to

the transducer in air stagnant conditions). The equipment uses a pneumatic device for weighing the samples at preset times and an impedance matching unit that permits the impedance output of the generator to be fitted to the transducer providing the system with a better electric yield.

2.2. Sorption isotherm

Fresh eggplant samples were dried at 40 ºC for different times (from 4 to 48 h) using an air forced tray oven in order to obtain samples with different moisture contents. Dry samples were milled and put in a hermetic glass container for 24 hours to make it easier for the samples to reach homogeneous moisture content. Thereafter, the water activity was measured at 40 ºC using an electric hygrometer (Model AW SPRINT TH500, NOVASINA, Air Systems for Air Treatment, Switzerland), which was previously calibrated using the followings salts: LiCl, $MgCl_2$, $Mg(NO_3)_2$, NaCl, $BaCl_2$ and $K_2Cr_2O_7$, according to the manufacturer's guidelines. Finally, the moisture content of each sample was measured (AOAC method Nº 934.06).[25] Thus, around 40 water activity-moisture content experimental points were obtained.

The sorption isotherm of eggplant was modeled using the GAB[13] (Guggenheim-Anderson-De Boer) equation (Eq. 1), describing the moisture content as a function of water activity.

$$W = W_m \frac{CKa_w}{(1-Ka_w)(1+(C-1)(Ka_w)} \quad (1)$$

The GAB model parameters (W_m, C and K) were identified using an optimization procedure that minimized the sum of the squared difference between the experimental and calculated average moisture contents of samples. For that purpose, the non-linear optimization algorithm of the Generalized Reduced Gradient (GRG), available in Microsoft Excel™ spreadsheet from MS Office 2007, was used.

2.3. Shrinkage

Cubic-shaped eggplant samples (side 18 mm) were used to determine the change of sample volume during drying. Cubes were dried at 40 ºC and 1 m/s for different times: 0.5, 1, 2, 4 and 6 hours. Moisture content (AOAC method Nº 934.06)[25] and volume were measured to estimate shrinkage. The volume measurement was taken

simultaneously by two different methodologies: image analysis and liquid displacement. For image analysis, digital images were taken (DSC-P100, Sony Corp. Japan) of each face of the fresh and dehydrated samples. The area of these surfaces was estimated using Sigma Scan Pro 5 software (SPSS Inc., USA). The measurement was done in pixels and afterwards converted into length. From this measurement, the volume was calculated by assuming that samples did not lose their cubic shape during drying. The volume was measured by liquid displacement using toluene (density 0.867 g/mL at 20 ºC), a volumetric standard picnometer (48.89 ml) and an analytical balance (PB 303-S, Mettler Toledo). The shrinkage was measured at least three times in 5 samples at the different drying times.

2.4. Modeling drying kinetics

In order to analyze the influence of power ultrasound on the drying kinetics of eggplant cylinders, three diffusion models based on the 2nd Fick's law with differing degrees of complexity and one empirical model (Weibull) were used.

2.4.1. Diffusion models

The differential equation for diffusion is obtained by combining Fick's law and the microscopic mass balance. For homogeneous and isotropic solids and finite cylinder geometry, the diffusion equation is expressed as follows considering effective moisture diffusivity to be constant in radial (r) and axial (x) directions (Eq. 2):

$$\frac{\partial W_p(x,r,t)}{\partial t} = D_e\left(\frac{\partial^2 W_p(x,r,t)}{\partial x^2} + \frac{\partial^2 W_p(x,r,t)}{\partial r^2} + \frac{1}{r}\frac{\partial W_p(x,r,t)}{\partial r}\right) \quad (2)$$

In Eq. 2, the solid symmetry and a uniform initial moisture content and temperature were considered as boundary and initial conditions (Table 1). To solve the diffusion equation, different models were tested (Table 1), which differ from the 2nd boundary condition used to describe the properties of the gas-solid interface ($x = L$ or $r = R$) and the assumption of considering a constant sample volume during drying. This strategy allowed testing the ability and reliability of describing the drying kinetics using different assumptions.

Table 1 Initial and boundary conditions for diffusion models considered for modeling the drying kinetics of eggplant cylinders.

Models	Initial condition			Equation	External resistance	Sample volume
Common	t=0	$0 \le x \le L; 0 \le r \le R$	$W_p(r,x,0)=W_0$	(3)		
Boundary conditions						
Common	t>0	$r = 0 ; 0 \le x \le L$	$\frac{\partial W_p(0,x,t)}{\partial r}=0$	(4)		
	t>0	$x = 0 ; 0 \le r \le R$	$\frac{\partial W_p(r,0,t)}{\partial x}=0$	(5)		
Negligible External Resistance **(NER)**	t>0	$r=R;0\le x\le L$	$W_p(R,x,t)=W_e$	(6)	Negligible	Constant
	t>0	$x=L;0\le r\le R$	$W_p(r,L,t)=W_e$	(7)		
External Resistance **(ER)**	t>0	$r=R;0\le x\le L$	$-D_e\rho_{ds}\frac{\partial W_p(R,x,t)}{\partial r}=k\left(\varphi_e(R,x,t)-\varphi_{air}\right)$	(8)	Significant	Constant
	t>0	$x=L;0\le r\le R$	$-D_e\rho_{ds}\frac{\partial W_p(r,L,t)}{\partial x}=k\left(\varphi_e(r,L,t)-\varphi_{air}\right)$	(9)		
External Resistance and Shrinkage **(ERS)**	t>0	$r=R;0\le x\le L$	$-D_e\rho_{ds}\frac{\partial W_p(R,x,t)}{\partial r}=k\left(\varphi_e(R,x,t)-\varphi_{air}\right)$	(10)	Significant	Variable L=f(W)
	t>0	$x=L;0\le r\le R$	$-D_e\rho_{ds}\frac{\partial W_p(r,L,t)}{\partial x}=k\left(\varphi_e(r,L,t)-\varphi_{air}\right)$	(11)		R=f(W)

2.4.2. Negligible external resistance model (NER)

The simplest diffusion model neglected the external resistance to mass transfer, thus, the water transfer is entirely controlled by water diffusion (Eq. 6 and Eq. 7, Table 1). The analytical solution[18] of the governing equation (Eq. 2) for the NER model is shown in Eq. 12 in terms of the dimensionless moisture content.

$$\psi(t)=\frac{W(t)-W_e}{W_0-W_e}=\left[\sum_{n=0}^{\infty}\frac{8}{(2n+1)^2\pi^2}e^{\left(-\frac{D_e(2n+1)^2\pi^2 t}{4L^2}\right)}\right]\cdot\left[\sum_{n=1}^{\infty}\frac{4}{\alpha_n^2}e^{\left(-\frac{D_e\alpha_n^2 t}{R^2}\right)}\right] \tag{12}$$

$\alpha_n : J_0(\alpha_n)=0$ where J_0 is the Bessel function of the first kind of the order zero. For resolution, 50 terms of the summatories were considered.

2.4.3. Model considering external resistance (ER)

This model considers as significant both the internal and external resistance to moisture transport.[23] The model took this fact into account through the boundary conditions stated in Eq. 8 and Eq. 9 (Table 1). An implicit finite difference method was used to solve the ER model, according to this method, the discretization of each term of Eq. 2 is as follows:

$$\frac{\partial W_p(x,r,t)}{\partial t}=\frac{W_p(x,r,t)-\tau(x,r,t-\Delta t)}{\Delta t} \tag{13}$$

$$\frac{\partial^2 W_p(x,r,t)}{\partial x^2}=\frac{W_p(x+\Delta x,r,t)-2W_p(x,r,t)+W_p(x-\Delta x,r,t)}{\Delta x^2} \tag{14}$$

$$\frac{\partial^2 W_p(x,r,t)}{\partial r^2}=\frac{W_p(x,r+\Delta r,t)-2W_p(x,r,t)+W_p(x,r-\Delta r,t)}{\Delta r^2} \tag{15}$$

$$\frac{\partial W_p(x,r,t)}{\partial r}=\frac{W_p(x,r+\Delta r,t)-W_p(x,r-\Delta r,t)}{2\Delta r} \tag{16}$$

For that purpose, the original volume of cylindrical samples was divided into a constant number of elements (20x20) that made up the subvolume network. According to this method, the local moisture content for an internal subvolume is obtained as a function of the moisture content of the surrounding subvolumes and of

the same subvolume at a given time (Eq. 17). The equation for each specific subvolume on the boundaries is obtained from Eq. 17 by combining the particular boundary conditions (Eq. 4, 5, 8 and 9).

$$W_p(r,x,t-\Delta t)=\frac{D_e\Delta t}{\Delta x^2\Delta r^2}\times$$
$$\times\left[\begin{array}{l} W_p(r,x,t)\left(\left(\frac{\Delta x^2\Delta r^2}{D_e\Delta t}\right)+2\left(\Delta x^2+\Delta r^2\right)\right)- \\ -\left(\begin{array}{l} W_p(r,x+\Delta x,t)\Delta r^2+W_p(r,x-\Delta x,t)\Delta r^2+ \\ +W_p(r+\Delta r,x,t)\Delta x^2\left(1+\frac{\Delta r}{2r}\right)+ \\ +W_p(r-\Delta r,x,t)\Delta x^2\left(1-\frac{\Delta r}{2r}\right) \end{array}\right) \end{array}\right] \quad (17)$$

The position of the subvolume in the radial and axial directions is characterized by the r and x parameters, the characteristic dimensions of the subvolume were determined by $\Delta r = R/(n-1)$ and $\Delta x = L/(n-1)$, the number of nodes in r or x direction by n (20) and, finally, the time interval by $\Delta t = 5$ seconds.[27] The values of Δr, Δx and Δt were refined in order to reach a good accuracy and stability in the programming code. A program was developed using Matlab® 7.1 SP3 (The MathWorks, Inc., Natick, MA, USA) to solve the set of implicit equations of the network. This program calculated the moisture distribution inside a finite length cylindrical body and the average moisture content as a function of the drying time, the effective moisture diffusivity and the mass transfer coefficient.

2.4.4. Model considering external resistance and shrinkage (ERS)

The most complex of the diffusion models tested considered not only the external resistance to mass transfer but also the sample shrinkage as significant phenomena affecting both axial and radial directions during drying.[7] In this case, mass transport was addressed as a moving boundary problem (Table 1).

As in the ER model, the diffusion equation was solved by applying an implicit finite difference method using MATLAB. In this case, the size of the subvolumes is reduced

due to the fact that the sample's shrinkage adjusts its dimension on the moving boundary and the dry matter remains constant during the process.

2.4.5. Empirical model

The Weibull empirical model[15] was used to compare its results with the theoretical models (Eq. 18).

$$W = W_e + (W_c - W_e) \cdot \exp\left(-\left(\frac{t}{\beta}\right)\right)^{\alpha} \tag{18}$$

Where α and β are the shape and kinetic parameters of the model, respectively. The β parameter is inversely linked to the drying rate. This parameter includes all the effects of the process variables (temperature, air velocity and particle size) on the drying kinetics,[28] thus, power ultrasound is expected to have an influence on this parameter.

2.5. Parameter estimation

The identification of Weibull parameters (α and β) and the NER model (D_e) were carried out using an optimization procedure that minimized the sum of the squared differences between the experimental and calculated average moisture contents of the samples. For that purpose, the non-linear optimization algorithm of the Generalized Reduced Gradient (GRG), available in Microsoft Excel™ spreadsheet from MS Office 2007, was used.

In the case of the ER and ERS models, the effective moisture (D_e) and the mass transfer coefficient (k) were simultaneously identified using the SIMPLEX method available in MATLAB (*fminsearch* function). The objective function minimized the sum of the squared differences between the experimental and calculated average moisture contents.

2.6. Model fitting evaluation and statistical analysis

The percentage of explained variance (% VAR) and the mean relative error (% MRE)[29] were computed to evaluate the fit of the models to the experimental data (Eq. 19 and Eq. 20).

$$\%VAR = \left[1 - \frac{S_{xy}^2}{S_y^2}\right] \cdot 100 \tag{19}$$

$$\%MRE = \frac{100}{N}\left[\sum_{i=1}^{N} \frac{\left|W_{ei} - W_{ci}\right|}{W_{ei}}\right] \tag{20}$$

In order to evaluate the significance of the differences between the identified parameters, the analysis of variance (ANOVA) was carried out and the LSD (least significant difference) intervals were identified. The statistical analysis was carried out using the Statgraphics Plus 5.1 software package (Statical Graphics Corp., VA, USA).

3. Results and discussion

3.1. Sorption isotherm

The experimental sorption isotherm determined at 40ºC is shown in Fig. 1. The experimental data ranged between 2.679 and 0.044 (kg water/kg dry solid) for average moisture content and between 0.993 and 0.174 for water activity. The sorption isotherm of eggplant showed the typical sigmoid curve. The GAB model provided a good description of experimental points, as observed in Fig. 1. The high percentages of explained variance obtained (> 99 %) also show the goodness of the fit. The parameters obtained by fitting the GAB model (Eq. 1) to the experimental data were W_m= 0.093 kg w/kg dry solid, K= 0.99 and C= 3.01, which are similar to what is reported in literature for other products at this temperature.[30]

The results of the GAB model were used in the modeling of drying kinetics to calculate the equilibrium moisture content values (average value of W_e=0.103 kg water/kg dry solid) in the NER and the Weibull model and the local water activity on the sample surface (φ_e) in the ER and the ERS model.

3.2. Eggplant shrinkage

As can be observed in Fig. 2, eggplant sample volume was significantly reduced during the drying process, thus, the lower the moisture content, the lower the volume. This fact is considered a common trend in vegetables and fruits.[7,22]

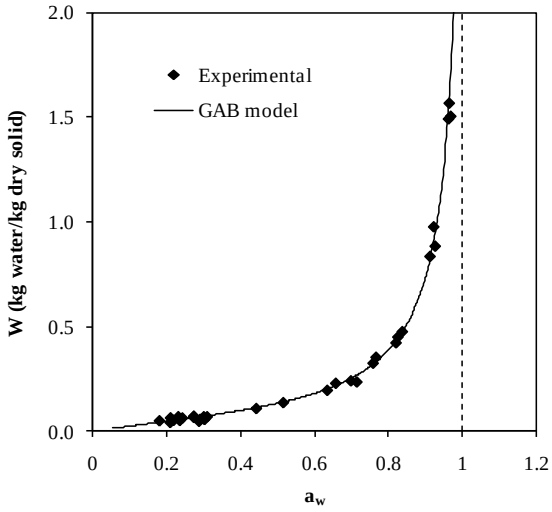

Fig. 1 Experimental sorption isotherm at 40 ºC and GAB model.

Although image analysis and liquid displacement provided a similar pattern in shrinkage data, significant differences between both methods were observed at low moisture contents. Sample volume measured at low moisture contents using image analysis was significantly higher than that measured by liquid displacement. Significant ($p<0.05$) linear relationships between the dimensionless volume and moisture content were established for both shrinkage measurement methods.

$$\frac{V}{V_0}=0.929\frac{W}{W_0}+0.112; \quad R^2=0.99 \tag{21}$$

$$\frac{V}{V_0}=0.621\frac{W}{W_0}+0.309; \quad R^2=0.95 \tag{22}$$

A better correlation was found for liquid displacement (Eq. 21, $R^2=0.992$) than for image analysis data (Eq. 22, $R^2=0.953$). For that reason, the shrinkage data obtained from liquid displacement analysis was chosen to be included in the ERS model. Using the liquid displacement methodology for evaluating drying shrinkage, Souma et al.[24] and Wu et al.[31] also studied the eggplant shrinkage for other cultivars and found very similar linear equation coefficient values to those obtained in this work. These results point to rather similar behavior, regardless of size, shape and cultivar.

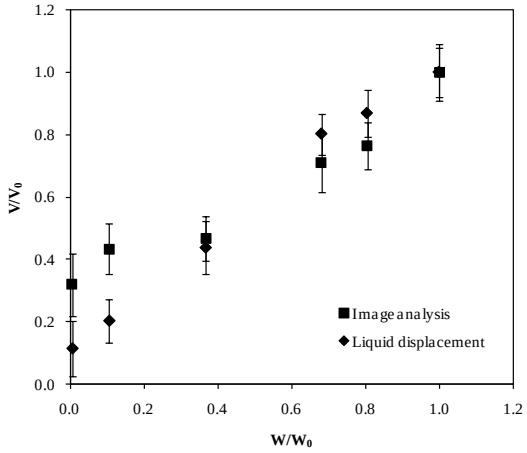

Fig. 2 Experimental shrinkage data for eggplant drying. V: Volume (m^3), W: Average moisture content (kg water/kg dry solid), subscript 0: Initial. Average ± standard deviation values are plotted.

3.3. Experimental drying kinetics

The experimental drying kinetics of eggplant cylinders at the different ultrasonic powers are shown in Fig. 3. The constant rate drying period was not observed in the drying kinetics, thus, the average initial moisture content of eggplant (14.70±0.17 kg water/kg dry solid) was considered as the critical moisture content.

Experimental data showed a very intense effect of power ultrasound (Fig. 3). The ultrasonic application sped up the drying kinetics. Thus, in comparison with the experiments carried out without ultrasonic application (0 kW/m^3), approximately 72 % less drying time was needed to reach an average moisture content of 2.9 kg water/kg dry solid, when applying the maximum ultrasonic power tested (37 kW/m^3). The drying time reduction induced by ultrasonic application was larger in the case of eggplant than when working on other products. Using the same ultrasonic set-up and similar experimental conditions, García-Pérez et al.[11] found drying time reductions of 32 and 53 % in the drying of carrot cubes and lemon peel slabs (40 ºC and 1 m/s), respectively. The intense effect of power ultrasound on the drying rate of eggplant may be linked to the material structure. In this sense, porosity is one of the most important variables in determining the effectiveness of power ultrasound application on food drying.[11] Hence, eggplant, which has a tissue with a highly unconsolidated porous structure,[31] may be considered as a material that has a greater propensity to be affected by ultrasonic energy than carrot and lemon peel.

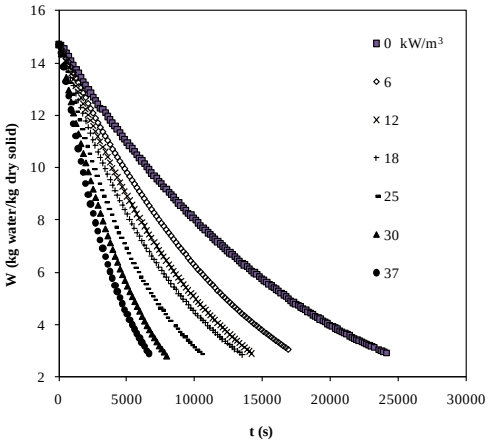

Fig. 3 Drying kinetics of eggplant cylinders at 40 ºC and 1 m/s, applying different ultrasonic powers (kW/m^3).

3.4. Drying modeling

In order to quantify the influence that power ultrasound application has on the mass transfer process during the convective drying of eggplant cylinders, it is convenient to consider modeling. In addition, modeling is useful to establish the influence of power ultrasound on external and internal mass transport. As already stated, theoretical and empirical approaches to the modeling of the drying kinetics of eggplant will be evaluated.

3.4.1. Negligible external resistance model (NER)

The NER diffusion model described by Eq. 12 was used as a first approach to model the experimental drying kinetics of eggplant cylinders. The average effective moisture diffusivity (D_e) identified from experimental results, the percentage of explained variance (% VAR) and mean relative error (% MRE) obtained are shown in Table 2.

In the experiments without ultrasound application (0 kW/m^3), the identified effective moisture diffusivity ($3.31\pm0.37 \times 10^{-10}$ m^2/s) is similar to those estimated by different authors for the convective drying of eggplant. Thus, Chaves et al.[32], reported a similar value (2.93×10^{-10} m^2/s) for eggplant slices dried at 50 ºC.

Table 2 NER model. Effective diffusivity (D_e). Percentage of explained variance (% VAR) and mean relative error (% MRE) identified from modeling. Subscripts (a,b,c,d) show homogeneous group established from LSD intervals ($p<0.05$).

UP (kW/m^3)	D_e (10^{-10} m^2/s)	VAR (%)	MRE (%)
0	$3.31\pm0.3_a$	85.9	16.5
6	$4.26\pm0.8_a$	85.2	18.1
12	$6.19\pm0.5_b$	85.8	18.1
19	$6.31\pm0.3_b$	84.9	18.5
25	$8.84\pm0.3_c$	86.7	17.3
31	$9.14\pm1.0_c$	85.9	18.0
37	$11.16\pm1.0_d$	86.8	16.8

As observed in Table 2, the ultrasonic power applied during drying showed a significant ($p<0.05$) influence on the identified effective moisture diffusivity. Thus, the maximum level of applied ultrasonic power (37 kW/m^3) increased the effective moisture diffusion coefficient by 237 % in comparison with the value identified in the experiments without power ultrasound application (0 kW/m^3). The ultrasonic effects were dependent on the power applied; the higher the applied ultrasonic power, the greater the identified effective diffusivity. In the range of the ultrasonic power level (UP) used in this work (0-37 kW/m^3), a significant ($p<0.05$) linear relationship between the ultrasonic power level and the effective moisture diffusivity was found (Fig. 4).

The improvement of the D_e values is associated with the mechanical effects brought about by applying ultrasound to the material being dried. The alternating cycles of expansions and contractions ("sponge effect") may contribute to easy water leaving the solid matrix, thus reducing the internal resistance to mass transfer. García-Pérez et al.[11] reported increases of 40 % and 131 % in the identified effective diffusivity (using a NER model) of carrot and lemon peel, respectively, when the same intensity of applied ultrasonic power (37 kW/m^3) was tested. Previous results indicate that high porosity products are more prone to the "sponge effect" showing a low internal resistance to the mechanical stress; therefore, the effects of ultrasound should be more intense in this type of products.[11]

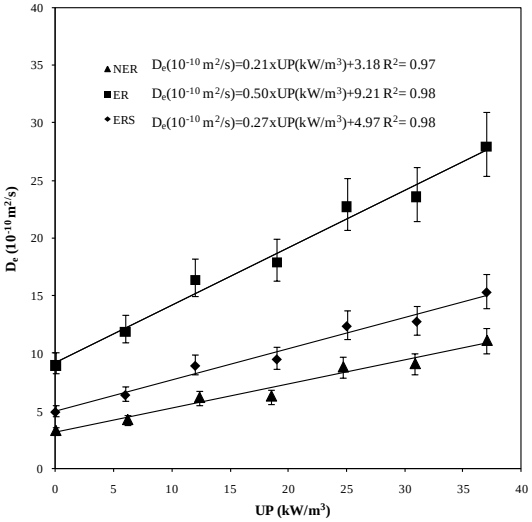

Fig. 4 Influence of the ultrasonic power (UP) on the effective moisture diffusivity. Average values ± LSD intervals ($p<0.05$) are plotted.

The NER model provided low percentages of explained variance (ranging between 84-87 %) and high percentages of the mean relative error (ranging between 16.5-18.5 %). The poor fit of the NER model may be linked to the proposed boundary conditions (Eq. 6 and Eq. 7, Table 1). Thus, the D_e values are simple fitting parameters, including not only the diffusion mechanisms but also other mechanisms and phenomena not considered in the modeling. In this sense, Akpinar and Bicer[33] reported that, at air velocities of 2.5 m/s or lower, the external mass transport resistance is significant and needs to be considered in the analysis of the eggplant drying data. Therefore, the use of a diffusion model that takes external resistance into account (ER model) would be necessary. In addition, as already mentioned, the ER model will permit the external and internal resistance to mass transfer to be separated.

3.4.2. Model considering external resistance (ER)

The ER model improved the description of the drying kinetics, achieving percentages of explained variance of over 99 % and mean relative errors of under 1.5 % in every case (Table 3). Thus, considering the external resistance seems to be adequate in order to describe the behavior of experimental eggplant drying. Considering diffusion moisture content dependent could also improve the fitting ability of the model.[34] This approach requires increasing the number of diffusion related parameters, which

makes difficult to highlight the effect of ultrasound application. As a consequence, an average/constant effective diffusivity was considered. The value of the mass transfer coefficient identified in the experiments without applying ultrasound (0 kW/m^3, Table 3) was very similar to the value calculated (1.35x10^{-3} kg water/m^2/s) using common correlations proposed in literature.[27]

Table 3 ER model. Effective diffusivity (De) and mass transfer coefficient (k). Percentage of explained variance (% VAR) and mean relative error (% MRE) identified from modeling. Subscripts (a,b,c,d,e,f) and (w,x,y,x) show homogeneous group established from LSD intervals ($p<0.05$).

UP (kW/m^3)	D_e (10^{-10} m^2/s)	k (10^{-3} kg water/m^{2}s^{-1})	VAR (%)	MRE (%)
	$8.9\pm1.3_a$	$1.87\pm0.4_w$	99.9	0.9
6	$11.8\pm2.7_{ab}$	$2.32\pm0.4_w$	99.9	0.9
12	$16.3\pm1.2_{bc}$	$3.35\pm0.3_x$	99.9	0.7
19	$17.8\pm3.2_{cd}$	$3.43\pm0.3_x$	99.8	1.3
25	$22.7\pm3.0_{de}$	$4.86\pm0.4_y$	99.9	0.9
31	$23.5\pm3.1_{ef}$	$4.79\pm0.7_y$	99.9	1.0
37	$27.9\pm3.0_f$	$6.16\pm0.9_z$	99.8	1.4

The power ultrasound application affected the external resistance to water transport. The mass transfer coefficient (k) was improved by 229 % when the maximum ultrasonic power (37 kW/m^3) was applied. As was already found for the effective diffusivity, a significant ($p<0.05$) linear relationship was observed between the mass transfer coefficient and the applied ultrasonic power (UP) (Figs. 4 and 5).

Studying the ultrasonic assisted drying of persimmon, Cárcel et al.[27] reported improvements of 34.5 % at 1 m/s and 31 kW/m^3 in the mass transfer coefficient, in comparison with the experiments carried out without power ultrasound application. These authors analyzed the influence of the drying air velocity on the external mass transport resistance during ultrasonic drying and concluded that, at low drying air velocities (< 4 m/s), the external resistance is significant and should be included in the modeling. The increase of the mass transfer coefficient is linked to the reduction of the boundary layer thickness due to different effects of ultrasound, like pressure

variations, oscillating velocities and micro-streaming on the solid-gas interfaces. Therefore, these effects should be responsible for the reduction of the boundary layer of diffusion and, as a consequence, the improvement in the rate of water transfer from the solid surface to the air medium.[10]

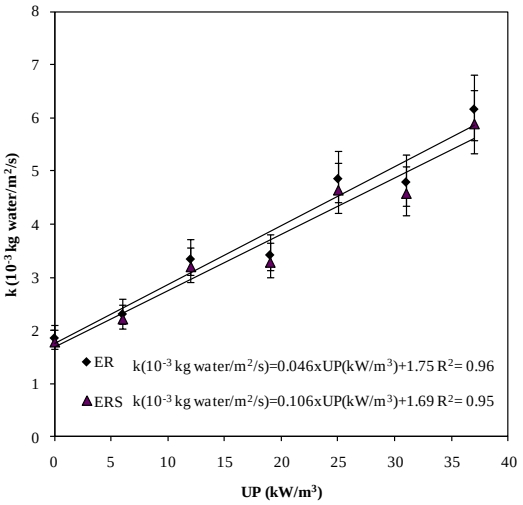

Fig. 5 Influence of the ultrasonic power (UP) on the mass transfer coefficient. Average values ± LSD intervals ($p<0.05$) are plotted.

Although the ER model provides a good description of drying curves, it could also be improved by considering the shrinkage of the product as a phenomenon which would explain the dehydration process better and also by increasing the confidence of the identified diffusion coefficient.

3.4.3. Model considering external resistance and shrinkage (ERS)

The most complex model showed high percentages of explained variance, over 99.9 % in every case, and low percentages of mean relative error, of under 1.2 % (Table 4). Both statistical parameters indicate a close fit between the calculated and experimental data, even better than that obtained in the ER model. The close fit confirms that the assumption of significant external resistance and shrinkage considered in the modeling seems to be adequate for the eggplant drying process. As in the ER model, significant ($p<0.05$) linear relationships were also found between the

mass transfer coefficient and effective moisture diffusivity and the applied ultrasonic power (UP) (Figs. 4 and 5).

Table 4 ERS model. Effective diffusivity (De) and mass transfer coefficient (k). Percentage of explained variance (% VAR) and mean relative error (% MRE) identified from modeling. Subscripts (a,b,c,d) and (w,x,y,z) show homogeneous group established from LSD intervals ($p<0.05$).

UP (kW/m^3)	D_e (10^{-10} m^2/s)	k (10^{-3} kg water/m^2s^{-1})	VAR (%)	MRE (%)
0	$4.9\pm0.9_a$	$1.79\pm0.4_w$	99.9	0.4
6	$6.3\pm1.4_a$	$2.22\pm0.4_w$	99.9	0.5
12	$8.9\pm1.8_b$	$3.20\pm0.2_x$	99.9	0.6
19	$9.4\pm1.7_b$	$3.29\pm0.3_x$	99.9	1.0
25	$12.3\pm1.4_c$	$4.65\pm0.3_y$	99.9	0.9
31	$12.7\pm1.7_c$	$4.58\pm0.7_y$	99.9	0.5
37	$15.2\pm1.8_d$	$5.89\pm0.8_z$	99.9	1.1

As can be observed in Fig.4, when shrinkage is not included in the modeling (ER model), the values of D_e are overestimated, in the range of 81.8-88.7 %. Following this assumption, Rahman and Kumar[35] analyzed the influence of shrinkage on the effective moisture diffusivity during the drying of potato cylinders (length 50 mm and thickness of 5,8,10 and 16 mm) and slices (thickness 10 mm). They found overestimated D_e values, in the range of 75.9-128.1 %, when shrinkage is not taken into account in the analysis. For banana drying (29.9-68.4 ºC), Queiroz and Nebra,[21] found overestimated D_e values, in the range of 20-50 %. Similar conclusions were also reported by Hernández et al.,[23] during the drying (50, 60 and 70 ºC and 3 m/s) of mango (thickness 5, 10 and 15 mm) and cassava (thickness 10, 20 and 30 mm) slices. The overestimated values of effective moisture diffusivity may be attributed to the fact that shrinkage reduces the distance for the diffusion of water molecules.

The mass transfer coefficients identified in the ERS model were slightly lower than in the ER model but the differences were not significant (Fig. 5). The sample shape may affect the water convective transport, but in this work, the inclusion of the shrinkage did not lead to any differences in the mass transfer coefficient.

3.4.4. Weibull model

The Weibull model adequately described the drying kinetics under the different experimental conditions tested in this work. The percentages of explained variance (% VAR) were, in every case, higher than 99.9 %, while the percentages of mean relative error (% MRE) were lower than 1.1 % (Table 5). The value of the statistical parameters were similar to that obtained using the ERS model. For real time applications, the use of the Weibull model may be advantageous due to its computational simplicity.

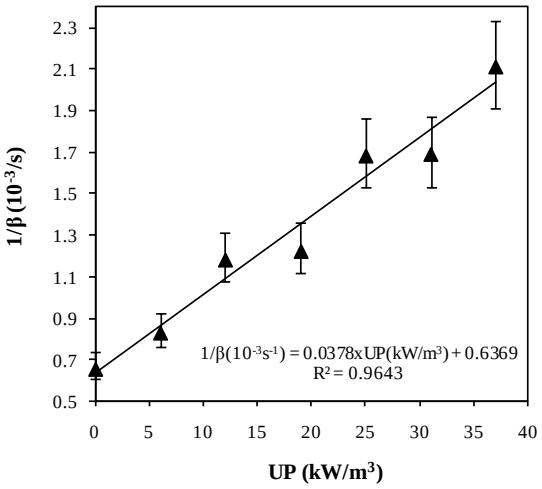

Fig. 6 Influence of ultrasonic power on kinetic parameter 1/β of eggplant cylinders at 1 m/s. Average values ± LSD intervals ($p<0.05$) are plotted.

On the one hand, the shape parameter, α, was not dependent on the level of applied ultrasonic power. On the other hand, the kinetic parameter, β, decreased as the applied ultrasonic power increased. As the β parameter is inversely proportional to the drying rate, a reduction of this value indicates an increase of the drying rate. A significant ($p<0.05$) linear relationship between the ultrasonic power level and 1/β was found in the range of the ultrasonic power level used in this work (0-37 kW/m^3) (Fig. 6). García-Pérez et al.[26] found a similar correlation in carrot cubes (18 mm) dried at 40 ºC and 0.6 m/s.

The Weibull model provided similar information to the diffusion models about the influences of the ultrasonic power on the kinetic parameters. However, the Weibull model has two main limitations: its results cannot be extrapolated to other working conditions or product geometries and does not provide information about mass transport mechanisms. Notwithstanding, this empirical model may be used as a first approach to more complex models, and its use in further industrial applications may also be considered relevant due to its simplicity.

Table 5 Weibull model. Parameters, α and β, percentage of explained variance and mean relative error. Subscripts (a,b,c,d,e) show homogeneous group established from LSD intervals ($p<0.05$).

UP (kW/m^3)	β (10^3 s)	α	VAR (%)	MRE (%)
0	$15.30\pm0.8_a$	1.08 ± 0.01	99.9	0.6
6	$12.46\pm0.9_a$	1.11 ± 0.02	99.9	0.6
12	$8.51\pm0.7_{ab}$	1.09 ± 0.02	99.9	0.5
19	$8.21\pm0.6_{bc}$	1.11 ± 0.10	99.9	0.7
25	$5.96\pm0.3_c$	1.07 ± 0.06	99.9	0.4
31	$6.00\pm0.8_d$	1.10 ± 0.03	99.9	0.6
37	$4.80\pm0.6_e$	1.07 ± 0.04	99.9	1.0

4. Conclusions

A diffusion model, considering the external resistance to mass transfer and shrinkage to be significant phenomena, provided a good description of eggplant drying kinetics. In addition, it allows the ultrasonic effects on the mass transport rate to be quantified. The Weibull empirical model also provides good results and could be useful for control purposes. From the results obtained in this piece of work, the application of power ultrasound in drying processes is considered to have great potential due to the improvement brought about in both the internal and external mass transport. Further research is required in order to apply this technology on an industrial scale.

Acknowledgments

The authors acknowledge the financial support of the Ministerio de Ciencia e Innovación (MICIN) of Spain from the project DPI2009-14549-C04-04 and the Generalitat Valenciana from the project PROMETEO/2010/062.

Nomenclature

a_w	Water activity
C	GAB model parameter, dimensionless (Eq. 1)
D_e	Effective diffusivity, m^2/s
K	GAB model parameter, dimensionless (Eq. 1)
k	Mass transfer coefficient, kg water/m^2/s
L	Half height, m
R	Radius, m
r	Radial co-ordinate, m
S_y	Standard deviation of the sample
S_{yx}	Standard deviation of the estimation
T	Temperature, K
t	Time, s
W	Average equilibrium moisture content, kg water/kg dry solid
W_c	Critical moisture content, kg water/kg dry solid
W_{ci}	Calculated moisture content, kg water/kg dry solid
W_e	Equilibrium moisture content, kg water/kg dry solid.
W_{ei}	Experimental moisture content, kg water/kg dry solid
W_m	Monolayer average equilibrium moisture content, kg water/kg dry solid
W_p	Local moisture content, kg water/kg dry solid
x	Axial co-ordinate, m
α	Weibull model parameter, dimensionless
α_n	Eigenvalues
β	Weibull model parameter, s
ρ_{ss}	Dry solid density, kg/m^3
φ_{air}	Relative humidity drying air
φ_e	Water activity
ψ	Dimensionless moisture

References

1. Mujumdar, A.S. An overview of innovation in industrial drying: current status and R&D needs. Transport in Porous Media **2007**, *66*, 3-18.
2. Chou, S.K; Chua, K.J. New hybrid drying technologies for heat sensitive foodstuff. Trends in Food Science & Technology **2001**, *12*, 359-369.
3. Lewicki P. P. Design of hot air drying for better foods. Trends in Food Science & Technology **2006**, *17*, 153-163.
4. Timoumi, S.; Mihoubi, D.; Zagrouba, F. Shrinkage, vitamin C degradation and aroma losses during infra-red drying of apple slices. Swiss Society of Food Science and Technology **2007**, *40*, 1648-1654.
5. Santos, P.H.S; Silva, M.A. Kinetics of L-ascorbic degradation in pineapple drying under ethanolic atmosphere. Drying Technology **2009**, *27*, 947-954.
6. Suvarnakuta, P.; Devahastin, S.; Mujumdar, A. S. Drying kinetics and β-carotene degradation in carrot undergoing different drying processes. Journal of Food Science **2005**, *70* (8), s520-s526.
7. Mayor, L.; Sereno, A.M. Modelling shrinkage during convective drying of food materials: a review. Journal of Food Engineering **2004**, *61*, 373-386.
8. Abasi, S.; Mousavi, S. M.; Mohebi, M.; Kiani, S. Effect of time and temperature on moisture content, shrinkage, and rehydration of dried onion. Iranian Journal of Chemical Engineering **2009**, *6*(3), 57-60.
9. Gallego-Juárez, J.A. High power ultrasound processing: recent developments and prospective advances. Physics Procedia **2010**, *3*, 35-47.
10. De la Fuente-Blanco, S.; Riera-Franco de Sarabia, E.; Acosta-Aparicio, V.M.; Blanco-Blanco, A.; Gallego-Juárez, J.A. Food drying process by power ultrasound, Ultrasonics **2006**, *44*, e523-e527.
11. García-Pérez, J.V.; Cárcel, J.A; Riera, E.; Mulet A. Influence of applied acoustic energy on the drying of carrots and lemon peel. Drying Technology **2009**, *27*, 281-287.
12. Mulet, A.; Cárcel, J.A.; Sanjuan, N.; García-Pérez, J.V. Food dehydration under forced convection conditions. In *Recent Progress in Chemical Engineering*; Delgado J. (Ed.), Studium Press LLC; Houston, TX, USA. **2010**, 153-177.
13. García-Pérez, J.V.; Cárcel, J.A.; Clemente, G.; Mulet, A. Water sorption isotherms for lemon peel at different temperatures and isosteric heats. LWT-Food Science and Technology **2008**, *41*, 18-25.

14. Mulet, A. Drying modelling and water diffusivity in carrots and potatoes. Journal of Food Engineering **1994**, *22*, 329-348.
15. Cunha, L.M.; Oliveira, F.A.R.; Oliveira, J.C. Optimal experimental design for estimating the kinetic parameters of processes described by the Weibull probability distribution function. Journal of Food Engineering **1998**, *37*, 175-191.
16. Azzouz, S.; Guizani, A.; Jomaa, W.; Belghith, A. Moisture diffusivity and drying kinetic equation of convective drying of grapes. Journal of Food Engineering **2002**, *55*, 323-330.
17. Simal, S., Femenía, A.; Garau, M.C.; Rosselló, C. Use of exponential, Page's and diffusional models to simulate the drying kinetics of kiwi fruit. Journal of Food Engineering **2005**, *66*, 323-328.
18. Crank, J. *The Mathematics of Diffusion*; Oxford University Press, London, 1975.
19. Maroulis, Z.B.; Saravacos, G.D.; Panagiotou, N.M.; Krokida, M.K. Moisture diffusivity data compilation for foodstuffs: effect of material moisture content and temperature. International Journal of Food Properties **2001**, *4*, 225-237.
20. Simal, S.; Femenía, A.; García-Pascual, P.; Rosselló, C. Simulation of the drying curves of a meat-based product: effect of the external resistance to mass transfer. Journal of Food Engineering **2003**, *58*, 193-199.
21. Queiroz, M.R.; Nebra, S.A. Theoretical and experimental analysis of the drying kinetics of bananas. Journal of Food Engineering **2001**, *47*, 127-132.
22. Hassini, L.; Azzouz, S.; Peczalski, R.; Belghith, A. Estimation of potato moisture diffusivity from convective drying kinetics with correction for shrinkage. Journal of Food Engineering **2007**, *79*, 47-56.
23. Hernández J.A.; Pavón G.; García M.A. Analytical solution of mass transfer equation considering shrinkage for modeling food-drying kinetics. Journal of Food Engineering **2000**, *45*, 1-10.
24. Souma, S.; Tagawa, A. A.; Limoto, M. Structural properties for fruits and vegetables during drying. Journal of the Japanese Society for Food Science and Technology **2004**, *51(11)*, 577-584.
25. Association of Official Analytical Chemists. Official Methods of Analysis; AOAC: Washington, DC, 1997.
26. García-Pérez, J.V.; Cárcel, J.A.; De la Fuente-Blanco, S.; Riera-Franco de Sarabia, E. Ultrasonic drying of foodstuff in a fluidized bed: Parametric study, Ultrasonics **2006**, *44*, e539-e543.

27. Cárcel, J.A.; García-Pérez, J.V.; Riera, E.; Mulet, A. Influence of high intensity ultrasound on drying kinetics of persimmon, Drying Technology **2007**, *25*: 185-193.
28. Blasco, M.; García-Pérez, J.V.; Bon, J.; Carreres, J.E.; Mulet, A. Effect of blanching and air flow rate on turmeric drying. Food Science and Technology International **2006**, *12*, 315-323.
29. Lypson, C.; Sheth, J.J. *Statistical Design and Analyisis of Engineering Experiments*; McGraw-Hill, New York, 1973.
30. Garau, M.C.; Simal, S.; Femenia, A.; Roselló, C. Drying of orange skin: drying kinetics modelling and functional properties. Journal of Food Engineering **2006**, *75*, 288-295.
31. Wu, L.; Orikasa, T.; Ogawa, Y.; Tagawa, A. Vacuum drying characteristics of eggplant. Journal of Food Engineering **2007**, 83, 422-429.
32. Chaves, M.; Sgroppo, S.C.; Avanza, J.R. Cinéticas de secado de berenjena (*Solanum melongena* L.). Comunicaciones Científicas y Tecnológicas (Universidad Nacional del Nordeste Corrientes Argentina), **2003,** *Resumen E-060*.
33. Akpinar, E.K.; Bicer, Y. Modelling of drying of eggplants in thin-layers. International Journal of Food Science and Technology **2005**, *40*, 273-281.
34. Lima, A.G.B.; Queiroz, M.R.; Nebra, S.A. Simultaneous moisture transport and shrinkage during drying of solids with ellipsoidal configuration. Chemical Engineering Journal **2002**, *86*, 85–93.
35. Rahman, N.; Kumar, S. Influence of sample size and shape on transport parameters during drying of shrinking bodies. Journal of Food Process Engineering **2007**, *30*, 186-203.

Ultrasonics Sonochemistry (Accepted)

Influence of Material Structure on Air-Borne Ultrasonic Application in Drying

César Ozuna[a], Tomás Gómez Álvarez-Arenas[b], Enrique Riera[b], Juan A. Cárcel[a], Jose V. Garcia-Perez[a,]*

[a] Grupo de Análisis y Simulación de Procesos Agroalimentarios. Departamento de Tecnología de Alimentos. Universitat Politècnica de València.

Camino de Vera. s/n. E46022. Valencia, Spain

[b] Dpto. Sensores y Sistemas Ultrasónicos (DSSU), ITEFI, CSIC.

Serrano 144. E28006. Madrid, Spain

Abstract

This work aims to contribute to the understanding of how the properties of the material being dried affect air-borne ultrasonic application. To this end, the experimental drying kinetics (40 ºC and 1 m/s) of cassava (*Manihot esculenta*) and apple (*Malus domestica* var. *Granny Smith*) were carried out applying different ultrasonic powers (0, 6, 12, 19, 25 and 31 kW/m^3). Furthermore, the power ultrasound-assisted drying kinetics of different fruits and vegetables (potato, eggplant, carrot, orange and lemon peel) already reported in previous studies were also analyzed. The structural, textural and acoustic properties of all these products were assessed, and the drying kinetics modeled by means of the diffusion theory.

A significant linear correlation ($r>0.95$) was established between the identified effective diffusivity (D_W) and the applied ultrasonic power for the different products. The slope of this relationship (SDUP) was used as an index of the effectiveness of the ultrasonic application; thus the higher the slope, the more effective the ultrasound application. SDUP was well correlated ($r\geq0.95$) with the porosity and hardness. In addition, SDUP was largely affected by the acoustic impedance of the material being dried, showing a similar pattern with the impedance than the transmission coefficient of the acoustic energy on the interface. Thus, soft and open-porous product structures exhibited a better transmission of acoustic energy and were more prone to the mechanical effects of ultrasound. However, materials with a hard and closed-compact structure were less affected by acoustic energy due to the fact that the significant impedance differences between the product and the air cause high energy losses on the interface.

Keywords:
Mass transport; Porosity; Cryo-SEM; Texture; Impedance acoustic

1. Introduction

The structural properties of vegetable tissues are of great scientific interest and an important subject of research [1,2]. The vegetable cell wall, which, among other functions, serves as mechanical support and external barrier, is the main structural component [3]. During fruit and vegetable processing, such as drying, the macrostructure, microstructure and composition of the cell walls undergo a series of changes that affect the functional properties [4] and also modify their ultrasonic properties [5]. In addition, the structure of the vegetable tissues itself can also largely influence the processing, e.g. affect the mass transfer rate during drying [6].

Convective drying is one of the most common unit operations used to dehydrate fruits and vegetables [7]. During drying, the plant tissue is subjected to high stress caused by the water removal and the high temperatures applied. These facts produce macroscopic changes, such as shrinkage or color and textural modifications, which are mostly linked to tissue alterations on a microscopic level [8].

The increasing need for the production of high quality dry products at reduced cost has led to traditional drying methods being combined with non-conventional energy sources [9]. In this regard, air-borne ultrasound application represents a very promising technique due to its low heating effect, which is particularly relevant for products containing thermo-labile compounds [10,11]. The improvement in the water transfer rate produced by ultrasound is linked to the effect it has, not only on the solid-gas interfaces (pressure variations, oscillating velocities and microstreaming) [12,13] but also on the internal structure (series of cyclical and rapid [> 20 kHz] compressions and expansions, a mechanism known as the sponge effect) [14,15]. The intensity of ultrasonic effects during drying has been shown to be largely dependent on the process variables, such as the temperature [16], air velocity [17], acoustic power applied [18], and also even on product characteristics [19]. In this sense, previous studies have shown that a minimum ultrasonic power must be applied in order to observe any significant effects of ultrasound. This ultrasonic power threshold depends on the product being dried [20], and it is likely that this could be linked to the different internal structure. Previous studies have highlighted the fact that porosity could explain how ultrasonic effects during drying are largely dependent on the product being dried [17,20]. This statement stems from the comparison between the air-borne ultrasound assisted drying of carrot and persimmon (low porosity products)

and that of lemon peel and analyzing how the effective diffusivity was dependent on the acoustic power [20] or the air velocity applied [17]. However, the comparison was merely qualitative and no quantitative analysis was performed. In addition, an analysis of instrumental texture and microstructure could also contribute to a better understanding of ultrasound-solid interaction [21].

Since the structural and textural properties affect the propagation of acoustic waves [22], the study of the materials' ultrasonic properties could also provide relevant information about how efficiently the energy is transferred during drying. The ultrasonic velocity and the attenuation are the most common parameters used for product characterization due to their good correlation with several physical and chemical properties of foodstuffs [23,24]. Conventional ultrasonic techniques involve an intimate contact between the transducer and the sample, and frequently require the use of a coupling medium (such as gel, water or oil) and a certain pressure, which, to a certain extent, delays the measurement and may contaminate and modify the product. Recently, novel non-contact ultrasonic techniques are being tested in which new sensors provide an efficient energy transmission using air as the coupling medium [25]. Thus, Sancho-Knapik et al. [5] used an air-borne broadband ultrasonic technique to characterize biological materials, such as leaves.

This works aims to contribute to understanding how the material being dried affects air-borne ultrasonic application in the drying of biological materials. For that purpose, how ultrasound affects drying kinetics will be correlated with the structural, textural and acoustic properties of different fruits and vegetables. Furthermore, microstructural observations (Cryo-SEM) will help to explain the results obtained.

2. Materials and methods

2.1. Ultrasonic assisted drying kinetics

Drying experiments were carried out with cassava (*Manihot esculenta*) and apple (*Malus domestica* var. *Granny Smith*) purchased in a local market. For both products, cubic samples (side 10 mm) were obtained from the flesh using a household tool. The drying experiments were conducted at 40 ºC and 1 m/s, applying different ultrasonic powers (UP: 0, 6, 12, 19, 25, 31 kW/m^3), defined as the electric power supplied to the ultrasonic transducer divided by the volume of the drying chamber. The drying

experiments were extended until a sample weight loss of 50% and 80% was achieved for cassava and apple, respectively. Drying kinetics were determined from the sample weight during drying, measured at preset times, and the initial moisture content (AOAC method Nº 934.06) [26]. For each condition tested, the drying experiments were carried out at least four times.

The drying experiments took place in a convective drier assisted by power ultrasound, already described in previous studies [27]. The drying chamber consists of an aluminum vibrating cylinder (internal diameter 100 mm, height 310 mm and thickness 10 mm) driven by a piezoelectric transducer (21.8 kHz). The ultrasonically activated drying chamber is able to generate a high-intensity ultrasonic field in the drying air, reaching an average sound pressure of 154.3 dB (measured by applying an acoustic power of 31 kW/m^3 in stagnant conditions). An impedance matching unit permits the impedance output of the generator to be tuned to the transducer resonance frequency providing the system with a better electrical yield.

2.2. Modeling

The experimental drying kinetics of apple and cassava were modeled according to the diffusion theory. The differential equation of diffusion was obtained combining Fick's law and the microscopic mass balance. For cubic geometry and considering the effective moisture diffusivity as constant and the solid as isotropic, the diffusion governing equation is shown as follows:

$$\frac{\partial W_p(x,y,z,t)}{\partial t} = D_W\left(\frac{\partial^2 W_p(x,y,z,t)}{\partial x^2} + \frac{\partial^2 W_p(x,y,z,t)}{\partial y^2} + \frac{\partial^2 W_p(x,y,z,t)}{\partial z^2}\right) \quad (1)$$

The diffusion equations were solved by assuming the solid to be symmetrical, the initial moisture content and temperature uniform and the product shape constant during the drying process. The external resistance to mass transfer was neglected, thus, mass transfer was assumed to be entirely controlled by diffusion mechanisms. The analytical solution [28] of the governing equation for cubic geometry in terms of the average moisture content is given in Eq. (2).

$$W(t) = W_e + (W_0 - W_e) \cdot \left[\sum_{n=0}^{\infty} \frac{8}{(2n+1)^2 \pi^2} e^{\left(-\frac{D_W (2n+1)^2 \pi^2 t}{4L^2} \right)} \right]^3 \quad (2)$$

Eq. (2) was fitted to the experimental drying kinetics in order to identify the effective moisture diffusivity (D_W). The identification was performed by minimizing the squared differences between the experimental and calculated average moisture contents. For that purpose, the Generalized Reduced Gradient (GRG) optimization method, available in the Microsoft Excel spreadsheet from Microsoft Office XP Professional, was used. In order to evaluate the goodness of fit (of Eq. (2) with the experimental drying kinetics), the explained variance (VAR (%), Eq. (3)) was computed [29].

$$VAR(\%) = \left[1 - \frac{S_{xy}^2}{S_y^2} \right] \cdot 100 \quad (3)$$

The analysis of variance (ANOVA) and the Least Significant Difference (LSD) intervals ($p<0.05$) were calculated using the Statgraphics Centurion XVI software package (Statistical Graphics Corp., Herdorn, USA) to statistically evaluate how the UP applied affected the D_W.

The purpose of modeling the drying kinetics of cassava and apple was to provide a relationship between the D_W and the UP. Thereby, in order to complete the results obtained in this work, similar data already reported in the literature on the ultrasonically assisted hot air drying of several fruits and vegetables, potato (*Solanum tuberosum* var. Monalisa) [18], eggplant (*Solanum melongena* var. Black Enorma) [30], carrot (*Daucus carota* var. Nantesa) [20], orange (*Citrus sinensis* var. Navelina) [31] and lemon (*Citrus limon* var. Fino) peel [20], were used. This allowed the comparison of the effects induced by ultrasound in the drying of products with very different properties. It should be emphasized that all collected data correspond with materials dried in the same ultrasonic assisted drier at 40 ºC, 1 m/s and in the same range of applied UP (0-31 kW/m^3). Moreover, the modeling of the experimental data was carried out using the same type of diffusion model. Therefore, the data presented in this work can be rigorously compared.

2.3. Structural, textural and acoustic analysis

In order to study the influence of material properties on the effects of air-borne ultrasonic application during drying, the microstructure, porosity, instrumental texture and acoustic properties of apple, cassava, carrot, potato, eggplant, orange peel and lemon peel were analyzed.

2.3.1. Cryo-scanning electron microscopy (Cryo-SEM)

Cubic samples (side 3 mm) of the raw products were immersed in slush Nitrogen (-210 ºC), and quickly transferred into a cryo-trans (CT 15000 C, Oxford Instruments, England) linked to a scanning electron microscope (JSM-5410, Jeol, Japan). Samples were cryo-fractured at -180 ºC, etched at -90 ºC and gold-coated, allowing cross-section visualization. The microscopic observations were carried out at 10 kV, at a working distance of 15 mm and a temperature below -130 ºC.

2.3.2. Porosity

The porosity (ε) represents the ratio between the volume of air present in the sample and its total volume. Thus, the porosity of the different products was calculated from the bulk (ρ_b) and particle density (ρ_s) [32] (Eq. (4)).

$$\varepsilon = 1 - \frac{\rho_b}{\rho_s} \tag{4}$$

The ρ_b was calculated as the ratio between the sample weight and its volume (Eq. (5)).

$$\rho_b = \frac{m_t}{V_t} \tag{5}$$

The volume was measured by liquid displacement using toluene (density 0.867 g/mL at 20 ºC), a volumetric standard picnometer (48.89 ml) and an analytical balance (PB 303-S, Mettler Toledo, Spain).

The particle density (ρ_s) was measured in a previously milled sample and calculated as the ratio between the sample mass and its volume (excluding pores) (Eq. (6)).

$$\rho_s = \frac{m_s}{V_s} \quad (6)$$

The porosity was measured at least 10 times for each one of the products tested.

2.3.3. Texture

The textural properties were assessed using a Texture Analyzer (TAX-T2®, Stable Micro System, United Kingdom). A texture profile analysis (TPA) was carried out by two compression cycles between parallel plates and performed on cylindrical samples (diameter of 7.70 mm, height of 6 mm) of raw products using a 75 mm flat cylinder probe (SMS P/75), a crosshead speed of 1 mm/s, a period of time between cycles of 5 s and a strain of 25%. In the case of orange and lemon peels, the TPA analysis was carried out on the albedo and flavedo sides and averaged. At least 15 measurements of each product were taken.

2.3.4. Acoustic properties

The acoustic properties were measured in cylinders (diameter of 365 mm and height of 30 mm), obtained from the flesh of raw products with the help of a cork-borer and a domestic slicer (V Mandoline, Ibili, Spain).

The ultrasonic measurements were taken using a pair of air-coupled piezoelectric transducers [33]. Briefly, the experimental set-up (Fig. 1) includes two pairs of specially designed air-coupled piezoelectric transducers with a center frequency of 0.1-1 MHz (ITEFI, CSIC, Spain). Supports were used to hold the sample between the transducers, but there was no contact between them. The transmitter and receiver transducers were placed vertically, facing each other at a distance of 2 cm apart. The transmitter was driven by a negative square semi-cycle tuned to the center frequency of the transducers at an amplitude of 200 V (P/R 5077, Panametrics, USA). This transducer transmits an ultrasonic signal that travels across the air-gap and the sample between transmitter and receiver and is eventually detected by the receiver. This converts the ultrasonic wave into an electrical signal that is then amplified and filtered by the receiver and digitalized in a digital oscilloscope (5052, Tektronix, USA). From the digitalized signal, the ultrasonic velocity was determined from which the impedance (Z) was calculated according to Eq. (7).

$$Z = \rho \cdot v \tag{7}$$

The air/solid transmission coefficient (TC) for a plane wave and normal incidence on a product surface, which constitutes a flat interface, was identified as [34]:

$$TC = \frac{4 \cdot Z_s \cdot Z_a}{(Z_s + Z_a)^2} \tag{8}$$

Where Z_s and Z_a are the acoustic impedances of the solid product and air, respectively.

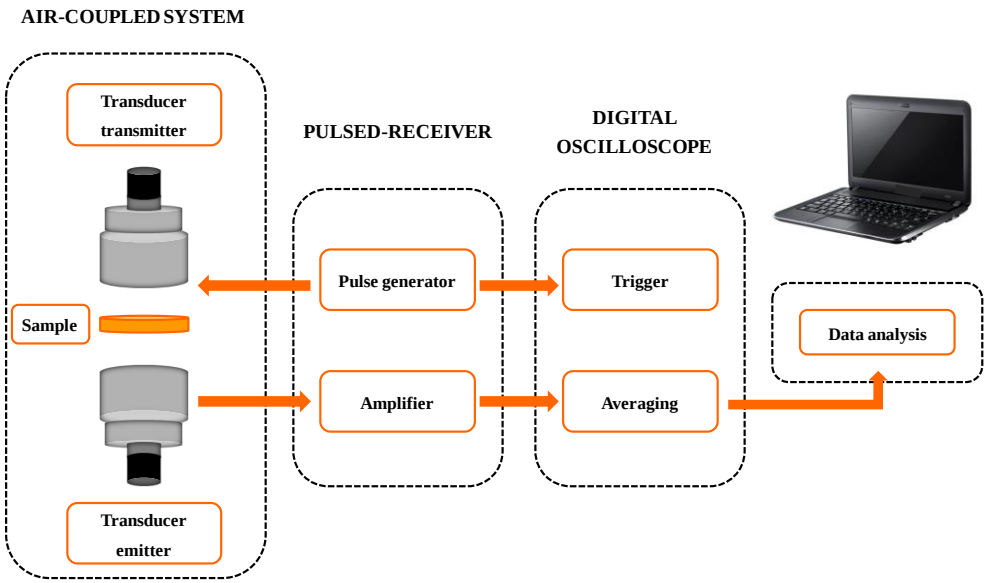

Fig. 1 Experimental set up for air-coupled ultrasonic measurements.

3. Results and discussion

3.1. Drying kinetics of cassava and apple

The average initial moisture contents for cassava and apple were 1.37±0.14 and 5.66±0.46 kg w/kg dry matter (d.m.), respectively. These figures may be considered as the critical moisture contents due to the fact that drying only took place in the falling rate period [9] (Fig. 2). The dried samples presented a final moisture content of

0.19±0.01 kg w/kg d.m. and 0.31±0.06 kg w/kg d.m., which corresponded to an initial weight loss of 50% and 80% for the cassava and apple, respectively.

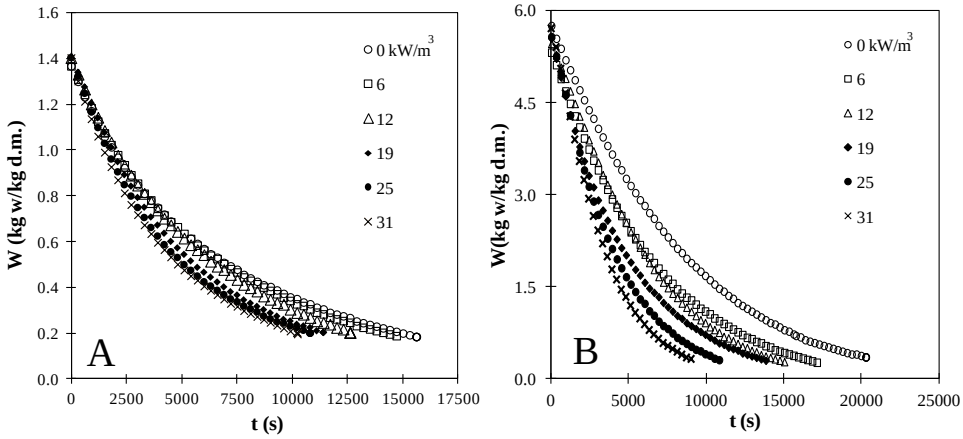

Fig. 2 Experimental drying kinetics of cassava (A) and apple (B) cubes (side 10 mm) carried out at 40 ºC and 1 m/s, applying different ultrasonic powers (UP, kW/m^3).

As can be observed in Fig. 2, the drying rate of both products, cassava and apple, increased when ultrasound was applied and the more UP applied, the faster the drying. For example, in the case of cassava (Fig. 2, A), the drying time needed to reach an average moisture content of 0.3 kg w/kg d.m. was shortened by 32% when the maximum acoustic power was applied (31 kW/m^3). In the case of apple, a time reduction (Fig. 2, B) of 56% was achieved by applying the same acoustic density The drying time reduction induced by ultrasonic application (31 kW/m^3) was in the range of others reported in previous studies for experiments carried out in similar conditions. Thus, the application of power ultrasound (31 kW/m^3) during the drying of potato [18], carrot and lemon peel [20] reduced the drying time by 39, 34 and 49%, respectively. In the case of eggplant drying [30], the time reduction achieved by the application of ultrasound reached 67%.

3.2. Influence of ultrasound on effective moisture diffusivity

The modeling of experimental drying kinetics allowed the influence that power ultrasound application had on the mass transfer process during the convective drying to be quantified and also permitted the comparison of the products.

The fitting of the proposed diffusion model (Eq. (2)) into the experimental data provided VAR (%) ranging between 85-92%. The fact that these values are low suggests that some of the assumptions considered in the model formulation were not close to the experimental conditions. However, the results achieved can be used to compare and quantify the effects of ultrasound application during drying. Thus, the figures for the identified effective moisture diffusivity (D_W) included all the phenomena related with water transfer removal during drying [35], not only those directly linked to the diffusion mechanism.

The identified effective moisture diffusivity in the experiments conducted on cassava and apple without ultrasound application (0 kW/m^3) (Table 1) were in the range of others reported in literature. Thus, in a compilation of data on the moisture diffusivity of foodstuffs, Zogzas et al. [35] reported D_W values ranging between 3.6 x 10^{-12} and 6.4 x 10^{-9} m^2/s for apple drying (30-76 ºC). In the case of the thin layer solar drying of cassava, Koua et al. [36] reported D_W values between 1.23 and 1.59 x 10^{-9} m^2/s.

As observed in Table 1, the UP applied during the drying of both products significantly ($p<0.05$) affected the D_W values. The higher the applied UP, the greater the effective diffusivity. Thus, at the maximum UP level tested (31 kW/m^3), D_W increased by 56% compared to experiments without ultrasonic application. In the case of apple, an increase of 87% was observed. The improvement in the D_W values brought about by ultrasonic application includes the effect ultrasound has not only on diffusion but also on the overall mass transport process [9,14]. Thus, ultrasound application could affect both the internal resistance, through the cyclical mechanical compression or the generation of microchannels, and also the external resistance by creating pressure variations, oscillating velocities or microstreaming, which reduce the boundary layer and, as a consequence, improve the movement of water from the solid surface to the air [12,13].

For cassava and apple, significant ($p<0.05$) linear correlations were found between the applied acoustic power and the D_W (Fig. 3). The slope of this linear relationship was 40% higher in apple than in cassava. This fact indicates that the application of power ultrasound during the drying of apple has a greater influence on water transfer than for cassava.

Table 1 Modeling of cassava and apple drying kinetics carried out at 40 ºC, 1 m/s and different ultrasonic powers (UP). Effective moisture diffusivity (DW) and percentage of explained variance (VAR %). Subscripts a, b, c, d (in cassava) and w, x, y, z (in apple) show homogeneous group established from LSD intervals ($p<0.05$).

	Cassava			Apple		
UP (kW/m^3)	$D_W(10^{-10})$ [m^2/s]	ΔD_W (%)	VAR (%)	$D_W(10^{-10})$ [m^2/s]	ΔD_W (%)	VAR (%)
0	$2.38\pm0.2_a$	-	91.3	$2.75\pm0.1_w$	-	86.1
6	$2.55\pm0.2_{a,b}$	7.1	92.3	$3.06\pm0.2_x$	11.3	87.9
12	$2.89\pm0.4_{a,b}$	21.4	88.3	$3.50\pm0.2_y$	27.3	87.2
19	$3.31\pm0.2_{b,c}$	39.1	88.9	$3.67\pm0.2_y$	33.5	87.5
25	$3.69\pm0.5_{c,d}$	55.1	89.6	$4.58\pm0.1_z$	66.6	88.8
31	$3.73\pm0.9_d$	56.7	88.0	$5.13\pm0.3_z$	86.6	85.0

ΔD_W= Increase in effective moisture diffusivity produced by US application.

The **S**lope of the linear relationship between the **D**iffusivity and the applied **UP** (**SDUP**) may be used as an index with which to measure the effectiveness of the ultrasonic application and could also be considered as an estimation of the material response to the mechanical phenomena provoked by ultrasonic waves. Different SDUP values have been reported in previous studies on orange peel [31], eggplant [30], potato [18], carrot and lemon peel [20] dried under the same conditions as apple and cassava (40 ºC, 1 m/s, UP range of 0-31 kW/m^3) with the same equipment and modeled by means of a similar diffusion model (see Section 2.2) (Table 2). The highest SDUP values have been found for eggplant, orange and lemon peel, which suggests that the ultrasound effects were more intense in these cases. On the other hand, the least intense effects were observed in potato and carrot, in which SDUP values of 0.027±0.003 and 0.017±0.003 m^5/kJ were found, respectively. The SDUP values for cassava (0.048 m^5/kJ) and apple (0.076 m^5/kJ) were located between both groups. Thereby, it seems that it is the material being dried which largely affects the intensity of the effects that ultrasonic application produces on drying. The characterization of the material structure, as well as the correlation between structural and textural variables and SDUP, could help to understand the response of fruits and vegetables to acoustic energy and explain why the observed effects are greatly product-dependent.

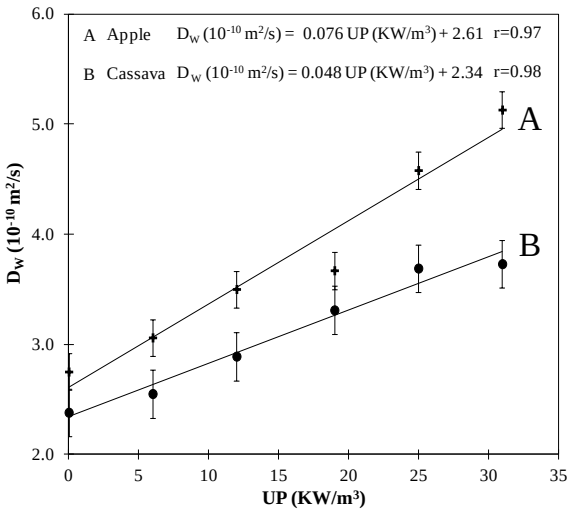

Fig. 3 Influence of applied ultrasonic power (UP) on effective moisture diffusivity (D_W) identified during the drying of cassava (A) and apple (B) cubes (side 10 mm) at 40 ºC and 1 m/s.

3.3. Material structure affecting ultrasound effectiveness

3.3.1. Microstructure and porosity

First of all, the microstructure of the materials being tested was analyzed by Cryo-SEM (Fig. 4) in order to analyze how it affects structural parameters, like porosity.

From the Cryo-SEM micrographs, it was observed that eggplant is composed of two main tissues, an external layer, named epicarp, and an internal one, the endocarp, which practically occupies all of the fruit's flesh (Fig. 4, I). In this sense, endocarp, which is responsible for the highly unconsolidated porous structure of the eggplant, is characterized by tubular, interconnected cells with large air-filled intercellular spaces. Orange (Fig. 4, II) and lemon peel (Fig. 4, III) are also made up of two characteristic tissues, the flavedo and the albedo. The flavedo (Figs. 4, II-F and III-F) constitutes the external layer and may be considered a compact structure with spherical or oval cells and without intercellular spaces. On the contrary, the albedo (Figs. 4, II-A and III-A) is characterized by long tubular cells and large intercellular spaces that give an open-pore structure to these products. Therefore, in overall terms, eggplant, orange and lemon peels are products that present large intercellular spaces filled by air. Therefore, these products may be considered as a cellular solid [37] with a low mechanical resistance to deformation.

Carrot is mainly constituted by two types of tissues: the phloem and the xylem (Fig 4, VII). The phloem (Fig. 4, VII-P) is composed of cells which are tightly-joined along their cell walls. Besides, the xylem (Fig. 4, VII-X) presents vessel elements, which have very thick and lignified walls (Fig. 4, VIII). The phloem and xylem provide a strong structure which means that carrot can be classified as a hard and dense product. The potato tissue also has a very close system of randomly positioned polyhedral cells (Fig. 4, V), containing numerous round and oval starch grains (Fig. 4, V-S) of crystalline structure. Cassava has a hard, compact structure because it is composed of small, elongated cells which are tightly-joined along their cell walls (Fig. 4, VI). Thus, the close-compact structures of carrot, potato and cassava provide these products with a high mechanical resistance to deformation due to their close intercellular spaces. Finally, apple (Fig. 4, IV) tissue is mainly made up of many irregular pores, different in shape and size, and numerous cells and intercellular spaces filled with liquid, which are the result of the cell-to-cell join.

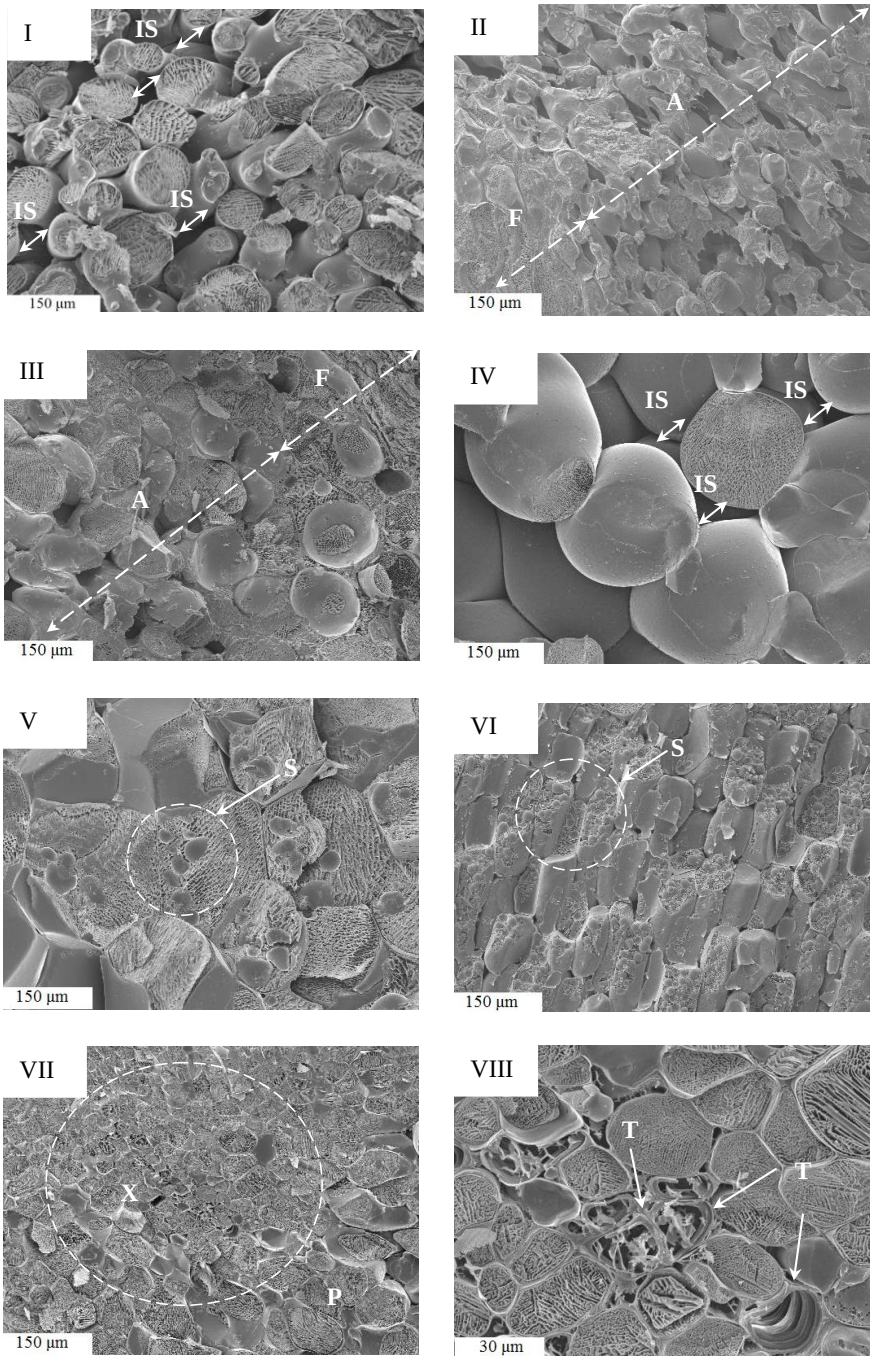

Fig. 4 Cryo-SEM images. Figs. I-VII (x200) and VIII (x1000). (I) Eggplant. (II) Orange peel. (III) Lemon peel. (IV) Apple. (V) Potato. (VI) Cassava. (VII) Carrot. (VIII) Details of phloem. IS: intercellular space; F: flavedo; A: albedo; S: starch; X: xylem, P: phloem and T: tracheid element.

The measurement of porosity aims to quantify the differences observed in the inner structure of the various products. Porosity is a key parameter in food processing since it determines the porous fraction in the material and indirectly, the degree of compactness. During drying, the sample does lose water but its volume also reduces so the porosity remains quite stable [32]. The porosity measurements for all the tested products are shown in Table 3; the figures identified are close to those reported in the literature [4,38,39]. While carrot, cassava and potato had the lowest porosity values, eggplant, orange and lemon peels exhibited the highest ones; the porosity figure for apple, meanwhile, was intermediate (Table 3).

Fig. 5, A relates SDUP with porosity; a significant ($p<0.05$) linear correlation with a negative slope was observed between both variables. Thereby, low porosity products (cassava, potato and carrot) exhibited low SDUPs. On the contrary, high porosity products (eggplant, orange and lemon peel) presented the highest SDUPs. Apple showed intermediate values of porosity and SDUP that confirm the relationship between both parameters. The influence of porosity on ultrasonic drying has already been reported [20]. However, as far as we are concerned, the relationship between SDUP and porosity has been never reported and quantified.

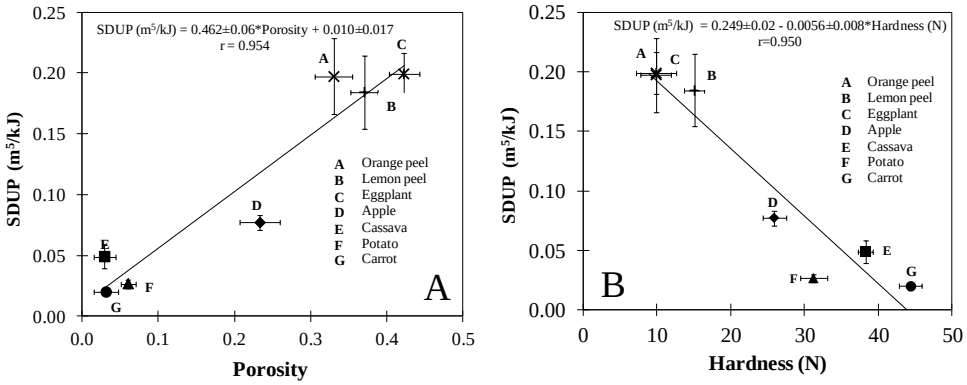

Fig. 5 Influence of porosity (A) and hardness (B) on the ultrasound effectiveness (SDUP) during the drying of different fruits and vegetables (40 ºC, 1 m/s).

Table 2 Influence of applied ultrasonic power (UP, kW/m^3) on effective moisture diffusivity during drying of different products at 40 ºC and 1 m/s.

Product	Linear relationship between D_W and UP	r	Reference
Eggplant	D_W (10^{-10} m^2/s)= 0.196 UP (kW/m^3) + 3.30	0.97	[30]
Orange Peel	D_W (10^{-10} m^2/s)= 0.195 UP (kW/m^3) + 8.62	0.95	[31]
Lemon Peel	D_W (10^{-10} m^2/s)= 0.178 UP (kW/m^3) + 5.01	0.97	[20]
Apple	D_W (10^{-10} m^2/s)= 0.076 UP (KW/m^3) + 2.61	0.97	Present work
Cassava	D_W (10^{-10} m^2/s)= 0.048 UP (KW/m^3) + 2.34	0.98	Present work
Potato	D_W (10^{-10} m^2/s)= 0.026 UP (kW/m^3) + 1.50	0.99	[18]
Carrot	D_W (10^{-10} m^2/s)= 0.017 UP (kW/m^3) + 1.01	0.97	[20]

r: correlation coefficient

Therefore, considering the same acoustic energy applied during the drying of a material, the mechanical compressions and expansions ("sponge effect") produced by ultrasound could be more intense in porous products, such as eggplant or orange and lemon peels, due to the fact that their level of mechanical weakness is relatively higher, which leads to a more effective water removal. Furthermore, the acoustic effects on the boundary layer of intercellular spaces could also be more intense in this type of products due to their larger porous net. In addition, a high degree of energy absorption could also be expected in the porous products, which increases the energy available to induce effects on the mass transport. All these facts help to explain why the application of ultrasound during drying is more effective in highly porous products than in those of low porosity. In the following sections, material properties, like texture and acoustic propagation which are highly dependent on structural properties, will be addressed and quantitatively related to SDUP.

Table 3 Porosity, hardness (H), acoustic impedance (Z) and air/solid transmission coefficient (TC) values measured for the different products tested. Average values and standard deviation.

Product	Porosity	H (N)	Z (MRayl)	TC
Eggplant	0.423±0.020	9.90±2.73	0.143	0.011
Orange peel	0.330±0.025	9.88±2.09	-	-
Lemon peel	0.370±0.017	15.07±1.39	-	-
Apple	0.233±0.026	25.92±1.63	0.177	0.009
Cassava	0.029±0.014	38.28±1.01	0.251	0.007
Potato	0.060±0.010	31.25±1.79	0.660	0.003
Carrot	0.031±0.016	44.37±1.53	0.286	0.006

3.3.2. Texture

Vegetable texture is closely related to the cell structure and composition of the product. For this reason, a TPA analysis was carried out on the different products considered in this work. From the experimental data obtained, the hardness, cohesiveness, springiness, adhesiveness and resilience parameters were calculated, of

which, hardness was the parameter that best permitted the products to be differentiated (Table 3).

The softest products were eggplant, orange and lemon peel. Although the hardness measured for eggplant and orange peel were quite similar (Table 3), lemon peel was significantly ($p<0.05$) harder than orange peel (15.07±1.39 and 9.88±2.09 N, respectively). This fact may be linked to the difference between the thickness of the flavedo of both citric peels. The hardest products were carrot, cassava, and potato, the hardness values of which ranged between 31.25±1.79 and 44.37±1.53 N. Finally, apple was considered as a product of intermediate hardness (25.92±1.63 N). The hardness results obtained coincided with the porosity measurement. Thus, the most porous products (eggplant and orange and lemon peels) were the softest ones, while the densest ones, such as cassava, carrot and potato, were the hardest. On the other hand, apple, an intermediate-porosity product, had an intermediate hardness value close to that of potato (Table 3). Both the fact that there is a high liquid content between the intercellular spaces and the irregularity of the apple pores may explain why its hardness value was close to that of potato.

As in the case of porosity, there was a significant ($p<0.05$) correlation ($r>0.95$) found between hardness and SDUP (Fig. 5, B). The softer products (high porosity), such as eggplant, orange and lemon peels, showed higher values of SDUP, while harder products (low porosity), such as potato, cassava and carrot, were less affected by ultrasound. The values for apple lay between both groups (Fig. 5, B). Thus, the correlation obtained between hardness and SDUP confirms that mechanical compressions and expansions produced in the materials by a specific amount of ultrasound energy should be more intense in soft products (like eggplant, orange and lemon peel), resulting in a more effective water removal. As regards the other estimated textural parameters (cohesiveness, springiness, adhesiveness and resilience), no significant relationship with the ultrasound effectiveness was found.

3.3.3. Acoustic properties

Relationships have been shown to exist between the textural and structural properties of materials and SDUP. It is likely that this relationship is linked to the different interaction between the acoustic waves and the solids being dried [5]. Therefore, analyzing how an acoustic signal changes when travelling across the material can be

used to study the acoustic wave-solid interaction [40,41] and also to determine how the material influences on the ultrasonically assisted drying.

The material impedance (Z), which is calculated by means of Eq. (7), mostly affects the coupling with the air and thus, the proportion of acoustic energy lost on the solid-gas interface and the amount penetrating into the solid material. This measurement can be an interesting means of determining the amount of ultrasonic energy that is actually available to produce changes. Thereby, the Z values for the different products tested were measured (Table 3); the figures for fresh products ranged from 0.14 (eggplant) to 0.67 MRayl (potato). On the one hand, products like eggplant had low Z values, suggesting that this product presented relatively better impedance coupling with the air leading to a low energy fraction reflected on the solid-gas interface, increasing the energy transmitted to the solid. On the other hand, other materials like potato showed higher Z values and thus a large impedance difference with the air which caused significant energy losses on the interfaces. The fact that there exists an inherent relationship between porosity, hardness and Z should be highlighted; so, the more porous the product and the softer it is, the lower the acoustic impedance.

From air and product impedances, the air/solid transmission coefficient (TC) for a plane wave with normal incidence on a flat interface was calculated by means of Eq. (8). According to the results obtained, TC values were in the range of 0.003-0.011, the highest being that of eggplant and the lowest that of potato (Table 3). This fact means that the highly unconsolidated porous structure of eggplant (Fig. 4, I) allowed a better transmission of acoustic waves than potato, which has a structure which is very close to that of polyhedral cells (Fig. 4, V)

As can be observed in Fig. 6, both SDUP and TC exhibited a very similar trend with Z (Fig. 6). To our knowledge, this fact has not previously been reported in the literature for any ultrasound- assisted mass transport process and suggests that the influence of ultrasound on the drying process could be explained, at least partially, through the energy transmitted in the interface from the air into the solid.

The slight differences observed in the evolution of SDUP and TC could be explained by considering that SDUP is not only dependent on the acoustic energy introduced into the solid but also on the internal energy transmission. Thus, two highly porous products, such as eggplant and apple, with a similar Z value (0.14 and 0.18 MRayl,

respectively) and TC, showed a very different SDUP (Fig. 6). This fact could be explained by their different structure. On the one hand, apple tissue is made up of intercellular spaces filled with liquid (Fig. 4, IV), while intercellular spaces in eggplant are mainly occupied by air (Fig. 4, I). Even considering the acoustic energy penetration into the material to be similar, the significant air fraction in the eggplant should increase the energy absorption, thereby increasing the energy available for water removal. In addition, TC can only be considered as a first approach to the actual amount of energy transmitted into the solid because, under real operating conditions, the acoustic field is not a single plane wave, incidence is not normal and the interface is not flat.

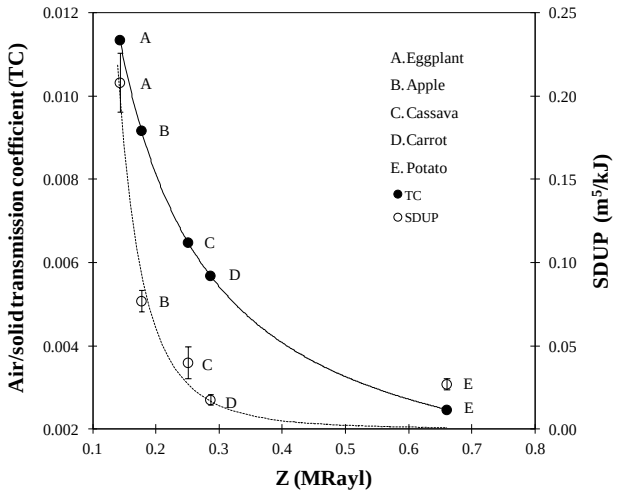

Fig. 6 Influence of acoustic impedance (Z, MRayl) of different fruits and vegetables on the ultrasound effectiveness (SDUP, m^5/kJ) during the drying of different fruits and vegetables (40 °C, 1 m/s) and the air/solid transmission coefficient (TC).

Further work should address the acoustic propagation on a particular commodity during the drying process and its effects on that process more concisely, since other, relevant parameters related to structure, such as type of pore (open or close) and size [42], tortuosity, the volumetric ratio of liquid or gas in the porous solid, largely contribute to the propagation of acoustic waves [43,44], and so to energy absorption. In such a way, mathematical models based on the product's structural properties could be developed in order to predict the acoustic propagation and so, the material response during ultrasound-assisted drying.

4. Conclusions

In this study, a quantitative analysis has been performed of how product properties affect ultrasonically assisted drying. The structure not only determines porosity and textural properties (hardness), but also controls acoustic propagation, so it influences the energy losses on the interface and thus the energy available in the particle for water removal. An acoustic analysis confirmed that soft and porous structures exhibited a higher acoustic impedance and so a better coupling with the air than hard and dense products, which involves a very different response to ultrasonically assisted drying.

Acknowledgments

The authors acknowledge the financial support of the Spanish Ministerio de Economía y Competitividad (Ref. DPI2012-37466-C03-03, DPI2012-37466-C03-03 and DPI2011-22438) and the assistance with the microstructural analysis provided by Dra. Ana Puig from Departamento de Tecnología de Alimentos of Universitat Politècnica de València (UPV). The author César Ozuna thanks UPV for an FPI grant (Ref. 2009-02).

Nomenclature

d. m.	Dry matter	
D_W	Effective moisture diffusivity	m^2/s
L	Half height	m
S_y	Standard deviation of the sample	
S_{yx}	Standard deviation of the estimation	
TC	Air/solid transmission coefficient	dimensionless
V	Volume	L
W	Moisture content	kg w/kg d.m.
Z	Acoustic impedance	MRayl
m	Mass	kg
t	Time	s
v	Ultrasonic velocity	m/s
x, y, z	Characteristic coordinates in cubic geometry	m

Greek letters

ρ	Density	kg/m^3
ε	Porosity	

Subscripts

0	Initial
b	Bulk
e	Equilibrium
p	Local
s	Solid particle

References

1. D. Witrowa-Rajchert, M. Rzaca, Effect of drying method on the microstructure and physical properties of dried apples, Drying Technol. 27 (2009) 903-909.
2. P.P. Lewicki, G. Pawlak, Effect of drying on microstructure of plan tissue, Drying Technol. 21 (2003) 657-683.
3. H. Kunzen, R. Kabbert, D. Gloyna, Aspects of material science in food processing: changes in plant cell walls of fruits and vegetables, Z. Lebensm. Unters. Forsch. A. 208 (1999) 233-250.
4. M. Krokida, Z. Maroulis, Quality changes during drying of food materials, in: A.S. Mujumdar (Ed.), Drying Technology in Agricultural and Food Sciences, Science Publishers, Enfield. 2000, pp. 61–106.
5. D. Sancho-Knapik, T. Gómez Álvarez-Arenas, J. J. Peguero-Pina, V. Fernández, E. Gil-Pelegrín, Relationship between ultrasonic properties and structural changes in the mesophyll during leaf dehydration, J. Exp. Bot. 62 (2011) 3637-3645.
6. I.N. Ramos, C.L.M Silva, A.M. Sereno, J.M. Aguilera, Quantification of microstructural changes during first stage air drying of grape tissue, J. Food Eng. 62 (2004) 159-164.
7. A. S. Mujumdar, Research and development in drying: recent trends and future prospects, Drying Technol. 22 (2004) 1-26.
8. S. Sansiribhan, S. Devahastin, S. Soponronnarit, Quantitative evaluation of microstructural changes and their relations with some physical characteristics of food during drying, J. Food Sci. 75 (2010) e453–e461.
9. A. Mulet, J.A. Cárcel, N. Sanjuan, J.V. García-Pérez, Food dehydration under forced convection conditions, in: J. Delgado (Ed.), Recent Progress in Chemical Engineering., Studium Press LLC; Houston, USA, 2010, pp. 153-177.
10. F. Chemat, Zill-e-Huma, M.K. Khan, Applications of ultrasound in food technology: processing, preservation and extraction, Ultrason. Sonochem. 18 (2011) 813–835
11. J.A. Gallego-Juárez, G. Rodriguez, V. Acosta, E. Riera, Power ultrasonic transducers with extensive radiators for industrial processing, Ultrason. Sonochem. 17 (2010) 953–964.

12. J.A. Cárcel, J.V. García-Pérez, J. Benedito, A. Mulet, Food process innovation through new technologies: use of ultrasound, J. Food Eng. 110 (2012) 200-207.
13. S. De la Fuente-Blanco, E. Riera-Franco de Sabaria, V.M. Acosta-Aparicio, A. Blanco-Blanco, J.A. Gallego-Juárez, Food drying process by power ultrasound, Ultrasonics. 44 (2006) e523-e527.
14. H.T. Sabarez, J.A. Gallego-Juárez, E. Riera, Ultrasonic-assisted convective drying of apple slices, Drying Technol. 30 (2012) 989-997.
15. T.J. Mason, L. Paniwnyk, J.P. Lorimer, The uses of ultrasound in food technology, Ultrason. Sonochem. 3 (1996) S253–S260.
16. J.V. García-Pérez, C. Rosselló, J.A. Cárcel, S. De la Fuente, A. Mulet, Effect of air temperature on convective drying assisted by high power ultrasound. Defect Diffus. Forum. 258-260 (2006) 563-574.
17. J.A. Cárcel, J.V. García-Pérez, E. Riera, A. Mulet, Influence of high intensity ultrasound on drying kinetics of persimmon, Drying Technol. 25 (2007) 185-193.
18. C. Ozuna, J.A. Cárcel, J.V. García-Pérez, A. Mulet, Improvement of water transport mechanisms during potato drying by applying ultrasound. J. Sci. Food Agr. 91 (2011) 2511-2517.
19. A. Puig, I. Pérez-Munuera, J.A. Cárcel, I. Hernando, J.V. García-Pérez, Moisture loss kinetics and microstructural changes in eggplant (Solanum melongena L.) during conventional and ultrasonically assisted convective drying, Food Bioprod. Process. 90 (2012) 624-632.
20. J.V. García-Pérez, J.A Cárcel, E. Riera, A. Mulet, Influence of applied acoustic energy on the drying of carrots and lemon peel, Drying Technol. 27 (2009) 281-287.
21. C. Ozuna, A. Puig, J.V. García-Pérez, A. Mulet, J.A. Cárcel, Influence of high intensity ultrasound application on mass transport, microstructure and textural properties of pork meat (Longissimus dorsi) brined at different NaCl concentrations, J. Food Eng. 119 (2013) 84-93.
22. J.V. Santacatalina, J.V. García-Perez, E. Corona, J. Benedito, Ultrasonic monitoring of lard crystallization during storage, Food Res. Int. 44 (2011) 146-155.
23. J.N. Coupland, Low intensity ultrasound, Food Res Int. 37 (2004) 537-543.

24. M. Nielsen, H.J. Martens, Low frequency ultrasonics for texture measurements in cooked carrots (Daucus carota L.), J. Food Sci. 62 (1997) 1167-1175.
25. T.E. Gómez Álvarez-Arenas, Simultaneous determination of the ultrasound velocity and the thickness of solid plates from the analysis of thickness resonances using air-coupled ultrasound, Ultrasonics. 50 (2010) 104-109.
26. Association of Official Analytical Chemists. Official Methods of Analysis, AOAC, Washington, 1997.
27. E. Riera, J.V. García-Pérez, J.A. Cárcel, V. Acosta, J.A. Gallego-Juárez. Computational Study of Ultrasound-Assisted Drying of Food Materials. In: Knoerzer, K., Juliano, P., Roupas, P., Versteeg, C. (Eds.), Innovative Food Processing Technologies: Advances in Multiphysics Simulation. John Wiley & Sons Ltd., 2011, pp. 265–301.
28. J. Crank, The Mathematics of Diffusion, Oxford University Press, London, 1975.
29. D.C. Montgomery, Design and Analysis of Experiments, John Wiley & Sons., Singapore, 2013
30. J.V. García-Pérez, C. Ozuna, C. Ortuño, J.A. Cárcel, A. Mulet, Modeling ultrasonically assisted convective drying of eggplant, Drying Technol. 29 (2011) 1499-1509.
31. J.V. García-Pérez, C. Ortuño, A. Puig, J.A. Cárcel, I. Pérez-Munuera, Enhancement of water transport and microstructural changes induced by high-intensity ultrasound application on orange peel drying, Food Bioprocess Tech. 5 (2012) 2256-2265.
32. L. Mayor, A.M. Sereno, Modelling shrinkage during convective drying of food materials: a review, J. Food Eng. 61 (2004), 373-386.
33. T.E. Gómez Álvarez-Arenas, Acoustic impedance matching of piezoelectric transducers to the air. IEEE T. Ultrason. Ferr. 51 (2004) 624-633.
34. S. Temkin, Elements of Acoustics, Wiley, John & Sons, Inc., 1981.
35. N.P. Zogzas, Z. B. Maroulis, D. Marinos-Kouris, Moisture diffusivity data compilation in foodstuffs, Drying Technol. 14 (1996) 2225-2253.
36. K.B. Koua, W.F. Fassinou, P. Gbaha, S. Toure, Mathematical modelling of the thin layer solar drying of banana, mango and cassava, Energy. 34 (2009) 1594–1602.

37. L.J. Gibson, M.F. Ashby, Cellular Solids: Structure and Properties, second ed., Cambridge University Press, 1997.
38. J. Martínez-Monzó, N. Martínez-Navarrete, A. Chiralt, P. Fito, Mechanical and structural changes in apple (Var. Granny Smith) due to vacuum impregnation with cryoportectants, J. Food Sci. 63 (1998) 499-503.
39. M. Cháfer, C. González-Martínez, A., Chiralt, P. Fito, Microstructure and vacuum impregnation response of citrus peels, Food Res. Int. 36 (2003) 35-41.
40. R. Saggin, J.N. Coupland, Non-contact ultrasonic measurements in food material, Food Res. Int. 34 (2001) 865-870.
41. D.J. McClements, Ultrasonic characterization of foods and drinks: principles, methods, and applications, Crit. Rev. Food Sci. Nutr. 37 (1997) 1–46.
42. T.E. Gómez Álvarez-Arenas, A non destructive integrity test for membranes filters based on air-coupled ultrasonic spectroscopy, IEEE T. Ultrason. Ferr. 50 (2003) 676-685.
43. D. Sancho-Knapik, T. Gómez Álvarez-Arenas, J.J. Peguero-Pina, E. Gil-Pelegrín, Air coupled broadband ultrasonic spectroscopy as a new non-invasive and non-contact method for the determination of leaf water status, J. Exp. Bot. 61 (2010) 1385-1391.
44. M. Nielsen, H.J. Martens, K. Kaack, Low frequency ultrasonics for texture measurements in carrots (Daucus carota L.) in relation to water loss and storage, Postharvest Biol. Technol. 14 (1998) 297-308.

5.Discusiones generales

A partir de los resultados obtenidos en esta Tesis Doctoral, se puede afirmar que la aplicación de Ultrasonidos de Alta Intensidad (**US**), tanto en sistemas sólido-líquido como en sistemas sólido-gas, tuvo efectos significativos ($p<0.05$) en las cinéticas de transporte de materia. Dichos efectos se vieron influenciados por las propiedades estructurales de la materia prima. Además, la aplicación de US afectó a la estructura de los productos tratados y, por lo tanto, a la calidad del producto final. Las discusiones generales de este trabajo se han dividido en dos apartados, siguiendo la misma estructura que en el resto de la Tesis. En primer lugar, se abordarán las discusiones de los resultados sobre la aplicación de US en sistemas sólido-líquido (**Capítulo 1 y 2**) y posteriormente los obtenidos en los sistemas sólido-gas (**Capítulo 3 y 4**).

5.1. Sistemas sólido-líquido

En los sistemas sólido-líquido, la aplicación de US intensificó las cinéticas de transporte de materia y afectó al contenido final de agua y sal tanto en el salado de carne (**Capítulo 1**) como en el desalado de bacalao (**Capítulo 2**). En el caso del salado de carne, se observó que el aumento de la concentración de sal en la salmuera (de 50 a 280 kg NaCl/m^3) incrementó significativamente ($p<0.05$) el contenido final de NaCl en las muestras tratadas e influyó en la dirección del transporte de agua. Las muestras tratadas con salmueras de baja concentración de sal (50 y 100 kg NaCl/m^3) se hidrataron, mientras que aquellas tratadas con salmueras de concentración superiores a 200 kg NaCl/m^3 se deshidrataron. En el caso de las concentraciones de 150 y 200 kg NaCl/m^3 no se observó una tendencia clara en la evolución del contenido de agua de las muestras y se identificaron, mediante técnicas de microscopía (Cryo-SEM), zonas deshidratadas y otras hidratadas.

La aplicación de US durante el salado de carne no afectó a la dirección del transporte de agua ni de sal pero sí produjo un aumento significativo ($p<0.05$) del contenido final de sal. Por el contrario, el contenido final de agua no llegó a ser significativamente diferente. Esto podría atribuirse a la necesidad de superar un umbral mínimo de potencia ultrasónica aplicada para provocar diferencias significativas (Cárcel et al., 2007a, b). Así, este umbral se habría alcanzado en el caso del transporte de sal y no en el de agua. En todo caso, la elevada variabilidad en el contenido de agua de las muestras podría enmascarar un posible efecto de los US (Siró et. al., 2009; Jayasooriya et al., 2007). El análisis microestructural (SEM-EDX) confirmó el incremento de la

concentración de sal por la aplicación de US y se observó que la distribución de la misma fue más homogénea en las muestras tratadas con US.

En el caso del proceso de desalado de bacalao, la aplicación de US incrementó significativamente la velocidad de ambos transportes, el de sal y el de agua. Así, los tiempos de tratamiento se redujeron en un 67% para la sal y un 50% para el agua (1500 W), respecto a un tratamiento convencional de 180 min. Además, la influencia de los US resultó mayor cuanto mayor fue la potencia aplicada (750 y 1500 W). De igual modo que para el salado de la carne, el estudio microestructural mostró que las muestras tratadas con US presentaron un menor contenido de sal. Además, éste disminuyó al aumentar la potencia ultrasónica aplicada al medio.

La influencia de la aplicación de US en ambos sistemas sólido-liquido, salado de carne y desalado de bacalao, se cuantificó mediante un modelo difusivo. Así, se observó que la aplicación de US incrementó significativamente ($p<0.05$) tanto la difusividad efectiva del agua ($\mathbf{D_W}$) como la de sal ($\mathbf{D_{NaCl}}$), lo que representó una intensificación global del proceso. En el salado de carne, el aumento de la D_{NaCl} osciló entre un 23% y un 45%. En cuanto a la D_W, estos aumentos llegaron a ser superiores al 100%. Incrementos similares se observaron el proceso de desalado de bacalao.

Por otro lado, la aplicación de US en medio sólido-líquido afectó significativamente ($p<0.05$) a la estructura interna de las muestras tratadas, lo que se observó a partir del análisis de la textura y de la microestructura. Respecto a los cambios texturales observados, los análisis de punción de carne mostraron que las muestras saladas con US presentaron un valor de dureza final significativamente ($p<0.05$) mayor que las saladas de manera convencional. Este hecho se relacionó con la intensificación del transporte de sal provocado por la aplicación de US durante el salado, lo cual, como se ha comentado con anterioridad, incrementó tanto su difusividad efectiva como el contenido final. Un mayor contenido de sal puede provocar cambios estructurales en las proteínas de la carne, favoreciendo su endurecimiento (Ruiz-Ramírez et al., 2005). Esto también se observó al incrementar la concentración de la salmuera, que produjo un mayor contenido final de sal y también un mayor endurecimiento de la carne.

El estudio de la evolución del hinchamiento y de la dureza de las muestras de bacalao durante el proceso de desalado también mostró la influencia de la aplicación de US en la estructura interna. Así, la aplicación de US incrementó significativamente ($p<0.05$)

tanto la velocidad de hinchamiento de las muestras como su tamaño final. De igual modo, los valores de dureza de las muestras desaladas con US fueron inferiores a los de las desaladas convencionalmente. La evolución del hinchamiento y de la dureza siguió una cinética de primer orden y se observó que el efecto de los US, tanto en el hinchamiento como en la dureza, se debió a la mejora cinética que su aplicación conlleva.

Los efectos de la aplicación de US en la estructura interna también se observaron a partir del estudio de la microestructura de los productos. En el salado de carne, la aplicación de US produjo la dispersión del tejido conectivo, la ruptura y la erosión de las miofibrillas de la carne. Esto se puede atribuir a los efectos mecánicos producidos por los US en medio líquido tales como la cavitación, el efecto esponja y la generación de microjets (Cárcel et al., 2012; Jayasooriya et al., 2007). Por otro lado, en el caso del desalado de bacalao, se observaron incrementos en el espesor de las fibras de las muestras tratadas con US de hasta un 27% superiores que en las desaladas convencionalmente.

Por lo tanto, la aplicación de US en los sistemas sólido-líquido estudiados supuso la intensificación de los fenómenos de transferencia de materia. Esta intensificación afectó a la estructura interna de los productos. Además, los US también produjeron cambios directos en dicha estructura interna. Todo esto se tradujo en cambios en las propiedades macroscópicas, como por ejemplo la dureza.

5.2. Sistemas sólido-gas

La aplicación de US en medios gaseosos es mucho más compleja que en medios líquidos debido a que la transmisión de energía acústica se ve dificultada por la gran diferencia de impedancias entre los sistemas emisores de US y los gases (Riera et al., 2011). Sin embargo, en los resultados obtenidos en esta Tesis Doctoral se observó que, de igual forma que en los sistemas sólido-líquido, la aplicación de US intensificó los procesos de transferencia de materia en diferentes sistemas sólido-gas.

El secado convectivo es ampliamente utilizado en la industria agroalimentaria. Sin embargo, la utilización de altas temperaturas puede afectar negativamente a la calidad del producto deshidratado (Krokida & Maroulis, 2000). En este sentido, el secado convectivo a baja temperatura representa una alternativa muy interesante en la búsqueda de productos deshidratados de elevada calidad, como es el caso del bacalao

seco-salado (Claussen et al., 2007). La principal desventaja de este proceso es la baja velocidad de secado, lo que reduce su aplicabilidad a productos de elevado valor económico. Así, la aplicación de US puede ser una alternativa interesante para intensificar el proceso debido al bajo efecto térmico que estos producen (Garcia-Perez et al., 2012a). En los resultados obtenidos en el **Capítulo 3,** se observó que la aplicación de US durante el secado de bacalao salado incrementó la velocidad de secado, alcanzando reducciones de tiempo de proceso entre un 35 y 54%. La pérdida de agua en las experiencias realizadas a 0, 10 y 20 ºC se describió de manera satisfactoria (varianza explicada mayor del 99%) considerando que la difusión es el único mecanismo controlante. Sin embargo, en el caso de las experiencias realizadas a -10 ºC, la varianza explicada disminuyó al 98.3% para los secados convencionales, valor que se redujo al 95.4% en las experiencias con aplicación de US. Esto indicaría que a temperaturas por debajo de 0 ºC, otros mecanismos de transporte diferentes a la difusión podrían tener una importancia relevante y, además, la aplicación de US podría influir sobre dichos mecanismos de manera que se modificara la importancia relativa entre ellos. En este sentido, García-Pérez et al. (2012a) observaron que la aplicación de US en el secado a baja temperatura de zanahoria (-14 ºC, 2 m/s) incrementó en mayor grado el coeficiente de difusión (407-428%) en comparación con el coeficiente de transferencia de materia (96-170%). Este hecho podría indicar que a temperaturas por debajo de 0 ºC, la aplicación de US provoca mayor reducción de la resistencia interna que de la resistencia externa al transporte de materia. Este hecho contribuye a que la difusión no sea el mecanismo predominante en el trasporte de agua.

De igual forma que en sistemas sólido-líquido, la aplicación de US incrementó significativamente ($p<0.05$) los valores de D_W. Estos incrementos oscilaron entre un 110% a la temperatura de 20 ºC y un 42% para 10 ºC. En ambos tipos de secados, con y sin aplicación de US, se observó una relación tipo Arrhenius entre la temperatura del aire de secado y la D_W, identificándose, en ambos casos, valores similares para la energía de activación. En procesos de secado por aire caliente, García-Pérez et al. (2006b) observaron una disminución de los efectos debidos a la aplicación de US a temperaturas por encima de 50 ºC, esto supuso que la ecuación de Arrhenius no describiera adecuadamente la influencia de la temperatura en los valores de D_W identificados para las experiencias con la aplicación de US.

Al igual que en los sistemas sólido-líquido, tanto la aplicación de US durante el secado como las variables de proceso, en este caso la temperatura de secado, influyeron en la

microestructura y en parámetros físicos del producto final. De esta forma, se estudió la capacidad de rehidratación, la dureza y el color de las muestras de bacalao salado deshidratadas. La aplicación de US conllevó una mayor capacidad de rehidratación y en consecuencia un incremento del contenido final de agua en las muestras rehidratadas. El análisis microestructural (SEM) de las muestras secadas a 0 ºC con aplicación de US mostró una estructura más degradada y con un mayor colapso celular que aquellas secadas de manera convencional. Al igual que en los tratamientos sólido-líquido (salado y desalado), la aplicación de US provocó rupturas en las fibras del bacalao, mayores espacios entre las miofibrillas y una mayor migración de la sal a la superficie de las mismas. Estas diferencias estructurales contribuyen a explicar la mayor capacidad de rehidratación de las muestras secadas con US.

Respecto a los cambios texturales observados, el incremento de la temperatura de secado provocó un mayor endurecimiento de las muestras deshidratadas y rehidratadas, lo cual podría estar relacionado con la desnaturalización del tejido conectivo y de las proteínas miofibrilares (Ortiz et al., 2013; Brás & Costa, 2010). Por el contrario, y en todas las temperaturas estudiadas, la aplicación de US produjo un descenso de la dureza tanto de las muestras deshidratadas como rehidratadas. Este hecho podría estar relacionado con las diferencias observadas en la microestructura de las muestras deshidratadas con US.

El color de las muestras también se vio afectado significativamente ($p<0.05$) por la temperatura y la aplicación de US durante el secado. Así, en las muestras secadas de manera convencional se observó que al incrementar la temperatura de secado, las muestras fueron menos luminosas y más amarillas (disminución de los valores de L* y b*, respectivamente). Respecto al color de las muestras secadas con US se observó que, las muestras secadas a -10 y 0 ºC fueron más luminosas y menos amarillas que las secadas de manera convencional, mientras que las muestras secadas a 10 y 20 ºC no presentaron diferencias significativas ($p<0.05$). Estas diferencias en color podrían deberse al tiempo de exposición de las muestras a la energía ultrasónica. Así, mientras que el tiempo de secado para las experiencias realizadas a -10 y 0 ºC osciló entre 6 y 8 h, el tiempo de secado para aquellas secadas a 10 y 20 ºC se redujo a la mitad. Por lo tanto, a mayores tiempos de aplicación de US, sus efectos en el color del producto final aumentaron.

En términos generales, la aplicación de US representa una interesante alternativa para intensificar el proceso de secado de bacalao salado a bajas temperaturas. La aplicación de US redujo el tiempo de secado y produjo cambios en la microestructura del producto, que incrementaron la capacidad de rehidratación de las muestras y el ablandamiento de las mismas. Además, los US aumentaron la luminosidad de las muestras secadas a bajas temperaturas, lo que se considera como un parámetro de calidad para este producto (Oliveira et al., 2012).

Como ya se ha comentado con anterioridad, los procesos de secado a baja temperatura representan una alternativa interesante para productos de elevada calidad y muy apreciados por los consumidores. Sin embargo, la importancia del secado por aire caliente sigue siendo muy alta en el secado de productos vegetales. Así, se estudió la aplicación de US en el secado por aire caliente (40 ºC y 1 m/s) de berenjena, patata, manzana y yuca (**Capítulo 4**) con el objetivo de identificar la influencia de la **P**otencia **U**ltrasónica (**PU**) aplicada en la cinética del proceso.

En todos los casos considerados, la aplicación de US aceleró el proceso de secado. Sin embargo, la efectividad de los mismos estuvo relacionada directamente con la PU aplicada en el medio. Así, mientras mayor fue la PU, mayores fueron las reducciones del tiempo de secado. Además, estas reducciones dependieron del producto. Por ejemplo, al aplicar una PU de 31 kW/m^3 y para alcanzar una pérdida de peso inicial del 50%, se obtuvieron reducciones del tiempo de secado del 68% en berenjena, del 58% en manzana, del 38% en patata y del 27% en yuca.

Para describir la cinética de secado de dichos productos (berenjena, patata, yuca y manzana) se ensayaron varios modelos difusivos con diferente grado de complejidad. En primer lugar, se consideró un modelo difusivo que considera la resistencia externa despreciable. Los ajustes obtenidos mostraron porcentajes de varianza explicada muy bajos (de hasta el 84%), lo que indica que la difusión no es el único fenómeno que controla el transporte de materia en estas condiciones.

Con objeto de mejorar los ajustes de las cinéticas de secado de berenjena y patata se elevó la complejidad del modelo difusivo considerando tanto la resistencia interna a la transferencia de materia como la externa en los fenómenos de transporte de materia. En este caso, se alcanzaron porcentajes de varianza superiores al 98% y porcentajes de error relativo medio inferiores al 5.7%.

Finalmente, se dio un paso más en la complejidad del modelo difusivo al introducir en el mismo, no solo la resistencia externa si no también el encogimiento del producto. En este caso, la bondad de los ajustes conseguidos fue mayor que la obtenida con los modelos anteriores. Por ejemplo, para la berenjena, se alcanzaron varianzas explicadas superiores al 99.9% en todos las PU ensayadas y errores relativos medios inferiores al 1.2%. Los valores de D_W obtenidos por este modelo indicaron que estos fueron sobreestimados en un rango comprendido entre de 81.8 y 88.7% al no considerar el encogimiento de la muestra en la modelización. Por el contrario, los coeficientes de transferencia de materia obtenidos en ambos modelos que consideran resistencia externa fueron similares, por lo que se puede afirmar que el análisis del transporte convectivo del agua durante el secado de berenjena no dependió de las hipótesis adoptadas en cuanto al encogimiento de las muestras.

Por otra parte, y como ya se ha comentado, el modelo difusivo sin considerar resistencia externa ni encogimiento no es el modelo que mejor ajustó a las cinéticas de secado por aire caliente. Sin embargo, este modelo permite obtener un único parámetro, la difusividad efectiva, que engloba todos los aspectos que afectan a la cinética del proceso. Este parámetro puede facilitar la comparación de resultados obtenidos con diferentes productos y, así, evaluar y cuantificar la influencia de la aplicación de US en los mismos. Así, con los valores de D_W obtenidos para el secado de berenjena, patata, manzana y yuca se establecieron relaciones lineales significativas entre PU y la D_W. Además, se consideraron valores de D_W obtenidos de bibliografía y estimados aplicando el mismo modelo al secado de otros productos, tales como la zanahoria (García-Pérez et al, 2009), piel de naranja (Garcia-Perez et al., 2012b) y piel de limón (García-Pérez et al, 2009). Así, se observó que el efecto de los US fue más intenso en materiales como la berenjena y las pieles de naranja y de limón, que en el caso de materiales como la zanahoria o patata, donde el efecto fue mucho menor. En todos los casos, se identificó una relación lineal entre PU aplicada y D_W, alcanzándose coeficientes de correlación superiores al 0.95 en todos los casos. Sin embargo, la pendiente de estas correlaciones lineales fue muy diferente para los productos considerados. Dicha **P**endiente de la relación lineal entre $\mathbf{D_W}$ y **PU** (**PDPU**) calculada para cada producto se puede utilizar como un índice para estimar la efectividad de los US en el proceso de secado. De igual modo, la PDPU puede ser también considerada como una estimación de la sensibilidad de los materiales a los efectos provocados por la aplicación de US.

Las micrografías obtenidas por Cryo-SEM mostraron diferencias importantes entre las estructuras internas de los productos analizados. Por un lado, la yuca, la zanahoria y la patata mostraron estructuras más compactas debido a que poseen pocos espacios intercelulares. La berenjena y el componente mayoritario de la piel de la naranja y de limón, el albedo, mostraron grandes espacios intercelulares, los cuales se encuentran rellenos principalmente de aire. Esta característica favorece que la estructura interna de estos productos sea menos compacta. El último producto considerado, la manzana, mostró células de mayor tamaño que los otros productos con grandes espacios intercelulares pero en este caso rellenos mayoritariamente de agua.

Con el objetivo de evaluar si la estructura interna del material influye en los efectos provocados por los US durante el secado, sus propiedades macroscópicas se relacionaron con la PDPU (**Capítulo 4**). Así, se puso de manifiesto que el efecto de los US fue más pronunciado en productos con una alta porosidad. De hecho, se identificó una relación lineal significativa ($r=0.95$) entre porosidad y PDPU. Esta relación indica que, para un mismo nivel de energía en el medio, los materiales porosos son más sensibles a los efectos de los US. Así, los efectos mecánicos producidos por las ondas acústicas o la influencia de los US en las interfases sólido-gas de los productos porosos pueden ser más intensos al poseer una mayor red interna de espacios intercelulares. Por otro lado, también se observó la existencia de una correlación lineal ($r=0.95$) entre PDPU y la dureza del producto, a menor dureza mayor PDPU. Este hecho sugiere que los efectos mecánicos producidos por los US fueron más intensos en aquellos productos de menor dureza (berenjena, piel de naranja y limón), y por tanto con menor resistencia a la deformación.

La estructura del producto influye enormemente en la propagación de las ondas acústicas. Así, a partir de la medida de la velocidad ultrasónica, se calculó la impedancia acústica (**Z**) como el producto de la velocidad y la densidad de la muestra. Esta variable determina el acople del material con el aire y, por lo tanto, la proporción de energía acústica que se pierde en la interfase o que penetra en el sólido. El valor de impedancia del aire es muy bajo. Por lo tanto, los materiales con menor impedancia tendrían un mejor acople de impedancias con el aire, lo que supondría una menor reflexión de energía en la interfase y por lo tanto una mayor penetración de energía en el material. En este sentido, los materiales más porosos y más blandos, como la berenjena, presentaron valores bajos de impedancia (0.14 MRayl), mientras que los materiales menos porosos y con mayor dureza, como por ejemplo la patata,

presentaron valores de impedancia más elevados (0.67 MRayl). Por lo tanto, se identificó una relación entre la dureza y la porosidad del material con su Z. Mientras más poroso y menos duro sea el producto, más alta resultó su Z. A partir de la Z del aire y del producto, se determinó el coeficiente de transmisión de energía acústica en la interfase (**CT**). Los valores que se obtuvieron para este parámetro oscilaron entre 0.003-0.011, siendo el valor más alto para la patata y el menor para la berenjena.

Se observó que la relación de PDPU con la Z fue muy similar a la obtenida entre CT y Z. Es decir, la eficiencia de la aplicación de US en el proceso de secado depende en gran medida de la fracción de energía ultrasónica que penetra en el sólido. Las diferencias observadas entre ambas curvas pueden explicarse considerando que PDPU no sólo depende de la energía acústica introducida en el sólido como la CT, sino también de la transmisión interna de la energía. Así, dos productos con alta porosidad como la berenjena y la manzana, mostraron valores similares de Z (0.14 y 0.18 MRayl, respectivamente) y de CT (0.011 y 0.009, respectivamente). Sin embargo, los valores de PDUP fueron muy diferentes, 0.196 para berenjena y 0.076 para manzana. Estas diferencia pueden deberse a la diferencia entre ambas estructuras. Por un lado, la manzana presenta muchos espacios intercelulares rellenos de agua, mientras que en la berenjena, estos espacios se encuentran ocupados principalmente por aire. Así, considerando que la misma cantidad de energía acústica penetra en el material, el alto contenido de aire presente en la berenjena en comparación con la manzana, podría incrementar la absorción de energía y, en consecuencia, la energía disponible para la eliminación de agua durante el secado por aire caliente.

6.Conclusiones

The main conclusions that can be extracted from the results obtained in the present work have been grouped into two sections depending on the system where High Intensity Ultrasound (**US**) is applied, **solid-liquid** and **solid-gas systems**.

6.1. Solid-liquid systems

Influence of US application on mass transport

- In meat brining, the US application significantly ($p<0.05$) increased the NaCl gain. However, the US effects on the final moisture content were not significant ($p<0.05$).
- In cod desalting, both the final NaCl content and the final water content were significantly ($p<0.05$) affected by US application. The US effects were dependent on the applied ultrasonic power, the higher the power, the larger the US effect.
- The effective NaCl and moisture diffusivities were significantly ($p<0.05$) increased by US application in brining and desalting, the increase ranged from 23 to 150%.

Influence of conventional solid-liquid treatments on the structure of the final product

- The NaCl gain during brining process promoted changes in meat texture. Thus, the higher the NaCl content, the harder the sample.
- Cod desalting brought about the tissue swelling and the hardness decrease.

Influence of US application on the structure of the final product

- In meat brining, US intensified the sample hardening, which was mainly linked to the increase of the NaCl gain.
- The swelling and the hardness reduction during cod desalting was sped-up by US application. In the case of swelling, this was only ascribed to the mass transfer enhancement produced by US. In the case of hardness, the US application also affected the internal structure of cod.
- The application of US during meat brining brought about the disruption, the dispersion of connective tissue and the rupture of myofibrils. Moreover, the NaCl distribution in brined samples with US was more homogeneous.

- In cod desalting, US provoked the enlargement of the muscle fibers and interfibrillar spaces.

6.2. Solid-gas systems

Influence of US on mass transport in low-temperature drying

- The application of US shortened the drying time of salted cod by up to 50%.
- At 0, 10 and 20 ºC the drying mechanism followed a diffusion pattern. However, at -10 ºC, other mass transport mechanisms were significant, especially when US was applied.
- The application of US increased significantly ($p<0.05$) the effective moisture diffusivity for every temperature tested being this increase laid between 42 and 110%.
- The relationship between effective diffusivity and temperature followed an Arrhenius type relationship.
- The identified activation energy was not affected by US application. Otherwise, the pre-exponential factor was higher for US assisted drying than for conventional drying process.

Influence of US on mass transport in hot-air drying

- In drying at 40 ºC of cassava, potato, apple and eggplant, a significant ($p<0.05$) shortening of the drying time was found by US application.
- For low air velocities (1 m/s), external resistance to mass transfer was considered to be a significant phenomenon. Then, it has to be considered in the diffusion model in order to accurately describe the drying kinetics. In addition, it also allows separating the effects of US over internal and external resistance to mass transfer.
- In those products which suffer shrinkage during drying, as eggplant, it is advisable to include this fact in the diffusion model in order to achieve an accurate estimation of the effective diffusivity.
- The effects of US on drying kinetics were significantly ($p<0.05$) dependent on the ultrasonic power applied. Linear relationships between the applied ultrasonic power level, at the range tested in this work (0-31 kW/m^3) and the identified effective moisture diffusivity were found, as well as with the mass transfer coefficient.

Influence of US application during drying on the physical properties of the dried product

- US application promoted changes of color of dried salted cod. Ultrasonically assisted dried samples at the lowest temperatures tested (-10 ºC) showed a significantly ($p<0.05$) higher lightness (L*) than those dried at the same temperature without US application.
- Microstructural analyses showed that, like in solid-liquid treatments, the US application in drying brought about changes in cod fibers, such as the increase in thickness.
- The microstructural changes linked to US application involve a higher rehydration capacity and lower hardness.

Influence of the material structure on US assisted drying

- The **S**lope of the linear relationship between the **D**iffusivity and the **U**ltrasonic **P**ower applied (**SDUP**) may be used as an index of the US application effectiveness, as well as an estimation of the material response to the mechanical phenomena provoked by ultrasonic waves. Thus, the higher the slope, the more sensitive the product to US application.
- SDUP was well correlated ($r\geq0.95$) with the product porosity and hardness. Thus, the highest SDUP corresponded to the softest (low porosity) products while, the hardest ones were less affected by ultrasound (lowest SDUP).
- Soft and porous products showed higher acoustic impedance than the hard and dense ones. High values of acoustic impedance involve a better acoustic coupling with the air. In this sense, the transmission coefficient in the interface air-product was also higher for soft and high porosity products.
- SDUP was greatly affected by the acoustic impedance of the material being dried.
- SDUP and the transmission coefficient of the acoustic energy at the interface showed a similar pattern with the acoustic impedance. Therefore, those products with the highest acoustic impedance and transmission coefficient (high porosity and low hardness products) presented the highest SDUP. Then, the internal structure of the product not only determines structural (porosity) and textural properties (hardness) but also controls acoustic

propagation, so it influences the energy losses on the interface and thus the energy available in the particle for water removal.

GENERAL CONCLUSION

In overall terms, US may be considered a feasible non-thermal technology for mass-transport intensification in solid-liquid and solid-gas systems if conveniently managed. In this regard, the interaction ultrasound/product should be highlighted, not only because the product structure affects the extension of US effects, but also because US may promote structural and quality trait modifications.

7.Recomendaciones

En base a los resultados obtenidos en esta Tesis Doctoral, se puede sugerir continuar la investigación haciendo énfasis en los siguientes aspectos:

Transporte de materia

- Profundizar en el estudio de la aplicación de Ultrasonidos de Alta Intensidad (**US**) en los procesos de secado a baja temperatura, tanto en matrices proteicas como vegetales, para determinar la influencia de variables de proceso, como la velocidad de aire o la potencia aplicada, en estas condiciones.
- Evaluar el potencial de la tecnología de US en el secado de productos líquidos o semi-sólidos (salsas, purés, etc.).
- En aplicaciones en medio líquido, estudiar procesos de impregnación de matrices sólidas asistida por US, por ejemplo, con extractos de alto contenido bioactivo.

Propiedades del producto final

- En productos vegetales, analizar la influencia de la aplicación de US en compuestos bioactivos, tales como polifenoles, vitaminas, etc.
- En el caso de productos con matrices proteicas, tal es el caso del lomo de cerdo y bacalao, estudiar el efecto de la aplicación de US en la estructura y calidad de la matriz proteica.

Propiedades del material que afectan a la efectividad de los US

- Profundizar en el estudio de la propagación acústica en el material y establecer relaciones entre las características de la onda acústica (potencia y frecuencia) con otros parámetros relacionados con la estructura del producto, como por ejemplo, el tipo de porosidad (abierta o cerrada), el tamaño del poro, la tortuosidad, la proporción volumétrica de fluido en el sólido poroso, etc. Además, sería muy interesante evaluar los cambios que ocurren durante el secado en las propiedades estructurales, texturales y acústicas, y determinar las relaciones existentes entre las diferentes variables.
- Desarrollar modelos matemáticos basados en las propiedades acústicas del material con el fin de predecir la propagación acústica y así establecer la influencia del producto en el secado asistido por US.

Ahorro energético

- Determinar si la intensificación de las cinéticas de transporte de materia en ambos sistemas, sólido-líquido y sólido-gas, se ve reflejada en un ahorro energético del proceso, con el fin de extrapolar esta tecnología a escala industrial.

8.Contribución científica

Research papers

García-Pérez, J.V., Ozuna, C., Ortuño, C., Cárcel, J.A. & Mulet, A. (2011). Modeling ultrasonically assisted convective drying of eggplant. *Drying Technology*. 29, 1499-1509.

Ozuna, C., Puig, A., García-Pérez, J.V., Mulet, A. & Cárcel, J.A. (2013). Influence of high intensity ultrasound application on mass transport, microstructure and textural properties of brined pork meat (*Longissimus dorsi*) at different NaCl concentrations. *Journal of Food Engineering*. 119, 84-93.

Ozuna, C., Cárcel, J.A., García-Pérez, J.V. & Mulet, A. (2011). Improvement of water transport mechanisms during potato drying by applying ultrasound. *Journal of the Science of Food and Agriculture*. 91, 2511–2517.

Ozuna, C., Gómez Álvarez-Arena, T., Riera, E., Cárcel, J.A. & García-Pérez, J.V. Influence of material structure on air-borne ultrasonic application in drying. *Ultrasonics Sonochemistry*. Accepted.

Ozuna, C., Puig, A., García-Pérez, J.V. & Cárcel, J.A. Ultrasonically enhanced desalting of cod (*Gadus morhua*). Mass transport kinetics and structural changes. *LWT- Food Science and Technology*. Submitted.

Ozuna, C., Cárcel, J.A, Walde P.M. & García-Pérez, J.V. Low-temperature drying of salted cod (*Gadus morhua*) assisted by high power ultrasound: kinetics and physical properties. *Innovative Food Science & Emerging Technologies*. Submitted.

Contributions to congresses

Ozuna, C. Puig, A., García-Pérez, J.V., Walde, P.M., Roselló, C. & Cárcel, J.A. (2013). Influence of high power ultrasound application on drying of salted cod (*Gadus Morhua*). Effects on rehydration capacity and structure of dried samples. European Drying Conference (EuroDrying'2013). Paris (France).

Ozuna, C., Walde, P.M., Riera, E., Mulet, A. & García-Pérez, J.V. (2013). Influence of high power ultrasound application on drying kinetics of salted cod (*Gadus Morhua*) at low temperature. European Drying Conference (EuroDrying'2013). Paris (France).

Ozuna, C., Hespos, T., Peña, R., García-Pérez, J.V., Mulet, A. & Cárcel, J.A. (2012). Influencia de la aplicación de ultrasonidos de alta intensidad en la cinética de desalado de bacalao (*Gadus morhua*). VII Congreso Español de Ingeniería de los Alimentos (CESIA 2012). Ciudad Real (Spain).

Ozuna, C., García-Pérez, J.V., Bon, J., Mulet, A. & Cárcel, J.A. (2011). Influence of brine concentration and high power ultrasound application on mass transport and meat texture during brining process. 12th Mediterranean Congress of Chemical Engineering. Barcelona (Spain).

Ozuna, C., Cárcel, J.A., Santacatalina, J.V., Mulet, A. & García-Pérez, J.V. (2011). Textural properties of vegetables: a key parameter on ultrasonic assisted convective drying. 11th International Congress on Engineering and Food (ICEF 11). Athens (Greece).

Ozuna, C., Cárcel, J. A., García-Pérez, J. V., Sanjuán, N. & Mulet, A. (2010). Improvement of water transport mechanisms during potato drying by ultrasonic application. 11th International Symposium on the Properties of Water (ISOPOW 11), Queretaro (Mexico).

Ozuna, C., Cárcel, J. A., García-Pérez, J. V., Peña, R. & Mulet, A. (2010). Influence of brine concentration on moisture and NaCl transport during meat salting. 11th International Symposium on the Properties of Water (ISOPOW 11), Queretaro (Mexico).

Ozuna, C., Cárcel P.C., García-Pérez, J.V., Mulet, A. & Cárcel, J.A. (2010). Influencia de la aplicación de ultrasonidos de alta intensidad en el transporte de agua y de NaCl durante el salado de carne en salmueras de diferente concentración. VI Congreso español de Ingeniería de Alimentos (CESIA), Logroño (Spain).

Santacatalina, J.V., Ozuna, C., Cárcel, J.A., García-Pérez, J.V. & Mulet, A. (2011). Quality assessment of dried eggplant using different drying methods: hot air drying, vacuum freeze drying and atmospheric freeze drying. 11th International Congress on Engineering and Food (ICEF 11). Athens (Greece).

Santacatalina, J.V., Ozuna, C., Cárcel, J.A., García-Pérez, J.V. & Mulet, A. (2011). A diffusion approach to describe hot air and atmospheric freeze drying kinetics of different products. European Drying Conference (EuroDrying'2011). Palma. Balearic Island (Spain).

9.Referencias

Agustí, M. (2010). Fruticultura. 2ª Edición. Mundi-Prensa, Madrid, España.

Ahmad-Qasem, M. H., Cánovas, J., Barrajón-Catalán, E., Micol, V., Cárcel, J. A., & García-Pérez, J. V. (2013). Kinetic and compositional study of phenolic extraction from olive leaves (var. Serrana) by using power ultrasound. *Innovative Food Science & Emerging Technologies*, 17, 120-129.

Awad, T. S., Moharram, H. A., Shaltout, O. E., Asker, D., & Youssef, M. M. (2012). Applications of ultrasound in analysis, processing and quality control of food: A review. *Food Research International*, 48, 410-427.

Awad, T. S. (2004). Ultrasonic studies of the crystallization behavior of two palm fats O/W emulsions and its modification. *Food Research International*, 37, 579-586.

Bantle, M., & Eikevik, T. M. (2011). Parametric study of high-intensity ultrasound in the atmospheric freeze drying of peas. *Drying Technology*, 29, 1230-1239.

Benali, M., & Kudra, T. (2010). Process intensification for drying and dewatering. *Drying Technology*, 28, 1127-1135.

Brás, A. & Costa, R. (2010). Influence of brine-salting prior to pickle salting in the manufacturing of various salted-dried fish species. *Journal of Food Engineering*, 100, 490–495.

Cárcel, J.A., García-Pérez, J.V., Benedito, J. & Mulet, A. (2012). Food process innovation through new technologies: Use of ultrasound. *Journal of Food Engineering*. 110, 200-207.

Cárcel, J. A., Garcia-Perez, J. V., Riera, E., & Mulet, A. (2011). Improvement of convective drying of carrot by applying power ultrasound—Influence of mass load density. *Drying Technology*, 29, 174-182.

Cárcel, J.A., Benedito, J., Roselló, C., & Mulet, A. (2007a). Influence of ultrasound intensity on mass transfer in apple immersed in a sucrose solution. *Journal of Food Engineering*, 78, 472-479.

Cárcel, J.A., Benedito, J., Bon, J., & Mulet A. (2007b). High intensity ultrasound effects on meat brining. *Meat Science*, 76, 611-619.

Cárcel, J.A., García-Pérez, J.V., Riera, E. & Mulet, A. (2007c). Influence of high intensity ultrasound on drying kinetics of persimmon, *Drying Technology*, 25, 185-193.

Cárcel, J.A. (2003). Influencia de los ultrasonidos de potencia en procesos de transferencia de materia. Tesis Doctoral. Universitat Politècnica de València.

Cardello, A. V., Schutz, H. G., & Lesher, L. L. (2007). Consumer perceptions of foods processed by innovative and emerging technologies: A conjoint analytic study. *Innovative Food Science & Emerging Technologies*, 8, 73-83.

Chandrapala, J., Oliver, C., Kentish, S., & Ashokkumar, M. (2012a). Ultrasonics in food processing–Food quality assurance and food safety. *Trends in Food Science & Technology*, 26, 88-98.

Chandrapala, J., Oliver, C., Kentish, S., & Ashokkumar, M. (2012b). Ultrasonics in food processing. *Ultrasonics sonochemistry*, 19, 975-983.

Chandrasekaran, S., Ramanathan, S., & Basak, T. (2013). Microwave food processing–a review. *Food Research International*, 52, 243-261.

Chemat, F., Zill-e-Huma, Khan & M.K. (2011). Applications of ultrasound in food technology: processing, preservation and extraction. *Ultrasonics Sonochemistry*, 18, 813–835.

Claussen, I. C., Ustad, T. S., Strømmen, I., & Walde, P. M. (2007). Atmospheric freeze drying-A review. *Drying Technology*, 25, 947-957.

Corona, E., Garcia-Perez, J. V., Alvarez-Arenas, T. E. G., Watson, N., Povey, M. J., & Benedito, J. (2013). Advances in the ultrasound characterization of dry-cured meat products. *Journal of Food Engine*ering, 119, 464-470.

Coupland, J. N. (2004). Low intensity ultrasound. *Food Research International*, 37, 537-543.

Cunha-Alves, A.A. (2002). Cassava botany and physiology. En: Cassava. Biology, production and utilization. Hillocks, R. J., Thresh, J.M., Bellotti, A.C. (editors) CABI Publishing, Reino Unido.

De la Fuente-Blanco, S., Riera-Franco de Sarabia, E., Acosta-Aparicio, V. M., Blanco-Blanco, A., & Gallego-Juárez, J. A. (2006). Food drying process by power ultrasound. *Ultrasonics*, 44, e523-e527.

Deng, Y., & Zhao, Y. (2008). Effects of pulsed-vacuum and ultrasound on the osmodehydration kinetics and microstructure of apples (Fuji). *Journal of Food Engineering*, 85, 84-93.

Esclapez, M. D., García-Pérez, J. V., Mulet, A., & Cárcel, J. A. (2011). Ultrasound-assisted extraction of natural products. *Food Engineering Reviews*, 3, 108-120.

Fernandes, F. A. N., & Rodrigues, S. (2008). Application of ultrasound and ultrasound-assisted osmotic dehydration in drying of fruits. *Drying Technology*, 26, 1509-1516.

Frias, J., Peñas, E., Ullate, M., & Vidal-Valverde, C. (2010). Influence of drying by convective air dryer or power ultrasound on the vitamin C and β-carotene content of carrots. *Journal of Agricultural and Food Chemistry*, 58, 10539-10544.

Fuentes, V., Ventanas, J., Morcuende, D., Estévez, M., & Ventanas, S. (2010). Lipid and protein oxidation and sensory properties of vacuum-packaged dry-cured ham subjected to high hydrostatic pressure. *Meat Science*, 85, 506-514.

Gabaldón-Leyva, C. A., Quintero-Ramos, A., Barnard, J., Balandrán-Quintana, R. R., Talamás-Abbud, R., & Jiménez-Castro, J. (2007). Effect of ultrasound on the mass transfer and physical changes in brine bell pepper at different temperatures. *Journal of Food Engineering*, 81, 374-379.

Gallego-Juárez, J. A., Rodríguez, G., Acosta, V., & Riera, E. (2010). Power ultrasonic transducers with extensive radiators for industrial processing. *Ultrasonics Sonochemistry*, 17, 953-964.

Gallego-Juarez, J. A., Rodriguez-Corral, G., Galvez Moraleda, J. C., & Yang, T. S. (1999). A new high-intensity ultrasonic technology for food dehydration. *Drying Technology*, 17, 597-608.

Gamboa-Santos, J., Soria, A. C., Villamiel, M., & Montilla, A. (2013). Quality parameters in convective dehydrated carrots blanched by ultrasound and conventional treatment. *Food Chemistry*, 141, 616-624.

Gamboa-Santos, J., Montilla, A., Soria, A. C., & Villamiel, M. (2012). Effects of conventional and ultrasound blanching on enzyme inactivation and carbohydrate content of carrots. *European Food Research and Technology*, 234, 1071-1079.

García-Pérez, J.V., Carcel, JA., Riera, E., Rosselló, C. & Mulet, A. (2012a). Intensification of low-temperature drying by using ultrasound. *Drying Technology,* 30, 1199-1208.

García-Pérez, J.V., Ortuño, C., Puig, A., Cárcel J.A. & Pérez-Munuera, I. (2012b). Enhancement of water transport and microstructural changes induced by high-intensity ultrasound application on orange peel drying. *Food and Bioprocess Technology*, 5, 2256-2265.

García-Pérez, J.V., Cárcel, J.A, Riera, E. & Mulet A. (2009). Influence of applied acoustic energy on the drying of carrots and lemon peel. *Drying Technology*, 27, 281-287.

García-Pérez, J.V. (2007). Contribución al estudio de la aplicación de ultrasonidos de potencia en el secado convectivo de alimentos. Tesis Doctoral. Universitat Politècnica de València.

Garcia-Perez, J. V., Cárcel, J. A., Benedito, J., & Mulet, A. (2007). Power ultrasound mass transfer enhancement in food drying. *Food and Bioproducts Processing*, 85, 247-254.

García-Pérez, J.V., Cárcel, J.A., De la Fuente-Blanco, S. & Riera-Franco de Sarabia, E. (2006a). Ultrasonic drying of foodstuff in a fluidized bed: Parametric study. *Ultrasonics*, 44, e539–e543.

García-Pérez, J. V., Rosselló, C., Cárcel, J. A., De la Fuente, S., & Mulet, A. (2006b). Effect of air temperature on convective drying assisted by high power ultrasound. *Defect and Diffusion Forum*, 258-260, 563-574.

Gerven, T. M., & Stankiewicz, A. (2009). Structure, energy, synergy, time-The fundamentals of process intensification. *Industrial & Engineering Chemistry Research*, 48, 2465-2474.

Gisbert, M. (2001). Influencia de las variables de proceso en la evolución físico-química y bioquímica del lomo embuchado. Tesis Doctoral. Universitat Politècnica de València.

Jaeger, H., Reineke, K., Schoessler, K., & Knorr, D. (2012). Effects of emerging processing technologies on food material properties. In B.R. Bhandari, & Y.H. Roos (Eds), Food Materials Science and Engineering, (pp. 222-254). Blackbell Publishing Ltd.

Jaeger, H., Balasa, A., & Knorr, D. (2009). Food industry applications for pulsed electric fields. In Electrotechnologies for Extraction from Food Plants and Biomaterials (pp. 181-216). Springer, New York.

Jayasooriya S.D., Torley P.J., D'Arcy B.R. & Bhandari B.R. (2007). Effect of high power ultrasound and ageing on the physical properties of bovine Semitendinous and Longissimus muscles. *Meat Science*, 75, 628-639.

Ji, J. B., Lu, X. H., Cai, M. Q., & Xu, Z. C. (2006). Improvement of leaching process of Geniposide with ultrasound. *Ultrasonics Sonochemistry*, 13, 455-462.

Knorr, D., Froehling, A., Jaeger, H., Reineke, K., Schlueter, O. & Schöessler, K. (2011). Emerging technologies in food processing. *Annual Review of Food Science and Technology*, 2, 203-235.

Krokida, M., & Maroulis, Z. (2000). Quality changes during drying of food materials. In: Drying technology in agriculture and food sciences, 61-106.

Lee, H. & Feng, H. (2011). Effect of power ultrasound on food quality. In Feng, H., Barbosa-Cánovas, G.M. & Weiss, J. (Eds.), *Ultrasound Technologies for Food and Bioprocessing* (pp. 559–582). London: Springer.

Lou, Z., Wang, H., Zhang, M., & Wang, Z. (2010). Improved extraction of oil from chickpea under ultrasound in a dynamic system. *Journal of Food Engineering*, 98, 13-18.

Luque de Castro, M.D., & Priego Capote, F. (2007). *Analytical applications of ultrasound*. Elsevier.

Mason, T. J., & Lorimer, J. P. (2002). Applied sonochemistry. The uses of power ultrasound in chemistry and processing. Weinheim: Wiley-VCH.

McClements, D. J. & Povey, M. J. W. (1992). Ultrasonic analysis of edible fats and oils. *Ultrasonics*, 30, 383-388.

Ministerio de Agricultura, Alimentación y Medio Ambiente (2013). Enciclopedia de los alimentos. www.alimentacion.es. (Fecha de consulta: 06-junio-2013).

Mizrach, A. (2008). Ultrasonic technology for quality evaluation of fresh fruit and vegetables in pre- and postharvest processes. Review. *Postharvest Biology and Technology*, 48, 315-330.

Mulet, A., Cárcel, J.A., Sanjuan, N. & García-Pérez, J.V. (2010). Food dehydration under forced convection conditions. In Recent Progress in Chemical Engineering; Delgado J. (Ed.), Studium Press LLC; Houston, TX, USA., 153-177.

Mulet, A., Cárcel, J. A., Benedito, J., Rosselló, C. y Simal, S. (2003). Ultrasonic mass transfer enhancement in food processing. En: Transport Phenomena in Food Processing. Welti-Chanes, J., Vélez-Ruiz, J. y Barbosa-Cánovas, G (editores). CRC Press. Boca Raton. EE.UU. 265-277.

Muralidhara, H.S., Ensminger, D. & Putnam, A. (1985). Acoustic dewatering and drying (low and high frequency): State of the art review. *Drying Technology* 1985, 3, 529-566.

Moy, J. H., & DiMarco, G. R. (1970). Exploring airborne sound in a nonvacuum freeze-drying process. *Journal of Food Science*, 35, 811-817.

Nakagawa S., Yamashita T., & Miura H. (1996). Ultrasonic drying of walleye pollack surimi. *Journal of the Japanese Society for Food Science and Technology*, 43, 388-394.

Oey, I., Lille, M., Van Loey, A., & Hendrickx, M. (2008). Effect of high-pressure processing on colour, texture and flavour of fruit-and vegetable-based food products: a review. *Trends in Food Science & Technology*, 19, 320-328.

Oliveira, H., Pedro S., Nunes, M.L., Costa, R., & Vaz-Pires, P. (2012). Processing of salted cod (Gadus spp.): a review. Comprehensive Reviews in Food Science and Food Safety, 11, 546-564.

Oliveira, F.I.P., Gallão, M. I., Rodrigues, S. & Fernandes, F. A. N. (2011). Dehydration of Malay apple (*Syzygium malaccense* L.) using ultrasound as pre-treatment. *Food and Bioprocess Technology*, 4, 610-615.

Ortuño, C., Martínez-Pastor, M. T., Mulet, A., & Benedito, J. (2013). Application of high power ultrasound in the supercritical carbon dioxide inactivation of *Saccharomyces cerevisiae*. *Food Research International*, 51, 474-481.

Ortuño, C., Martínez-Pastor, M. T., Mulet, A., & Benedito, J. (2012). Supercritical carbon dioxide inactivation of *Escherichia coli* and *Saccharomyces cerevisiae* in different growth stages. *The Journal of Supercritical Fluids*, 63, 8-15.

Ortiz, J., Lemus-Mondaca, R., Vega-Gálvez, A., Ah-Hen, K., Diaz-Puente, L., Zura-Bravo, L. & Aubourg, S. (2013). Influence of air-drying temperature on drying kinetics, colour, firmness, and biochemical characteristics of Atlantic salmon (*Salmo salar* L.) fillets, *Food Chemistry*, 139, 162-169.

Patterson, M. F. (2005). Microbiology of pressure-treated foods. *Journal of Applied Microbiology*, 98, 1400-1409.

Perrut, M. (2012). Sterilization and virus inactivation by supercritical fluids (a review). *The Journal of Supercritical Fluids*, 66, 359-371.

Picó, Y. (2013). Ultrasound-assisted extraction for food and environmental samples. *TrAC Trends in Analytical Chemistry*, 43, 84-99.

Pingret, D., Fabiano-Tixier, A. S., & Chemat, F. (2013). Degradation during application of ultrasound in food processing: a review. *Food Control*, 31, 593-606.

Puig, A., Perez-Munuera, I., Carcel, JA., Hernando, I. & Garcia-Perez, J.V. (2012). Moisture loss kinetics and microstructural changes in eggplant (*Solanum melongena L.*) during conventional and ultrasonically assisted convective drying. *Food and Bioproducts Processing*, 90, 624-632.

Ravigione, A.F.M. (2002). Estudio para la caracterización microestructural de la zanahoria (*Daucus Carota L.*) encurtida : relación con los principales cambios macroscópicos experimentados.

Rawson, A., Tiwari, B. K., Tuohy, M. G., O'Donnell, C. P., & Brunton, N. (2011). Effect of ultrasound and blanching pretreatments on polyacetylene and carotenoid content of hot air and freeze dried carrot discs. *Ultrasonics Sonochemistry*, 18, 1172-1179.

Riera, E., García-Pérez, J.V., Cárcel, J.A., Acosta, V., Gallego-Juárez, J.A. (2011). Computational Study of Ultrasound-Assisted Drying of Food Materials. In: Knoerzer, K., Juliano, P., Roupas, P., Versteeg, C. (Eds.), Innovative Food Processing Technologies: Advances in Multiphysics Simulation. John Wiley & Sons Ltd., pp. 265–301.

Riera, E., Blanco, A., García, J., Benedito, J., Mulet, A., Gallego-Juárez, J. A., & Blasco, M. (2010). High-power ultrasonic system for the enhancement of mass transfer in supercritical CO_2 extraction processes. *Physics Procedia*, 3, 141-146.

Riera, E., Gallego-Juárez, J. A., & Mason, T. J. (2006). Airborne ultrasound for the precipitation of smokes and powders and the destruction of foams. *Ultrasonics Sonochemistry*, 13, 107-116.

Rodríguez-Barona, S. (2003). Estudio del proceso de salado y desalado de bacalao (*Gadus morhua*). Evaluación de alternativas a los procesos tradicionales. Tesis Doctoral. Universidad Politécnica de Valencia.

Rodríguez, G., Riera, E., Gallego-Juárez, J. A., Acosta, V. M., Pinto, A., Martínez, I., & Blanco, A. (2010). Experimental study of defoaming by air-borne power ultrasonic technology. *Physics Procedia*, 3, 135-139.

Rodríguez, J., Melo, E. C., Mulet, A. & Bon, J. (2013). Optimization of the antioxidant capacity of thyme (*Thymus vulgaris* L.) extracts: Management of the convective drying process assisted by power ultrasound, *Journal of Food Engineering*, 119, 793-799.

Ross, K. A., Pyrak-Nolte, L. J. & Campanella, O. H. (2004). The use of ultrasound and shear oscillatory test to characterize the effect of mixing time on the rehological properties of dough. *Food Research International*, 37, 567-577.

Roupas, P. (2008). Food Innovation: Emerging Science, Technologies and Applications (FIESTA) conference. *Innovative Food Science & Emerging Technologies*, 9, 139.

Ruiz-Ramírez, J., Arnau, J., Serra, X., & Gou, P. (2005). Relationship between water content, NaCl content, pH and texture parameters in dry-cured muscles. *Meat Science*, 70 (4), 579-587.

Sabarez, H.T., Gallego-Juarez, J.A. & Riera, E. (2012). Ultrasonic-assisted convective drying of apple slices. *Drying technology*, 30, 989-997.

Sanchez, E. S., Simal, S., Femenia, A., Llull, P., & Rosselló, C. (2001a). Proteolysis of Mahon cheese as affected by acoustic-assisted brining. *European Food Research and Technology*, 212, 147-152.

Sanchez, E. S., Simal, S., Femenia, A., Benedito, J., & Rosselló, C. (2001b). Effect of acoustic brining on lipolysis and on sensory characteristics of Mahon cheese. *Journal of Food Science*, 66, 892-896.

Sánchez, E. S., Simal, S., Femenia, A., Benedito, J., & Rosselló, C. (1999). Influence of ultrasound on mass transport during cheese brining. *European Food Research and Technology*, 209, 215-219.

Schössler, K., Thomas, T., & Knorr, D. (2012a). Modification of cell structure and mass transfer in potato tissue by contact ultrasound. *Food Research International*, 49, 421-435.

Schössler, K., Jäger, H., & Knorr, D. (2012b). Effect of continuous and intermittent ultrasound on drying time and effective diffusivity during convective drying of apple and red bell pepper. *Journal of Food Engineering*, 108, 103-110.

Schössler, K., Jäger, H., & Knorr, D. (2012c). Novel contact ultrasound system for the accelerated freeze-drying of vegetables. *Innovative Food Science & Emerging Technologies*, 16, 113-120.

Simal, S., Benedito, J., Sánchez, E. S., & Rosselló, C. (1998). Use of ultrasound to increase mass transport rates during osmotic dehydration. *Journal of Food Engineering*, 36, 323-336.

Siró, I., Vén, C., Balla, C., Jónás, G., Zeke, I., & Friedrich, L. (2009). Application of an ultrasonic assisted curing technique for improving the diffusion of sodium chloride in porcine meat. *Journal of Food Science*, 91, 363-362.

Soria, A. C., & Villamiel, M. (2010). Effect of ultrasound on the technological properties and bioactivity of food: a review. *Trends in Food Science & Technology*, 21, 323-331.

Soria, A. C., Corzo-Martínez, M., Montilla, A., Riera, E., Gamboa-Santos, J., & Villamiel, M. (2010). Chemical and physicochemical quality parameters in carrots dehydrated by power ultrasound. *Journal of Agricultural and Food Chemistry*, 58, 7715-7722.

Spilimbergo, S., Mantoan, D., & Dalser, A. (2007). Supercritical gases pasteurization of apple juice. *The Journal of Supercritical Fluids*, 40, 485-489.

Stojanovic, J., & Silva, J. L. (2007). Influence of osmotic concentration, continuous high frequency ultrasound and dehydration on antioxidants, colour and chemical properties of rabbiteye blueberries. *Food Chemistry*, 101, 898-906.

Tao, Y., & Sun, D. W. (2013). Enhancement of food processes by ultrasound: a review. *Critical Reviews in Food Science and Nutrition*. DOI: 10.1080/10408398.2012.667849.

Toepfl, S., Mathys, A., Heinz, V., & Knorr, D. (2006). Review: Potential of high hydrostatic pressure and pulsed electric fields for energy efficient and environmentally friendly food processing. *Food Reviews International*, 22, 405-423.

U.S. Department of Agriculture. Agricultural Research Service (2013). USDA Nutrient Database for Standard Reference, Release 25. Nutrient Data Laboratory Home Page, http://ndb.nal.usda.gov/ndb/search/list. (Fecha de consulta: 03-junio-2013).

Venkatesh, M. S., & Raghavan, G. S. V. (2004). An overview of microwave processing and dielectric properties of agri-food materials. Biosystems Engineering, 88, 1-18.

Wei, F., Gao, G. Z., Wang, X. F., Dong, X. Y., Li, P. P., Hua, W., Wang, X., Wu, X. M. & Chen, H. (2008). Quantitative determination of oil content in small quantity of oilseed rape by ultrasound-assisted extraction combined with gas chromatography. *Ultrasonics sonochemistry*, 15, 938-942.

Ying, Z., Han, X., & Li, J. (2011). Ultrasound-assisted extraction of polysaccharides from mulberry leaves. *Food Chemistry*, 127, 1273-1279.

Zhang, G., He, L., & Hu, M. (2011). Optimized ultrasonic-assisted extraction of flavonoids from *Prunella vulgaris* L. and evaluation of antioxidant activities in vitro. *Innovative Food Science & Emerging Technologies*, 12, 18-25.

Zhang, H. F., Yang, X. H., Zhao, L. D., & Wang, Y. (2009). Ultrasonic-assisted extraction of epimedin C from fresh leaves of *Epimedium* and extraction mechanism. *Innovative Food Science & Emerging Technologies*, 10, 54-60.

Zhang, M., Tang, J., Mujumdar, A. S., & Wang, S. (2006). Trends in microwave-related drying of fruits and vegetables. T*rends in Food Science & Technology*, 17, 524-534.

Zhao, S., Kwok, K. C., & Liang, H. (2007). Investigation on ultrasound assisted extraction of saikosaponins from *Radix Bupleuri*. *Separation and Purification Technology*, 55, 307-312.

Zou, Y., Xie, C., Fan, G., Gu, Z., & Han, Y. (2010). Optimization of ultrasound-assisted extraction of melanin from *Auricularia auricular* fruit bodies. *Innovative Food Science & Emerging Technologies*, 11, 611-615.